DEVELOPMENTS IN SEDIMENTOLOGY

24

R.E. GRIM
N. GÜVEN

BENTONITES

GEOLOGY, MINERALOGY, PROPERTIES AND USES

ELSEVIER

DEVELOPMENTS IN SEDIMENTOLOGY 24

BENTONITES

FURTHER TITLES IN THIS SERIES

1. *L.M.J.U. VAN STRAATEN, Editor*
DELTAIC AND SHALLOW MARINE DEPOSITS
2. *G.C. AMSTUTZ, Editor*
SEDIMENTOLOGY AND ORE GENESIS
3. *A.H. BOUMA* and *A. BROUWER, Editors*
TURBIDITES
4. *F.G. TICKELL*
THE TECHNIQUES OF SEDIMENTARY MINERALOGY
5. *J.C. INGLE Jr.*
THE MOVEMENT OF BEACH SAND
6. *L.VAN DER PLAS*
THE IDENTIFICATION OF DETRITAL FELDSPARS
7. *S. DZULYNSKI* and *E.K. WALTON*
SEDIMENTARY FEATURES OF FLYSCH AND GREYWACKES
8. *G. LARSEN* and *G.V. CHILINGAR, Editors*
DIAGENESIS IN SEDIMENTS
9. *G.V. CHILINGAR, H.J. BISSELL* and *R.W. FAIRBRIDGE, Editors*
CARBONATE ROCKS
10. *P. McL. D. DUFF, A. HALLAM* and *E.K. WALTON*
CYCLIC SEDIMENTATION
11. *C.C. REEVES Jr.*
INTRODUCTION TO PALEOLIMNOLOGY
12. *R.G.C. BATHURST*
CARBONATE SEDIMENTS AND THEIR DIAGENESIS
13. *A.A. MANTEN*
SILURIAN REEFS OF GOTLAND
14. *K.W. GLENNIE*
DESERT SEDIMENTARY ENVIRONMENTS
15. *C.E. WEAVER* and *L.D. POLLARD*
THE CHEMISTRY OF CLAY MINERALS
16. *H.H. RIEKE III* and *G.V. CHILINGARIAN*
COMPACTION OF ARGILLACEOUS SEDIMENTS
17. *M.D. PICARD* and *L.R. HIGH Jr.*,
SEDIMENTARY STRUCTURES OF EPHEMERAL STREAMS
18. *G.V. CHILINGARIAN* and *K.H. WOLF*
COMPACTION OF COARSE-GRAINED SEDIMENTS
19. *W. SCHWARZACHER*
SEDIMENTATION MODELS AND QUANTITATIVE STRATIGRAPHY
20. *M.R. WALTER, Editor*
STROMATOLITES
21. *B. VELDE*
CLAYS AND CLAY MINERALS IN NATURAL AND SYNTHETIC SYSTEMS
22. *C.E. WEAVER* and *K.C. BECK*
MIOCENE OF THE SOUTHEASTERN UNITED STATES
23. *B.C. HEEZEN, Editor*
INFLUENCE OF ABYSSAL CIRCULATION ON SEDIMENTARY ACCUMULATIONS IN SPACE AND TIME

DEVELOPMENTS IN SEDIMENTOLOGY 24

BENTONITES

Geology, Mineralogy, Properties and Uses

RALPH E. GRIM

Research Professor of Geology,
University of Illinois, Urbana, Ill., U.S.A.

NECIP GÜVEN

Professor of Geology,
Texas Tech University, Lubbock, Texas, U.S.A.

ELSEVIER SCIENTIFIC PUBLISHING COMPANY

AMSTERDAM — OXFORD — NEW YORK 1978

ELSEVIER SCIENTIFIC PUBLISHING COMPANY
335 Jan van Galenstraat
P.O. Box 211, 1000 AE Amsterdam, The Netherlands

Distributors for the United States and Canada:

ELSEVIER NORTH-HOLLAND INC.
52, Vanderbilt Avenue
New York, N.Y. 10017

Library of Congress Cataloging in Publication Data

Grim, Ralph Early, 1902-
Bentonites : geology, mineralogy, properties and uses.

(Developments in sedimentology ; 24)
Bibliography: p.
Includes index.
1. Bentonite. I. Güven, Necip, joint author.
II. Title. III. Series.
QE391.B55G74 553'.61 78-3842
ISBN 0-444-41613-7

ISBN: 0-444-41613-7 (Vol. 24)
ISBN: 0-444-41238-7 (Series)

Printed in The Netherlands

PREFACE

In the course of many years one of us (Grim) had many opportunities to study deposits of bentonite and collect samples of bentonites in many parts of the world. This collection of bentonite samples was augmented by additional material kindly donated by colleagues and commercial producers of bentonite. The mineralogical study of these samples was started at the University of Illinois by Güven and continued by him at Texas Tech University when he moved there from the University of Illinois. At the University of Illinois Mrs. Neriman Güven assisted in catalogging the samples and organizing them into a collection.

The mineralogical analytical procedure was to survey several hundred samples by X-ray diffraction and electron micrography and then select representatives for further detailed investigation. In this volume Grim is responsible for the geological part of the monograph: the description of the field occurrences, the consideration of the origin and distribution of bentonites, and the final chapter on Properties and Uses of Bentonite. Güven is responsible for the mineralogical and chemical data and for the chapters on Methods of Investigations, and Selected Area Electron Diffraction Studies on Muscovite, Beidellite, and Montmorillonite.

In the course of the preparation of his part of the volume, Güven had the assistance of Mr. Rodney W. Pease, who obtained a large number of micrographs, Mr. Roger W. Lee, who did the chemical analyses, and Mr. N.M. Gazdar, who determined the exchangeable cations. Güven also had the assistance of Professors R.B. Mattox and V.L. Yeats, who were always ready to help choose the "right" word or to find the "natural way" of saying things in English, and he had very instructive correspondence with Professors P.P. Ewald and B.B. Zvyagin, which helped to clarify matters while preparing Chapter 4 on Electron Diffraction.

Special thanks should be expressed to the management of Industrial Mineral Ventures, Inc., Golden, Colorado for their financial support of this project. Finally, thanks are due to Mr. Robert Suddarth for his careful drawings and for making the prints in this monograph.

R.E.G.
N.G.

This Page Intentionally Left Blank

CONTENTS

Chapter 1

INTRODUCTION

The name bentonite was suggested in 1898 by Knight for a peculiar clay-like material with soapy properties from its occurrence in the Fort Benton unit of Cretaceous age formations in Wyoming (U.S.A.). Hewitt (1917) and Wherry (1917) first established that this particular clay is an alteration product of volcanic ash, although an earlier observation by Condra (1908) suggested this origin for a similar clay from northern Nebraska. Ross and Shannon (1926) presented the following definition which has been widely quoted: "Bentonite is a rock composed essentially of a crystalline clay-like mineral formed by the devitrification and the accompanying chemical alteration of a glassy igneous material, usually a tuff or volcanic ash". These authors further stated that, "the characteristic clay mineral has a micaceous habit and facile cleavage, high birefringence, and a texture inherited from the volcanic tuff or ash, and it is usually the mineral montmorillonite, but less often beidellite". The term bentonite is now well established (Wright, 1968) for any clay which is composed dominantly of a smectite clay mineral, and whose physical properties are dictated by this clay mineral; this is the definition used in this volume.

As indicated later in this volume, there are many clays now designated as bentonite which have not originated by the alteration of volcanic ash or tuff, or whose origin cannot be established definitely. Consequently, the definition of bentonite used herein does not include mode of origin.

The term fuller's earth refers to any natural material which has the capacity to decolorize oil to an extent to be of commercial value. The term does not imply any mode of origin, or any particular mineral composition. However, fuller's earths are generally composed of attapulgite or a smectite clay mineral, although not all clays composed of these clay minerals have the decolorizing capacity necessary for their classification as fuller's earths.

The unique physical properties of the Wyoming clay quickly gave it high commercial value. Its use in oil well drilling muds, as a bonding agent for foundry molding sands, and in other commercial processes caused the development of an important bentonite producing industry in Wyoming, and led to a search in other regions for similar clays with the same properties. Such clays were soon found in Mississippi, Texas, Arizona, and California of the U.S.A., and in England, Germany, U.S.S.R., Japan, and many other countries. A bentonite producing industry developed rapidly outside of the United States beginning in the late 1920's. Grim has had an opportunity for many years to visit and study the occurrence of bentonites in many parts of the world. Samples were collected from many of the deposits visited, and

additional samples from other deposits were kindly supplied by friends and colleagues. A collection of approximately 1,000 world-wide bentonite samples was developed and is now housed in the Department of Geosciences at Texas Tech University in Lubbock, Texas. Much information was gathered in the field on the mode of occurrence of bentonites, including the types of formations with which they are associated, their relationship to hydrothermal and/or deuteric activities, and their association with unaltered volcanic ash, tuff, or other volcanic material.

The first objective of this volume is to describe the geologic and geographic occurrence of bentonites world-wide. No claim is made that all known deposits are listed, but it is hoped that no large significant deposits have been overlooked. The information recorded is from the literature and from data obtained by one of us (Grim) on visits to many of the deposits in the field.

It is obviously impossible to list all available references to the various deposits. An attempt was made to select papers of general interest that especially were concerned with occurrence and origin of the bentonites. There are many additional publications which are concerned with the properties and uses of particular bentonites.

Very limited information regarding bentonites is available for some countries, e.g. China, Cuba, Colombia. Consequently, it should not be concluded from the brief statements regarding some countries that substantial deposits of bentonites may not occur there or may be unknown. Similarly, there are other countries for which no reference to bentonite could be found, e.g. Chile, but based on geological considerations, it seems likely that bentonites should be present in some of these countries.

No mention is made regarding the so-called metabentonites, i.e. clays probably of volcanic origin, usually of Paleozoic age, which are composed of illite-smectite mixed-layers, and which do not have the colloidal properties associated with the term bentonite.

The second objective of the volume is to consider the variations in the mineral and chemical composition of bentonites. Detailed mineralogical analyses of the samples have been made by Güven. Because of the submicron crystallite size and poor crystallinity of the major component (smectite) in bentonites, X-ray diffraction analyses were of limited use. Therefore, modern electron-optical methods were used extensively in studying the morphology and structure of the smectite particles.

Members of the montmorillonite—beidellite series form the smectites commonly occurring in bentonites. The smectites are examined with respect to their atomic structure, chemical composition, and crystal morphology (habit, particle size, and mode of aggregations). Electron optics, which are probably the most powerful methods for precise analyses of the above properties of smectites, are discussed in detail. An attempt is made to classify the smectite particles according to their morphological character-

istics. The habit of single crystallites and the morphological features of smectite aggregates are discussed with respect to crystal growth mechanisms and to the factors governing crystal growth processes.

The chemistry of smectites is examined using a rapid method of analysis by atomic absorption spectroscopy and a single-solution decomposition technique. The problems related to the calculation of chemical formulae for smectites are discussed. 152 chemical analyses of smectites are compiled from the literature and subjected to a factorial analysis in order to elucidate the correlations between the chemical components in these minerals.

The third, and last, objective is to consider the physical properties of bentonites, and the manner in which the physical properties determine the commercial usage of these clays. An attempt is made to correlate the properties with the fundamental mineral and chemical character of the bentonites.

REFERENCES

Knight, W.C., 1898. Bentonite. Eng. Min. J., 66: 491.

Hewitt, D.F., 1917. The origin of bentonite. J. Wash. Acad. Sci., 7: 196—198.

Wherry, E.T., 1917. Clay derived from volcanic dust in the Pierre of South Dakota. J. Wash. Acad. Sci., 7: 576—583.

Condra, G.E., 1908. Geology and water resources of a portion of the Missouri River valley in northwestern Nebraska. U.S. Geol. Surv., Water-Supply Pap., 215: 59 pp.

Ross, C.S. and E.V. Shannon, 1926. Minerals of bentonite and related clays and their physical properties. J. Am. Ceram. Sci., 9: 77—96.

Wright, P.C., 1968. Meandu Creek bentonite — a reply. J. Geol. Soc. Aust., 15: 347—350.

This Page Intentionally Left Blank

METHODS OF INVESTIGATIONS

Detailed mineralogical examinations were made on selected samples using X-ray diffraction, electron microscopy, and atomic absorption spectroscopy. These analyses helped to establish the mineralogical and chemical composition of the bentonites, as well as the morphological characteristics of smectite particles in them. The most important mineralogical component in bentonites is the smectite. The prime emphasis is, therefore, put on the mineralogical analysis of the smectites. The smectite minerals are divided into two subgroups: trioctahedral and dioctahedral. Major trioctahedral smectites occurring in bentonites are represented by the hectorite—saponite series within the range of the following ideal formula:

$$[(Mg_{3.00-z}Li_z)(Si_{4.00-u}Al_u)O_{10}(OH)_2]M^+_{z+u}$$

where the mineral with $z = 0.0$, i.e., no lithium, represents the saponite end-member of this series. The lithium content of the smectite forms, therefore, a good indicator for the position of the smectite in this series. The major dioctahedral smectites of this group are represented by a ternary system consisting of the end-members montmorillonite, beidellite, and nontronite within the range of the following formula.

$$[(Al_x Fe^{3+}_y Mg_z)_{2.00}(Si_{4.00-(u+v)}Fe^{3+}_v Al_u)O_{10}(OH)_2]M^+_{u+v+z}$$

where the subscript $(u + v + z)$, i.e. the layer charge, can vary between 0.25 to 0.6. The ferrous iron, which might occupy octahedral positions, has not been included in the above formula. For the end-member montmorillonite u, v, and y subscripts are zero, while for the end member beidellite v, y, and z subscripts are zero. For the end-member nontronite, v, x, and z subscripts are assumed to be zero. The boundary in the montmorillonite—beidellite series $(v,y = 0)$ is defined by Greene-Kelly (1953) at the composition at which $u = z$; the smectite with $z > u$ being a montmorillonite. For the ignited (at 1000°C) samples, the MgO content of the montmorillonite end-member varies from 3.0% at the layer charge of $z = 0.25$ to 7.2% at the maximum layer charge of $z = 0.6$ (on the basis of $MgO + Al_2O_5 + SiO_2 = 100$). The magnesia content of the sample may be used as an indicator with respect to the position of the smectite in this series provided the ferrous iron content is not significant. The chemical analyses published by Ross and Hendricks (1945) suggest that the montmorillonite—beidellite series is a continuous one, whereas the beidellite—nontronite series seems to be a discon-

tinuous one. The smectites commonly occurring in bentonites are the members of the montmorillonite—beidellite series with small amounts of iron in them.

2.1. X-RAY DIFFRACTION ANALYSIS

A Philips X-ray diffractometer, with Ni-filtered CuKα-radiation, at a scanning speed of one degree per minute (2θ), was used to obtain X-ray diffraction data. From the X-ray data, crystalline phases in the samples were identified and their amounts were semiquantitatively estimated. For the identification of clay minerals, oriented slides were prepared from the -1 μm fractions of the samples; these were separated by centrifugation using the suspensions of the samples in distilled water. Oriented slides were air dried at room temperature and at a relative humidity of 40—50% in the laboratory. After the air-dried slides were X-rayed, they were sprayed with ethylene glycol and left overnight in ethylene glycol atmosphere, and X-rayed again. The X-ray diffraction patterns obtained on these slides give the variations in the basal interplanar distances of the clay minerals. In order to obtain X-ray data on the b lattice parameters of the smectites, the (06) reflection is separately scanned at a speed of $(\frac{1}{4})^\circ$/min. (2θ) using randomly powdered clay samples.

2.2. ATOMIC ABSORPTION SPECTROSCOPY

Data on the chemistry of the samples are obtained by atomic absorption spectroscopy (AAS). This method has been widely known for its precision in the determination of alkaline and earth alkaline elements. Recently other major elements of silicates have been also rather satisfactorily analyzed by the same method by a number of investigators (Bernas, 1968; Langmyhr and Paus, 1968; Van Loon and Parissis, 1969; and Abbey, 1970, 1973). The decomposition of silicates with hydrofluoric acid in a pressure vessel (Bernas, 1968; Langmyhr and Paus, 1968) and subsequent complexing of the fluorides with boric acid provides a salt-free single solution. From this solution with a matrix of fluoboric—boric acids, major and minor elements of silicates can be directly determined by atomic absorption spectroscopy. Recently, Lee and Güven (1975) reported how chemical interferences among the major elements of silicates in the fluoboric—boric acids (HBF_4—H_3BO_3) matrix could be compensated.

The following procedure has been adopted for the preparation of bentonites for the AAS analysis. Five grams of clay are equilibrated overnight in 75 ml of 1N ammonium acetate solution adjusted to a pH of 7. The ammonium saturated clay is washed several times with distilled water, and the

leachate is collected. The latter contains not only the exchangeable cations of the clays but also other material dissolved during the process. The leachate is analyzed for the cations Na, K, Ca, and Mg. The ammonium clay in the residue, while still wet, is transferred to centrifuge tubes and the $-1\ \mu m$ fraction of the clay is separated by centrifugation. A small portion of the moist clay from the $-1\ \mu m$ fraction is dried at 110°C on a watch glass and then removed in a porcelain crucible and heated with a cover to 400°C for 30 min. The sample is then ignited for an hour at 1000°C in a muffle furnace. Since the ammonium, which occupies the interlayer positions of the smectites, is lost during the ignition, the material now contains oxides of the constituents making up the silicate layer of the smectites. During the ignition process all ferrous iron becomes oxidized to ferric state. Duplicates of about 100 mg of the ignited material are weighed after it has been cooled in a desiccator, and transferred into the teflon cup of an acid pressure vessel. The vessel is similar to the one described by Bernas (1968), and was obtained from Parr Instrument Co., Moline, Illinois. The decomposition of the samples is accomplished in 3 ml of HF at 100—110°C within an hour by placing the sealed pressure vessel into an oven at that temperature. Subsequently, the content of the bomb is transferred to a polypropylene beaker containing 2.8 g analytical reagent H_3BO_3, and about 100 ml distilled-deionized water. The beaker is heated at 80°C until a clear solution is obtained, and then diluted to 250 ml in order to provide optimum concentration ranges for the AAS determinations of the common elements in bentonites. These elements (Si, Al, Ca, Mg, Fe, Na, K, and Li) are analyzed under the instrumental conditions listed in Table 2.1. Because of the high magnesium concentrations of the solutions, the secondary absorption line (2025 Å) of magnesium is preferred over the resonance line (2852 Å). Checks made using both lines showed no appreciable differences between them.

As seen from the sensitivity values listed in Table 2.1, atomic absorp-

TABLE 2.1

Experimental conditions for atomic absorption analysis of bentonites

Element	Flame type	λ(Å)	Width of the receiving slit (μm)	Lamp current (mA)	Sensitivity (μg/ml/1% Abs.)
Silicon	N_2O—C_2H_2	2516	150	12	1.0
Aluminum	N_2O—C_2H_2	3093	150	10	0.5
Calcium	N_2O—C_2H_2	4227	100	10	0.07
Magnesium	Air—C_2H_2	2025	100	10	0.05
Iron	Air—C_2H_2	2483	100	10	0.05
Sodium	Air—C_2H_2	5890	100	6	0.01
Potassium	Air—C_2H_2	7665	100	12	0.02
Lithium	Air—C_2H_2	6708	100	12	0.02

tion spectroscopy provides highly precise analyses for most of the elements except for silicon and aluminum. Conventional methods (gravimetric and colormetric) of silicate analyses were shown (Fairbairn, 1953) to have a relative standard deviation (coefficient of variation) of 0.5% for silica (SiO_2) and 2.2% for alumina (Al_2O_3) for a granitic composition. The plots of absorbance vs. concentration have a rather low slope for Al and Si. This, combined with the sensitivity values of the same elements, results in about 1% relative deviation for both silica and alumina as inferred from our limited number of determinations. A thorough statistical analysis, using larger number of analyses, has yet to be done in order to evaluate exactly the errors involved in silica and alumina determinations using atomic absorption spectroscopy. For the present we will consider the silica and alumina values of the samples to have an error of ±1% of the amount listed for the sample. Both titanium (TiO_2) and manganese (MnO) have not been determined, since these elements are believed, for the most part, to occur not in smectites but in separate phases in the clays. The total of the oxides varies from 98 to 101% because of the above factors related to silica, alumina, titanium, and manganese.

Cations (Ca, Mg, K, Na) extractable from the bulk sample by the NH_4^+-acetate method (Jackson, 1956) are determined by atomic absorption spectroscopy, and they are given in mequiv./100 g. For those clays with high amounts of extractable cations, the cation exchange capacity (C.E.C.) was also determined by resaturating the NH_4^+-clay with sodium. The values of the C.E.C. and the basal spacings of the smectites were found helpful in deciding whether all the extractable cations originate from the clay minerals or from the other components in the sample. For this purpose two samples representative of Wyoming and Cheto-type montmorillonites (samples 1 and 9) have been saturated with the cations Na, Ca, and Mg from their 1*N* chloride solutions at pH = 7. X-ray diffraction data on the oriented slides dried at relative humidity of 50% showed the following variations on the basal spacings of the samples. Wyoming montmorillonite gives a basal spacing of 12.3 Å for Na, 14.1 Å for Mg, and 14.5 Å for Ca whereas the basal spacing of Cheto montmorillonite reaches 12.6 Å for Na, 14.9 Å for Mg, and 15.0 Å for Ca. Complete data on the basal spacings of montmorillonites saturated with different cations is available in the literature (Hendricks et al., 1940).

Discrepancies between the total of extractable cations and the C.E.C. values may occur in the following circumstances: (a) the total of extractable cations may be larger than the C.E.C., if some of the extractable cations originate from dissolution of other material in the clay; (b) the C.E.C. may be larger than the total of extractable cations, if clay has already lost some of the exchangeable cations prior to the extraction, e.g., during the weathering.

Chemical formulae for smectites are derived from the above analyses *only* for the samples in which no detectable (with X-rays) impurities are found in the -1 μm fractions.

Chemical formulae for minerals can be calculated from their chemical analyses under the assumption of fixed anionic charges, or that of fixed cationic numbers. These two methods are described in Section 3.8 with respect to the formulae calculations for dioctahedral smectites. For the reasons mentioned there the method of fixed cationic numbers has been adopted for the formulae calculations in this volume.

The total iron is given as Fe_2O_3, and iron is considered to be in ferric state and located in octahedra. These assumptions introduce a small error into the resulting formulae since the ferrous content of dioctahedral aluminum smectites is generally low, and a part of the ferric iron may be located in the tetrahedral positions in the structure. In fact, Osthaus (1955) showed a long time ago the presence of tetrahedral iron in smectites. The small amounts of Na, K, and Ca found in the NH_4^+-saturated samples are probably related to the impurity minerals such as micas and feldspars, rather than to the smectites. The samples with large iron contents (>5% Fe_2O_3) have been reanalyzed after removing the "free" iron using the treatment of Jackson (1956). Prior to this treatment, the sample was, however, boiled in 5% Na_2CO_3 for 5 min.

2.3. ELECTRON-OPTICAL METHODS

The morphological features, modes of aggregations, and crystal structure of smectites are vitally related to the rheological behavior and other properties of these clays. Various applications of this material in industry, technology, and science are directly related to the above characteristics of smectites. Electron optics provide rather powerful methods to study the basic properties of the smectite particles. The smectites in bentonites have been, therefore, studied extensively using electron optics. The electron-optical data on the samples consist of transmission images and selected area electron diffraction (SAD) patterns. The properties of the SAD patterns can reveal the type of texture present in a polycrystalline aggregate even when the individual crystallites and their mutual arrangement are not discernable in the transmission electron images. Smectite aggregates generally possess a sheet texture because of the approximately parallel orientation of the (001) planes of smectite crystallites. The SAD pattern of such aggregates, with the electron beam parallel to the [001] direction, are expected to display only *hk* rings with uniform intensities along them. Any additional preferred orientation between the crystallites may cause a nonuniform distribution of intensity along each *hk* ring. Finally if a certain *hk* direction becomes common to each crystallite in addition to the common (001) planes, the aggregate will become identical to a single crystal and will give a spot SAD pattern. With respect to its origin, a texture may be formed mechanically during the aggregation or packing of crystallites, especially when they possess a pre-

dominant habit (columnar, lamellar, fibrous, etc.). The origin of a texture may also be related to the growth process, and therefore, be an intrinsic property of the aggregate. Regardless of its origin, the presence of a certain texture may have a bearing on the physical properties of the crystalline aggregate. A JEM-7 electron microscope operated at 80 kV, and a Hitachi electron microscope operated at 75 kV were used to obtain electron-optical data. The electron microscope grids were prepared from very dilute suspensions of the 0.2—2 μm and —0.2 μm fractions of the natural samples in a 0.007*N* solution of tertiary butylamine. Similarly, grids were prepared from the suspensions of the Na-saturated samples, after they had been subjected to a special dispersion treatment. This procedure (Jackson, 1956) consists of boiling the sample first with 5% Na_2CO_3 and subsequently with sodium-citrate-dithionite. The dispersion procedure may dissolve amorphous silica, alumina, and iron oxides which might cement the smectite layers. After such treatment one can find even 10 Å thick lamellae. In the following presentation, the observations on the samples prior to the dispersion treatment are described. Whenever different or additional observations are made on the same sample after the dispersion treatment, they are also noted. The electron microscope grids were shadowed with carbon-platinum (Bradley, 1959) for the purpose of thickness determinations and by gold for the purpose of providing an internal standard for the SAD data. The thickness of the particles have been measured by the shadow lengths with a precision of ±5 Å, and they are given as rounded to tens of Ångstrøms. Various shadowing angles were used, ranging from 14 to 27 degrees.

Different habits of smectite single crystallites are depicted in Fig. 2.1 with their predominant forms. Real fibers (or whiskers) of dioctahedral aluminium smectites have not been observed, but the laths of these minerals do occur. Güven and Pease (1975) classified the smectite crystallites in the

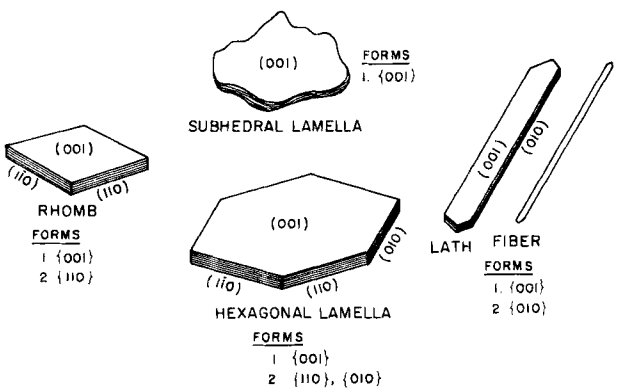

Fig. 2.1. Common habits of smectite single crystallites. The predominant forms for each habit are indicated.

montmorillonite—beidellite series into three groups according to their morphological features. Such a classification should correlate better with the physical and rheological properties of this material:

(1) Lath-shaped or L-type particles: these are genuine laths or laths formed by folding of thin lamellae.

(2) Euhedral lamellae or E-type particles: these are lamellae with polygonal outlines displaying the presence of well-developed {*hk*0} forms in addition to the prominent basal {001} forms. These euhedral lamellae are often in form of hexagonal platelets, or in diamond shaped units (rhombs).

(3) Subhedral lamellae or S- and H-type particles: these particles occur as lamellae with irregular outlines, i.e. no {*hk*0} forms, but with well-developed basal forms. Those with a thickness below 60—70 Å are designated as S-type particles. Thicker ones (H-type particles) resemble a single crystal, but their SAD patterns indicate no three-dimensional periodicity.

Morphological features of smectite aggregates also show a wide range of variations. Distinctions between smectite aggregates can be made on the basis of the habit of individual crystallites and on their arrangements in the aggregate. One or several of the following types of smectite aggregates are rather frequently observed for a given sample:

(1) *Globular aggregates (Otay-type).* These consist of randomly arranged tiny globules. The Otay smectite aggregates, described later in Chapter 3 (Figs. 3.8A and 3.8B), represent this type.

(2) *Mossy aggregates (Cheto-type).* In these aggregates individual crystallites resemble flexible fibrous units that seem to form by the curling of extremely thin layers or ribbons, and the aggregate has a mossy appearance. Typical examples are found in the Cheto samples (Fig. 3.7).

(3) *Lamellar aggregates.* Distinct smectite lamellae are discernible as components of these aggregates. Depending on the characteristics of these lamellae (large folded sheets vs. smaller S-type platelets) and their packing (loose vs. compact), one may distinguish the following types:

(a) *Foliated aggregates.* These consist of individual lamellae which are folded and crumbled sheets and which are loosely packed together. These flexible thin layers often branch and curl, and give a foliated appearance to the aggregates. Curling and folding of these thin and flexible lamellae may partially be caused by the drying process during sample preparation.

(b) *Compact lamellar aggregates.* Individual subhedral lamellae (S-type) form a compact aggregate. If such a compact aggregate resembles a single crystal, it is classified as H-type smectite particle.

Typical examples of foliated and compact lamellar aggregates are found in Wyoming samples as shown in Fig. 3.4.

(c) *Reticulated aggregates (Santa Rita-type).* These consist of euhedral (hexagonal or diamond-shaped) platelets and they form a more or less net-like (reticular) arrangement. Typical examples are shown in the Santa Rita sample described in Chapter 3 (Fig. 3.12).

The reader is advised to familiarize himself with the above morphological terms. They will be used in the description of smectite particles (single crystallites or aggregates) throughout this volume.

REFERENCES

Abbey, S., 1970. Analysis of rocks and minerals by atomic absorption spectroscopy. 3. A lithium fluoboric scheme for seven major elements. Geol. Surv. Can., Pap., 70: 23.

Abbey, S., 1973. Studies in standard samples: of silicate rocks and minerals; Part 3. Geol. Surv. Can., Pap., 73: 36.

Bernas, B., 1968. A new method for decomposition and comprehensive analysis of silicates by atomic absorption spectrometry. Anal. Chem., 40: 1682—1686.

Bradley, D.E., 1959. High resolution shadow-casting technique using simultaneous evaporation of platinum and carbon. Br. J. Appl. Phys., 10: 198—203.

Fairbairn, H.W., 1953. Precision and accuracy of chemical analysis of silicate rocks. Geochim. Cosmochim. Acta, 4: 143—156.

Greene-Kelly, R., 1953. The identification of montmorillonoids in clay. J. Soil Sci., 4: 233—237.

Güven, N. and Pease, R.W., 1975. Electron-optical investigations on montmorillonites, II. Clays Clay Miner., 23: 182—191.

Hendricks, S.B., Nelson, R.A. and Alexander, L.T. 1940. Hydration mechanism of the clay mineral montmorillonite saturated with various cations. J. Am. Chem. Soc., 62: 1457—1464.

Jackson, M.L., 1956. Chemical Analysis — Advanced Course. Published by the author, Madison, Wisc., pp. 57—62.

Langmyhr, F.J. and Paus, P.E., 1968. The analysis of inorganic siliceous materials by atomic absorption spectrophotometry and the hydrofluoric acid decomposition technique. Anal. Chim. Acta, 43: 397—408.

Lee, R.W. and Güven, N., 1975. Chemical interferences in atomic absorption spectrometric analyses of silicates in the fluoboric-boric acids matrix. Chem. Geol., 16: 53—58.

Osthaus, B.B., 1955. Kinetic studies on montmorillonites and nontronite by the acid-dissolution technique. Clays Clay Miner., 4: 301—321.

Ross, C.S. and Hendricks, S.B., 1945. Minerals of the montmorillonite group. U.S. Geol. Surv., Prof. Pap., 205-B: 23—79.

Van Loon, J.C. and Parissis, C.M., 1969. Scheme of silicate analysis based on the lithium metaborate fusion followed by atomic absorption spectrometry. Analyst (London), 94: 1057—1062.

Chapter 3

GEOLOGICAL FEATURES AND MINERALOGICAL STUDIES OF MAJOR BENTONITE OCCURRENCES

In this chapter geological features of the major bentonites occurrences will be described. Detailed mineralogical data will be given for some of these bentonites. The occurrences of the bentonites are listed in a geographical framework. First (in Sections 3.1 and 3.2), bentonites from the American (north, central, and south) continents are discussed beginning with the deposits in the U.S.A. The bentonite occurrences in Africa are described in Section 3.3. The European (excluding U.S.S.R.) and Eastern Mediterranean bentonite occurrences are discussed together in Section 3.4. The bentonites from Asia and Australia, along with descriptions of U.S.S.R. deposits, are given in Section 3.5. In Section 3.6 the origin of bentonite deposits is discussed while in Section 3.7 morphological features of smectites are interpreted in terms of present crystal growth theories. In the final section a summary of the geological and mineralogical data is given for the major bentonite occurrences in the world.

3.1. BENTONITES IN THE UNITED STATES OF AMERICA

Bentonites are widely distributed in the United States, especially in formations of Upper Cretaceous and Tertiary ages and they are extensively produced commercially in about a half dozen areas.

The principal producing area is in the Black Hills region of South Dakota, Wyoming, and Montana, in the general area where bentonite was first described, named, and found to be valuable for many industrial uses. Bentonites are also well known and commercially developed in several Gulf Coast states, principally in Texas and Mississippi. There are many deposits of bentonite in the Rocky Mountain states, where the best known deposits are in the Cheto district of Arizona, and in the Amargosa Valley of Nevada. Bentonites are also known in several areas in California, and in Alaska. Clays thought to be bentonites are reported in several other states, including Illinois, Georgia and Delaware.

Black Hills region

Geological features. Many beds of bentonite occur in a section of about 4000 ft. of mostly marine shales, marls, and argillaceous sandstones of Lower and Upper Cretaceous ages in the Black Hills area. A single section may contain as many as twenty separate beds of bentonite (Fig. 3.1). In the area as a whole, the bentonite beds vary in thickness from a fraction of an inch to 10 ft. or more. In some instances, the thicker beds appear to be composites of several layers, i.e. they represent a sequence of ash falls (see p. 19) rather than a single one. Many of the beds are lenticular but some can be traced continuously for many miles. The structure of the area is a broad northwest plunging anticline with some subordinate folds. The bottom of the bentonite horizons is usually sharply defined from subjacent material which is commonly a shale and which is locally silicified to a chert-like layer up to a foot in thickness (Fig. 3.2). The thickness of the silicified zone tends

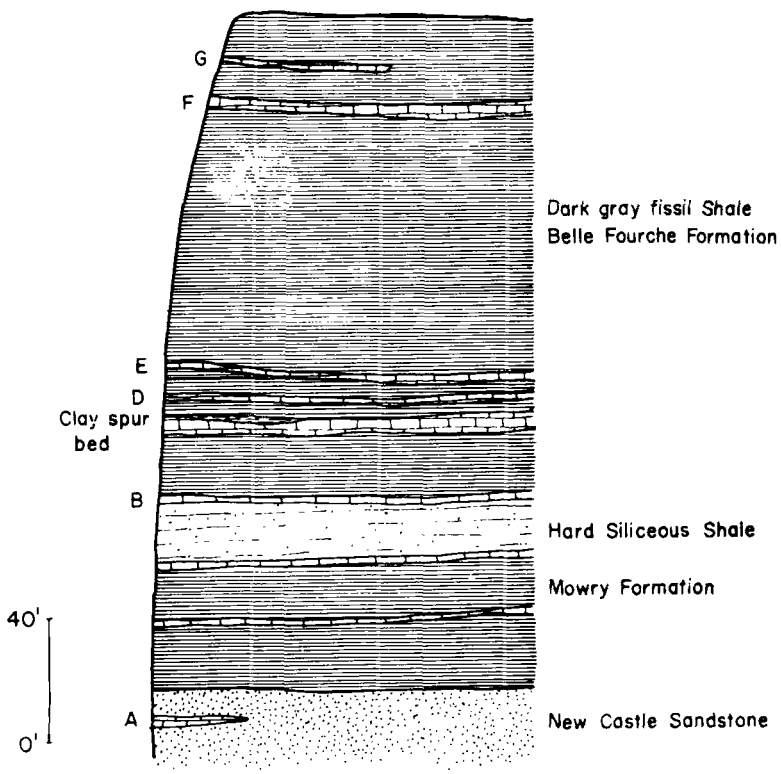

Fig. 3.1. Section of New Castle, Mowry, and Belle Fourche formations showing bentonite horizons (after Patterson, 1955).

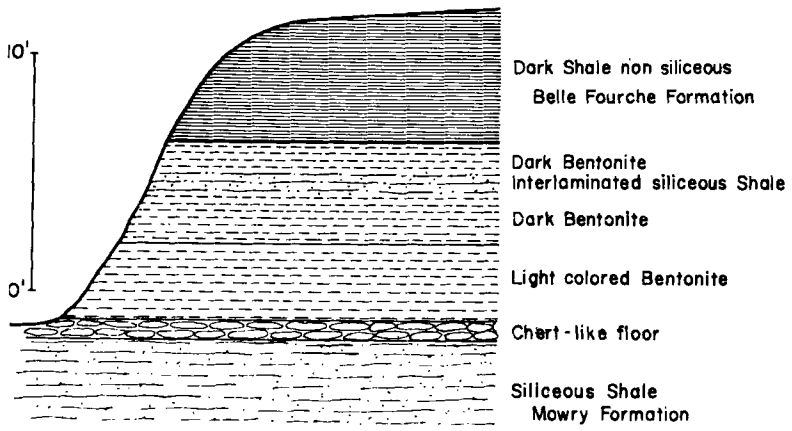

Fig. 3.2. Section of Clay Spur Bentonite (after Patterson, 1955).

to increase as the thickness of the bentonite bed increases, and in general is not present beneath thin bentonite horizons. The silicification requires the addition of only a few percent of silica. The top of the bentonite horizons is less definite and grades through gradual transitions or interlaying to the overlying formation.

The bentonite at the outcrop is generally light yellow or green and becomes bluish away from the outcrop. Knechtel and Patterson (1962) have pointed out that the change in color is due to the oxidation of ferrous iron, and that the accompanying increase in colloidal properties is not the result of this oxidation of iron, but rather is due to the leaching replacement of some exchangeable sodium by calcium. The quality of bentonite in a given bed commonly also varies vertically, with the central part having the highest colloidal properties. The lowermost few inches is frequently somewhat sandy. The uppermost part of a bed is likely to be brownish in color and is frequently discarded. Limestone concretions up to 15 ft. in diameter are associated with some of the bentonite horizons, and veins of gypsum frequently cut across the bentonite. Concretions of siderite, frequently manganiferous, are also found in some beds. The bentonite has a waxy character, and at the outcrop weathers to a flakey or granular form. The outcrop bloom frequently has a popcorn-like appearance resulting from the expansion and contraction caused by successive wetting and drying. Weathering in general tends to enhance the colloidal properties of the bentonite. Interesting features of some bentonite horizons are masses of concentric layers of blue bentonite. These so-called "blue eggs" may be a foot or more in diameter. They have the same composition as the remainder of the bentonite. Their origin is obscure.

It is generally agreed that the bentonite in this area has formed by the in-

TABLE 3.1A

Location, geological and mineralogical data on bentonites from U.S.A.

Sample no.	Location and formation	Geologic age	Smectite's spacings (Å)		MgO * (%)	Extractable cations (mequiv./100 g)					C.E.C. (mequiv./100 g)
			(001)	(06,33)		Mg	Ca	K	Na	total	
	Wyoming										
1	Weston County, Belle Fourche	U. Cretaceous	12.9	1.497	2.77	16	6	2	85	109	120
2	Natrona County, Frontier	U. Cretaceous	12.6	1.496	2.91	5	22	2	66	95	
3	Natrona County, Mowry	L. Cretaceous	12.4	1.496	2.12	10	95	3	94	202	96
4	Natrona County, Steele	U. Cretaceous	12.3	1.497	3.66	14	12	2	67	95	
5	Crook County, Belle Fourche, Clay Spur bed	U. Cretaceous	11.8	1.496	2.55	17	25	1	106	149	119
6	Crook County, Belle Fourche	U. Cretaceous	12.4	1.497	2.68	5	22	2	70	99	105
7	Crook County, Belle Fourche, "blue egg"	U. Cretaceous	11.6	1.497	2.35	14	12	2	67	95	
8	Crook County, Mowry	L. Cretaceous	14.2	1.498	2.11	20	50	3	27	100	104
	Arizona										
9	Apache County, Bidahochi, "Cheto"	Pliocene	14.5	1.500	5.83	7	50	2	59	118	104
10	Apache County, Bidahochi, "Cheto"	Pliocene	14.3	1.498	4.96	22	120	1	14	157	62
11	Apache County, Bidahochi, "Chambers"	Pliocene	15.5	1.497	5.44	25	92	1	4	122	126
	California										
12	San Diego County, "Otay"	Pliocene	14.7	1.500	6.35	75	18	2	36	131	
	Nevada										
13	Nye County, Amargosa, "Dry Lake"	Pleistocene	15.3	1.515	19.6						
14	Nye County, Amargosa, "Dry Lake"	Pleistocene	14—15	1.515	17.2						
15	Nye County, Amargosa, "Dry Lake"	Pleistocene	14.3	1.516	16.7						

16	Nye County, Amargosa, "Dry Lake"	Pleistocene	14.5	1.515	15.3						
	New Mexico										
17	Santa Rita (API-11), New Mexico		14.8	1.497	5.37	29	66	1	20	116	
	Mississippi										
18	Smith County, Vicksburg, "Polkville"	Oligocene	15.2		n.d.						
	Texas										
19	Gonzales County, Jackson, "Helms"	Eocene	15.1		2.70						
20	Gonzales County, Jackson, "Helms"	Eocene	14.7		2.88	24	59	1	13	97	
21	Gonzales County, Jackson, "Helms"	Eocene	15.1	1.497	3.61	24	59	1	16	100	
22	Gonzales County, Jackson, "Helms"	Eocene	14.4	1.496	2.15	27	73	1	14	115	
23	Gonzales County, Jackson, "Syler shales"	Eocene	14.3	1.499	2.52	19	48	3	12	82	
24	Gonzales County, Jackson, "Clark Yenna"	Eocene	14.7		2.56	18	28	2	13	61	
25	Gonzales County, Jackson, "Hamon"	Eocene	14.7	1.497	1.40	9	20	2	8	39	73
	Georgia										
26	Jefferson County		14.3	1.500	3.41	27	72	1	24	124	
27	Jefferson County		14.7	1.490	0.55	5	11	1	2	19	29
28	Jefferson County		14.3	1.502	1.57	8	12	1	3	24	47
29	Jefferson County		15.2		1.05	9	14	1	3	27	46
	Alaska										
30	Northern Alaska, Colville group, "Umiat"	U. Cretaceous	12.4	1.497	2.92	7	7	2	94	110	

* On ignited material from —1 μm fraction of clay that was stripped off exchangeable cations.

TABLE 3.1B

Chemical analyses of bentonites from U.S.A. (on ignited material from —1 μm fractions of ammonium saturated clays except for the data from the literature)

Sample no.	SiO_2	Al_2O_3	Fe_2O_3	MgO	Li_2O	CaO	Na_2O	K_2O	Total	Impurities *
1	66.05	25.10	3.98	2.77	0.0	0.23	0.03	0.37	98.53	—
2	71.86	22.62	2.95	2.91	0.0	0.06	0.05	0.05	100.50	crist(20), Q(20)
3	68.20	23.17	4.91	2.12	0.0	0.02	0.05	0.11	98.58	Q(5)
4	70.33	20.32	4.65	3.66	0.0	0.0	0.0	0.0	98.96	Q(5)
5	68.25	25.05	4.40	2.55	0.0	0.01	0.07	0.02	100.35	Q(5)
6	69.11	24.80	4.00	2.68	0.0	0.03	0.08	0.04	100.74	Q(5)
7	67.36	26.03	3.66	2.35	0.0	0.02	0.01	0.06	99.49	crist(10)
8	78.68	15.70	2.42	2.11	0.0	0.03	0.05	0.11	99.10	crist(30), Q(10)
9	69.61	21.94	2.36	4.97	0.0	0.04	0.06	0.04	99.02	—
10	68.50	22.19	3.52	4.96	0.0	0.02	0.07	0.0	99.26	—
11	70.51	22.30	1.84	5.44	0.0	0.02	0.02	0.06	100.19	—
12	68.96	20.90	2.38	6.35	0.0	0.03	0.04	0.22	98.88	—
13	52.20	6.60	2.40	19.60	0.16	1.40	1.40	0.0	83.76	see text
14	50.50	6.10	2.20	17.20	0.30	1.50	2.00	0.0	79.80	see text
15	50.90	7.40	2.30	16.70	0.25	2.80	1.10	0.0	81.45	see text
16	47.20	9.40	2.50	15.30	0.17	1.00	0.63	0.0	76.20	see text
17	71.21	20.73	1.44	5.37	0.0	0.22	0.05	0.19	99.21	crist(10)
18	65.00	22.80	3.07	3.90	0.0	0.05	0.17	0.13	95.12	—
19	71.35	20.41	5.16	2.70	0.0	0.02	0.02	0.67	100.33	crist(10)
20	79.60	17.35	0.31	2.88	0.0	0.03	0.02	0.03	100.22	crist(30)
21	79.83	15.58	0.80	3.61	0.0	0.03	0.03	0.02	99.90	crist(40)
22	68.57	24.67	3.26	2.15	0.0	0.03	0.05	0.05	98.78	Q(5)
23	67.72	22.37	5.84	2.52	0.0	0.04	0.0	0.0	98.49	Q(5)
24	75.41	18.54	2.57	2.56	0.0	0.02	0.05	0.47	99.62	crist(20)
25	66.97	27.43	3.99	1.40	0.0	0.02	0.06	1.08	100.95	crist(20) kaol(10)
26	78.54	17.36	1.09	3.41	0.0	0.02	0.03	0.01	100.46	crist(10)
27	79.96	17.04	1.48	0.55	0.0	0.05	0.03	0.42	99.53	crist(40) kaol(10)
28	80.97	12.49	3.22	1.57	0.0	0.74	0.01	0.45	99.45	crist(50)
29	80.42	8.02	9.66	1.05	0.0	0.03	0.02	0.27	99.47	crist(50)
30	67.98	23.93	4.07	2.92	0.0	0.02	0.03	0.17	99.12	—

* Impurities are semiquantitatively estimated from the X-ray diffraction data. (crist = cristobalite; kaol = kaolinite; Q = quartz.) Data for sample 18 are from Grim and Kulbicki (1961) that was obtained on the —2 μm fraction of H-clay. Samples 13—16 were analyzed by Terrasearch, Inc., Denver, Colorado without any pretreatment.

situ alteration of volcanic ash. The parent ash is believed to have been rhyolitic in composition and to have come from a western source. It is of interest that the magnesium content of the smectite is higher than that of the probable parent ash. Fragments of unaltered ash, grains of feldspar, quartz, and biotite commonly make up less than 10% of the bentonite. Cristobalite is present in some horizons in amounts up to about 25%. The cristobalite is not restricted to particular horizons and is not always present in a given bed. The smectite in the producing horizon commonly makes up about 90% of the material.

Of the many bentonite beds in the area about seven are sufficiently thick, continuous, and rich enough in smectite to be of commercial interest. The best known producing horizon is the so-called "Clay Spur" bed in the top part of the Mowry shale at about the top of the Lower Cretaceous (Fig. 3.2). This bed, which ranges in thickness from $2\frac{1}{2}$ to 4 ft., has produced most of the sodium bentonite with the extremely high colloidal properties for which the district is famous. In some other beds, the component smectite carries calcium as the dominant adsorbed cation. Knechtel and Patterson (1962) have pointed out that there is no general correlation between the presence of sodium versus calcium and the associated beds, i.e. marine versus non-marine. The nature of the exchangeable cation must be derived from the composition of the ash.

A distinctive feature of the sodium Wyoming bentonite is that the smectite disperses in water into relatively large and extremely thin flakes. As a consequence of this feature, the bentonite has important colloidal, plastic, and bonding properties.

Mineralogical studies. Detailed mineralogical studies have been carried out on bentonites samples 1—8 from Wyoming listed in Table 3.1A. The X-ray diffraction data on the basal spacings and the data on the extractable cations in this table indicate that all the above Wyoming samples contain a predominantly Na-montmorillonite except sample 8, which contains calcium as its main interlayer cation. Their magnesia contents suggest that all of these samples are close to the boundary line in the montmorillonite—beidellite series. Because of the impurities even in -1 μm fraction, a structural formula has been calculated only for sample 1 from the chemical data in Table 3.1B:

$$[(Si_{3.86}Al_{0.14})(Al_{1.58}Fe^{3+}_{0.17}Mg_{0.24})O_{10}(OH)_2]M^{+}_{0.38}$$

Micas, feldspars, quartz, and minor amounts of kaolinite are the other components in the samples. In addition, samples 2, 7, and 8 contain about 10—20% cristobalite. Zeolite (clinoptilolite) is also found in small amounts in samples from Natrona. Two of the Natrona samples (2 and 4) contain about 5—10% calcite. Electron-optical observations on the Wyoming samples show that the morphological features of the smectite particles in samples 1, 5, 6,

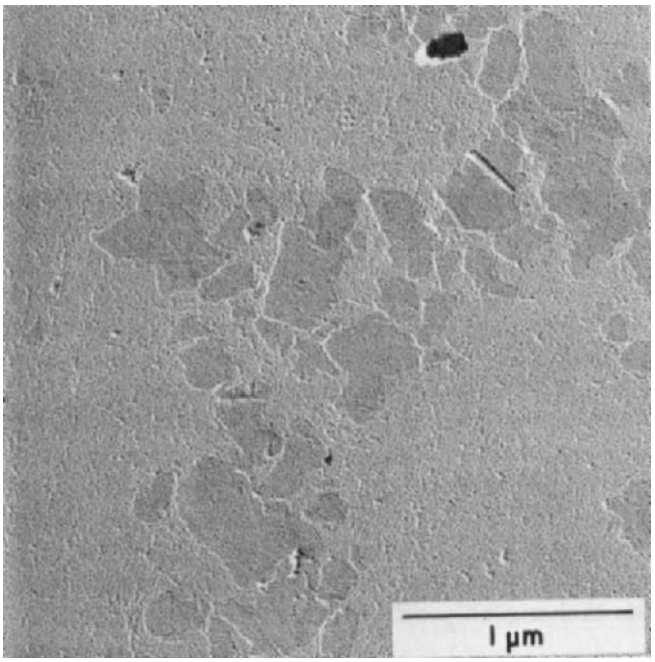

Fig. 3.3. The S-type lamellae of Wyoming montmorillonite, Weston County (sample 1).

in three samples from Natrona county (2, 3 and 4), and in "blue eggs" (sample 7) are very similar. Smectites in these samples occur mainly as lamellar aggregates and as single crystallites. The crystallites are in the form of S- and H-type lamellae; the S-type lamellae are shown in Fig. 3.3. Typical aggregates in Wyoming montmorillonites are shown in Figs. 3.4 and 3.5. In these aggregates thin but large smectite sheets are irregularly folded and branched, which gives the aggregate a foliated appearance. The foliation of the aggregate is shown and designated by the letter *F* in Fig. 3.4A. A more intensely foliated aggregate is displayed in Fig. 3.5 from sample 2. In these foliated aggregates the existence of individual thin smectite sheets is discernible, although they are folded and loosely packed. Some of the lamellar aggregates are, however, compact, and they consist of flat, (unfolded) compactly packed particles. Such a compact aggregate is designated by the letter *C* in Fig. 3.4A. The rheological properties of the samples 5 and 6 are reported to be different, sample 5 being a "high-yield" and sample 6 a "low-yield" bentonite. However, no significant difference between the morphological features of smectites is noted in either sample, except that sample 5 with "low-yield" seems to contain a larger number of H-type, thicker lamellae. In sample 8, mossy aggregates also occur in addition to the foliated aggregates,

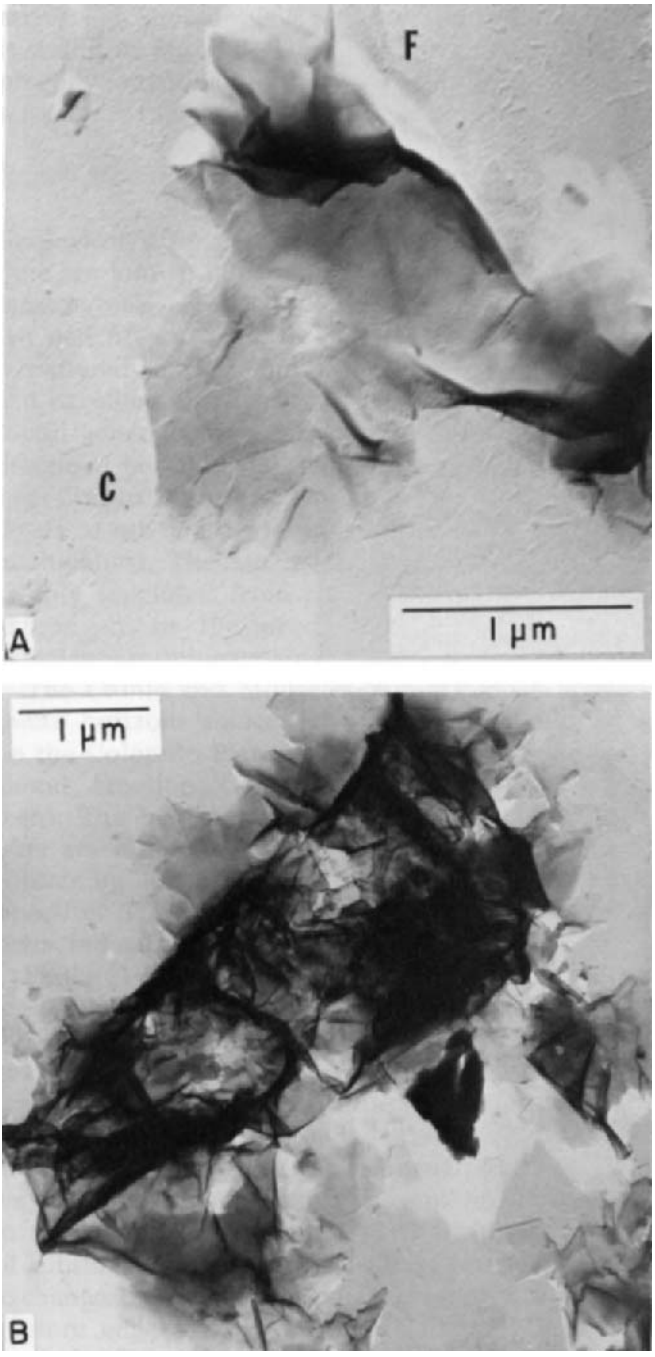

Fig. 3.4. Typical foliated aggregates consisting of irregularly folded layers in Wyoming montmorillonites. A. Weston County. B. Thixogel sample from Natrona. (Explanation of *C* and *F* in text.)

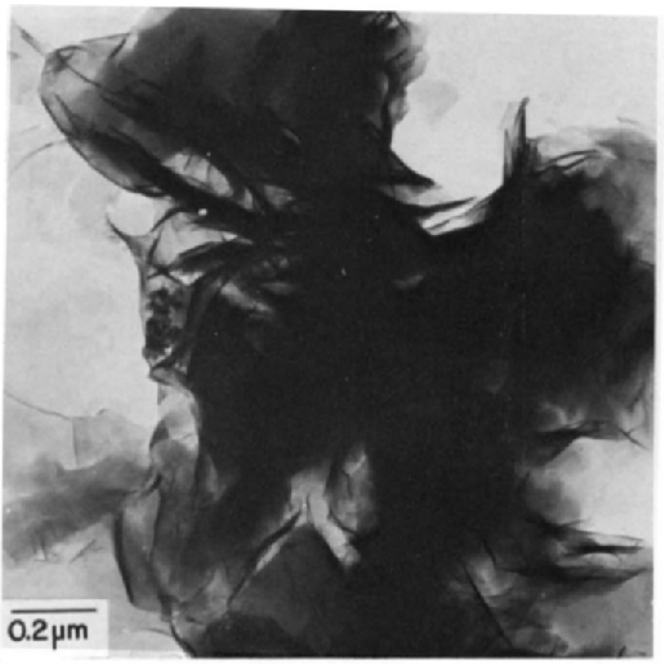

Fig. 3.5. Typical foliated aggregates in sample 2 from Wyoming.

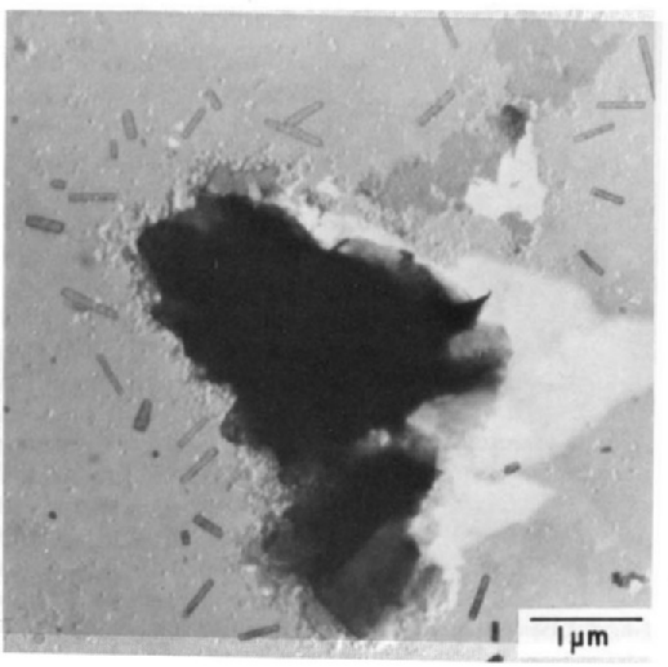

Fig. 3.6. Irregular aggregates (Cheto-type) in Na-saturated sample 8 from Wyoming.

even when the sample is saturated by sodium. One of these mossy aggregates is shown in Fig. 3.6. The tiny, lath-shaped crystallites in the same figure are probably cristobalite that was identified by X-ray diffraction in the bulk sample.

Rocky Mountain and California areas

Geological features. Bentonite deposits ranging in age from Triassic to Pleistocene are known in many of the Rocky Mountain states. The best known and most extensively developed deposit is at Cheto, Arizona, where a thick ±20 ft.) bed of ash of latitic composition in the Pliocene Bidahochi Formation has altered to a calcium smectite. The alteration of the ash is not complete, and excellent shard fragments can be found in the white bentonite which is found generally in a series of beds of sand. Sloan and Gilbert (1966) have described in detail the sequence of the alteration of the volcanic glass to the smectite. In this area there are interesting occurrences of many interbedded layers of ash and bentonite with the individual layers only a matter of inches in thickness. The ash layers show substantially no alteration, and they are sharply separated from the bentonite layers. The Cheto bentonite is used extensively in the production of acid activated decolorizing clay and petroleum refining catalysts.

The Chinle and Morrison formations of Triassic age contain several bentonite horizons associated with a wide variety of sediments at many places on the Colorado Plateau. Such bentonites are well known in the vicinity of Grand Junction, Colorado, but there has been little commercial development. The bentonites are the calcium variety, and in some cases are quite pure smectite. Allen (1930) described bentonites in the Chinle formation containing associated clay pellets, indicating rapid alteration of the ash to smectite. These bentonites also contain fragments of silicified wood and bone, indicating migration of silica.

Papke (1969) has described many occurrences of bentonite in Nevada varying in age from Miocene to Pliocene. Many of these deposits are altered ash, but some of them are due either to hydrothermal action or the reaction of ground water with glassy rhyolitic volcanic rocks. Papke (1969) states that the saponite variety of smectite is the dominant component of these clays in the Ash Meadows area of the Amargosa Valley of Nevada. In the so-called Eastern Dry Lake area of the Amargosa Valley beds of pure sepiolite and clays composed of a mixture of sepiolite and saponite are present. Elsewhere in the Amargosa area (notably in Ewing and Kinney) bentonites composed of substantially pure montmorillonite carrying sodium and/or calcium as the exchangeable cation occur in beds 2—8 ft. thick in a sand section. Along the western edge of the Amargosa Valley a vertical vein-like mass of carbonate containing up to 20% hectorite is to be found.

An interesting occurrence of a smectite clay is found near Hector, Califor-

nia, where lithium and flourine bearing hot waters rising along a fault zone have reacted mainly with travertine to produce the magnesium trioctahedral smectite called hectorite (Ames et al., 1958).

Berg (1969) has reported bentonite from many localities in Montana.

Many deposits of bentonite are found in the Tertiary formations of California. At Otay, in the extreme southern part of the state, several beds of calcium bentonite were mined several years ago for use in petroleum refining. The bentonites were white and occurred in a sand section. Of the many other occurrences of bentonite in California, one found at Tehachapi is particularly interesting because of the presence of clinoptilolite as an important component with the smectite. This bentonite is overlain and underlain directly by unaltered tuff. Kerr (1931) has described other zeolitic bentonites from the Rincon and Modela formations of Miocene age from Ventura, California.

Mineralogical studies. The analytical data in Table 3.1 suggest that the three samples (9, 10 and 11) from the Cheto district (Arizona) contain a predominantly Ca-montmorillonite. The extractable cations consist largely of calcium except in sample 9, which contains about equal amounts of sodium and calcium as the predominant interlayer cations. All three samples are distinguished by having high magnesia, in the range of 5—6%. The chemical formulae of these smectites, as calculated from the data in Table 3.1B are:

Sample 9: $[(Si_{3.93}Al_{0.07})(Al_{1.40}Fe^{3+}_{0.10}Mg_{0.50})O_{10}(OH)_2]M^{+}_{0.57}$

Sample 10: $[(Si_{3.93}Al_{0.07})(Al_{1.42}Fe^{3+}_{0.15}Mg_{0.42})O_{10}(OH)_2]M^{+}_{0.49}$

Sample 11: $[(Si_{3.98}Al_{0.02})(Al_{1.46}Fe^{3+}_{0.08}Mg_{0.46})O_{10}(OH)_2]M^{+}_{0.48}$

Micas, kaolinite, quartz, and feldspars are the common impurities in these bentonites.

Electron-optical observations indicate similar morphological features for the smectite particles in all three samples. The common aggregates consist of fiber-like units that are formed by extensive curling of thin layers. Such an aggregate is shown in Fig. 3.7 obtained from sample 10. The aggregate resembles a piece of a moss, and it is soft and flexible. The term "mossy aggregates" is, therefore, adopted to designate this type of smectite aggregate. Another less common form of smectite particles consists of compact lamellar aggregates. These aggregates consist of S-type, flat (unfolded) lamellae compactly packed on top of each other. The single smectite crystallites in these samples occur mainly in the form of S- and H-type lamellae. A few euhedral lamellae are also observed.

The Otay sample contains a montmorillonite with very high magnesia content (6.35%). As indicated in Table 3.1A, magnesium is also the predominant

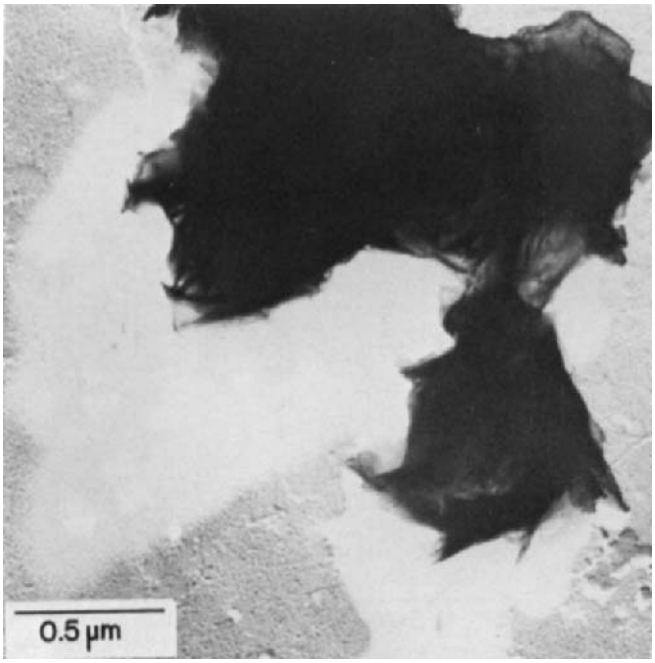

Fig. 3.7. Typical irregular aggregates with "mossy appearance" of Cheto montmorillonite.

cation in the interlayer region of this mineral. The chemical formula of the Otay montmorillonite is calculated from data in Table 3.1B as:

$$[(Si_{3.95}Al_{0.05})(Al_{1.36}Fe^{3+}_{0.10}Mg_{0.54})O_{10}(OH)_2]M^{+}_{0.59}$$

Electron-optical examination shows that montmorillonite particles occur mainly as aggregates. The individual crystallites in these aggregates are discernible in the form of globular grains (Fig. 3.8A), especially after the dispersion treatment of the sample (Fig. 3.8B). As shown in this figure, the larger diameters of these globules range from 150 to 250 Å. The term "globular" aggregates is proposed for these aggregates. The SAD patterns of these aggregates display only spotty *hk*-rings indicating random orientation of the units. Micas, cristobalite and feldspars are the common impurities in the Otay bentonites.

Bentonites listed in Table 3.1A from Amargosa Valley, Nevada, contain magnesian (trioctahedral) smectites. Some of the other bentonites in the same area contain sepiolite in addition to the above smectites, and still others are composed of montmorillonite. The mineral composition of the four samples in Table 3.1A from the Eastern Dry Lake region of the Amargosa Valley are similar. Samples 13, 14 and 15 contain about 70% smectite,

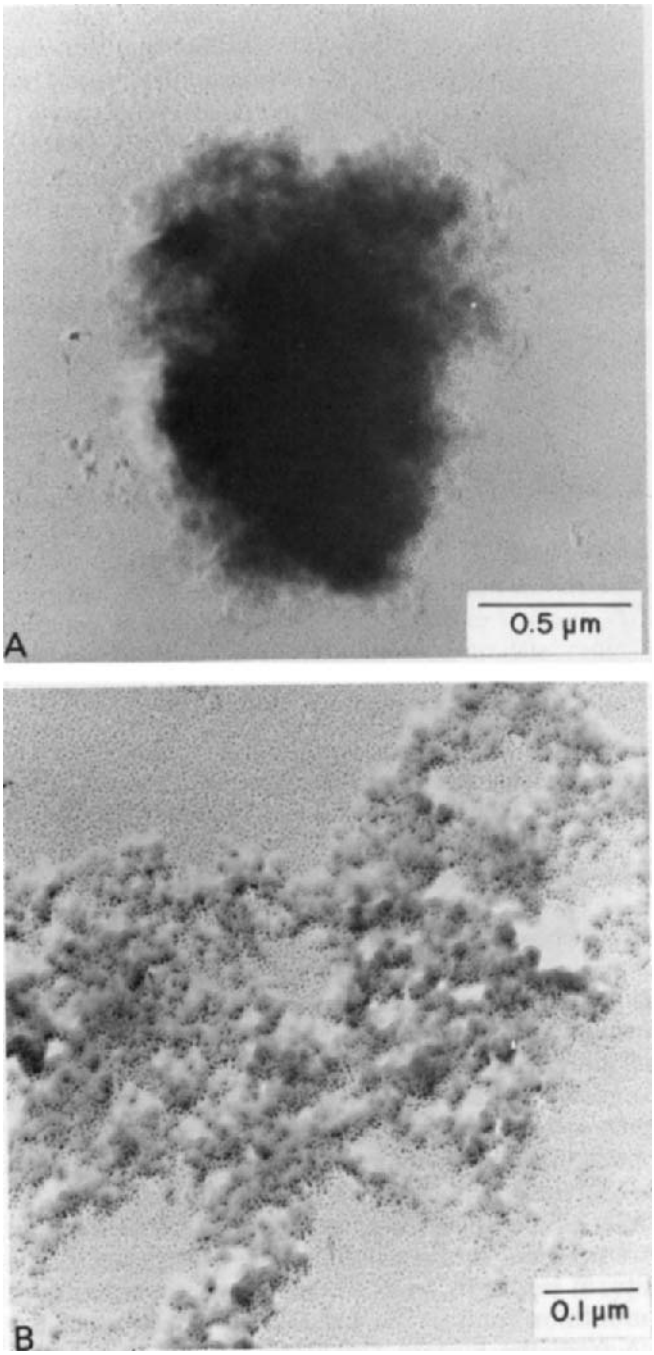

Fig. 3.8. A. Typical globular montmorillonite aggregate in the Otay sample. B. Montmorillonite aggregates after the dispersion treatment in the Otay sample, displaying globular grains.

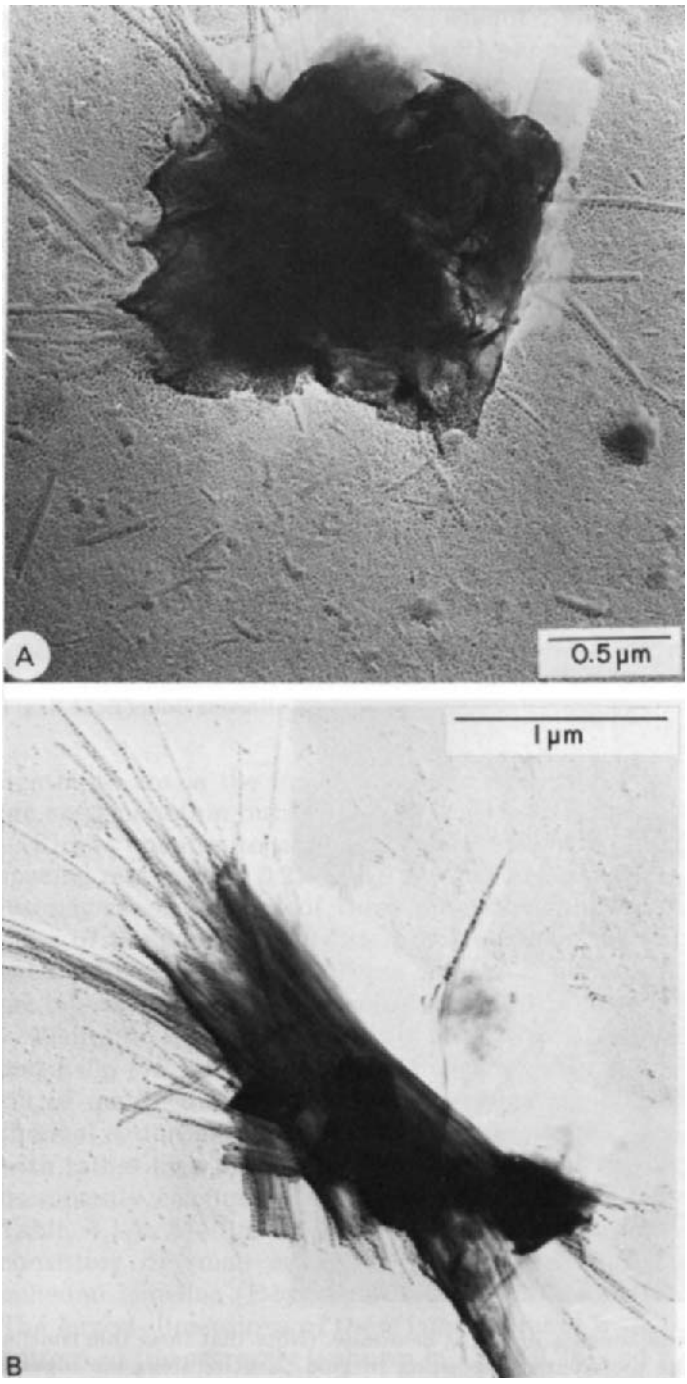

Fig. 3.9. A. Aggregates of fibrous units and thin curled layers of smectites. (Sample 13 in Eastern Dry Lake Area, Amargosa Valley, Nevada.) B. Aggregates of smectite fibers. Note also the carbonate rhombs in the sample. (Sample 16, Eastern Dry Lakes, Amargosa Valley, Nevada).

20% mica, and 10% carbonate (dolomite and calcite). Relative to the other samples, the mica content of sample 16 seems to be higher (about 30—40%) and the smectite content correspondingly smaller. The basal spacings of these smectites range between 14.2 and 15.3 Å.

Electron-optical observations show similar morphological features for the smectites in the samples from the Eastern Dry Lake area of the Amargosa Valley. Mossy (Cheto-type) aggregates form the common smectite particles. These mossy aggregates are often associated with fibrous units which seem to grow from them (Fig. 3.9A). In addition, genuine individual fibers and sheaf-like aggregates of them (Fig. 3.9B) make up about 30% of the smectites in the samples. As seen in the last figure, rhombs of carbonates are often found in these fibrous aggregates.

In Ewing bentonite Na-montmorillonite makes up about 80—90% of the rock. The basal spacing of these smectites in various samples from the Ewing deposit ranges from 12.3 to 12.7 Å. Individual smectite lamellae and Wyoming-type smectite aggregates occur in about equal quantities in these samples. The crystallinity of the individual lamellae seem to be higher than those found in Wyoming bentonites. Typical euhedral lamellae in Ewing

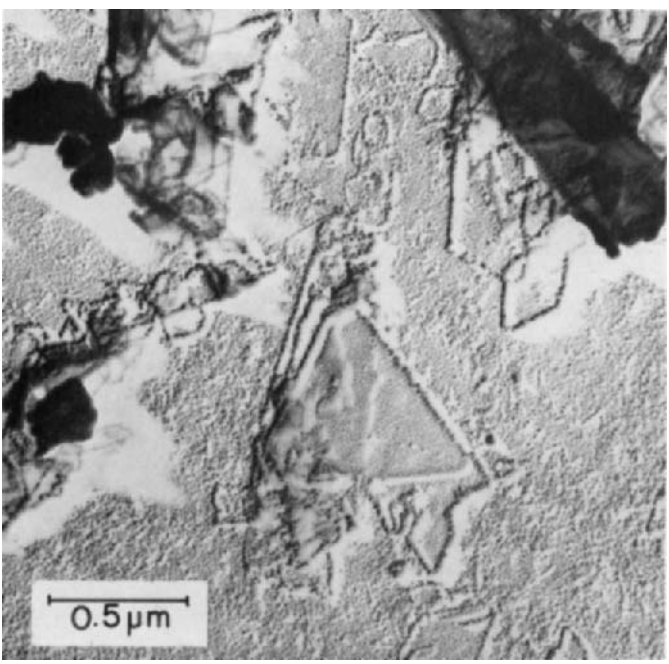

Fig. 3.10. Euhedral smectite lamellae in Ewing bentonite. (Note that these thin lamellae are clearly outlined by the preferential deposition of gold particles along the edges of these lamellae.)

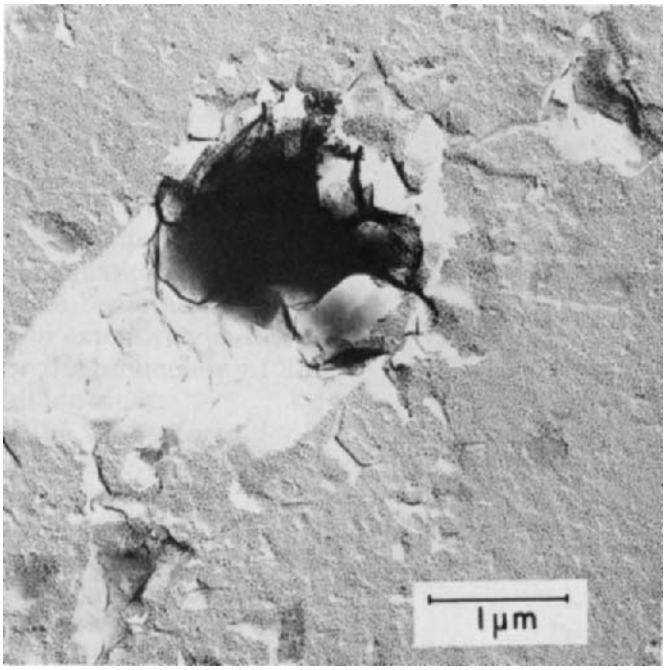

Fig. 3.11. Typical smectite aggregates in Kinney bentonite.

bentonite are in the form of rhombs as shown in Fig. 3.10. These lamellae are extremely thin but their lateral dimensions are on the average 0.5 μm.

Kinney bentonite contains about 90% a montmorillonite whose basal spacing ranges from 12.6 to 15.2 Å in various samples. This suggests that the interlayers occupancy of these montmorillonite is not uniform in various parts of the deposit. Smectite particles occur typically in the form of aggregates shown in Fig. 3.11. These aggregates have morphological features that are intermediate between Cheto-type and Wyoming-type aggregates.

Bentonite occurrence in Santa Rita, New Mexico, was described by Kerr and Kulp (1949). According to them, the clay is an alteration product of a sill of quartz diorite or of the underlying granodiorite porphyry by hydrothermal action along a fault zone. This bentonite contains a montmorillonite with rather high magnesium content (5.37%). The interlayer cations are predominantly calcium with appreciable amount of magnesium as indicated in Table 3.1A. Montmorillonite particles occur predominantly as aggregates consisting of small euhedral crystallites. In some instances, rather large euhedral lamellae (E-type particles) are developed as shown in Fig. 3.12A. The largest dimensions of these lamellae range from 0.1 to 0.2 μm. The SAD pattern of the aggregate is shown in Fig. 3.12B, and it displays a spot pattern like that of a single crystal, indicating that the individual crystallites estab-

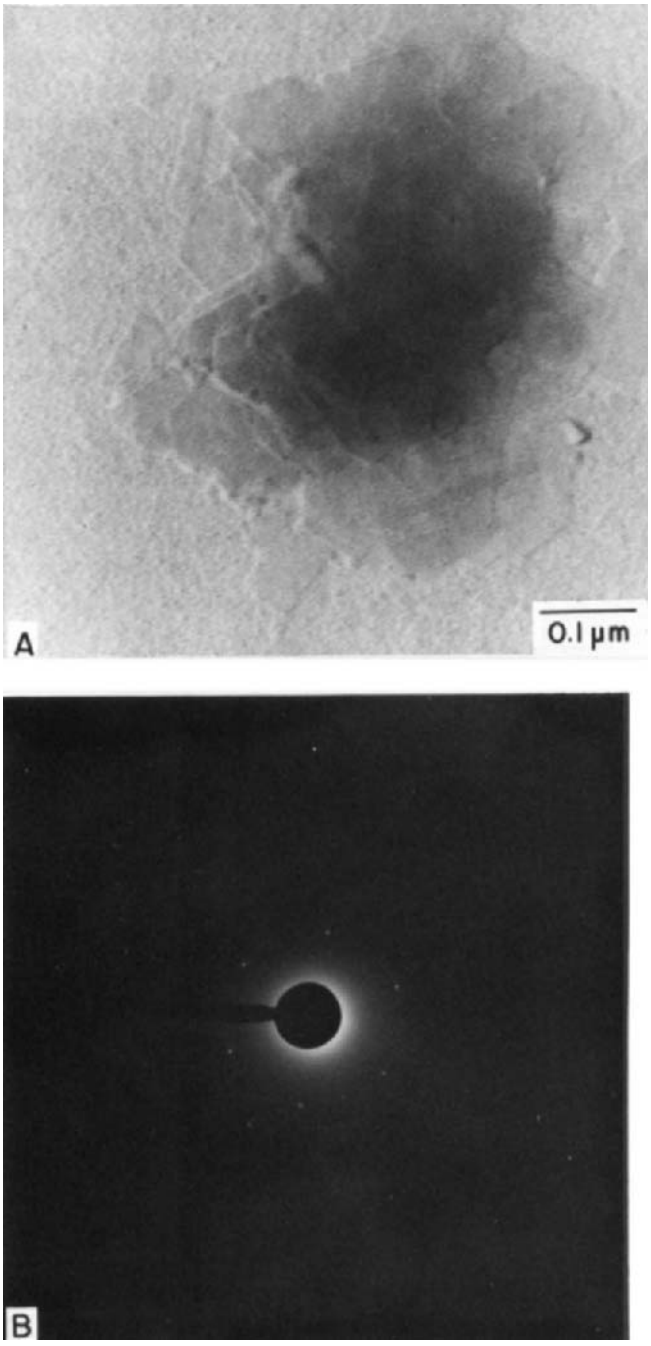

Fig. 3.12. A. Perfectly reticulated aggregate of E-type lamellae of Santa Rita montmorillonite observed after the dispersion treatment. B. Its SAD pattern displaying only 02, 11, and $\bar{1}1$ spots.

lished an almost perfect crystallographic orientation with respect to each other. Such aggregates are therefore called "reticulated" or "net-like" aggregates.

Micas, quartz and feldspars are the common impurities in the sample.

Gulf Coast area

Bentonite is widely distributed in the Coastal Plains of the Gulf of Mexico in formations ranging in age from Upper Cretaceous to Middle Tertiary. These bentonites are best known in Mississippi and Texas where they have been extensively developed, particularly for bonding foundry molding sands, for the production of decolorizing agents, and to a lesser extent for oil well drilling muds.

The Eutaw formation of Upper Cretaceous age in northeastern Mississippi contains several beds of bentonite, some reaching a thickness of 14 ft. The bentonites are best known in Itawamba and Monroe counties where there is substantial commercial production. The material is waxy and blue in color when fresh, and yellow when weathered. The overlying material is a friable sand, and the underlying material varies from argillaceous, micaceous sand to glauconitic sand. In general, both the upper and lower contacts are gradational. Bentonite of a similar character was formerly produced in Pontotoc County in northern Mississippi from the Ripley formation of Uppermost Cretaceous age. The Ripley formation in Alabama contains bentonite at Sandy Ridge.

Substantial quantities of bentonite have been produced from the Tertiary Vicksburg formation in Wayne and Smith counties in central Mississippi. Several beds of bentonite are known in these counties, ranging up to about 4 ft. in thickness. The beds are overlain and underlain by shales but occur in a generally calcareous section. Some of these bentonites are almost pure smectite and are white in color, while other beds are gray to yellow. The smectite of all the Mississippi bentonites carry calcium as the adsorbed cation. There is no silicification of underlying beds.

Reynolds (1940) has described interesting claystones in formations of Eocene age in Alabama believed to have formed from rhyolitic ash. These claystones in the Clayton and Nanafalia formations are composed of montmorillonite, cristobalite, and heulandite, while those in the Lower Tallahatta claystones are composed only of clinoptilolite. Upper Tallahatta claystones are composed only of cristobalite in western Alabama, and of both cristobalite and montmorillonite in eastern Alabama.

In Texas, bentonites are found in a wide belt paralleling the coast and marking the outcrop of Cretaceous and Tertiary sediments. They are known in the Upper Cretaceous, but are best developed in the Tertiary Jackson and Gueydan formations in Gonzales and Lafayette counties where there is extensive commercial production. In general, all deposits show several beds

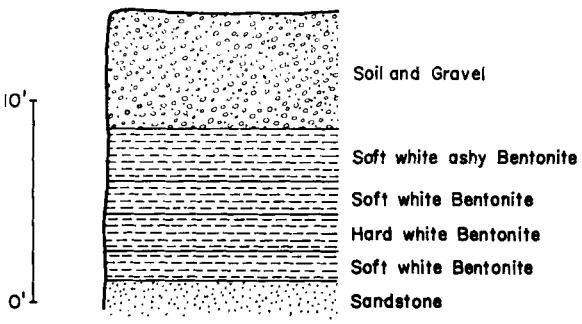

Fig. 3.13. Generalized section of bentonite occurrence in Gonzales County, Texas.

of bentonite interbedded with soft sands and shales, Fig. 3.13.

Calcium smectite is the clay mineral component of the Texas bentonites, in some cases mixed with kaolinite, especially, according to Hagner (1939), in deposits in the northeastern part of the outcrop area. According to Roberson (1964), the composition of the smectite varies considerably in the Texas bentonites. Also, some bentonites contain appreciable amounts of unaltered ash and/or cristobalite, and they are present in amounts up to about 25% in horizons in some areas. The relative abundance of the ash increases as the formations are traced to the southwest grading into ash beds in Mexico. The bentonite varies in color from white to yellow. There is no silicification of the underlying beds.

Bentonites are reported in Arkansas by Branner (1929) in formations of Tertiary Wilcox age in Saline, Hot Springs, and Ouachita counties. Ross (1925) has reported bentonites in the Upper Cretaceous formations of southwest Arkansas. Bentonites are also known in the Tertiary formations of Louisiana. Some of the bentonites in Louisiana are nontronitic in character.

Mineralogical studies on Mississippi bentonites. The Itawamba county sample contains a Ca/Mg montmorillonite according to the X-ray and chemical data in Table 3.1A. Quartz, feldspars, and micas form the nonclay components in the sample. The Polkville sample was previously studied by Grim and Kulbicki (1961). They reported a basal spacing of 14.7 Å for the montmorillonite (in H-saturated state) and a MgO content of 3.90% for the $-2\ \mu$m fraction of the H-clay. The sample (in H-state) has been examined with electron optics. It was found that the montmorillonite particles occur in thick and compact aggregates almost opaque to the electrons. In addition, there is an appreciable number of globular (Otay-type) aggregates. Some of these globular particles are as large as 400—500 Å in diameter (Fig. 3.14). Upon using the dispersion treatment, H- and S-type lamellae are frequently found in the fine fraction ($-2\ \mu$m) of the sample.

Micas and quartz are the common impurities in the sample.

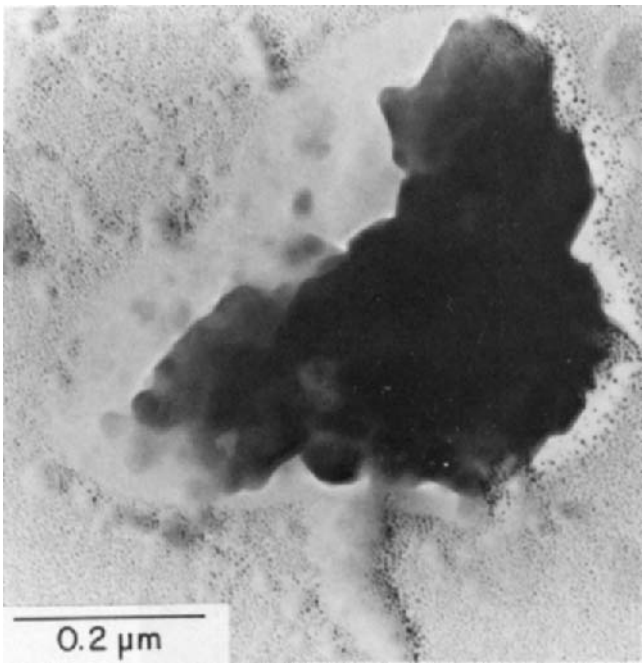

Fig. 3.14. Montmorillonite aggregates consisting of oval-shaped grains in the Polkville Mississippi bentonite.

Mineralogical studies on Texas bentonites. The samples studied are listed in Table 3.1A along with the analytical data for them. The chemical composition of the samples is given in Table 3.1B. The data indicate that the basal spacings of the montmorillonites in these bentonites range from 14.3 to 15.1 Å. Furthermore, calcium is the predominant interlayer cation, but magnesium and sodium are also present among the extractable cations. Quartz, feldspars, mica and kaolinite are the other components in the samples. Cristobalite, mixed with tridymite, occurs in large amounts in samples 19, 20, 21, 24 and 25.

Montmorillonite particles in Helms sample 19 are, for the most part, in the form of (Cheto-type) mossy aggregates, but H- and S-type lamellae are occasionally observed. Tridymite and montmorillonite are often intergrown in aggregates with a sieve-like texture as shown in Fig. 3.15A. The presence of the montmorillonite is not discernible in the latter figure, but the SAD pattern (Fig. 3.15B) of the aggregate distinctly shows two rings at 4.45 Å (for montmorillonite) and at 4.12 Å (for tridymite). Kaolinites usually occur in particles consisting of a number of euhedral crystallites (Fig. 3.16). The SAD pattern of the entire aggregate is distinguished by distinct spots like those from a single crystal, indicating that the individual crystallites have

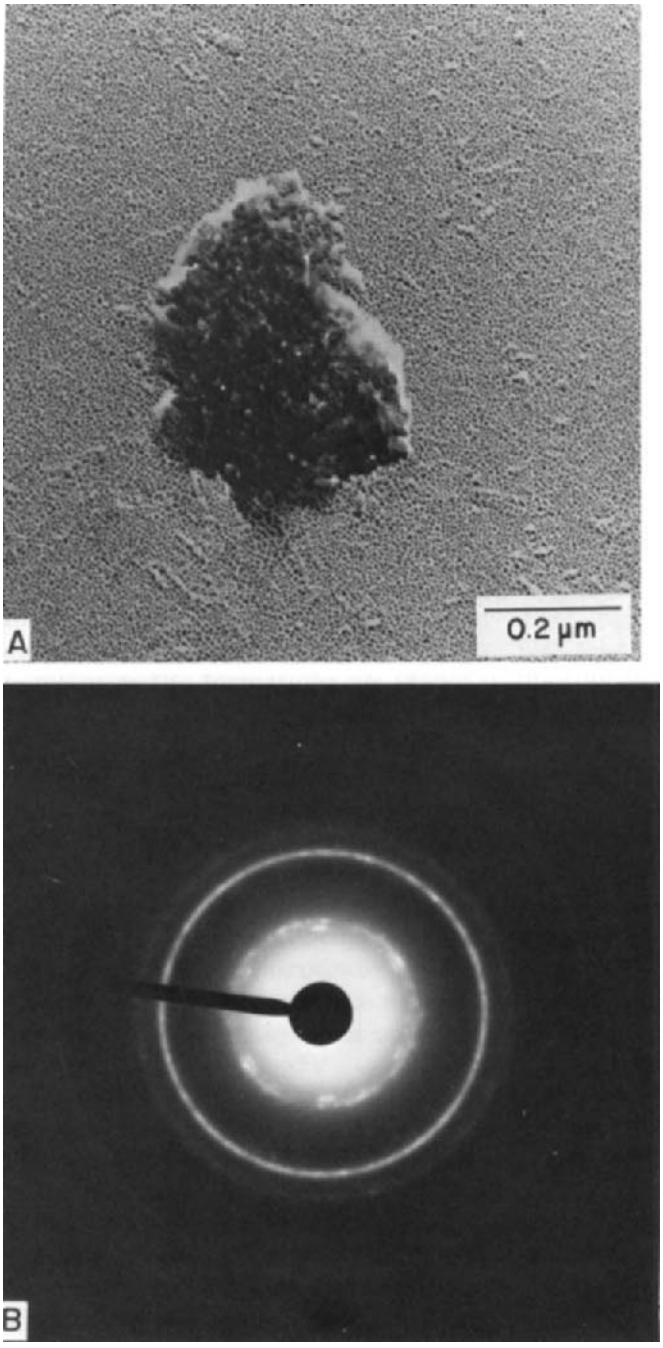

Fig. 3.15. A. Intergrowth of tridymite and montmorillonite. B. Its SAD pattern displaying a double ring corresponding to 4.45 Å (montmorillonite) and 4.12 Å to tridymite. (Sample 19, Gonzales, Texas.)

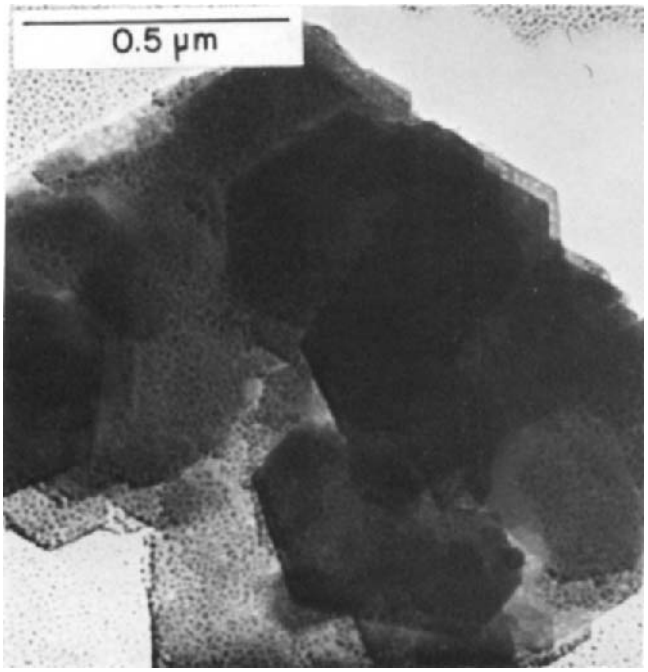

Fig. 3.16. Kaolinite in bentonite (sample 19) from Gonzales, Texas.

strict crystallographic orientations and are reticulated with respect to each other. Similarly, micas, in the form of regular and irregular arrangements of laths, make up about 20% of the sample.

In the Helms bentonite (sample 20) the smectite particles occur mainly in two types of aggregates, in Cheto-type and foliated ones. The S-type crystallites make up about 10% of the smectite particles. Kaolinites occur in the form of intergrown multiple crystallites and mica is found in aggregates of laths similar to those described in the previous sample.

Typical montmorillonite aggregates, shown in Fig. 3.17, make up about 80% of the smectites in the other Helms bentonite (sample 21). In Fig. 3.17A, the aggregates consist partly of laths and rhombs and partly of curled layers. The individual crystallites, making up the aggregate in Fig. 3.17B, are not quite distinguishable. Its superimposed SAD pattern displays a strong preferred orientation of the crystallites in the [02], [1$\bar{1}$], and [11] directions. The S-type montmorillonite crystallites are rarely observed. Kaolinites occur again in this sample in the forms described above for the sample 19.

In the Helms bentonite (sample 22), Cheto-type aggregates of smectites occur along with the lath-shaped units as shown in Fig. 3.18. Individual laths have a *b*-dimension of 9.02 Å. These laths are probably micas. The above aggregates consisting of smectites and laths make up about 80% of the

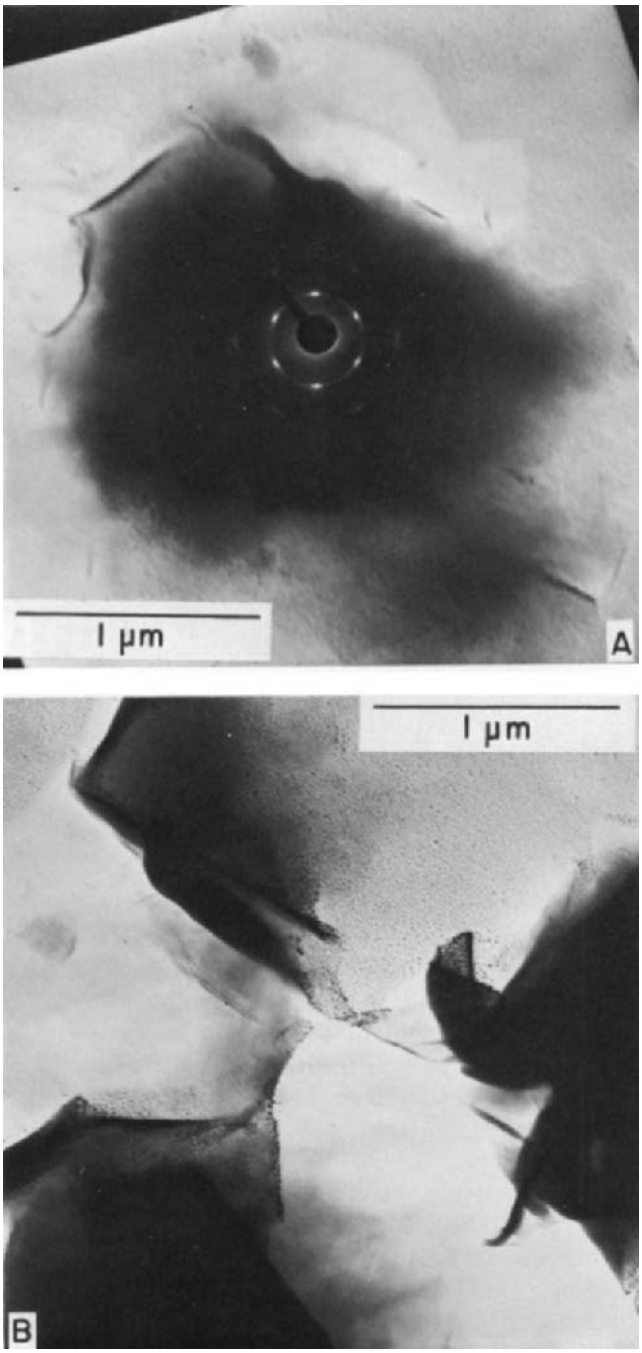

Fig. 3.17. Typical montmorillonite aggregates in the Helms bentonite, Texas (sample 21).

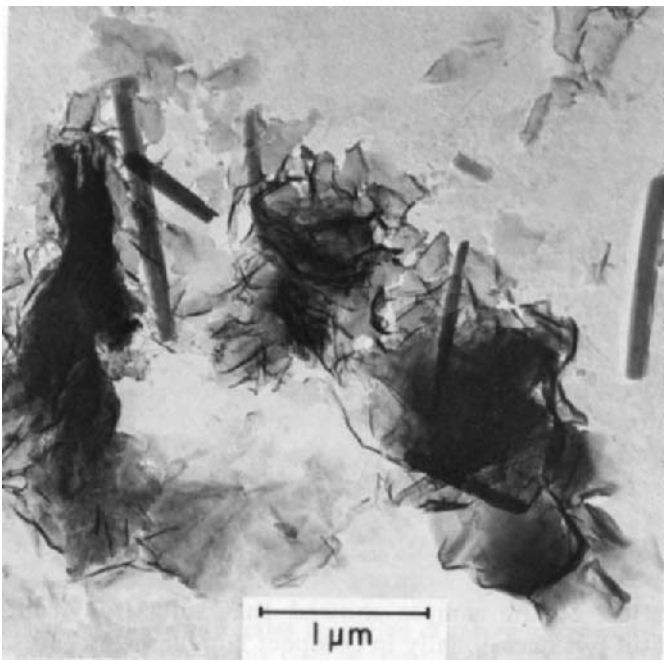

Fig. 3.18. Montmorillonite aggregates and lath-shaped units in the Helms bentonite (sample 22).

$-2\,\mu$m fraction of the sample. The remainder consist of E- and S-type lamellae of montmorillonite.

In the Syler top shale (sample 23), reticulated aggregates of smectites are made up of tiny rhombs and laths similar to those in the Santa Rita-type aggregates. Mica and kaolinites are common impurities in the sample.

In the Clark Yenna bentonite (sample 24), Cheto-type aggregates make up about 80% of the smectites in the sample. The S- and E-type lamellae of montmorillonite are occasionally observed.

In the Hamon clay (sample 25), smectites make up about half of the sample. The rest consists of micas, quartz, feldspar, kaolinite, and cristobalite. Smectites occur mostly in Cheto- and Santa-Rita-type aggregates.

Other areas

Clays thought to be bentonites have been reported elsewhere in the United States. The fuller's earth in the Eocene Porters Creek formation in Illinois and Missouri is so classified by Allen (1934). Jordan and Adams (1962) have reported a bentonite from Delaware also from an Eocene formation.

In the Wrens area of Georgia, a bed of clay ranging up to 30 ft. thick commonly designated as fuller's earth occurs in a section of sands of Lower Tertiary age. The Wrens area also contains sedimentary kaolins which are lower in the section and consequently older than the fuller's earth which is the clay extensively produced commercially because of its adsorbent properties.

Anderson and Reynolds (1966) report the presence of about 20 beds of bentonite in the Colville Group of Upper Cretaceous age in northern Alaska. Most of the beds are only a few inches thick, but at Umiat the thickness is a foot or more. Some of the bentonites are interbedded with marine formations, others with coal and other non-marine horizons. Many of the bentonites are quite pure montmorillonite, but others contain clinoptilolite and cristobalite. The clinoptilolite is most common in the bentonites associated with the coal. There is no evidence of any reworking of the ash. The Umiat bentonite contains a predominantly sodium-bearing montmorillonite (Table 3.1A). The chemical formula of this smectite is calculated from the data in Table 3.1B:

$$[(Si_{3.84}Al_{0.16})(Al_{1.58}Fe^{3+}_{0.16}Mg_{0.25})O_{10}(OH)_2]M^{+}_{0.42}$$

Electron-optical examination of the sample showed that smectites occur mostly in foliated aggregates but occasionally in compact lamellar aggregates. There are also an appreciable number of S-type montmorillonite particles. The *b*-dimensions of these morphologically distinct particles, as obtained from the SAD patterns, are very close to each other (9.02 ± 0.02 Å).

Mineralogical studies on fuller's earth from the Wrens area of Georgia. The X-ray diffraction and chemical data in Table 3.1 indicate the presence of a predominantly calcium montmorillonite in these samples. Cristobalite, quartz, feldspars, micas, and kaolinite make up more than half of the sample; therefore, the amounts of extractable cations and C.E.C. (Table 3.1A) are rather low for these clays. The cristobalite content is about 50% in samples 27, 28, and 29, and about 10% in sample 26. The amounts of magnesia in the samples 27, 28, and 29 are exceedingly low even after the high cristobalite content is accounted for.

In sample 26 smectites occur mostly as compact lamellar aggregates. Cristobalite intergrown with montmorillonite forms aggregates with a sieve-like texture, and micas occur in lath-shaped units. In the "flint clay" (sample 27), aggregates of intergrown cristobalite and montmorillonite make up about 80% of the particles in the sample. The aggregates show a fine granular aggregate with a sieve-like texture similar to that given in Fig. 3.15A. Its SAD pattern gives distinct rings corresponding to 4.04 Å (cristobalite) and 4.45 Å (montmorillonite).

In the "white clay" (sample 28), the $-2\,\mu$m fraction of the sample consists of montmorillonite, cristobalite, and micas in about equal proportions.

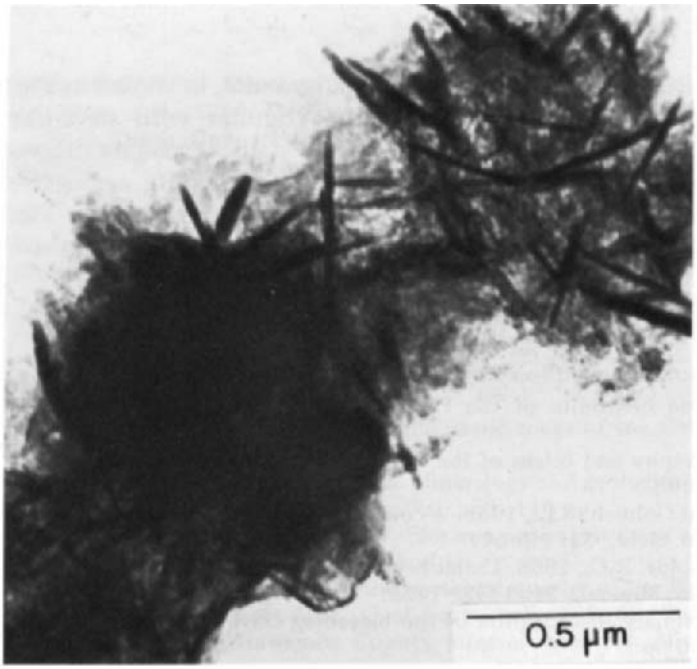

Fig. 3.19. Silica aggregates consisting of mixed-layered cristobalite and tridymite in the "white clay" from Wrens, Georgia (sample 28).

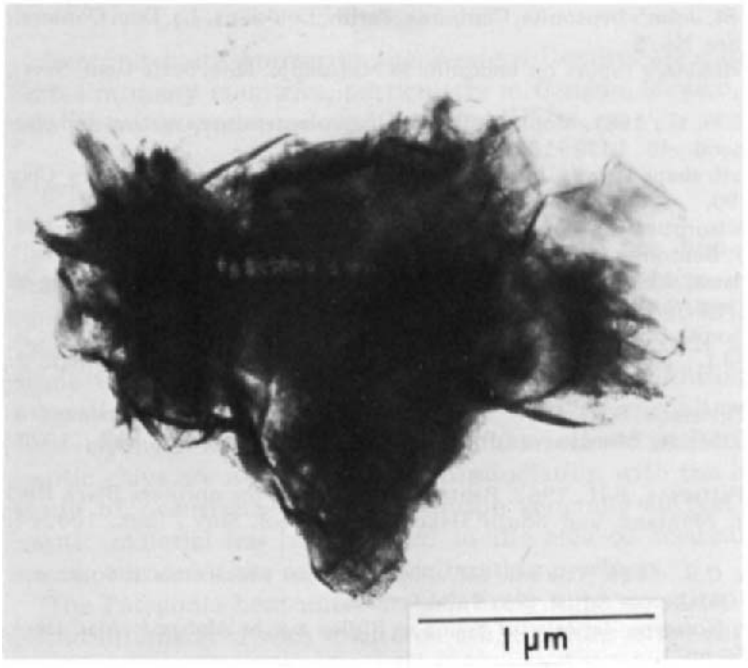

Fig. 3.20. Montmorillonite aggregates in the "white clay" from Wrens, Georgia (sample 28).

Some of the cristobalite aggregates consist of acicular units, as shown in Fig. 3.19, while other cristobalite aggregates are fine granular with sieve-like texture. The SAD patterns of these aggregates give a 4.11 Å spacing suggestive of a mixed layering of cristobalite and tridymite. Smectite aggregates (Fig. 3.20) are similar in appearance to the fibrous silica aggregates in Fig. 3.19. Micas exhibit regular (reticulated) arrangements of laths, and they are described by Güven (1974) elsewhere.

References

Allen, V.T., 1930. Triassic bentonite of the Painted Desert. Am. J. Sci., Ser. 5, 19: 283—288.

Allen, V.T., 1934. Petrography and origin of the fuller's earth of southeastern Missouri. Econ. Geol., 29: 590—598.

Ames, L.L., Sand, L.B. and Goldich, S.L., 1958. A contribution on the Hector, California, bentonite deposit. Econ. Geol., 53: 22—37.

Anderson, D.M. and Reynolds, R.C., 1966. Umiat bentonite. An unusual montmorillonite from Umiat, Alaska. Am. Mineral., 51: 1443—1456.

Bay, H.X., 1935. A preliminary investigation of the bleaching clays of Mississippi. Miss. Geol. Surv. Bull., 29: 60 pp.

Berg, R.G., 1969. Bentonite in Montana. Mont., Bur. Mines. Geol., Bull., 74: 34 pp.

Branner, J.C., 1929. Occurrence of bentonite in Southern Arkansas. Am. Inst. Min. Metall. Eng., Tech. Pub., 239: 11 pp.

Cleveland, G.B., 1960. Geology of the Otay bentonite deposit, San Diego County, California. Calif. Dep. Nat. Resour., Div. Mines, Spec. Rep., 64: 1—16.

Durham, C.O., 1962. St. John's bentonite, Clarborne, Parish, Louisiana. La. Dep. Conserv., Geol. Surv., Folio Ser. No. 2.

Grim, R.E., 1928. Preliminary report on bentonite in Mississippi. Miss. State Geol. Surv., Bull., 22: 14 pp.

Grim, R.E. and Kulbicki, G., 1961. Montmorillonite: high temperature reaction and classification. Am. Mineral., 46: 1329—1369.

Güven, N., 1974. Lath-shaped units in fine-grained micas and smectites. Clays Clay Miner., 22: 385—390.

Hagner, A.F., 1939. Adsorptive clays of the Texas Gulf Coast. Am. Mineral., 24: 67—108.

Heathman, J.H., 1939. Bentonite in Wyoming. Wy. Geol. Surv., Bull., 28: 22 pp.

Jordan, R.R. and Adams, J.K., 1962. Early Tertiary bentonite from the subsurface of central Delaware. Geol. Soc. Am. Bull., 73: 395—398.

Kerr, P.F., 1931. Bentonite from Ventura, California. Econ. Geol., 26: 153—168.

Kerr, P.F. and Kulp, J.L., 1949. Reference clay localities. Am. Pet. Inst., Proj. Rep., 2: 108 pp.

Knechtel, M.M. and Patterson, S.H., 1956. Bentonite deposits in marine Cretaceous formations, Hardin District, Montana and Wyoming. U.S., Geol. Surv., Bull., 1023: 115 pp.

Knechtel, M.M. and Patterson, S.H., 1962. Bentonite deposits of the northern Black Hills District, Wyoming, Montana, and South Dakota. U.S., Geol. Surv., Bull., 1082-M: 893—1029.

Miser, H.D. and Ross, C.S., 1925. Volcanic rocks in the Upper Cretaceous of Southwest Arkansas and S.E. Oklahoma. Am. J. Sci., 9: 113—126.

Monroe, W.H., 1941. Notes on deposits of Selma — Ripley age in Alabama. Ala., Geol. Surv., Bull., 48: 150 pp.

Papke, K.G., 1969. Montmorillonite deposits in Nevada. Clays Clay Miner., 17: 211—222.
Patterson, S.H., 1955. Geology of the Northern Black Hills Bentonite Mining District. Ph.D. Thesis, Univ. of Illinois, 37 pp.
Reynolds, R.C. and Anderson, D.M., 1967. Cristobalite and clinoptilolite in bentonite beds of the Colville Group of Northern Alaska. J. Sediment. Petrol., 27: 966—969.
Reynolds, W.R., 1940. Mineralogy and stratigraphy of Lower Tertiary clays and claystones of Alabama. J. Sediment. Petrol., 40: 829—838.
Roberson, H.E., 1964. Petrology of Tertiary bentonites of Texas. J. Sediment. Petrol., 43: 401—411.
Ross, C.S., 1925. Volcanic rocks in the Upper Cretaceous of Southeast Oklahoma and Southwest Arkansas. Am. J. Sci., 9: 113—126.
Ross, C.S. and Hendricks, S.B., 1945. Minerals of the montmorillonite group. U.S., Geol. Surv., Prof. Pap., 205-B; 77 pp.
Schultz, L.G., 1963. Clay minerals in Triassic rocks of the Colorado Plateau. U.S., Geol. Surv., Bull., 1147—C: 70 pp.
Slaughter, M. and Early, J.M., 1965. Mineralogy and geological significance of the Mowry Bentonites. Geol. Soc. Am., Spec. Pap., 83: 116 pp.
Sloan, R.L. and Gilbert, J.M., 1966. Electron-optical study of alteration in the Cheto clay deposit. Clays Clay Miner., 15: 35—44.
Torries, T.F., 1964. Geology of the northeast quarter of the West Point, Miss. quadrangle and related bentonites. Miss., Geol. Surv., Bull., 102: 62—98.
Vestal, F.E., 1947. Itawamba County mineral resources. Miss., Geol. Surv., Bull., 64: 150 pp.

3.2. BENTONITES IN THE WESTERN HEMISPHERE (EXCLUDING THOSE IN THE U.S.A.)

Bentonites are known in the Western Hemisphere outside of the United States in many countries, particularly in Canada, Mexico, Brazil, and Argentina where they are produced commercially.

Argentina

Geological features. In Argentina bentonites are best known from the Triassic formations in Mendoza and San Juan Provinces, and from the Paleocene and Eocene formations of Patagonia (Bordas, 1943). The bentonites of Triassic age are altered tuffs interbedded with sands and conglomerates. Some of the beds contain detrital material in addition to the smectite, suggesting transportation and redeposition of the altered tuff. These are some of the few occurrences that could be classed as detrital bentonite. Bentonitic clays are not uncommon in association with the bentonites, but the mode of occurrence and composition generally suggest that the non-bentonitic material has been carried to the area of accumulation rather than transportation of the ash and its alteration products.

The Patagonia bentonites are relatively pure smectite, and are frequently found interbedded with unaltered ash. Sections often show an interbedding of many thin (2—10 inches) bentonite and ash layers. The bottoms of the

ash layers tend to be sharply separated from the underlying bentonite, whereas the ash grades upward into bentonite. A feature of the deposits is the presence of many manganese nodules in both the bentonite and the ash. Fossils of land mammals are found in some horizons and of marine animals in other beds, indicating that the ash accumulated in a littoral environment varying from marine to non-marine. In such an interlamination sequence it is difficult to understand why some beds of ash were altered and others were not. Certainly the environment of accumulation was not a significant factor. Possibly the composition of the ash was most important; some ash being wetter than other ash with the wet ash favoring alteration. The bentonite grading downward to ash suggests that in some cases weathering has been a factor in the alteration. The bentonite-ash sequence is in a generally sandy section that is frequently capped by a basalt flow.

Mason and Sand (1960) have described a bed of zeolite (clinoptilolite) interbedded with bentonitic clays of Eocene age in Patagonia. According to these authors, the zeolite has formed by the alteration of volcanic ash probably of different composition from that yielding the bentonite. There is no evidence for a different environment for the zeolite as compared to the bentonite.

Mineralogical studies. X-ray diffraction and chemical data on the representative samples from Argentina in Table 3.2A indicate that a predominantly sodium bearing smectite is the major component in these bentonites. The basal spacings of samples 31 and 32 suggest that the extractable calcium in these samples probably originates from other minerals. The magnesia contents of samples 31, 32, and 34 are unusually low, and these smectites can be specified as beidellites. The smectite in sample 33, on the other hand, has a high magnesia content (6.12%), and represents a montmorillonite end-member. Its chemical composition is calculated as:

$$[(Si_{3.98}Al_{0.02})(Al_{1.54}Fe^{3+}_{0.09}Mg_{0.52})O_{10}(OH)_2]\,M^{+}_{0.55}$$

The chemical formulae of the other smectites are calculated from the data in Table 3.1B:

Sample 35: $[(Si_{3.98}Al_{0.02})(Al_{1.54}Fe^{3+}_{0.19}Mg_{0.27})O_{10}(OH)_2]M^{+}_{0.29}$

Sample 36: $[(Si_{3.91}Al_{0.09})(Al_{1.52}Fe^{3+}_{0.20}Mg_{0.28})O_{10}(OH)_2]M^{+}_{0.45}$

Sample 37: $[(Si_{3.96}Al_{0.04})(Al_{1.20}Fe^{3+}_{0.38}Mg_{0.41})O_{10}(OH)_2]M^{+}_{0.45}$

Quartz, micas, and kaolinite are the common impurities in the samples.

The coarser fraction (>10 μm) of the above bentonites contains large amounts of feldspars except for sample 32. In the latter sample, a zeolite

TABLE 3.2A

Location, geological and mineralogical data on bentonites from the Western Hemisphere (excluding U.S.A.)

Sample no.	Location and formation	Geologic age	Smectite's spacings (Å)		MgO * (%)	Extractable cations mequiv./100 g					C.E.C. (mequiv./100 g)
			(001)	(06,33)		Mg	Ca	K	Na	total	
	Argentina										
31	Mendoza, Potrelilos, San Gabriel mine	Triassic	12.0	1.497	1.37	5	64	2	61	132	105
32	Mendoza, Challae, La Florencia mine	Triassic	12.1	1.494	1.11	6	51	1	79	137	112
33	San Juan, Ramblon	Tertiary	12.4		6.12	22	9	4	137	172	119
34	Mendoza, Las Heras	Triassic	13.4		1.36	7	7	2	115	131	99
35	Rio Negro, Cineo Saltos	Tertiary	12.3		3.09	23	7	1	75	106	107
36	Neuguen, Cuenca del Anelo	Tertiary	13.0		3.24	18	1	4	120	143	113
37	Chubut, Las Chapas	Tertiary	12.2		4.73	16	4	1	75	96	126
	Brazil										
38	Minas Gerais, Ponta Alba	Tertiary	14.3	1.495	3.31	35	58	2	7	102	114
	Canada										
39	Manitoba, Vermillion River Formation	U. Cretaceous	14.4	1.498	3.68	22	228	2	5	257	97
40	Manitoba, Vermillion River Formation	U. Cretaceous	13.4	1.496	1.92	29	22	1	61	113	118
41	Manitoba, Vermillion River Formation	U. Cretaceous	14.9	1.497	4.63						
	Jamaica										
42	Montego Bay, South of Cacoon, Montpelier Formation	Oligocene	14.8	1.500	6.14	11	304	1	6	322	47
	Mexico										
43	Tatatilla, Vera Cruz		15.1	1.493							

* On ignited material from —1 μm fraction of clay stripped off exchangeable cations.

TABLE 3.2B

Chemical analyses of bentonites from Western Hemisphere outside U.S.A. (on ignited material from —1 μm fractions of ammonium saturated clays except for the data from the literature)

Sample no.	SiO_2	Al_2O_3	Fe_2O_3	MgO	Li_2O	CaO	Na_2O	K_2O	Total	Impurities *
31	66.87	23.96	6.42	1.37	0.0	0.0	0.26	0.19	99.07	Q(5)
32	66.84	27.25	3.48	1.11	0.0	0.02	0.32	1.24	100.26	Q(5)
33	69.69	21.13	2.08	6.12	0.0	0.02	0.07	0.11	99.22	—
34	69.81	22.12	3.89	1.36	0.0	0.03	0.63	0.61	98.45	Q(10)
35	68.83	22.86	4.41	3.09	0.0	0.24	0.49	0.16	100.08	—
36	67.20	23.38	4.62	3.24	0.0	0.01	0.29	0.36	99.10	—
37	67.37	17.91	8.67	4.73	0.0	0.16	0.36	0.10	99.30	—
38	63.09	27.58	3.75	3.31	0.0	0.01	0.06	1.13	98.93	mica(5)
39	62.88	20.57	10.04	3.68	0.0	0.36	0.38	0.72	98.63	Q(20), mica(20)
40	71.71	23.37	1.86	2.39	0.0	0.12	0.06	0.08	99.59	—
41	68.60	23.21	2.44	4.63	0.0	0.02	0.12	0.21	99.33	—
42	64.90	19.92	8.16	6.14	0.0	0.12	0.01	0.01	99.26	—
43 **	52.09	17.68	0.06	3.54	0.0	3.28	0.0	0.0	76.65	—

* Impurities are semiquantitatively estimated from the X-ray diffraction data. (crist = cristobalite; kaol = kaolinite; Q = quartz.)
** Data for sample 43 is from Ross and Hendricks (1945) on bulk sample without any pretreatment.

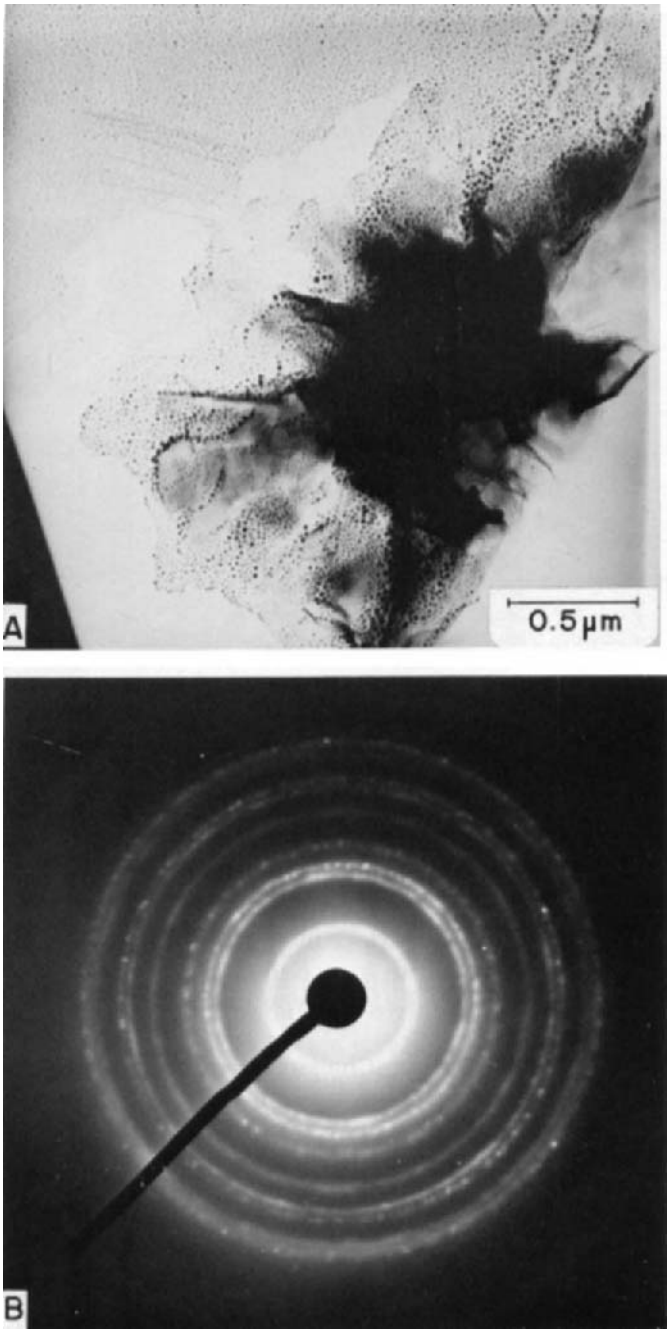

Fig. 3.21. A. Typical montmorillonite aggregate in the bentonite from San Gabriel Mine, Mendoza (Argentina). B. Its SAD pattern.

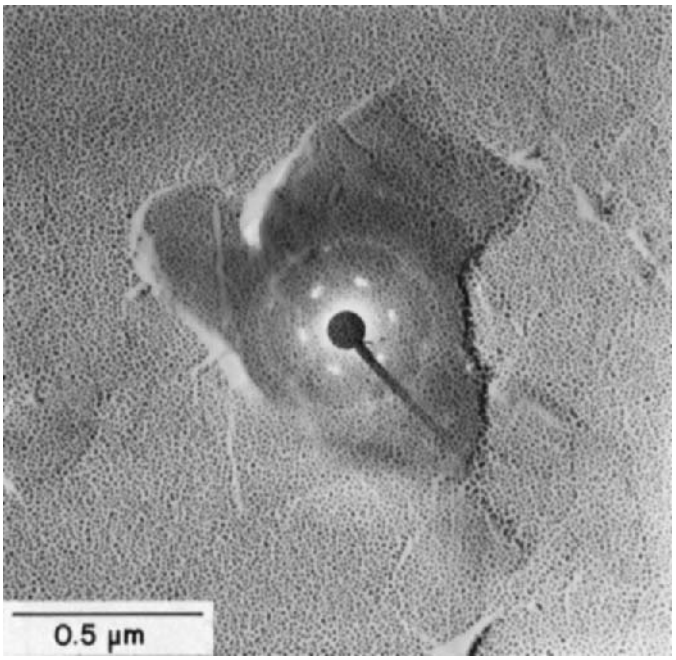

Fig. 3.22. Thicker smectite lamellae in sample 32 with its superimposed SAD pattern. (The uniform ring belongs to the gold-coating material.)

occurs, instead of the feldspar, as the major component in the coarser fraction. The zeolite is characterized as analcite by its prominent X-ray reflections corresponding to 5.60, 4.85, 3.42, 2.92, 2.68, 2.50, 1.90, and 1.74 Å.

Smectite particles occur for the most part as mossy (Cheto-type) aggregates and as S-type lamellae in the bentonite from San Gabriel Mine (sample 31). A typical aggregate is shown in Fig. 3.21. H-type particles and laths of smectites are rarely observed.

In the bentonite from La Florencia Mine, Challao, Mendoza (sample 32) S- and H-type montmorillonite lamellae make up about 70% of the smectites. An H-type lamellae is shown in Fig. 3.22. Although this particle has the appearance of a single crystal, its SAD pattern (superimposed) indicates that the particle does not possess a three-dimensional periodicity. The other common forms of the smectites are foliated and compact lamellar aggregates in about equal amounts. L-type smectites are rarely observed, and an unusual aggregate of laths is shown in Fig. 3.23, in which at least two sets of parallel ribbons are discernible.

In the Ramblon bentonite from San Juan (sample 33), smectites occur in a variety of forms: aggregates, S- and H-type lamellae, and laths. The aggre-

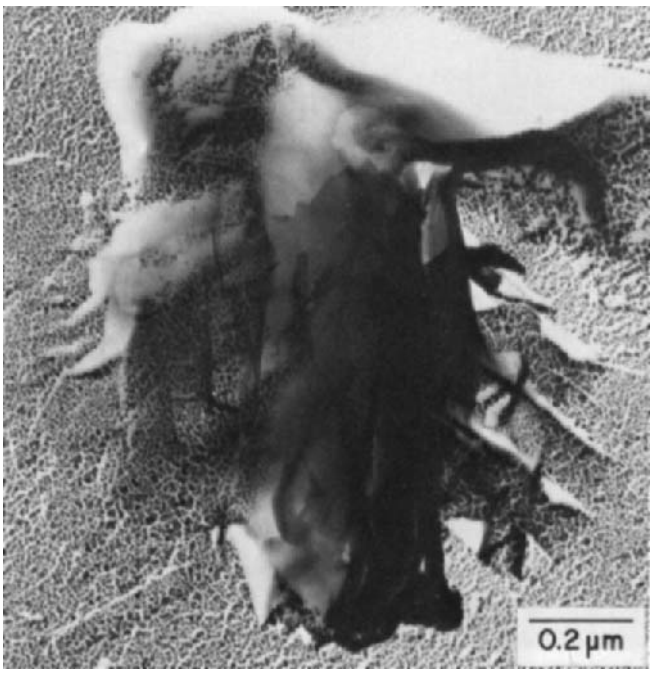

Fig. 3.23. An unusual aggregation of lath-shaped montmorillonite particles in sample 32 from the La Florencia Mine, Mendoza (Argentina).

gates are mainly Cheto-type, and they make up about 70% of smectite particles.

In the bentonite from Las Heras, Mendoza (sample 34), foliated aggregates make up about half of the smectites in the sample. Some of these aggregates display tree-like branchings that end in lamellar forms at their tips, as shown in Fig. 3.24. The H-type lamellae are the next common form in the sample, and they make up about 30—40% of the smectites. The E-, S-, and L-type montmorillonite particles are rarely observed in the sample.

In the bentonite from Cineo Saltos, Rio Negro (sample 35), foliated aggregates make up about half of the smectite particles. The rest consist of compact lamellar aggregates, and H-, S-, and E-type particles in about equal proportions.

Similarly, in the bentonite from Cuenca del Anelo, Neuguen (sample 36), smectites occur predominantly (about 50%) in the form of foliated aggregates. The H-, S-, and L-type particles make up the remainder of the smectites in about equal amounts.

The bentonite from Las Chapas, Patagonia (sample 37) also contains foliated aggregates as the common form of smectites. The S-type lamellae are also occasionally observed.

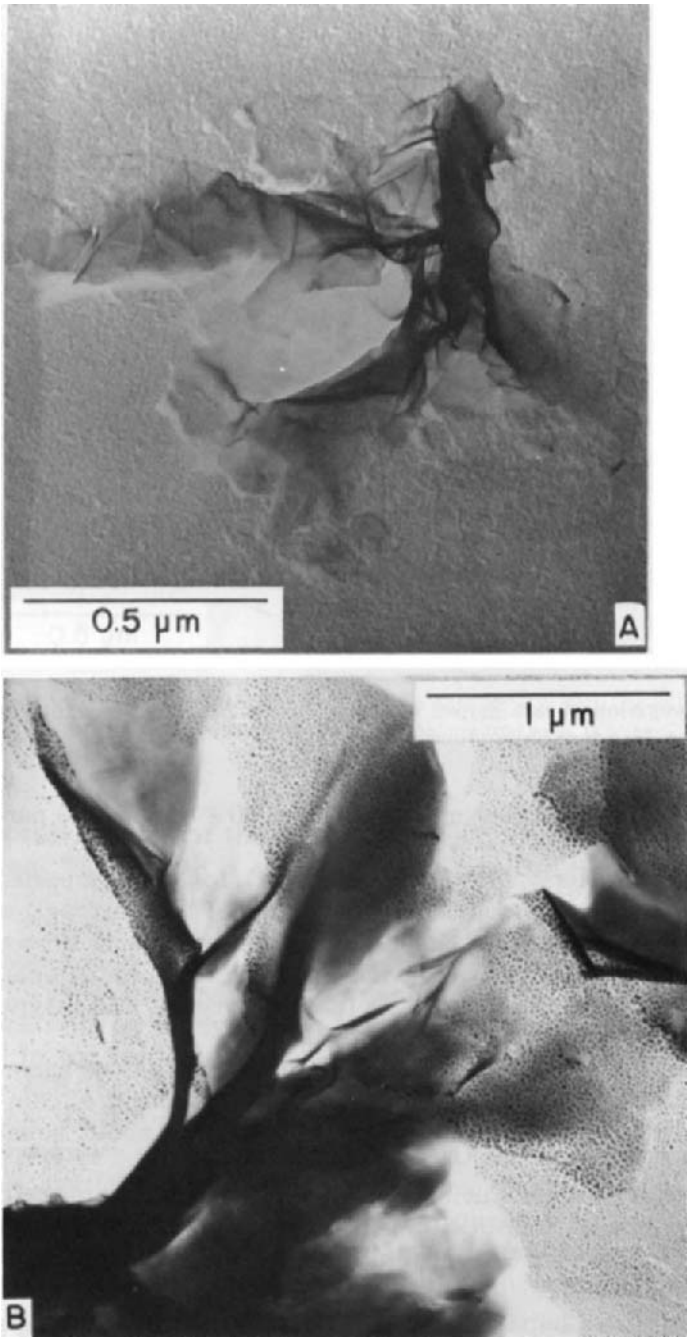

Fig. 3.24. Smectite aggregates displaying tree-like branchings in the bentonite from Las Heras, Mendoza (Argentina).

Brazil

De Souza Santos and Santini (1966) and recently Zanonadi et al. (1970) have presented detailed reviews, including extensive bibliographies, of the occurrence of clays containing smectite in Brazil. Such clays are widely distributed, particularly in the states of Minas Gerais, Santa Catarina, Rio Grande do Sul, Paraiba, Paraná, and São Paulo. However, in most cases the amount of smectitic clay is small, or the smectite is diluted with substantial amounts of other minerals.

An exception to the foregoing statement is in the Ponta Alta area of Minas Gerais, where a clay of relatively pure montmorillonite composition is produced as a bentonite. This clay is decomposed volcanic ash of Cretaceous age, and occurs in a fresh water limestone sequence, which indicates the accumulation of the ash in a lacustrine environment. Other similar occurrences of montmorillonite clays are reported in this area.

In Rio Grande do Sul near Sao Gabriel and in Santa Catarina near Lages, montmorillonite clays of considerable quantity and purity have been reported. Pintaude et al. (1972) have described a bed of montmorillonite clay 30 cm thick in the Permian Estrada Nova formation at Acegua in Rio

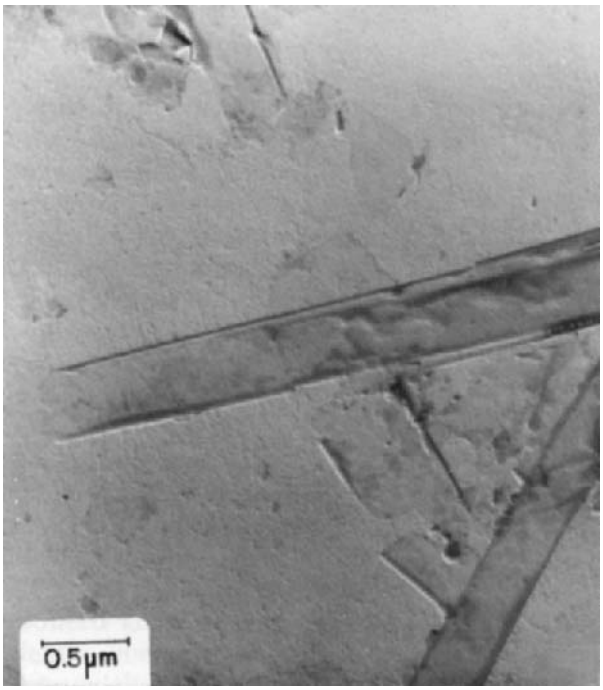

Fig. 3.25. Lath-shaped smectite particles in sample 38 with typically curved long edges.

Grande do Sul. Very recently, discoveries of possible economic significance have been made at numerous places in Paraná where De Paiva Netto and Nascimento (1956) reported a bentonitic clay in a Tertiary bituminous shale in the Paraiba Valley.

Mineralogical studies. The X-ray diffraction and chemical data for sample 38 (Table 3.2) from Ponta Alta indicate the presence of a smectite carrying calcium and magnesium as the main exchangeable cations. Quartz, feldspars, and micas are the common impurities in the sample. Smectite particles occur predominantly in the form of laths, S-type lamellae, and Wyoming-type foliated aggregates. Typical laths, as shown in Fig. 3.25, are as long as 4.0 μm. The long, straight edges of these laths are not sharp but gently curved. These laths seem to form by backfolding of thin lamellae on themselves. The S-type lamellae are also developed to unusually large lateral dimensions as shown in Fig. 3.26. The lamellae in the latter figure has about 2 $\times$ 2 μm lateral dimensions and a thickness of about 50 Å. The superimposed SAD patterns show the predominance of 02, 11, and $1\bar{1}$ spots that are equally strong in intensity. The *b*-dimension of the lamellae is calculated from the

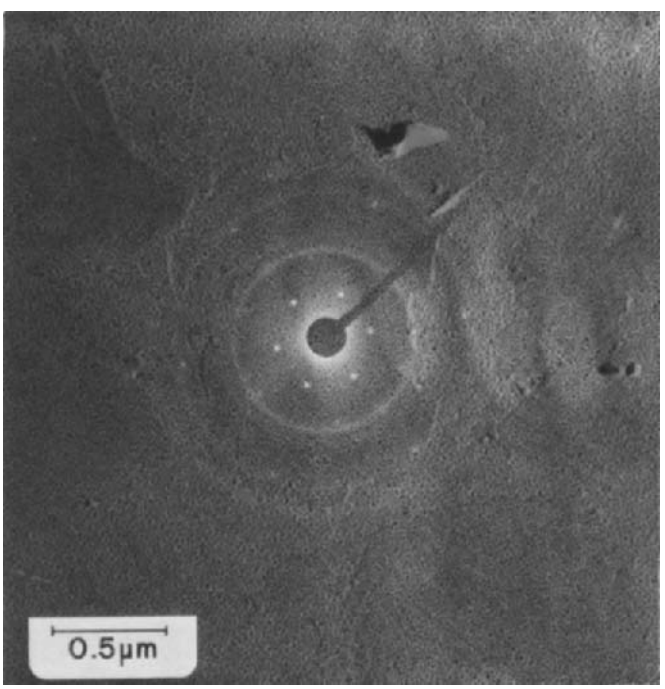

Fig. 3.26. S-type lamellae with their superimposed SAD patterns in the bentonite from Minas Gerais, Brazil (sample 38).

SAD pattern to be 8.90 ± 0.02 Å. The foliated aggregates are similar to those of Wyoming bentonites, but the individual lamellae in them have larger lateral dimensions.

Canada

Geological features. Bentonites are widely distributed in the Prairie Provinces of Canada (Manitoba, Saskatchewan and Alberta) in sediments of Cretaceous and Lower Tertiary ages. They are most extensively developed in horizons of Uppermost Cretaceous age. These bentonites are of about the same geologic age as those in Montana and the Dakotas of the U.S.A. There are frequently many beds in a given section ranging in thickness from a fraction of an inch to 10 ft. or more. The bentonites are most often in marine shales and limestones, but occur in all types of sediments, even as partings in beds of coal. In many instances, the associated shales contain considerable smectite and are described as bentonitic. It is clear from the occurrences of bentonite in Canada that there is no type of associated sediment that particularly favors the formation or occurrence of bentonites. Alteration of volcanic ash is the accepted mode of origin of these bentonites. The ash was dacitic to rhyolitic in composition, and is believed to have had a western source. At places the bentonites are reported to contain unaltered ash, for example, in the Ravenscrag formation in Saskatchewan, pumice is frequently interbedded in the bentonites. In some instances the underlying formations are silicified indicating some downward migration of silica.

Most of the bentonites in the Prairie Provinces carry calcium as the major exchangeable cation, but sodium bentonites are known also. Cristobalite is a common minor component of the bentonites. There appears to be no correlation between the physical appearance of the bentonites or the character of the associated beds and the presence of calcium versus sodium as the dominant exchangeable cation. Scott and Booker (1968) state that there is a marked increase in the sodium content of the bentonites toward the base of the Bearpaw formation, suggesting that environment of accumulation may have influenced the type of bentonite. Elsewhere there seems to be no such correlation, and the composition of the ash was probably the controlling factor.

An unusual occurrence of a natural hydrogen bentonite is found in the Pembina area of Manitoba. In this region the Pembina member of the Cretaceous Vermillion River formation contains several bentonite horizons interbedded with black carboniferous, pyritic shales of marine origin (Fig. 3.27). Oxidation of the pyrite in the association shales is believed to have produced an acid which reacted with the clay to form the acid bentonites. Selenite, melanterite, and jarosite incrustations are found along bedding planes in the bentonite. Bentonites are processed commercially with acid to enhance their decolorizing properties for oils. The Pembina bentonites have

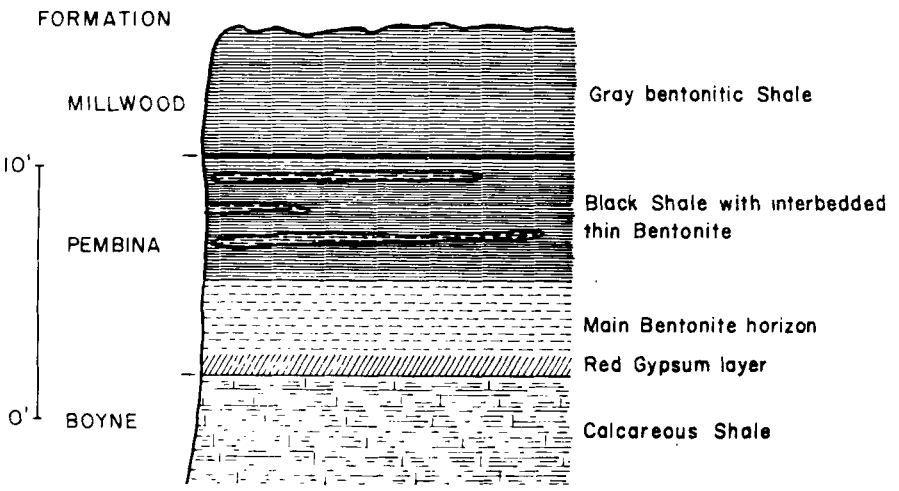

Fig. 3.27. Section of Upper Cretaceous formations showing occurrence of bentonite in Pembina Valley, Manitoba, Canada (after Torell, 1951).

been activated naturally and are processed for this purpose.

Bentonites are also known in British Columbia, where beds, up to 3 ft. in thickness, have been described in fresh water sediments of Lower Tertiary age from near Princeton and Quilchena. At places, the bentonites are interbedded with lignitic coals.

Commercial production of bentonites is reported from several areas in Canada, notably from the Edmonton formations of Upper Cretaceous age in Alberta. In these formations, beds of bentonite attain a thickness of 8—10 ft., and are commonly underlain by carbonaceous shale containing thin seams of coal.

Smith (1967) has described bentonites from Lower Devonian formations of Gaspo which are composed of mixed-layer illite—montmorillonite. They have formed by the alteration of ash.

Mineralogical studies. Sample 39 from Manitoba contains a Ca-montmorillonite and appreciable amounts of gypsum. The dissolution of the latter during the extraction process gives rise to an unusually large calcium content of the extractable cations (Table 3.2A). The other sample (40) from Manitoba consists almost entirely of a smectite with a rather low magnesia content. The chemical formula of the smectite in sample 40 is calculated from the data in Table 3.2B to be:

$$[(Si_{3.83}Al_{0.17})(Al_{1.67}Fe^{3+}_{0.17}Mg_{0.17})O_{10}(OH)_2]\,M^{+}_{0.34}$$

Quartz, plagioclases, micas, and kaolinite are the common impurities in the above samples from Canada.

Electron-optical observations show that the smectites in a Manitoba bentonite (sample 39) consist mostly of Cheto-type aggregates and H-type particles. Smectite particles in sample 40 also from Manitoba occur mostly in (Wyoming-type) foliated aggregates. The S-type montmorillonite lamellae are occasionally found in both samples from Manitoba. In the "Pembina mountain clay", sample 41, smectites consist mostly of Cheto-type mossy aggregates. A large number of micas, in the form of subhedral and euhedral crystallites are observed in the clay fraction of this sample.

Colombia

Bentonite deposits are reported in the vicinity of Marquita, Fresno, and Falan in the Tolima area by Varon (1960). They occur in the Honda formation of Tertiary age.

Cuba

Bentonitic clays composed of 90—95% montmorillonite overlying Cretaceous limestone were encountered in several bore holes near Rodas in the Province of Las Villas (Cech and Martiny, 1963).

Equador

Stoll (1962) reports an occurrence of bentonite near Quito that is used in oil well drilling muds, but gives no further information on its characteristics or mode of occurrence.

Jamaica

According to Eyles (personal communication), a bed of bentonite (sample 42) about 8 inches thick occurs in a limestone sequence of the Oligocene Montpelier formation in a road cut about one mile south of Cacoon and 9 miles southwest of Montego Bay.

The sample contains a Ca-montmorillonite (about 70%) and appreciable amounts of calcite (about 30%). The latter mineral seems to be the cause of the large values for the extractable calcium in Table 3.2A. Smectites with high magnesia content (6.14%) occur mostly in the form of globular aggregates.

Bentonite is also reported in Westmoreland Parish by Hose (1950). Davis et al. (1970) report two impure bentonites from Benbow and Kirkvine. The former contains about 30% of illite, and the latter contains appreciable gibbsite and goethite, presumably due to the proximity to bauxite.

Mexico

Geological features. Bentonite and fuller's earth, which consist mainly of smectites, are widely distributed in the central volcanic area of Mexico, but there is little specific information on the size of the deposits and on the properties of the clays. In general they are all altered volcanic materials, but whether by hydrothermal action, deuteric action, simple devitrification of ash, or a combination of such processes is not clear. Examples of such bentonites are in Queretoro, Michoacan, and Guanajuato. Some of the bentonites are quite pure smectite, and they contain calcium as the exchangeable cation.

An example of fuller's earth is found at Huajumbano, Michoacan, where an andesite and associated pyroclastics are hydrothermally altered to the earth. The alteration is incomplete as the earth contains masses of unaltered andesite. Also of interest is the occurrence of chalcedony overlying and underlying the earth. At Comonfort, Gto., basaltic pyroclastics are altered to the earth.

Clays classed as sub-bentonites are reported by Arellano (1961) at Petlalcingo, Pueblo; Puente de Tierra, Michoacan; and S. Pedro and S. Pablo, Oaxaca. In each instance, the clays are altered pyroclastics generally acidic in composition.

Clays classed as bentonites are reported by the same author at several other localities. At Guadalupe, Pueblo, bentonite occurs in a Tertiary sedimentary sequence of clays, sands, and felspathic conglomerates. The bentonite is said to have formed by hydrothermal alteration of the conglomerate. At Pena Miller, Queretoro beds of rhyolitic ash in a marine Tertiary sequence are altered to bentonite. Other beds of rhyolite in the sequence have not been altered. At Atenango del Rio, Guanajuato bentonite is found in a Tertiary marine section. At Buenavista, Pueblo, bentonite has formed from Tertiary pyroclastics with associated chalcedony and at San Juan de Dios, Pueblo, by hydrothermal alteration of pyroclastics.

An interesting occurrence of a substantially pure smectite clay is at Tatatilla, Vera Cruz. No information is available on the mode of occurrence or origin of this smectite.

Mineralogical studies. The smectite from Tatatilla is distinguished by its exceedingly low iron content (0.06% Fe_2O_3) as reported by Ross and Hendricks (1945). The same investigators gave a cation exchange capacity of 81 mequiv./100 g, all of which is calcium, and the following chemical formula:

$$[(Al_{1.58}Mg_{0.43})(Si_{3.90}Al_{0.19})O_{0.10}(OH)_2]M^{+}_{0.53}$$

An electron-optical examination of the sample from Tatatilla (U.S. National Museum No. 101836) showed that montmorillonite particles occur

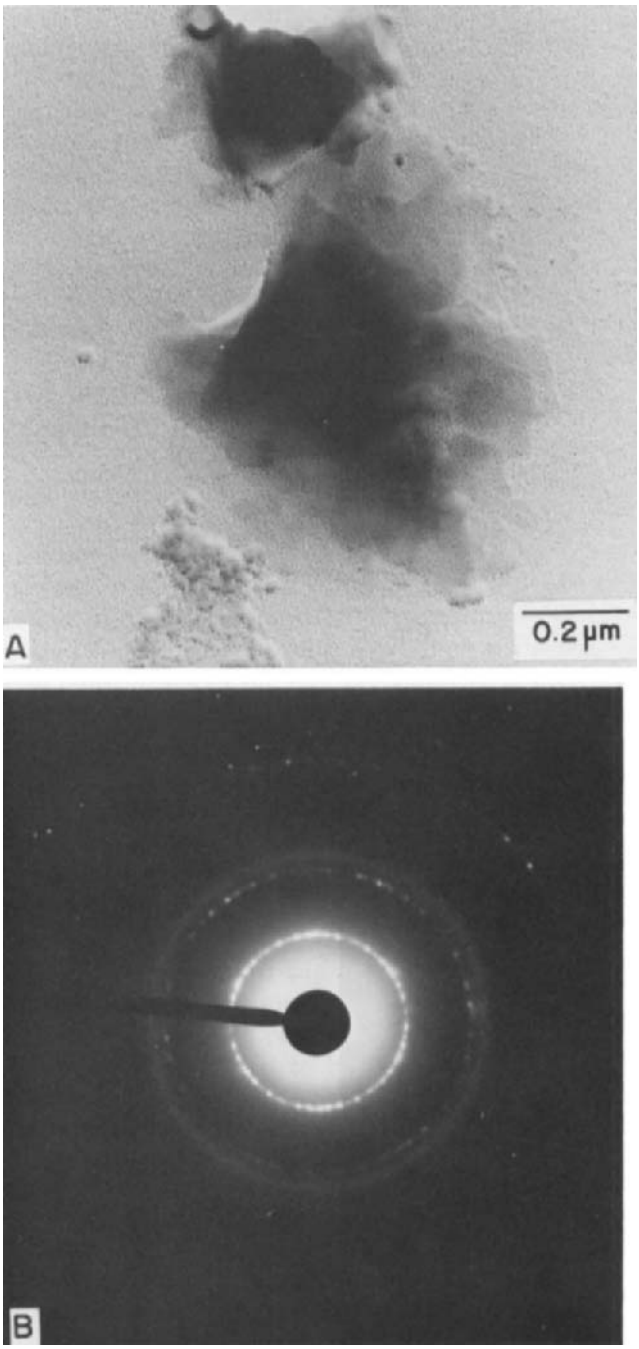

Fig. 3.28. A. A compact lamellar aggregate (in the center of the figure) of Tatatilla montmorillonite in natural state. B. Its SAD pattern.

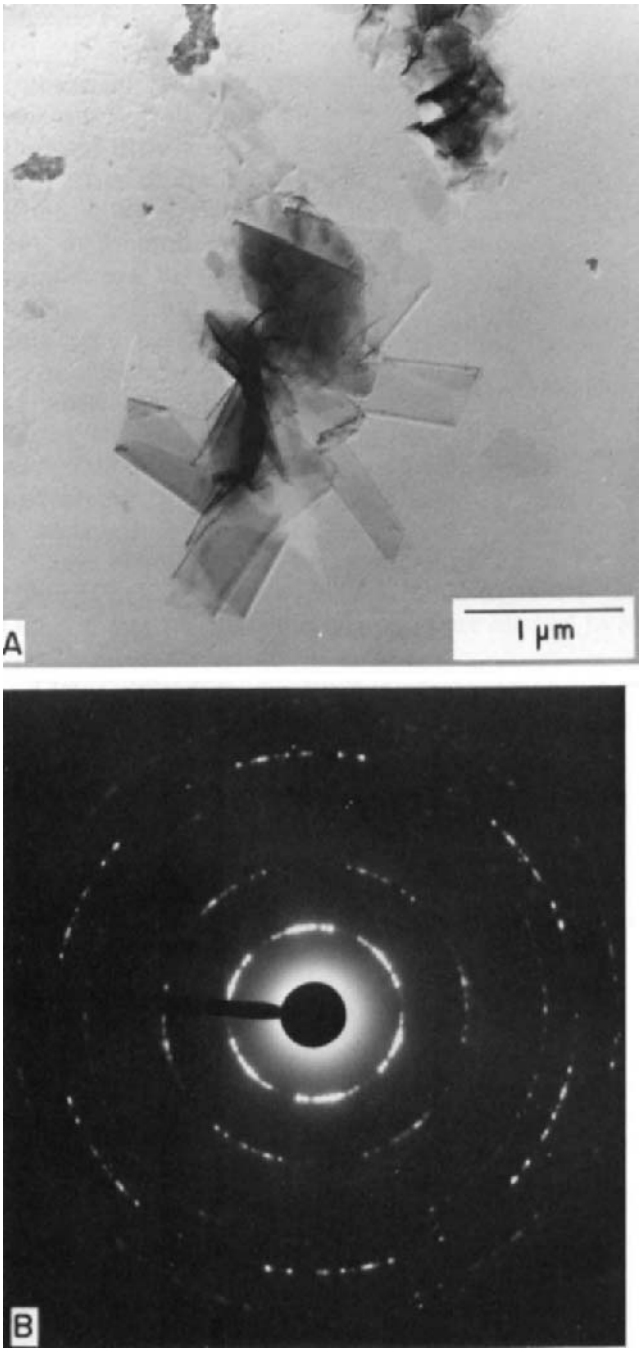

Fig. 3.29. A. Aggregate of back-folded lamellae in Tatatilla montmorillonite subjected to the dispersion treatment. B. Its SAD pattern.

in a variety of form: compact lamellar aggregates, globular (Otay-type) aggregates, and S-, E-, and L-type single crystallites. One of the lamellar aggregates is shown in Fig. 3.28A, in which E- and S-type individual lamellae are discernible. The SAD pattern of this lamellar aggregate displays spotty *hk*-rings (Fig. 3.28B), indicating increased crystallite size of lamellae. The dispersion procedure disintegrates some of the above lamellar aggregates into single crystallites, with L-, E-, and S-type morphologies. This process seems to completely break down the globular aggregates, inasmuch as they are rarely observed after the dispersion treatment. About two-thirds of the smectite particles occur in the form of aggregates with back-folded thin lamellae as shown in Fig. 3.29A. In the latter figure, lath-shaped and envelope-like units seem to be formed by back-folding of thin lamellae. The SAD pattern (Fig. 3.29B) of the aggregate displays a pronounced preferred orientation along the [02], [11], and [1$\bar{1}$] directions.

Peru

A deposit of bentonite is reported in the Paracas area of the Pisco Province of Peru in a formation of Oligocene age (Saldana, 1947). According to this author the clay is composed of montmorillonite and has formed by the alteration of trachyte—andesite ash which accumulated under marine conditions. The bentonite can be acid activated to produce a decolorizing earth. It is of interest that the bentonite occurs interstratified with diatomaceous earth.

Cabrera La Rosa (1963) has reported the occurrence of many deposits of bentonite in Tertiary formations in the coastal ranges in northern and south central Peru. Details of the occurrence of these bentonites have not been reported.

Puerto Rico

The central part of the island of Puerto Rico consists of a complex series of volcanic rocks, mostly of Upper Cretaceous age. Lava flows and pyroclastics are frequent components of this complex. At some places these tuffs and lavas have altered to bentonites, at other places to kaolinite, and at still other places to tripoli. The alteration process seems to be hydrothermal and/or deuteric, rather than weathering.

Important bentonite deposits are located in the Aguada area in the western part of the island. Here beds up to 10 ft. thick are composed of relatively pure montmorillonite. They are overlain abruptly by lateritic soil, and it is clear that the development of the laterite was unrelated to the origin of the bentonites. Other deposits of bentonitic material are known near Barrio Palo Hincado and Hacienda Lecaro in the Barranquitas area, along the Utuado—Lares road in the central part of the island, and in the vicinity of Guaynabo south of San Juan. According to Smith and Guillou (1953), the

deposits at Aguada are in the Rio Blanco volcanic series of probable Upper Cretaceous age.

Uruguay

The Cretaceous and possibly younger formations of the coastal region of Uruguay are reported by Bucaram (1966) to contain substantial tuffaceous material and the presence of soapy clays is noted, which could probably be classed as bentonite.

References

Argentina

Bordas, A.F., 1943. Contribucion al conocimientos de las bentonites argentinas. Rev. Minera, Geol. Mineral., 14: 1—60.

Krenkel, T.G., Pereira, E. and Chamorro, H.J., 1968. Bentonitas argentinas. Ind. Quim., 26: 329—334.

Lombardozzi, V. and Freixas, A., 1945. Mendoza Province clays. Ind. Minera, 5(47): 69—71.

Manjor, F., 1952. Bentonitas argentinas. Rev. Fac. Cienc. Quim. (Univ. de La Plata), 27: 3—18.

Mason, M. and Sand, L.B., 1960. Clinoptilolite from Patagonia. Am. Mineral., 45: 341—350.

Brazil

Berg, E. and De Souza Santos, P., 1968. Occurrences of montmorillonite clays in the State of Parana. Min. Metal., 48 (283): 25—30.

Delaney, P.J. and Formosa, M.L., 1960. Occurrence of bentonite in Sao Gabriel, Rio Grande do Sul. Univ. Rio Grande do Sul, Esc. Geol., Bol., 2: 13 pp.

De Paiva Netto, J.E. and Nascimento, A.C., 1956. Bentonite clays in the Tertiary of the Paraiba Valley. Bol. Soc. Bras. Geol. B, 5: 5—15.

De Souza Santos, P. and Santini, P., 1966. Occurrence of montmorillonite clays in Brazil. Ceramica (Sao Paulo), 11, 44: 36—64.

Pintaude, R.S., Alves, D. and Formosa, M.L., 1972. Montmorillonite clay beds in Acegua. Inst. Tech. Rio Grande do Sul., 57: 40 pp.

Sturdze Visconti, Y., 1951. Clays and Clay Minerals: Structure, Properties, Tests and Analyses. Inst. Tech., Rio de Janeiro, 189 pp.

Zanonadi, A.R., De Souza Santos, P. and Lourenco, D.B., 1970. Preliminary laboratory study of montmorillonite clays and their industrial use. Ceramica (Sao Paulo), 16, 64: 263—303.

Canada

Bannatyne, B.B., 1963. Cretaceous bentonite deposits in Manitoba. Manit. Dep. Mines Nat. Resour., Mines Branch, Publ., 62-5: 20 pp.

Byrne, P.J.S., 1955. Bentonite in Alberta. Res. Counc. Alberta, Rep., 71: 20 pp.

Cummings, J.M. and McCammon, J.W., 1952. Clay and shale deposits of British Columbia. B. C. Dep. Mines, Bull., 30: 64 pp.

Lebekmo, J.F., 1968. Chemical and modal analyses of some Upper Cretaceous and Paleocene bentonites from Western Alberta. Can. J. Earth Sci., 5: 1505—1511.

Scafe, D.W., 1973. Bentonite characteristics from deposits near Rosalind, Alberta. Clays Clay Miner., 21: 437—449.

Scott, J.S. and Booker, E.W., 1968. Geological and engineering aspects of Upper Cretaceous shales in Western Canada. Geol. Surv. Can., Pap., 66—37: 75 pp.
Smith, D.G.W., 1967. The petrology and mineralogy of some Lower Devonian bentonites from Gaspo, P.Q. Can. Miner., 9: 141—165.
Spence, H.S., 1924. Bentonite in Canada. Can. Dep. Mines, Mines Branch, Bull., 626: 36 pp.
Torell, C.S., 1951. Geology of the Pembina Valley, Headhorse Creek Area. Man. Dep. Mines Nat. Resour., Rep., 47-7: 7 pp.
Worcester, W.C., 1937. Saskatchewan bentonites. Trans. Can. Inst. Min. Metall., 40: 438—451.

Cuba
Cech, F. and Martiny, E., 1963. Investigation of argillaceous rocks in the locality of Rodas. Havana Univ., Fac. Sci., Mem., 1: 1—21.

Columbia
Ellswanger, R., 1967. Report on the analyses of clays by the laboratories of the Colomb., Min. Minas Pet., Serv. Geol. Nac., Bol. Geol., 14: 5—132.
Varon, M.V., 1960. Bentonite deposits of the municipios Marquita, Fresna, and Falan (Tolima). Colomb., Min. Minas Pet., Bol. Minas, (80—81): 3—10.

Ecuador
Stoll, W.C., 1962. Notes on the mineral resources of Ecuador. Econ. Geol., 57: 799—808.

Jamaica
Davis, C.E., Taylor, W.A., Thompson, B.E. and Holdridge, D.B., 1970. Two Jamaican bentonite clays. J. Sci. Res. Counc., Jamaica, 1: 71—81.
Hose, H.R., 1950. The geology and mineral resources of Jamaica. Colon. Geol. Miner. Resour., 1: 11—36.

Mexico
Arellano, A.R.V., 1961. Geological and geographical distribution of some ceramic raw materials. Publs. Ceramicas (Mex.), 1: 105—118.
Aquilera, N., 1958. Clays of some Campeche Calcareous sediments. Publs. Ceramicas (Mex.), 1: 31—34.
Esquivol, J. and Zamora, S., 1966. Information on non-metallic minerals. Mex., Cons. Recur. Nat. No Renov., Bol., 44: 226 pp.
Ross, C.S. and Hendricks, S.B., 1945. Minerals of the montmorillonite group. U.S., Geol. Surv., Prof. Pap., 205-B: 23—79.

Peru
Cabrera la Rosa, A., 1963. Bentonite. Non-metallic minerals of Peru. Peru Inst. Nac. Invest. Fom., Miner. Ser., 7: 1—65.
Saldana, L.B., 1947. The activation of bentonite from Paracas for decolorizing oils. Bol. Soc. Quim. Peru, 12: 197—210.

Puerto Rico
Smith, R.J. and Guillou, R.B., 1953. Bentonite deposits, Aguada, Barrio Malpasa, U.S., Geol. Surv., Open File Rep., 173: 2 pp.

Uruguay
Bucaram, R., 1966. Geological Report of the Coast of Uruguay. Republic of Uruguay, Ministry of Industry and Commerce, 132 pp.

3.3. BENTONITES IN AFRICA

Valuable bentonite deposits are located in many parts of Africa with important commercial production in Morocco, Algeria, Union of South Africa, and Mozambique.

Algeria and Morocco

Geological features. These two north African countries are considered together because of the similarity of their geologic setting and bentonite occurrences. In general the areas containing the bentonites are in the northern part of the countries and consist of a series of Cretaceous and Tertiary sediments with interbedded pyroclastics and lava flows, and into which volcanic rocks of varying composition have been intruded. Bentonites of varying types and modes of origin occur in these rocks, and they have been extensively developed commercially at several places. Following are examples of these deposits, but not a complete presentation of all deposits.

In Algeria, about 25 miles east of Mostaganem along the Chelif River, a series of five separate bentonite beds occur interlayered with ashy silts of Miocene age, Fig. 3.30A (sample 46). Ash structures are preserved in the bentonite indicating its mode of origin. The bentonite beds, varying in thickness from 5 inches to 15 ft., are not sharply separated from the silt. There is no silification of underlying beds, nor any suggestion of downward leaching. The fresh bentonite is blue, quickly weathering to brown, and contains many "egg" structures similar to those found in the Wyoming, U.S.A. material. The weathered brown clay is said to have higher colloidal properties than the blue bentonite. Some of the bentonites carry sodium as the dominant exchange cation rather than calcium, which is interesting in view of its interlamination with calcareous sediments. The cation exchange composition together with the gradational contact with the enclosing beds suggest that alteration of the ash was contemporaneous with accumulation. Diatomaceous earth is found in the same area in sediments of the same age.

At Lalla Maghnia in the Oran area of Algeria, a rhyolite plug occurs in a Tertiary marine sequence. At some places the rhyolite has altered to smectite, at other places to kaolinite or halloysite. Sadran et al. (1955) attribute the formation of this deposit to hydrothermal alteration of the rhyolite. The texture of the rhyolite is retained in the clay and the volume is unchanged, even though the chemical composition of the smectite and rhyolite indicate that magnesium has been added and alkalies and silicon have been removed in the transition. The hydrothermal action is believed to have been followed by the circulation of magnesium-bearing waters, probably meteoric, which added the magnesium and leached the alkalies and silicon.

On the south side of the Tafna Valley about 10 miles from Tyrene in Algeria, five beds of bentonite — 3 inches to 15 ft. thick — are found inter-

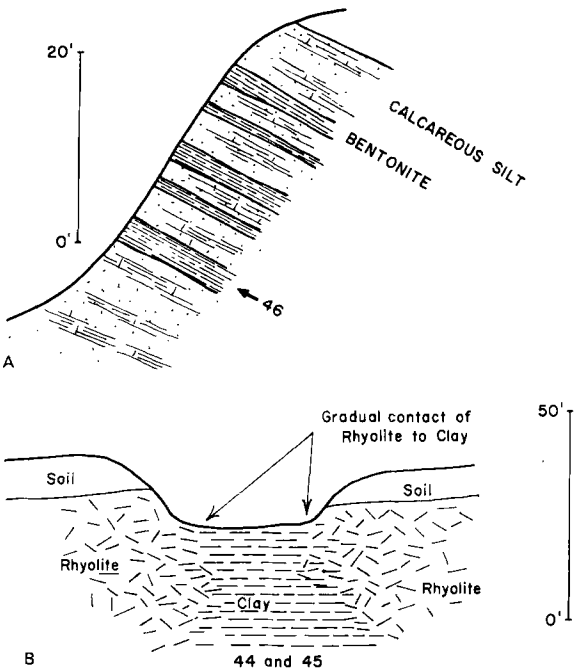

Fig. 3.30. A. Section of Miocene age formations in Chelif Valley, 5 km north of Bellevue in Mostaganem area, Algeria. B. Clay deposit northeast of Marnia in Nemours area, Algeria.

bedded with calcareous brown silts of Miocene age. The bentonite is white and contains occasional fragments of rhyolite. There is no silicification of underlying beds nor any evidence of leaching. There are intrusive masses of rhyolite and basalt nearby. Deuteric alteration of rhyolitic material is the probable mode of origin.

About 4 miles north of Marnia in Algeria on the road to Nemours and thence 5 miles east, there is a large deposit of bentonite which supplied the clay for the production of acid activated decolorizing earth at the plant in Marnia. A dike of rhyolite dipping about 60° cuts through a sequence of Miocene sediments (Fig. 3.30B). The central part of the dike is altered to clay, preserving the texture of the rhyolite (samples 44 and 45). The clay is white and translucent in appearance. The composition of the clay is quite variable and ranges from pure montmorillonite to material with considerable halloysite. Probable factors controlling the composition are not obvious. Hydrothermal or possibly deuteric processes are possible modes of origin of the clay minerals. As in the case of the deposit at Lalla Maghnia, the alteration must have been accompanied by the addition of magnesium and the removal of silicon and alkalies.

Termier et al. (1956) have described bentonites of varying modes of origin between Menerville and Dra-el-Mizane in Algeria. Some of the bentonites are interbedded with obsidian and are believed to be due to autopneumatolytic (deuteric) action in rhyolitic material. Other occurrences in sediments suggest alteration of volcanic breccia in a saline lacustrine environment.

There are many occurrences of bentonite in the Taourirt area of Morocco. The Gara Zjad deposit about 15 miles northeast of Taourirt consists of layers of bentonite about 2 inches thick in a Miocene section of bentonitic clays, volcanic ash, and marine fossiliferous sand. The bentonite grades upward into ash, and the association of bentonite beds with unaltered ash beds are of interest, as the upward gradation of bentonite to ash precludes origin by a weathering process. Perhaps the ash fell in very shallow water with only the wetted ash altering to bentonite, or possibly the composition of the ash was not constant — the earlier lower ash being wetter or different in chemical composition from the later ash. The Miocene section is overlain by about 30 ft. of gravel. Many of the hills in the area are capped by basalt of Pliocene age.

At Camp-Berteaux, also in the Taourirt area, beds of bentonite are found in a marine Miocene fossiliferous sequence (sample 47). The Taourirt bentonite is said to have outstanding properties for decolorizing oil. Current bentonite production is reported at Tamdafelt and in the Beni Aukil districts.

Mineralogical studies. In the bentonite (sample 44) from Marnia (Algeria), montmorillonite carries largely magnesium with relatively smaller amount of sodium as indicated by the data on extractable cations in Table 3.3A. Smectite particles in this sample are commonly in the form of (Cheto-type) mossy aggregates. In the other sample from Marnia (sample 45), montmorillonite particles occur mostly in the form of (Santa Rita-type) reticulated lamellar aggregates. The bentonite from Tafna contains Cheto-type aggregates as the common form of montmorillonite. As shown in Fig. 3.31, these aggregates are often entangled with lath-shaped units. These laths seem to grow from the montmorillonite aggregates. Kaolinites are also found in the sample in the form of hexagonal platelets that are often in edge-to-edge association. In the bentonite from Mostaganem, Algeria, sample 46, smectite particles occur mainly in the form of Cheto- and Santa Rita-type aggregates, with H- and L-type particles occurring rarely. The smectite has the structural formula:

$$[(Si_{3.96}Al_{0.04})(Al_{1.56}Fe^{3+}_{0.11}Mg_{0.33})O_{10}(OH)_2]M^{+}_{0.37}$$

In all the above bentonites from Algeria, quartz, mica, and feldspars form the common impurities.

The bentonite from Camp-Berteaux, Morocco (sample 47) contains a montmorillonite with a basal spacing of 14.7 Å. Na, Ca, Mg are about equally present in the extract of exchangeable cations from this sample

TABLE 3.3A

Location, geological and mineralogical data on bentonites from Africa

Sample no.	Location and formation	Geologic age	Smectite's spacings (Å)		MgO * (%)	Extractable cations (mequiv./100 g)					C.E.C. (mequiv./100 g)
			(001)	(06,33)		Mg	Ca	K	Na	total	
	Algeria										
44	Marnia	Pliocene	14.3	1.496	3.94	61	18	2	35	116	
45	Marnia	Pliocene	15.0	1.496	3.22 +						
46	Mostaganem, Bellevue	Miocene	13.8	1.496	3.81	61	5	3	28	97	
	Morocco										
47	Camp Berteaux	Miocene	14.7	1.497	4.24	58	59	2	57	176	109
	Union of South Africa										
48	Natal, Zululand, Stormberg Series, "Mkuzi green"	Liassic	12.3	1.493	0.82	20	6	2	20	48	
49	Natal, Zululand, Stormberg Series, "White"	Liassic	12.2	1.495	1.67	47	14	1	35	97	
50	Orange Free State, Parys, Karoo System "Ocean"	Liassic	12.5	1.500	3.98	44	60	1	120	225	103
51	Orange Free State, Parys, Karoo System "Ocean top"	Liassic	13.6	1.500	3.55	6	42	2	3	53	
52	Orange Free State, Parys, Karoo System "Ocean bottom"	Liassic	15.0	1.497	4.77	46	45	2	7	100	
53	Orange Free State, Parys, Karoo System "Ocean middle"	Liassic	14.4	1.499	3.96	55	64	2	7	128	128
54	Cape Province, Plettensberg Bay	Tertiary	15.0	1.501	4.89	14	127	2	5	148	57
	Mozambique										
55	Laurenco Marques, Stormberg Series, "ultra white"	Liassic	12.3	1.497	0.93	32	8	1	32	73	
56	Laurenco Marques, Stormberg Series, "perlite"	Liassic	12.3		3.52						
57	Laurenco Marques, Stormberg Series, "portal"	Liassic	12.6	1.497	1.17	21	7	1	22	51	

* On ignited material from —1 μm fraction of clay stripped off exchangeable cations.

+ Grim and Kulbicki (1961) on 110°C basis.

TABLE 3.3B

Chemical analyses of African bentonites (on ignited material from —1 μm fractions of ammonium saturated clays except for the data from the literature)

Sample no.	SiO_2	Al_2O_3	Fe_2O_3	MgO	Li_2O	Na_2O	CaO	K_2O	Total	Impurities *
44	69.34	23.62	1.85	3.94	0.0	0.01	0.03	0.02	98.81	Q(5)
45 **	63.37	23.37	3.82	3.22	0.0	0.0	0.63	0.0	94.88	—
46	68.47	23.55	2.55	3.81	0.0	0.02	0.04	0.09	98.53	—
47	67.01	24.92	2.56	4.24	0.0	0.06	0.04	0.21	99.04	—
48	71.39	24.20	2.25	0.82	0.0	0.03	0.03	0.03	98.75	crist(30) kaol(10)
49	68.93	25.60	3.02	1.67	0.0	0.03	0.04	0.03	99.32	crist(5) kaol(5)
50	63.64	27.92	4.78	3.98	0.0	0.03	0.05	0.32	100.72	Q(5)
51	67.83	22.35	5.35	3.55	0.0	0.01	0.05	0.39	99.53	—
52	62.18	28.78	4.42	4.77	0.0	0.01	0.01	0.12	100.29	Q(5)
53	66.26	22.19	5.60	3.96	0.0	0.02	0.05	0.42	98.50	—
54	67.36	23.72	1.67	4.89	0.0	0.11	0.33	1.60	99.68	feldspar (10)
55	88.92	8.67	1.02	0.93	0.0	0.01	0.02	0.02	99.59	crist(60)
56	73.74	18.24	3.65	3.52	0.0	0.03	0.16	0.13	99.47	crist(20)
57	84.77	11.33	1.20	1.17	0.0	0.01	0.01	0.09	98.58	crist(60)

* Impurities are semiquantitatively estimated from the X-ray diffraction data. (crist = cristobalite; kaol = kaolinite; Q = quartz.)
** Grim and Kulbicki (1961) on the —2 μm fraction of H-clay.

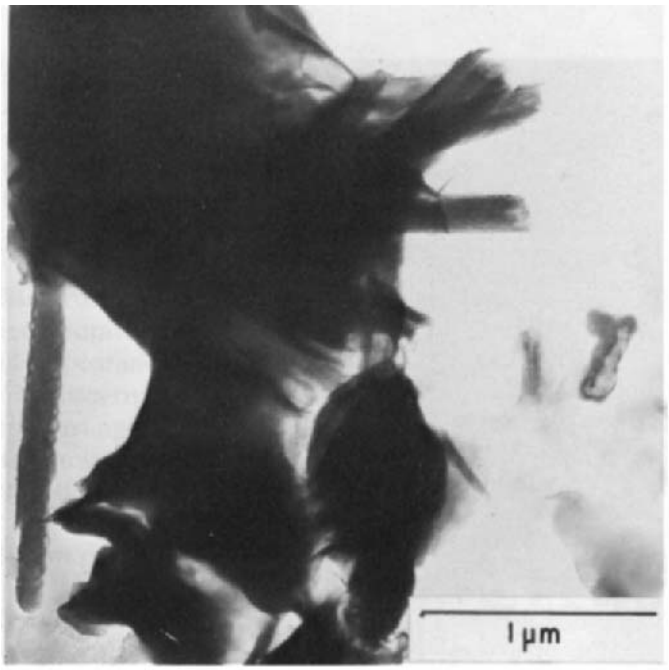

Fig. 3.31. Montmorillonite aggregates and lath-shaped units associated with them in bentonite from Tafna, Algeria.

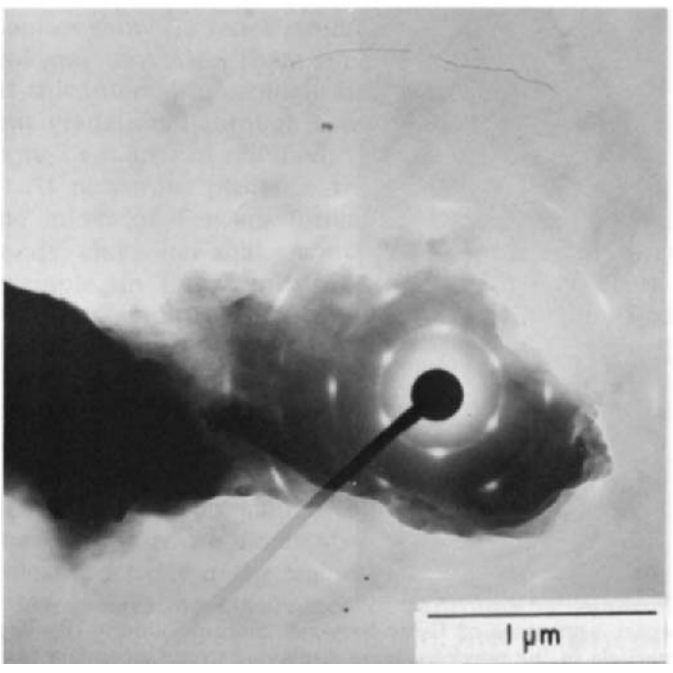

Fig. 3.32. A compact montmorillonite aggregate in the Camp-Berteaux sample with its superimposed SAD pattern.

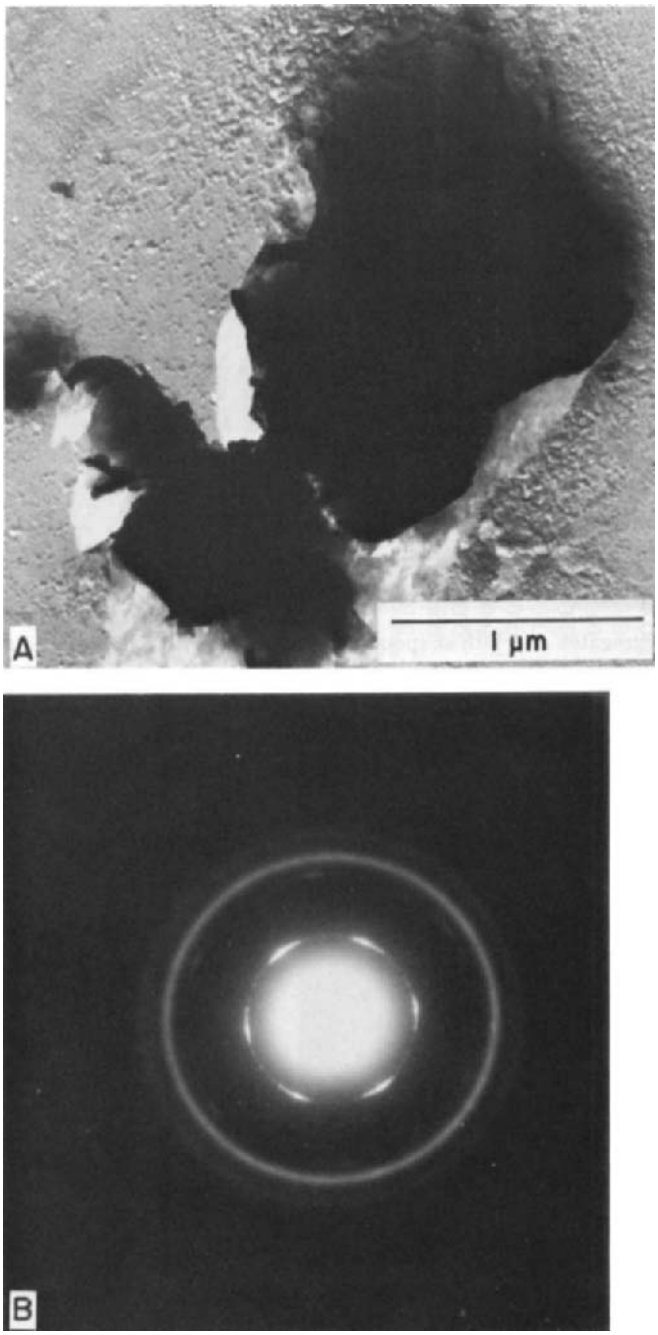

Fig. 3.33. A. Typical compact aggregates of Camp-Berteaux montmorillonite. B. The SAD pattern of the larger particle in the previous figure displaying strong secondary textures along the [02], [11], and [$\bar{1}$1] directions.

(Table 3.3A). However, the cation exchange capacity (109 mequiv./100 g) and 14.7 Å basal spacing suggest that some of the extractable sodium and magnesium probably originate from other minerals in the sample rather than from the smectite. The chemical formula of this smectite is calculated from the data in Table 3.3B to be:

$$[(Si_{3.84}Al_{0.16})(Al_{1.53}Fe^{3+}_{0.11}Mg_{0.36})O_{10}(OH)_2]M^{+}_{0.52}$$

Electron-optical observations on Camp-Berteaux sample show that montmorillonite particles occur mostly in the form of aggregates that are compact in appearance (Figs. 3.32 and 3.33A), and in which individual crystallites are not discernable. The SAD patterns indicate a strong preferred orientation in the arrangement of the crystallites along the [02], [11], and [$1\bar{1}$] directions as shown in Figs. 3.32 and 3.33B. The individual crystallites of smectites are occasionally observed as E- or S-type lamellae after the dispersion treatment.

Union of South Africa

Geological features. Bentonites are known and produced commercially from several places in South Africa. Several beds up to 8 ft. thick interbedded with shales and sands are found in formations of the Karoo System of Liassic age in the vicinity of Parys in the Orange Free State (samples 50, 51, 52, and 53). These beds carrying calcium as the exchangeable cation are composed of substantially pure montmorillonite. It is interesting to note that these bentonites show no relict structures nor non-smectite minerals indicating parent volcanic ash. Also, there is no evidence of any volcanic activity in the region at this interval in geologic time. The beds are sharply bounded at their base, but gradational through a short interval to the overlying shale. The underlying beds are not silicified.

At numerous places in the Cape Province along the Indian Ocean, there are inliers of Tertiary formations from the coast westward. These beds of sands, clays and shales contain layers of bentonite at several localities. For example, in the vicinity of Plettensberg Bay, there are lenticular beds of very pure montmorillonite up to 6 ft. thick in a shale section (sample 54). Similarly in the vicinity of Albertinia to the south, there are beds of similar thickness which in some instances are relatively pure montmorillonite, while other beds contain considerable illite, quartz, and other minerals. These Tertiary bentonites are sharply separated from underlying beds, but gradational with overlying soft shales. There is no silicification of the underlying beds, and they are similar to the bentonites from the Orange Free State in that there are no relict structures in the bentonite, and no evidence of volcanic activity in the region at the time of their formation.

An interesting occurrence of bentonite is found in northern Zululand in the Natal Province (samples 48, 49). Here a glassy, perlitic, rhyolitic lava in a volcanic sequence near the top of the Stormberg Series of the Karoo System

in places is altered by deuteric action to smectite. The alteration of the perlite to smectite is extremely irregular. At some places the perlite is completely unaltered; at other places, the alteration is so complete that there are pockets of almost pure smectite; at still other places, the smectite is scattered through the glass, or the perlite contains disseminated smectite. Occasionally the alteration product is kaolinite or a mixture of kaolinite and smectite with some cristobalite. There is no suggestion of any variation with fractures or the penetration of hydrothermal agents from outside sources. It seems clear that the alteration took place as a consequence of reactions between gases and vapors included within the parent igneous rock and the perlite, and was concentrated where the gases and vapors were most abundant. The geologic setting and character of this deposit are similar to those that will be described in Mozambique (see pp. 71—72).

Mineralogical studies on the bentonites from Natal Province, Zululand. The X-ray diffraction data (Table 3.3A) indicate the presence of a Na-montmorillonite with basal spacings of 12.3 and 12.2 Å (samples 48, 49). Large amounts of magnesium are, however, found among the extractable cations. Some of this magnesium might originate from biotites in these samples. Samples 48 and 49 contain about 50% and 20% cristobalite respectively in their coarser (>10 μm) fractions. These large amounts of cristobalite may account for the low values of total extractable cations. Kaolinite is also present in small quantities (5—10%) in these samples. The cristobalite is still a major component in the fine fractions (—1 μm) of the sample 48 as indicated in Table 3.3B. The latter table also shows that the magnesium contents of these smectites are below 2% even after accounting for the cristobalite in the samples, and consequently, these smectites are to be specified as beidellites.

Electron-optical examination of sample 48 shows that Cheto-type aggregates make up about 70% of the smectite particles. The S-type lamellae are the next common form of smectites in the sample. Aggregates of cristobalite and montmorillonite are frequently observed.

In the "white clay" (sample 49), montmorillonite aggregates display tree-like branchings similar to those of dendrites. Such an aggregate is shown in Fig. 3.34, in which triangular smectite lamellae are developed at the tips of the branches like the leaves of a tree. Such dendritic aggregates make up about 70% of the smectite particles, the E- and S-type lamellae make up the remainder. These E-type lamellae are shown in Fig. 3.35. The smectites of the dendritic (tree-like) aggregates, E-, and S-type lamellae all have a *b*-dimension of 9.00 ± 0.02 Å.

Mineralogical studies on the bentonites from Parys, Orange Free State, Plettensberg Bay, Cape Province. Sample 50 was a commercial product pretreated with Na_2CO_3. The analytical data on the sample in Table 3.3 indicate a basal

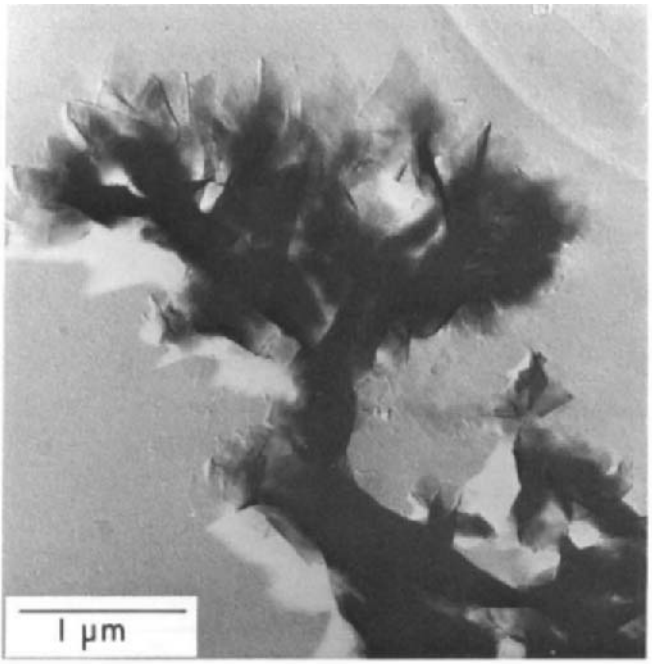

Fig. 3.34. Dendritic aggregates of montmorillonite in sample 49, Zululand, Natal Province, South Africa.

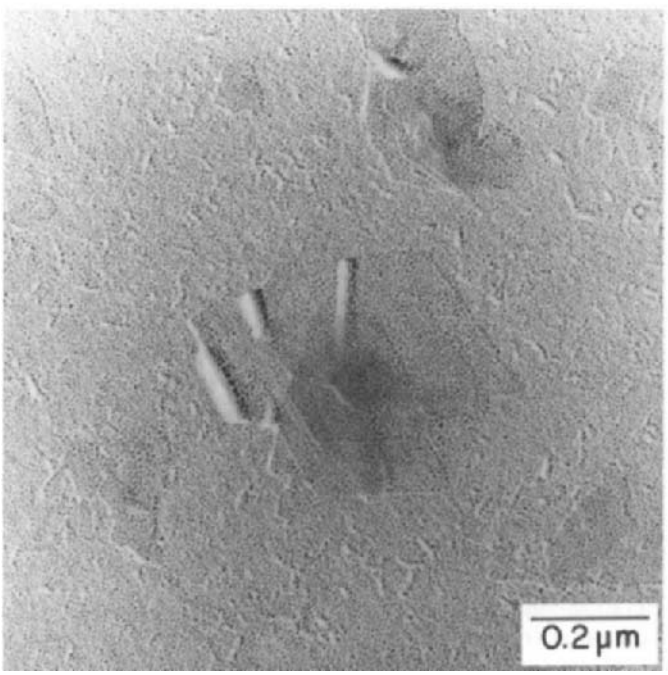

Fig. 3.35. Two E-type montmorillonite lamellae (in center), and S-type lamellae in Mkuzi bentonite (sample 49), Natal Province, South Africa.

spacing of 12.5 Å as expected from a Na-montmorillonite. Large amounts of Ca and Mg are also found among the extractable cations in the same sample, probably originating from other minerals than the montmorillonite. A predominantly calcium bearing montmorillonite occurs in samples 51 and 54. Smectites in samples 52 and 53 carry both calcium and magnesium as exchangeable cations. The smectites have the following formula in samples 51 and 53, as calculated from the data in Table 3.3B:

Sample 51: $[(Si_{3.91}Al_{0.09})(Al_{1.45}Fe^{3+}_{0.24}Mg_{0.31})O_{10}(OH)_2]M^{+}_{0.40}$

Sample 53: $[(Si_{3.88}Al_{0.12})(Al_{1.41}Fe^{3+}_{0.25}Mg_{0.35})O_{10}(OH)_2]M^{+}_{0.47}$

Quartz, mica, kaolinite, and feldspars are the common impurities in the above samples from Parys. The sample from Cape Province (sample 54) contains, in addition, about 20% cristobalite in the coarser fractions (>10 μm).

Electron-optical observations show that Cheto- and Wyoming-type aggregates, H-, S-, and L-type particles are equally common forms of smectites in sample 50. In the top layer of the Parys bentonite (sample 51), Wyoming-

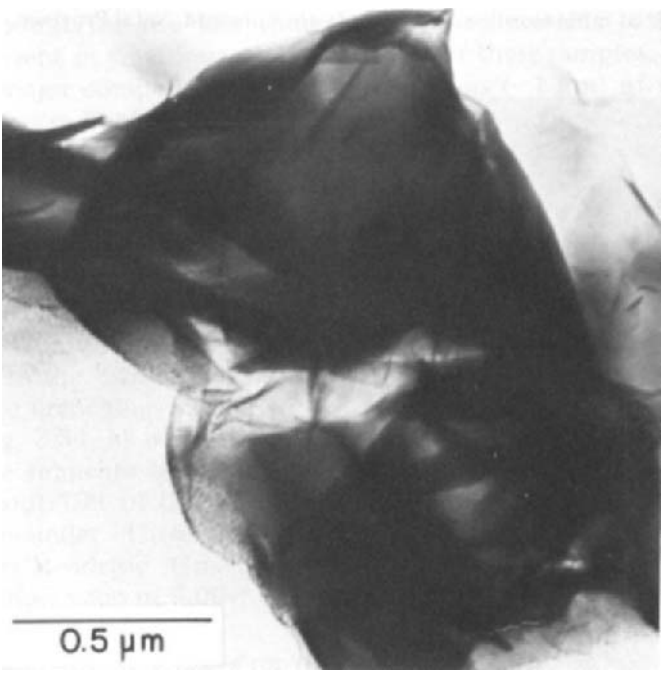

Fig. 3.36. Wyoming-type montmorillonite aggregates in the top layer Parys bentonite (sample 51) from South Africa.

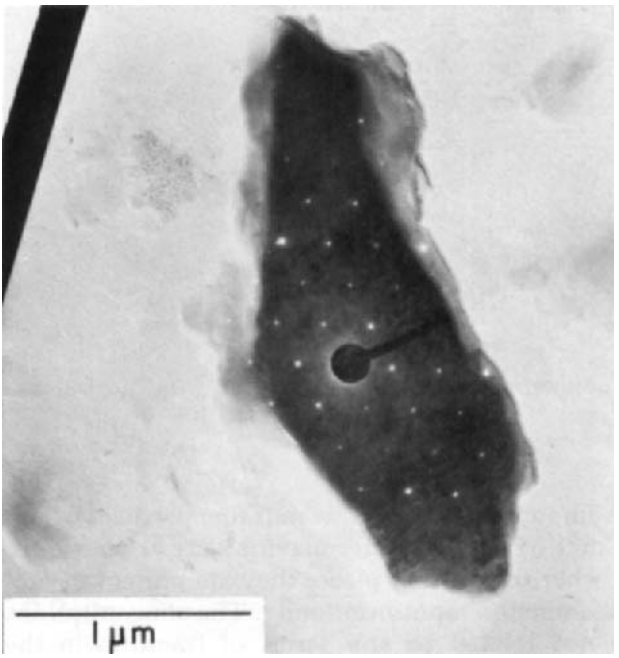

Fig. 3.37. A typical mica flake with its SAD pattern in sample 51 from Parys, South Africa.

type aggregates make up about 50% of the smectite particles. Such an aggregate is shown in Fig. 3.36. Mica flakes are the common impurities in all the above samples, and Fig. 3.37 shows a typical mica with its SAD pattern from sample 51. In the middle and bottom layer of Parys bentonite (samples 52 and 53), smectite particles occur mostly as S-type lamellae and as compact lamellar or foliated aggregates.

In the bentonite from Plettensberg Bay (sample 54), Wyoming-type aggregates and H-type lamellae are the common forms of smectites. After the dispersion treatment, these aggregates break down into a large number of S-type lamellae.

Mozambique (Portuguese East Africa)

There is an interesting occurrence of bentonite adjacent to the main highway about 25 miles east of Laurenco Marques (Fig. 3.38). Here glassy perlitic lava of the Stormberg Series of the Karoo System of Liassic age has been altered irregularly by deuteric action to bentonite. In this deposit, the alteration has produced masses of bentonite tens of feet thick. The bentonite varies from relatively pure montmorillonite (sample 55) to material contain-

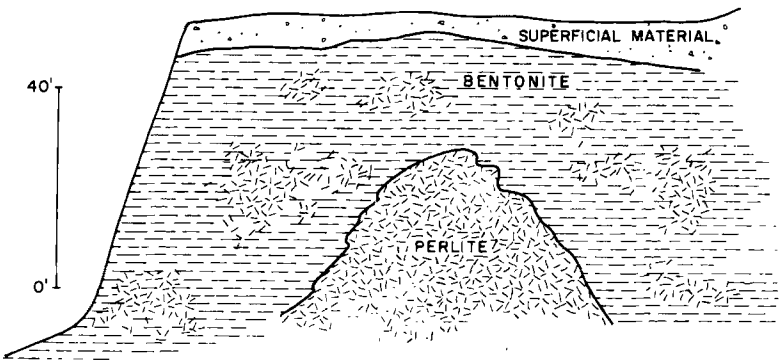

Fig. 3.38. Sketch of bentonite occurrence in perlite, Laurenco Marques, Mozambique (sample 57).

ing variable but considerable amounts of cristobalite and fine particles of unaltered rhyolite (samples 56 and 57). These latter materials are at places disseminated through the clay, whereas at other places they are present in substantial masses containing disseminated montmorillonite. The concentrations of the montmorillonite are not related to any series of fractures in the rhyolite, which would suggest hydrothermal alteration beginning along such fractures. Rather, the masses of bentonite are isolated and randomly distributed in the rhyolite, indicating that the alteration process developed within the rhyolite. The bentonite is the calcium variety. It has been extensively developed commercially.

The perlitic beds of the Stormberg Series continue to the south in Zululand of the Natal Province, Union of South Africa (p. 67). As for the Natal bentonite, deuteric processes are believed to have been the mode of origin of these Mozambique deposits.

In the northern part of Mozambique there is a large basin of Cretaceous and Tertiary sediments. There appears to be no record of bentonite in this area, but based on the common occurrence of bentonite in rocks of this age, its presence is likely.

Mineralogical studies on Mozambique bentonites. The X-ray diffraction data on the three samples in Table 3.3A indicate that they all contain a Na-montmorillonite with a basal spacing between 12.3—12.6 Å. These are samples which have been processed with the addition of soda ash. Tridymite or cristobalite is a major component in these samples. The free silica (tridymite, cristobalite) content of the samples 55 and 57 is as high as about 60%, which accounts for the low amount of total extractable cations. The appreciable amounts of magnesium among the extractable cations for samples 55 and 57 must be related to some other minerals than the mont-

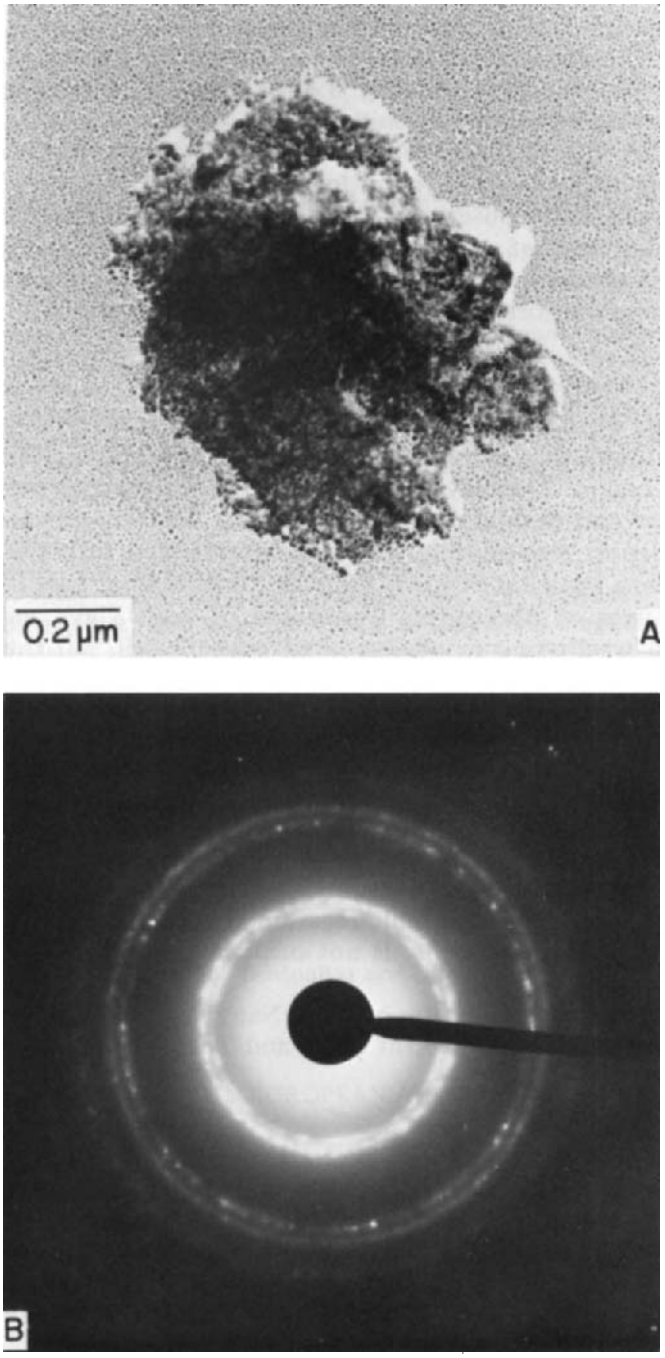

Fig. 3.39. A. Fine granular aggregate consisting of tridymite and montmorillonite. B. Its SAD pattern displaying two diffraction rings for these minerals. (Sample 55, Mozambique.)

morillonite. Tridymite occurs in fine granular aggregates as shown in Fig. 3.39A. The aggregate also contains smectite as revealed by the 4.45 and 4.11 Å rings in the SAD pattern of the aggregate (Fig. 3.39B). The 4.11 Å spacing suggests that the silica phase consists of tridymite.

Smectite particles occur mostly in the form of Wyoming-type aggregates in samples 55 and 57. In these samples, laths formed by back folding of smectite lamellae are occasionally observed. The perlite bentonite (sample 56) contains appreciable amounts of montmorillonite—cristobalite aggregates similar to those described above. In addition, H-type particles and Wyoming-type aggregates are the common forms of smectites.

Egypt

Information concerning possible bentonites in Egypt is very scant. Gindy and Badra (1968) have described clays which appear to be bentonites from the northwestern desert region. The clays occur alternating with marine carbonate beds in the lower and middle members of Middle Miocene formations. The authors also report montmorillonite marls interbedded with gypsum deposits in Pleistocene lagoonal deposits between fossil coastal bars of the Mediterranean Sea west of Alexandria. The origin of these clays and marls may be related to weathering or alteration of volcanic ash, but this cannot be established definitely. Basta et al. (1971) have recently reported bentonite from Faiyum.

Kenya and Tanganyika

Analyses of several samples of clay from the Rift Valley of Kenya and Tanganyika supplied by the Geological Survey of Kenya indicate that a smectite is the dominant clay mineral. The samples are Tertiary to Recent in age, but no specific information is available regarding occurrence, associated beds, etc. The occurrence of bentonite is not surprising in view of the presence of volcanics in the area.

Shackleton (1946) has reported bentonites between Nanyuki and Maralal in Kenya. Bentonite is also reported in the Athi River and Timau areas by Du Bois and Walsh (1971).

Sudan Republic

Whiteman (1971) reports the presence of bentonitic clays in a Mesozoic section encountered in a bore hole for the foundation of a bridge across the Nile River at Shambat.

Southwest Africa

Bentonites are known in several areas in Southwest Africa, but no specific information concerning them could be obtained.

References

Algeria and Morocco

Anonymous, 1973. Bentonite in Europe. Ind. Miner. (London), 64: 9—20.

DeLapparent, J., 1937. Origin of bentonites from North Africa. C. R. Soc. Geol. Fr., 10: 126—128.

DeLapparent, J., 1945. Deposits of the smectitic clays in North Africa. C. R., 221 (13): 335—337.

Frey, R., Yovanovich, B. and Burghelle, J., 1936. Composition and probable genesis of some decolorizing clays of North Africa. Serv. Min. and Carte Geol. Morocco, Mem., 38: 65 pp.

Grim, R.E. and Kulbicki, G., 1961. Montmorillonite: high temperature reaction and classification. Am. Mineral., 46: 1329—1369.

Sadran, G., Millot, G. and Bonifas, M., 1955. The origin of bentonite deposits at Lalla Maghnia (Oran). Serv. Carte Geol., Algeria, Bull., 5: 213—234.

Termier, H., Termier, G. and Korenko, V., 1956. On the occurrence of bentonite of Miocene age between Menerville and Dra-el-Mizane, Algeria. Serv. Carte Geol., Algeria, B.n.s., 8: 291—301.

Egypt

Basta, E.Z., El-Kadi, M.B. and Maksoud, M.A., 1971. Mineralogy of some bentonitic clays from Faiyum. Cairo Univ. Fac. Sci., Bull., 43: 271—284.

Gindy, A.R. and Badra, A., 1968. Bentonite-like clays and marls in the northwestern desert of Egypt. Proc. Egypt. Acad. Sci., 21: 11—36.

Kenya and Tanganyika

DuBois, C.O.D. and Walsh, J., 1971. Minerals of Kenya. Geol. Surv. Kenya, Bull., 11: 1—82.

Shackleton, R.M., 1946. Geology of the country between Nanyuki and Maralal. Geol. Survey Kenya, Rep., 11: 54 pp.

Sudan Republic

Whiteman, S.J., 1971. Geology of the Sudan Republic. Clarendon Press, Oxford, 291 pp.

Mozambique

Tavares, A.F., 1973. Bentonitas nos Limbobas. Men. Inst. Invest. Cient. Mozambique, Ser. b, 9: 1—15.

3.4. BENTONITES IN EUROPEAN AND EASTERN MEDITERRANEAN COUNTRIES

Bentonites are well known and have been extensively studied in many countries of Europe. Important producers of bentonite are located in England, Spain, Germany, Hungary, Poland, Romania, Czechoslovakia, Yugoslavia, Italy, Greece, and Bulgaria.

Austria

The Tertiary formations, particularly of Lower and Middle Miocene age, of Austria contain volcanic ash and tuff which in some places has altered

directly to bentonite. At other places, according to Kopetsky (personal communication), "trachy-andesites" of Miocene age were altered by solutions of silica and sulfate to produce the "Austrian Trass", a mineral aggregate composed mainly of opal and alunite. Finally, weathering of the "Trass" produced smectite. The weathered material attains a thickness of 60 ft. The bentonite varies in color from gray to blue. The blue bentonite at places contains as much as 10% pyrite.

The Miocene sections containing the bentonites are made up of both marine and non-marine sediments with the bentonites showing no preference for either type of sediment. The associated beds range in character from gravel and lignite to marine sands and calcareous clays. Paulitsch (1953) has described relict structures in some of the bentonites. The volcanic tuff and ash is reported to be dacitic in composition. The thickness of the bentonite horizons varies from 1 to 3 ft.

Bulgaria

Bentonites are found in several areas in Lower Tertiary sequences of calcareous sediments and volcanic tuffs and lavas of rhyolitic to andesitic composition. The bentonites are reported to have formed by the devitrification of volcanic glass with some superimposed hydrothermal action causing a zonal arrangement of the clay minerals, and the deposition of calcite, barite, and quartz in fissures. The clay near the conducting channels is kaolinitic, whereas smectite has developed farther away from the contact. Montmorillonite has developed from the more acid tuffs, whereas beidellite has formed from the more basic ones. Deposits with the foregoing characteristics are best known and developed in the Kurdjali area. Other occurrences at Dimitrovgrad and Chirpan are reported to be secondary sedimentary deposits of smaller size and of lesser purity than the Kurdjali deposits.

Cyprus

A bed of bentonite is reported near the village of Troulli resting on pyritic montmorillonite clay. The bentonite is cut by veins of gypsum, and is believed to have formed by the alteration of volcanic ash.

Pantazis (1967) reported bentonitic clay in the Pharmakas—Kalarasas area in the Moni and Parapedhi formations of Cretaceous Campanian age. The bentonitic clays are thinly bedded and are associated with radiolarian tuffaceous silts and pillow lavas. The radiolaria of the Moni formation are reportedly deep-sea varieties, indicating an interesting site of accumulation of the ash believed to be the parent material of the bentonite. Production of bentonite is reported near Cambia.

Electron-optical studies on this sample showed that smectite particles occur largely as Cheto-type aggregates. The S- and H-type lamellae are also frequently observed.

Czechoslovakia

Geological features. Konta (1957) has reported two bentonite occurrences in Czechoslovakia. One at Branany in northwest Bohemia has formed by the decomposition of Tertiary basaltic tuffaceous material. Some of the bentonite is calcareous, and a small amount (10%) of kaolinite and illite is frequently mixed with the smectite. The other deposit is at Kuzmice in eastern Slovakia (sample 58) where decomposition of tuffaceous material in a lacustrine environment has formed the bentonite. The tuff is associated with volcanics ranging in composition from andesites to fairly acid rocks, all in a sequence of Upper Tertiary lake sediments.

Bentonites are known at several other places in eastern Slovakia, for example, at Fintice and Nizne Hrabovce. Cristobalite is a common component with the smectite in these bentonites which have formed by the alteration of Tertiary pyroclastic sediments. Currently bentonite production is reported at Zelenice in northern Bohemia. Bentonite occurrences are also known in Upper Silesia at Radzionkow.

Mineralogical studies. The sample from Branany contains a montmorillonite carrying predominantly calcium and magnesium as exchangeable cations. The cation exchange capacity (130 mequiv./100 g) of the sample is much higher than the total extractable cations (66 mequiv./100 g). This suggests that the clay must have lost part of its interlayer cations, e.g., by exchanging with hydrogen or hydronium (H_3^+O). Kaolinite, mica, quartz, feldspars are the common impurities in this sample. The bentonite from Kuzmice contains about 40—50% cristobalite as indicated by the X-ray diffraction data and by the chemical analysis of the sample (Table 3.4). The magnesia content of the smectite is unusually low even after accounting for the cristobalite content of the sample. The smectite is, therefore, specified as a beidellite.

The smectites in the Kuzmice and Branany bentonites occur in a variety of forms: Wyoming-type aggregates, S-, and E-type lamellae, and laths.

England

Geological features. Clays, composed almost entirely of smectite, called fuller's earth in the English literature, are well known in formations of Upper Cretaceous age in the London basin, and in sediments of Jurassic age in Somerset. Recently zeolites have been reported along with the smectite as a component of some of the Cretaceous bentonites. Calcium is the dominant exchangeable cation in bentonites of both geologic ages.

The Upper Cretaceous fuller's earth is produced extensively near Nutfield in Surrey for a wide variety of commercial uses: bonding foundry molding sands, oil well drilling muds, acid activated decolorizing clays, etc. At the Nutfield locality, several beds of clay ranging in thickness from a few inches

TABLE 3.4A

Location, geological and minerological data on bentonites from Europe and Eastern Mediterranean countries

Sample no.	Location and formation	Geologic age	Smectite's spacings (Å)		MgO * (%)	Extractable cations (mequiv./100 g)					C.E.C. (mequiv./100 g)
			(001)	(06,33)		Mg	Ca	K	Na	total	
	Czechoslovakia										
58	E. Slovakia, Kuzmice	U. Tertiary	14.7	1.497	0.67	nd	nd	nd	nd	nd	nd
	England										
59	Surrey, Nutfield, Lower green sand "gray"	U. Cretaceous	15.2	1.499	3.56	18	36	2	4	60	
60	Surrey, Nutfield, Lower green sand "blue lump"	U. Cretaceous	14.9	1.501	3.92	6	129	3	4	142	75
61	Surrey, Nutfield, Lower green sand "yellow"	U. Cretaceous	14.3	1.501	3.84	10	89	1	6	106	83
62	Bedfordshire, Woburn, Lower green sand	U. Cretaceous	13.4	1.505	3.38	23	82	1	5	111	66
	Germany										
63	Bavaria, Landshut, Molasse, "green"	U. Miocene	14.5	1.497	3.38	33	64	2	6	105	64
64	Bavaria, Landshut, Molasse, "yellow"	U. Miocene	14.0	1.501	2.83	43	84	1	8	136	76
	France										
65	Vienne, Montmorillon	Tertiary	15.1	1.492	2.70	18	87	—	5	110	108

	Greece										
66	Milos Island	Pliocene	14.2	1.499	0.90	22	41	1	8	72	106
67	Milos Island	Pliocene	13.8	1.497	1.28	30	18	3	22	73	45
68	Milos Island	Pliocene	15.1	1.502	2.98	24	61	1	5	91	107
	Israel										
69	Negev, Ramon Makhtesh, Cenonian, "green"	U. Cretaceous	13.4	1.495	2.49	30	18	3	33	84	70
	Italy										
70	Ponza Island, La Forna, "ivory"	Tertiary	12.4	1.499	3.47	30	26	4	70	130	73
71	Ponza Island, La Forna, "white"	Tertiary	14.5	1.500	3.14	47	41	4	19	111	99
72	Ponza Island, La Forna	Tertiary	14.7	1.496	2.63	46	22	3	14	85	
73	Enna, Regabuto, Sicily	Tertiary	11.8	1.495	1.46						
	Spain										
74	Cabo de Gata, Minas de Gador	Tertiary	13.4	1.490	2.31	45	10	4	47	106	102
75	Granada	Cretaceous	14.7	1.502	2.41	18	9	3	40	70	
76	Granada	Cretaceous	15.5	1.501	3.71	13	175	4	44	236	91
	Switzerland										
77	Bischofszell, Molasse, "lower"	U. Miocene	14.3	1.499	6.46	92	130	1	10	233	89
78	Bischofszell, Molasse, "Ashrock"	U. Miocene	14.5	1.498	5.52	29	59	2	4	94	
	Yugoslavia										
79	Montenegro, Petrovac	Triassic	12.3	1.497	4.36	9	21		52	82	

* On ignited material from —1 μm fraction of clay stripped off exchangeable cations

TABLE 3.4B

Chemical analyses of bentonites from European and Eastern Mediterranean countries (on ignited material from —1 μm fractions of ammonium saturated clays)

Sample no.	SiO_2	Al_2O_3	Fe_2O_3	MgO	Li_2O	CaO	Na_2O	K_2O	Total	Impurities *
58	80.43	13.99	2.03	0.67	0.0	0.10	0.20	1.20	98.62	crist(50)
59	64.67	29.99	1.43	3.56	0.0	0.02	0.02	0.07	99.76	—
60	67.64	19.15	7.49	3.92	0.0	0.06	0.02	0.18	98.46	—
61	67.12	18.77	8.89	3.84	0.0	0.05	0.03	0.12	98.82	—
62	65.81	18.14	11.66	3.38	0.0	0.04	0.34	0.46	99.83	—
63	64.46	21.98	8.03	3.38	0.0	0.02	0.03	0.79	98.69	—
64	67.10	22.85	5.69	2.83	0.0	0.01	0.01	0.03	98.52	—
65	67.41	29.38	0.41	2.70	0.0	0.01	0.01	0.01	99.93	—
66	74.52	21.45	1.44	0.90	0.0	0.03	0.03	0.26	98.63	crist(20)
67	78.86	15.66	2.51	1.28	0.0	0.02	0.03	0.15	98.51	crist(40)
68	77.09	18.29	1.89	2.98	0.0	0.03	0.02	0.13	100.43	crist(30)
69	63.98	26.05	5.18	2.49	0.0	0.02	0.05	1.77	99.54	kaol(20)
70	78.71	14.84	2.06	3.47	0.0	0.04	0.09	0.60	99.81	crist(20)
71	77.79	16.88	1.16	3.14	0.0	0.02	0.02	1.23	100.24	crist(30)
72	72.92	21.72	1.63	2.63	0.0	0.11	0.02	0.18	99.21	crist(30)
73	80.06	14.35	2.46	1.46	0.0	0.07	0.06	0.26	98.72	crist(50)
74	61.47	29.64	1.96	6.02	0.0	0.20	0.08	0.49	99.86	—
75	58.01	24.24	11.26	2.41	0.0	0.26	0.14	2.40	98.72	kaol(10) mica(10)
76	61.98	20.74	7.76	3.71	0.0	0.03	0.16	4.50	98.88	Q(5)
77	70.00	19.52	2.53	6.46	0.0	0.08	0.06	0.17	98.82	Q(5)
78	67.78	24.39	2.21	5.52	0.0	0.33	0.19	0.35	100.77	—
79	69.51	21.91	2.35	4.36	0.0	0.03	0.04	0.72	98.92	crist(5)

* Impurities are semiquantitatively estimated from the X-ray diffraction data. (crist = cristobalite; kaol = kaolinite; Q = quartz.)

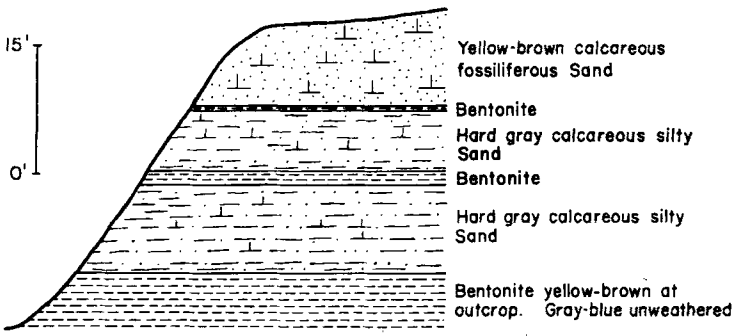

Fig. 3.40. Section of bentonite, Redhill, Surrey, England.

to several feet are found in a section of fairly hard, calcareous sands in the Sandgate formation of the Lower Greensand (Fig. 3.40). The clay is waxy and blue in color (sample 60) becoming yellow (sample 61) at the weathered outcrop. The blue clay contains nodules of pyrites and other sulfides. A similar clay from the same stratigraphic position is mined near Woburn in Bedfordshire (sample 62) and other occurrences are reported in the London basin.

Two beds of Fuller's earth near the base of the Jurassic Bathonian formation are found at Combe Hay in Somerset. The clay is blue when fresh and weathers to a yellow color. The beds are several feet thick and are separated by a sandy marl.

Both of the above fuller's earths can be classed as bentonites on the basis of their composition and properties. Also both of these clays are believed to have formed by the alteration of volcanic ash (Grim, 1933; Hallam and Selwood, 1968). However, the absence of volcanic activity in the area in these geologic intervals has caused this mode of origin to be questioned by some English geologists (Robertson, 1961; Poole et al., 1971).

Recently, Poole et al. (1971) have described the occurrence of several beds of fuller's earth in the middle silty and sandy group of the Lower Greensand in the Fernham area of Berkshire. In this area there are two main beds of bentonite, one of which attains a thickness of 12 ft. and has a calcium montmorillonite content of 80—85%. A small amount of zeolite (clinoptilolite) and quartz are also present. These authors accept the early thesis of Robertson (1961) that direct chemical precipitation in a marine environment was the major process of formation. Very recently Cowperthwaite et al. (1972) have agreed with the early conclusion of Grim (1933) that "the English Mesozoic fuller's earth are considered to be montmorillonite-rich deposits derived both directly from crystal-vitric ash falls that accumulated in small lagoons and indirectly from the rapid penecontemporaneous erosion of the ash falls covering adjacent land masses".

Mineralogical studies. The X-ray diffraction and the chemical data in Table 3.4A indicate that the samples investigated contain a predominantly Ca-montmorillonite as their major component. Furthermore three of these montmorillonites (samples 60, 61 and 62) contain unusually large amounts of Fe_2O_3 (Table 3.4B). The chemical formulae of the smectites, as calculated from the data in Table 3.4B, are given in the following:

Sample 59: $[(Si_{3.65}Al_{0.35})(Al_{1.64}Fe^{3+}_{0.06}Mg_{0.30})O_{10}(OH)_2]M^{+}_{0.65}$

Sample 60: $[(Si_{3.99}Al_{0.01})(Al_{1.32}Fe^{3+}_{0.33}Mg_{0.34})O_{10}(OH)_2]M^{+}_{0.35}$

Sample 61: $[(Si_{3.96}Al_{0.04})(Al_{1.27}Fe^{3+}_{0.39}Mg_{0.34})O_{10}(OH)_2]M^{+}_{0.38}$

Sample 62: $[(Si_{3.91}Al_{0.09})(Al_{1.18}Fe^{3+}_{0.52}Mg_{0.30})O_{10}(OH)_2]M^{+}_{0.39}$

Quartz, feldspars, and micas are the common impurities in the samples, and they are concentrated in coarser fractions (>10 μm).

Electron-optical observations show that the smectite particles occur

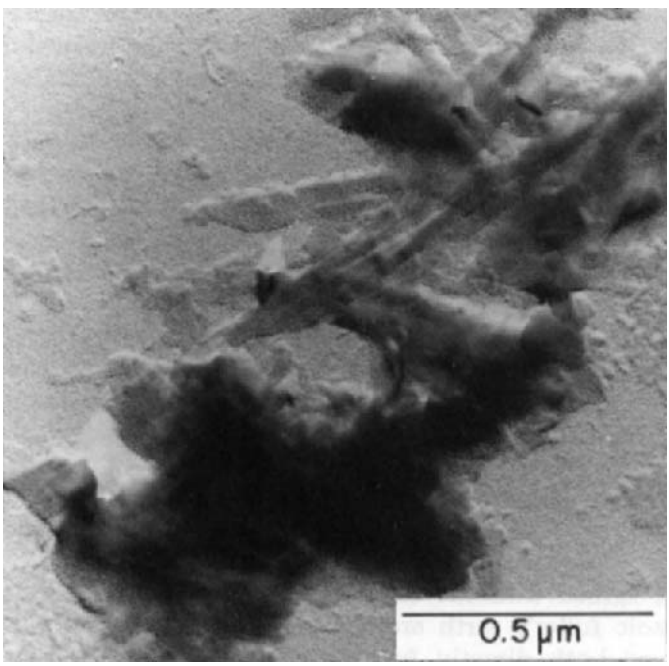

Fig. 3.41. Lath-shaped units and their aggregates in fuller's earth (sample 60) from England.

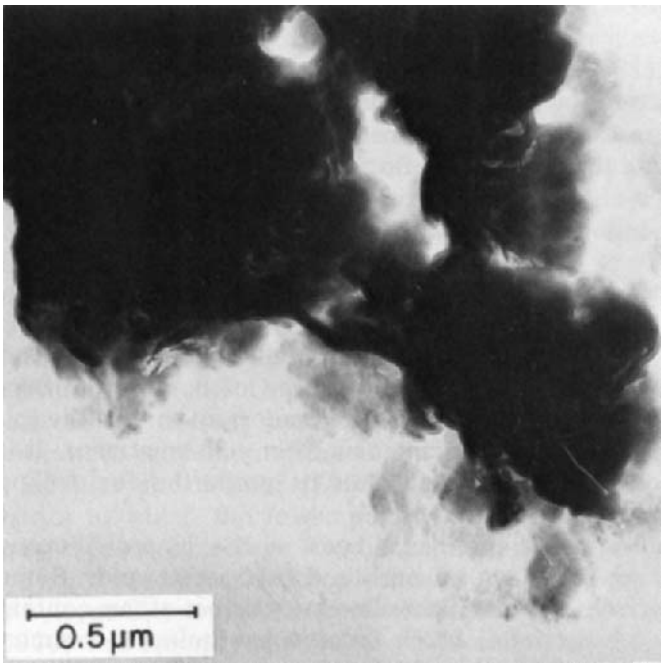

Fig. 3.42. Typical montmorillonite aggregates in fuller's earth from Woburn, England (sample 62).

mostly in the form of Cheto-type and compact lamellar aggregates in sample 59. The S-type crystallites of montmorillonites are also common, but they are often aggregated and form the compact lamellar aggregates. In the "blue lump" (sample 60), Cheto-type aggregates and lath-shaped units make up the smectite particles in about equal proportions. The laths are often aggregated in a haphazard manner as shown in Fig. 3.41. Similar smectite particles (Cheto-type aggregates and laths) are found in the "yellow earth" (sample 61). Smectites in the fuller's earth from Woburn (sample 62) occur again as Cheto-type aggregates (Fig. 3.42) and as aggregates of ill-defined laths.

Denmark

Unmack (1949) reports the occurrence of montmorillonite clays in the "fish clay" from Stevns, the Eocene "moler" from Siltstrup Sydklint, in Recent clays from Refsnaes, and in the Eocene clay from the vicinity of Hadsten. Whether or not any of these clays should be classed as bentonites is not clear.

Faroe Islands (Denmark)

According to Sabine (1971), a mudstone composed essentially of beidellite resulting from the alteration of tuff is found beneath coal in a Tertiary sedimentary series among Tertiary basalts in the Faroe Islands. The alteration of the tuff is reported to be "in situ". Bogvad (1937) reported a bleaching earth at Vaago with a chemical composition suggesting that montmorillonite is the dominant component.

Federal Republic of Germany

Extensive deposits of bentonite in the vicinity of Mainburg, Mossburg, and Landshut in Bavaria have been an important source of commercial bentonites for the European and world markets. The crude bentonite is the calcium variety and is an excellent decolorizing clay after acid treatment. It is also subject to treatment with soda ash to alter its properties for drilling mud, bonding molding sands, etc.

The Bavarian bentonites occur in several beds in the Upper Miocene Molasse, in a generally marine section of marls and tuffaceous sands. Some of the bentonites are relatively pure montmorillonite, whereas others contain considerable illite and some kaolinite, which restricts or eliminates commercial usage. Some beds attain a thickness of 10 ft. It is generally agreed that the bentonite has formed by the alteration in situ of acid vitreous tuff.

The occurrence of bentonite at Landshut illustrates the foregoing occurrence of the German bentonites (Fig. 3.43). At this location a 10 ft. bed of bentonite (sample 64) overlain by sand and underlain by green sandy bentonitic clay (sample 63) is worked in an open cut. The bentonite is fairly uniform, light yellow gray in color with the lower part being reportedly the highest grade. A characteristic of the upper part of the bentonite horizon is

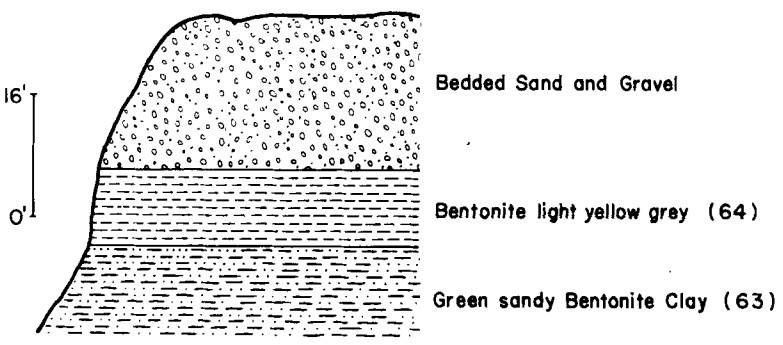

Fig. 3.43. Section of bentonite at Landshut, Bavaria, Germany.

the presence of nodular masses up to 2 ft. in diameter of worthless material consisting of hard blueish clay. The nodules appear similar to the "blue eggs" in some of the Wyoming, U.S.A., bentonite. As in the case of the "blue eggs", in the Wyoming bentonite, a smectite is the dominant component and the cause of poor quality of the material is not evident.

Much of the Bavarian bentonite is obtained by underground mining. The soft sandy overburden requires extensive timbering. In a few cases the bentonite beds are overlain by a hard strata which facilitates the mining, but in general such bentonites are reported to be low grade. At some places a soft white siliceous material directly underlies the bentonite horizons.

Numerous other occurrences of bentonite have been reported from Germany. Valeton (1960) described a bentonite derived from tuff in a calcareous bed of the Upper Chalk in northwest Germany. Several bentonite horizons are present and some of them contain the zeolite heulandite, in addition to calcium montmorillonite.

Schüller and Köhler (1953) describe an occurrence at Steinberg, near Ostritz in which the lower part of a nepheline basanite has altered, apparently by deuteric action, to a calcium montmorillonite.

Fahn (1965) has reported occurrences of bentonite at Thannhausen in Swabia, at Unterrupsroth on the Rhine, and in the Fichtelgebirge. Antiorgitis (1970) has recently described a bentonite from Rossberg near Darmstadt that has formed by the alteration of a tuffaceous basalt.

Mineralogical studies. The X-ray diffraction and chemical data in Table 3.4 indicate that the samples 63 and 64 contain a montmorillonite carrying mostly calcium with possibly some magnesium as exchangeable cations. The discrepancy between the C.E.C. and total extractable cations suggest that part of the extractable calcium and magnesium must be derived from other minerals. The smectites are distinguished by their unusually high iron contents. Their structural formulae are given in the following:

Sample 63: $[(Si_{3.81}Al_{0.19})(Al_{1.34}Fe^{3+}_{0.36}Mg_{0.30})O_{10}(OH)_2]M^{+}_{0.49}$

Sample 64: $[(Si_{3.93}Al_{0.07})(Al_{1.50}Fe^{3+}_{0.25}Mg_{0.25})O_{10}(OH)_2]M^{+}_{0.32}$

The samples contain appreciable amounts of micas, kaolinite, quartz, and feldspars. The "green sandy clay" (sample 63) has a high content of mica (about 40—50% of the material in the $>10\,\mu m$ fraction), whereas the "yellow clay" (sample 64) contains only 5—10% mica.

Electron-optical examination of the "green sandy clay" (sample 63) showed that montmorillonites occur mostly as (Otay-type) globular aggregates. Micas are frequently observed in the clay fraction, and one of them is shown in Fig. 3.44 with its superimposed SAD pattern. Micas formed by reticulated laths intersecting at 120° are seen in Fig. 3.45A, from the "yel-

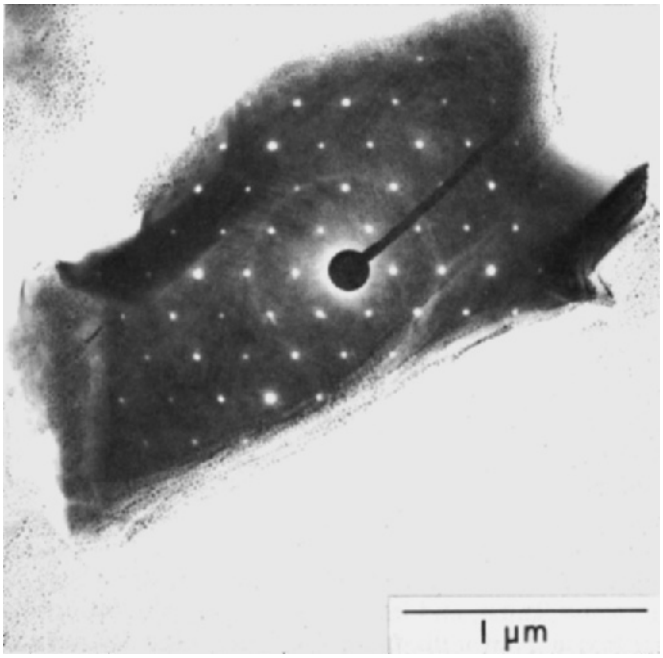

Fig. 3.44. A mica flake in bentonite (63) from Bavaria, Germany.

low clay" (sample 64). Although one of the sets of laths is not as well developed as the other, their SAD pattern (Fig. 3.45B) displays a spot pattern similar to that of a $2M_1$ dioctahedral mica. Similar sets of mica laths were described by Güven (1974), but in this sample, the original particle (Fig. 3.45A) seems to be a montmorillonite aggregate from which the laths of mica are developing.

The smectites in the yellow bentonite (sample 64) occur mostly as Chetotype aggregates but occasionally as compact lamellar aggregates.

France

There has been little commercial development of bentonites in France, apparently because the deposits have not been large or very high grade, and also because of the extensive development of bentonites in North Africa by French interests.

Fuller's earths composed largely of smectite have been known for a long time in the Paris Basin, and in the vicinity of Vaucluse, Apt, Moimoiron, and Sommières (Charrin, 1951). These clays do not have the high colloidal properties of bentonites generally, but on the basis of their clay mineral

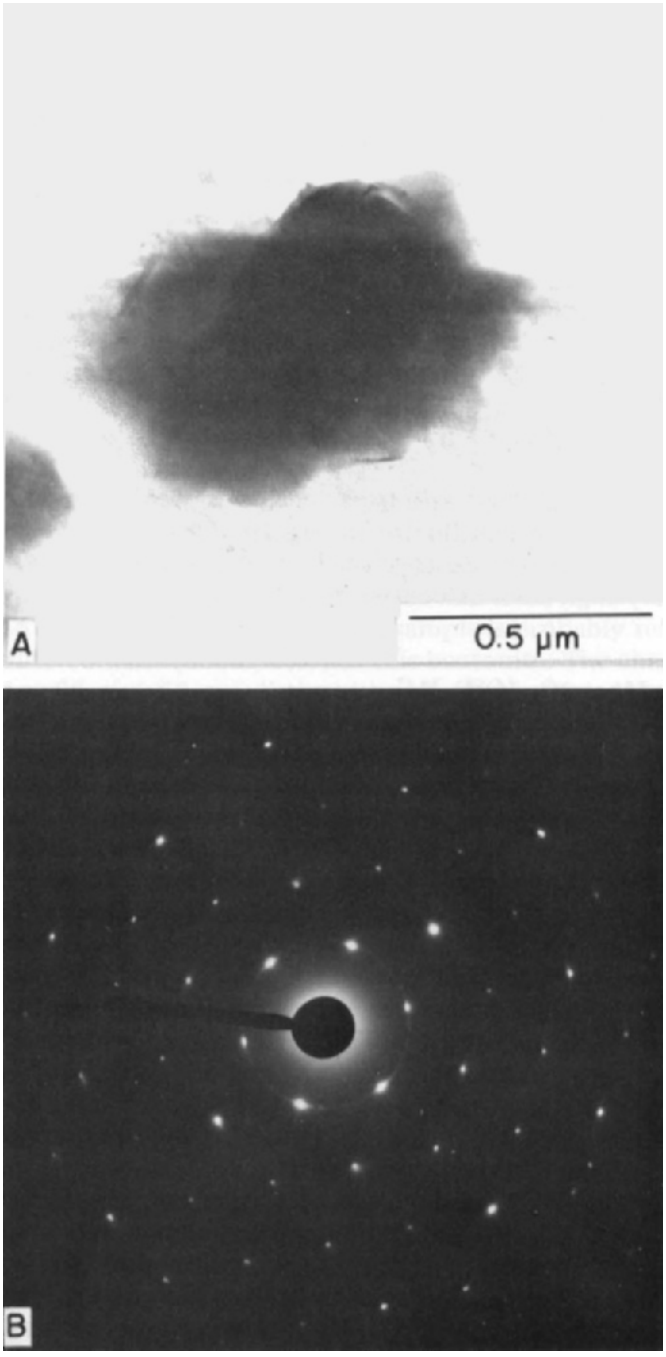

Fig. 3.45. A. Two sets of laths (intersecting at 120°) that seem to have developed from a montmorillonite aggregate in the bentonite (63). B. Its SAD pattern.

composition could be so classified. The same author reports the occurrence of lenticular beds of relatively pure montmorillonite in formations of Lower Eocene age on the western flank of the Perigord region. These beds extend from the Lot Valley to the Gironde estuary, and are particularly well developed near Bouillac and Cadoun.

Déribéré and Esme (1951) have reported the occurrence of clays in the Pyrenees and Limousin in Tertiary beds which have colloidal properties that seem to warrant the term bentonite. The same author notes a deposit at Caillard near d'Alzon in the Card area which has been used as fuller's earth and could be classed as bentonite.

Small deposits of clay, some of which are composed of montmorillonite, are found in the Tertiary formations of the central region. One of these deposits at Montmorillon (Vienne) has supplied the type mineral montmorillonite (Damour and Salvétat, 1847).

Mineralogical studies. The sample from the type locality at Montmorillon contains a predominantly Ca-montmorillonite as suggested by the data in Table 3.4A. This montmorillonite is distinguished by its exceedingly low iron content and unusually high alumina content (Table 3.4B). Its structural formula is calculated as:

$$[(Si_{3.80}Al_{0.20})(Al_{1.76}Fe^{3+}_{0.02}Mg_{0.23})O_{10}(OH)_2]M^{+}_{0.43}$$

Kaolinite and feldspars are present in small quantities (5—10%) in the $>10\,\mu m$ fraction of the sample. Our electron-optical observations showed that smectite particles in the sample occur mostly as compact lamellar and foliated aggregates. The S-type lamellae make up about 20% of the smectites.

Greece

Geological features. Several of the volcanic islands of Greece are known to contain bentonites of which the large extensively developed deposit on the Island of Milos is the best known (samples 66, 67, and 68). Geologic maps of Milos show it to be composed mostly of relatively acid igneous material with some interbedded limestone of Pliocene and Recent ages. The bentonites have formed from liparite, dacite, and associated tuffs. The tuffaceous material is glassy, perlitic, and spherulitic in character. The bentonite commonly retains the macroscopic aspects of the parent rock. The genesis of these deposits has not been described, but it is probable that deuteric action and hydrothermal activity have been important in their formation. At some places the perlitic tuffaceous material is unaltered, or small pockets and disseminated masses of clay are found in the glass. At other places the alteration is fairly complete with some perlitic glassy material disseminated through the clay. At still other places the alteration is essentially complete, and there are large masses

of quite pure smectite. Possibly the amount and location of the alteration depended on the presence and abundance of gaseous material in the parent tuffaceous rock. The bentonite is the calcium variety, and in some cases small amounts of cristobalite and kaolinite or halloysite are also present. It is of interest that deposits of kaolinite and relatively pure soft silica are also present on the Island of Milos, so that at some places the alteration has been to kaolinite or silica rather than to smectite.

The type of alteration product appears related to the type of parent igneous rock as well as to the nature of the hydrothermal agents.

Bentonite is also known on the island of Polivos, northeast of Milos, and from Kimolos. Robertson (1958) pointed out that the Kimolos earth has been known and used from very early times as a fuller's earth. The Kimolos bentonite contains appreciable cristobalite. The geologic setting and origin of the Kimolos bentonite is similar to that on Milos.

Mineralogical studies. The bentonites (samples 66 and 68) contain a smectite carrying primarily calcium with some magnesium as exchangeable cations (Table 3.4A). The smectite in sample 67 seems to carry more magnesium and sodium than calcium according to the data in Table 3.4A. The low C.E.C. (45 mequiv./100 g) of the latter sample is probably related to the high cristobalite content (about 40%) of this bentonite. The chemical analyses of smectites 66 and 67 are distinguished by their exceedingly low magnesia values (Table 3.4B) even after accounting for the cristobalite in the analyzed material. These smectites are probably beidellites. Quartz, feldspars, micas, and kaolinite are common impurities in the above samples from Greece, but the kaolinite content in sample 68 is much higher than in the other samples. The morphological features of smectites in samples 66 and 67 are very similar. Wyoming-type (foliated) aggregates and S-type lamellae are the common forms of smectites. The individual smectite lamellae (S-type) have unusually large lateral dimensions ($2 \times 3\ \mu m$). Cristobalite and smectite form fine-grained intergrown aggregates in these samples. In sample 68, Wyoming-type aggregates make up half of the smectite particles. The rest of the smectites is made up of S- and E-type lamellae in about equal amounts. Lath-shaped units of smectite are rarely observed.

Hungary

Bentonite production in Hungary began in the 1930's, and in recent years the country has become an important producer of bentonite from a considerable number of deposits. Szeky-Fux (1957) has classified Hungarian bentonites in two groups on the basis of their origin as follows: (1) derived dominantly by hydrothermal alteration of rhyolites and pyroxene andesites as illustrated by deposits at Komloska, Mad, and Vegardo, and (2) derived by the alteration of rhyolitic-dacitic tuff which fell in the sea and altered under

marine conditions, as illustrated by deposits at Istenmezo, Nagyteteny, and Band. The latter deposits are Sarmatian (Tertiary) in age, and the former deposits are tied to Tertiary volcanism.

Szeky-Fux (1957) has studied the Komloska deposit in detail, and the following data are from her report. Dikes of rhyolitic tuff and pyroxene andesite have been altered by siliceous magnesium-rich hydrothermal solutions to about pure montmorillonite except for slight alteration locally of feldspar to illite and kaolinite. The alteration appears to have started from fractures and spread outward. The center of the dikes is generally altered completely to clay with gradations to partially altered rock at the edges. The texture of the parent rock tends to be preserved in the bentonite. Two types of bentonite occur in the Komloska deposit: a hard white to green variety derived from the rhyolite, and a more plastic yellow-green variety derived from the andesite. The hardness of the white bentonite is probably due to the presence of opaline material. All of the Komloska bentonite is the calcium variety. Small quantities of sulfide minerals (galena, pyrite, and sphalerite) are found in the bentonites.

The sedimentary bentonites are altered rhyolitic tuffs in a marine sequence of Sarmatian Tertiary age. The beds are reported to attain a thickness of 10 m, but some times the alteration to montmorillonite is not complete, in which case the clays are of no commercial value as illustrated by the bentonite from Kobanya in the Budapest region (Szeky-Fux, 1948).

Barna (1956) has described a bentonite formed by the alteration of basalt from Monostorapati. The smectite component is the high iron variety (9.41% Fe_2O_3) and carries calcium and magnesium as exchangeable cations.

Israel

Beds of bentonite are exposed along the road going down the north side of the Ramon Makhtesh in the Negev. According to Weissbrod (1962), the bentonite is in the lower part of the Cenomanian sequence (Fig. 3.46). In addition to montmorillonite, illite is also a component, but is usually of minor importance. The bentonite occurs in a fossiliferous marine section — in fact some of the bentonite beds contain marine fossils. Five beds of bentonite are reported by Weissbrod (1962), ranging in thickness from a few inches to about 6 ft. The thickest bed is made up of three distinct layers differing from one another in color and composition. The color varies from green-yellow to gray-black. Thin layers of limestone are interbedded with the thicker bentonites. Gypsum, halite and alunite (?) are distributed in the bentonites in the form of veins and fissile planes. According to Wolff and Minkoff (1962), the smectite in the bentonites is the high magnesium variety (6% MgO). Bentor (1966) states that "it must be concluded that the Ramon bentonites represent a normal marine sediment" because no contemporaneous volcanic activity is known short of Mount Carmel 220 km to the north.

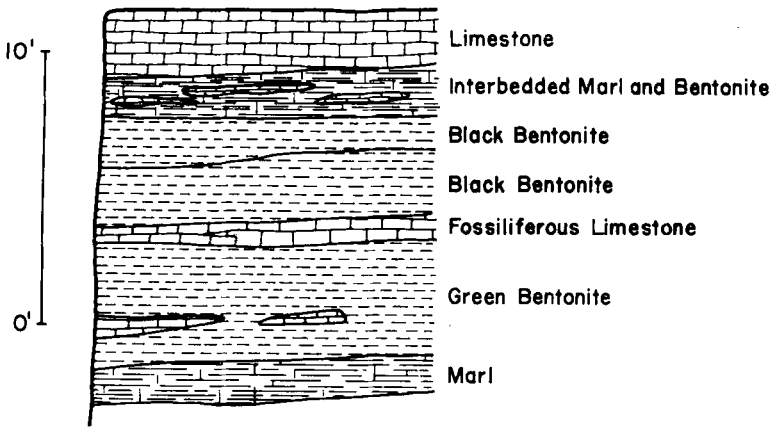

Fig. 3.46. Generalized section showing bentonite occurrence, Makhtesh Ramon, Israel (after Weissbrod, 1962).

However, as has been mentioned frequently, there are many deposits of bentonite in areas where there is no record of contemporaneous volcanic activity. These bentonites have very probably formed by the alteration of volcanic material.

Bentor (1966) recorded the presence of bentonites in a section of Late Jurassic age in Makhtesh Hazera. In the Ramon bentonite the montmorillonite carries both sodium and magnesium as the major extractable cations (Table 3.4A). Its chemical composition is calculated from the data in Table 3.4B as:

$$[(Si_{3.64}Al_{0.36})(Al_{1.30}Fe^{3+}_{0.44}Mg_{0.26})O_{10}(OH)_2]M^{+}_{0.62}$$

Italy

Geological features. Bentonites are found at many places in Italy, but the large deposit at La Forna on the Island of Ponza is the most widely known. The Ponza bentonite (Fig. 3.47) occurs in a mass 20 ft. or more in thickness, and dips at an angle of about 60°. Vertical drilling has proven bentonite to at least 150 ft. The uppermost part of the bentonite is soft, and grades downward from ivory (sample 70) to blue-white (sample 71) in color. At depth the bentonite becomes hard with a loss of some plastic and colloidal characteristics. The bentonite is quite pure smectite, and calcium is the dominant exchangeable cation.

Rhyolitic glassy tuff encloses the Ponza bentonite, and the smectite is believed to have formed by a combination of deuteric and hydrothermal alteration of the rhyolite. At places the bentonite is

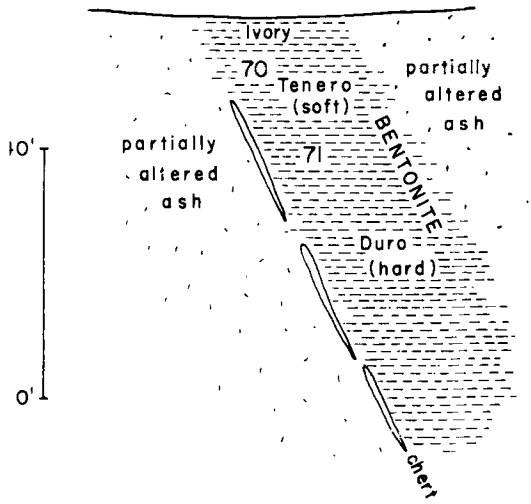

Fig. 3.47. Generalized section of Ponza bentonite deposit at La Forna, Island of Ponza, Italy.

underlain by silicified tuff indicating some downward movement of silica.

Bentonites are reported also from many other localities in Italy, for example at Puglia, Publiese, Foggia, Apulia, Forti, and Campobasso. Poppi (1972) has recently reported an occurrence of bentonite formed by the alteration of basic rocks in the vicinity of Lessini and Berici.

Cavinato (1957) has concluded that many of the Italian bentonites are due to late magmatic alteration, i.e. following intrusion, alteration took place during cooling by the action of gasses and vapors present in the intruded rock.

Alietti (1962) has described an interesting bentonite from Gemmano (Forli) containing both calcium and sodium montmorillonites which can be separated by sedimentation methods. The deposit is said to be of sedimentary origin.

Bentonites are also well known in the Sadali, Cagliari, Urix, and Vallanova Tulo areas of Sardinia where they are reported to have formed by the hydrothermal alteration of trachytes and trachytic tuffs (Annedda, 1956). Production is reported at Nurallo.

Pietracaprina et al. (1972) have recently described a deposit at Uri, Sardinia, where the bentonite forms a succession of lenticular beds 1—2 m thick within trachy-andesites. The bentonization process seems to have proceeded entirely at the expense of the pyroclastic lenses. In general, the bentonite lenses are entirely enclosed in non-argillized lavas. The bentonite contains, at places, masses of unaltered or partially altered lava. Cristobalite and "hydrated silica" make up 20—30% of these bentonites. Deuteric alteration

appears to have been the dominant process for the formation of these bentonites.

Wayland (1971) has recently noted a bentonite in Miocene marine sediments near Alghero in Sardinia.

Bentonites are also reported in Sicily (sample 73) as alteration products of volcanic material.

Mineralogical studies. The Ponza bentonites (samples 70, 71, and 72) as well as the Enna bentonite from Sicily (sample 73) contain large amounts of cristobalite (40—50%) in addition to smectites in the >10 μm fractions of the samples. The fine fractions (—1 μm) of the same samples also carry large quantities of cristobalite as indicated by high SiO_2 values in Table 3.4B. Quartz, feldspars, micas, and kaolinite are the common impurities. The plagioclase content of samples 70 and 71 is especially high, and it makes up about 30—40% of the >10 μm fraction. The basal spacings and the extractable cations of smectites in Table 3.4A suggest that the smectites 71 and 72 carry predominantly Ca and Mg as exchangeable cations, whereas the samples 70 and 73 contain a predominantly Na-montmorillonite.

Morphological features of smectite particles are very similar in all the

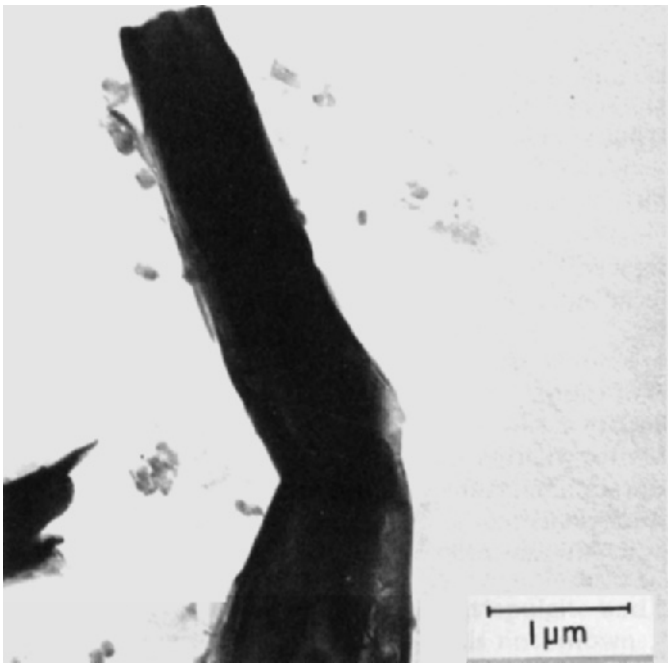

Fig. 3.48. Ribbon of montmorillonite in the Ponza bentonite (72) from Italy.

above four samples. Wyoming-type (foliated) aggregates are predominant in these samples. A large number of S-, E-, and L-type crystallites are also found in all of them. The laths and ribbons seem to be formed by backfolding of the thin lamellae. A typical ribbon is shown in Fig. 3.48 from the sample 72. Aggregates of fine-grained cristobalite with montmorillonite ribbons were described from the latter sample by Güven and Grim (1972).

Poland

Bentonites have been described from many places in Poland. They are particularly well known in Middle Tertiary formations in the Carpathian area where they are thought to have formed by the hydrolysis of volcanic glass blown from the inner Carpathian region during the intensive Tertiary volcanic activity within the Carpathian arc (Tokarski, 1953). This same author (Tokarski, 1948) earlier described such bentonites from Podolia and Volhynia where they occur interbedded with Sarmathian—Tortonian sands of Miocene age. Heflik (1959) has described bentonites of similar age and mode of origin in a sequence of bentonitic clays from Ciecierze near Chmielnik. Sujkowski (1934) and Kamienski (1935) also described bentonites from altered ash in the Miocene from Krzemienca and Lwow, and pointed out the connection with volcanic activity in Transylvania. Langier-Kuzniarowa (1967) has recorded several occurrences of bentonite in bore holes penetrating Miocene beds in the Szydlow area, and has particularly noted many alternations of bentonite and clay. The alteration of the parent volcanic ash is quite variable, at places unaltered ash and fresh feldspars are dominant whereas elsewhere the ash and feldspar are thoroughly altered to smectite.

Sikora and Wieser (1959) have recorded bentonite beds in variegated Eocene shales of the Magura nappe south of Grybow. The non-clay mineral components provide evidence for a volcanic origin of the bentonite. Gucwa and Koszarski (1960) describe bentonite horizons interlaminated with glauconitic sands in Oligocene Krosno beds at Zagorz near Sanok in the Carpathians. These same authors record other occurrences of bentonite in the Carpathians.

Alexandrowicz and Parachoniak (1958) and Krauss and Rutkowski (1962) have described bentonites of Cretaceous age in the Miechow region of Poland. Bentonites near the boundary between the Lower and Upper Cretaceous are almost pure montmorillonite, whereas those in the Lower Maastrichtian are more nontronitic and contain admixtures of kaolinite. These bentonites are interbedded with limestones and marls, and are believed to be associated with volcanic activity in the external zone of the Carpathian geosyncline.

Portugal

Galopim de Carvalho (1970) reports the occurrence of montmorillonite-rich sediments in formations of Tertiary age at many places in Portugal,

notably near Lisbon at Lantarem and Torres Novas, in the Setubal Peninsula, and near Ponte de Soro. At the last locality smectites carrying sodium as the exchangeable cation are reported. This same author states that attapulgite beds are frequently associated with the montmorillonite clays.

Montmorillonite is also reported at several localities by Silva and Neiva (1948) in pegmatites as a hydrothermal alteration product.

Rumania

Bentonites of Cretaceous and Tertiary age are extensively developed in many areas in Rumania. They are particularly well known in the Banat, Dobrogea, and Transylvania areas (Cardew, 1952; Ghergariu and Mirza, 1961; Neaesu, 1962). Alteration of volcanic ash has been the general mode of origin of these clays. Of special interest is the occurrence of some bentonites in a lacustrine series of sediments, and the andesitic composition of some of the parent ash. According to Nedelcu (1968) both calcium and sodium varieties are known in the Oarda area. Popescu and Mares (1971) report that beds of diatomaceous earth are associated with the bentonites of southern Dobrogea.

Bentonites are known also which have been formed by hydrothermal action. For example, Dittler and Kirnbauer (1933) described an occurrence at Tomesti where a liparite has been hydrothermally altered to smectite, but still retains its original texture. Depth of alteration is cited as evidence for the hydrothermal mode of origin.

The composition and properties of the Rumanian bentonites have been extensively investigated and reported in a series of papers by Felszeghy and his associates (1963—1968). These studies have indicated a wide variety of bentonites — both calcium and sodium types are indicated. Leonida-Zamfirescu (1943) has stated that some of the bentonites are good decolorizing clays either in the natural state or after acid activation.

Spain and Spanish Morocco

Geological features. Numerous deposits of bentonite have been developed in the vicinity of Almeria in the Cabo de Gata area of eastern Spain (sample 74). According to Martin-Vivaldi and Linares Gonzales (1969), these deposits have formed by hydrothermal alteration of Tertiary rhyolite-dacites. The process has involved the removal of some silica, iron, alkalies, and alkaline earths, and the addition of aluminum and magnesium. In some occurrences, there have been relatively large additions of magnesium with the formation, frequently in veins, of attapulgite and sepiolite rather than smectite. The source of the magnesium is not known. At still other places, relatively large amounts of silica remain in the clay in the form of cristobalite.

Linares et al. (1972) have further considered the process of hydrothermal alteration of the Cabo de Gata bentonites. According to them, chromium, nickel, and cobalt are concentrated in the colored bentonites.

The Cabo de Gata deposits are quite large and relatively uniform, particularly for deposits of hydroxythermal origin. Some working faces are 25 ft. or more in height, and exploration has indicated continuation of the bentonite to depths of 50 ft. or more. The clay appears to be rather sharply bounded laterally by unaltered igneous material, but this has not been studied in detail. The texture of the parent rock is preserved in the bentonite. These bentonites are another example of the puzzling occurrence of a large mass of igneous rock altered to a smectite — all of the parent minerals being altered to a single clay mineral. At least part of the explanation must reside in the character of the altering agents — in this case perhaps due to their high magnesium content. It is difficult to understand the retention of the texture of the parent rock by the bentonite in the face of substantial changes in chemical composition accompanying the alteration process.

Martin-Vivaldi (personal communication) has reported bentonite in sediments of Cretaceous age in the vicinity of Granada (samples 75 and 76). In the vicinity of Cabana de la Sagra on the highway from Madrid to Toledo, bentonite is found in beds up to 4 ft. thick in a series of dolomites and dolomitic sands of Miocene age. It is of interest that the magnesium smectite saponite is the component of these bentonites.

Bentonites similar to those at Cabo de Gata are reported in Spanish Morocco by Gutierrez-Rios and Hernando (1947). An example is the deposit at Tidinit in which the parent material is andesite. Other deposits are reported at Gurugu and Cabo Quilates. In some of these places smectite is associated with considerable kaolinite (or possibly halloysite) and consequently the processes of alteration are more readily understood. Near Mount Maaza, there is a sedimentary deposit in which beds of smectite are very regularly interstratified with beds of sand.

Mineralogical studies. Sample 74 contains a montmorillonite carrying both magnesium and sodium as exchangeable cations (Table 3.4A). The latter montmorillonite with its chemical formula:

$$[(Si_{3.56}Al_{0.44})(Al_{1.69}Fe^{3+}_{0.11}Mg_{0.20})O_{10}(OH)_2]M^{+}_{0.64}$$

has an unusually high alumina content (29.64%). The bentonites from Granada contain smectites with exceedingly high iron contents (Table 3.4B). The chemical formula of the sample 76 is calculated to be:

$$[(Si_{3.80}Al_{0.20})(Al_{1.30}Fe^{3+}_{0.36}Mg_{0.34})O_{10}(OH)_2]M^{+}_{0.54}$$

Quartz, feldspars, mica, and kaolinite are the common impurities in the

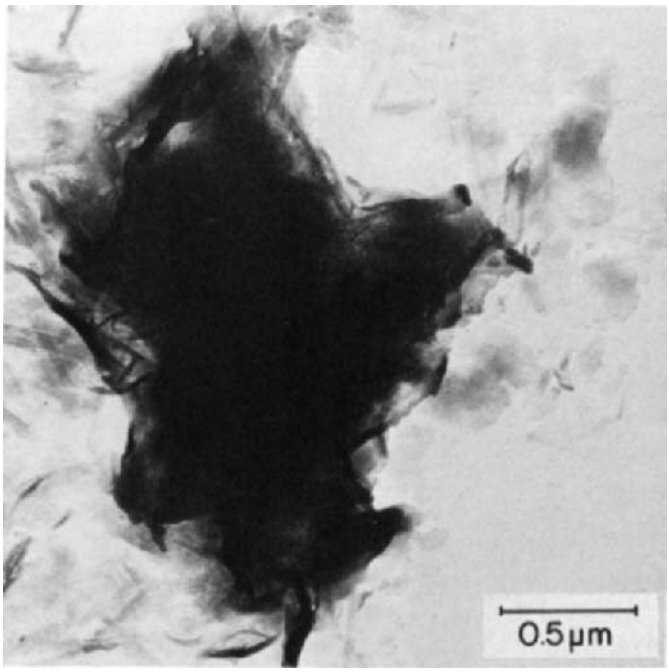

Fig. 3.49. An aggregate containing fibrous units in bentonite from Cabana de la Sagra, Spain.

above samples. In addition, a small amount of gypsum (10%) is present in sample 76 and calcite (10%) in sample 75.

In the bentonite of Minas de Gador (sample 74), montmorillonite particles occur almost entirely (80—90%) in the form of Cheto-type irregular aggregates. The S- and H-type lamellae are rarely observed.

In the bentonite from Cabana de la Sagra, saponites occur mostly as aggregates of fibrous or lath-shaped units. The chemical analysis of the sample gives 34% magnesia. A typical aggregate is shown in Fig. 3.49 in which fibers seem to grow from a flaky smectite mass. The lath-shaped units from this sample are described elsewhere by Güven (1974).

In the bentonites from Granada (samples 75 and 76), the morphological features of smectites are very similar. Otay-type globular aggregates make up about 80—90% of the smectite particles. These aggregates are associated with laths as shown in Fig. 3.50 from sample 76. Some of the laths seem to grow from the smectite aggregates and others simply to be entangled with them.

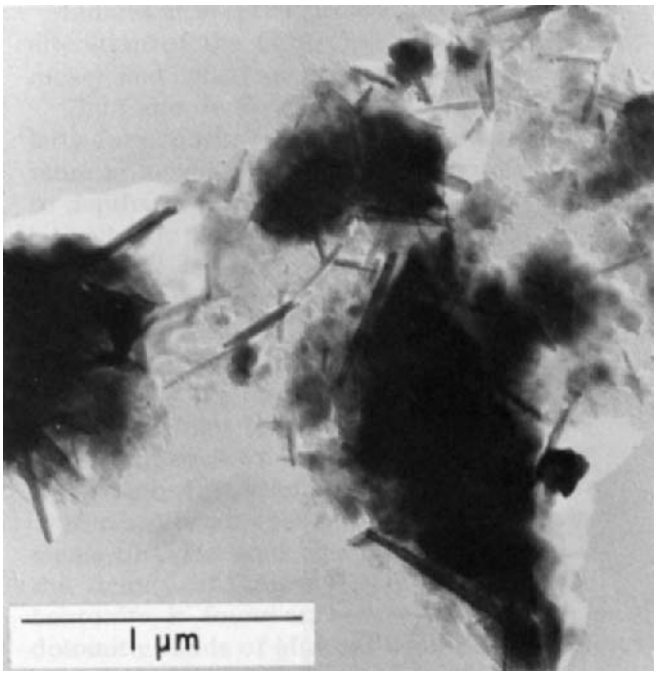

Fig. 3.50. Typical aggregates of smectites associated with lath-shaped units in the Granada bentonite from Spain (sample 76).

Switzerland

Geological features. Bentonite in beds up to 2 ft. thick has been described as an alteration product of andesitic and trachytic ash and tuff in the Miocene Molasse of Switzerland. More than two dozen deposits have been described. The clays are commonly associated with fresh water marls. The locations of the volcanic vents producing the ash have not been determined. At Bischofszell, Hofmann (1956) has described a section (Fig. 3.51) in which several layers of unaltered and partially altered ash (sample 78) sharply separated from each other abruptly overlie a bentonite horizon (sample 77). This has led Hofmann et al. (1975) to the concept that the ash was converted to montmorillonite as a result of hydrothermal conditions during the eruption in the volcanic pipes. Clearly what is akin to deuteric action, as visualized in the present volume, is contemplated. It is emphasized that weathering has played no part in the origin of the bentonites.

Saponite clays derived from the alteration of basaltic tuff have been described from the Molasse at Karolihof (Hofmann, 1959). The crude brown clay contains considerable calcite and unaltered grains of pyroxene and

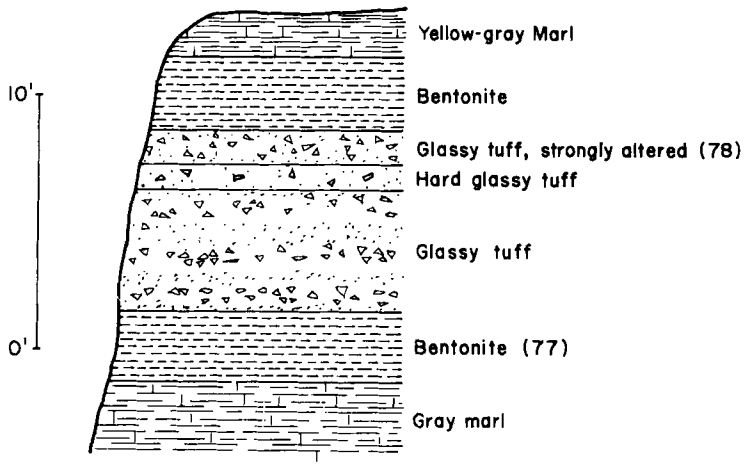

Fig. 3.51. Section at Bischofszell — Niederhelfenschwil, Switzerland (after Hofmann, 1956 — Eclogae Geol. Helvetiae, 49: 113—133).

magnetite. An analysis of purified saponite shows 42.30% SiO_2; 7.48% Al_2O_3; 7.10% Fe_2O_3; 4.56% CaO; 17.19% MgO and 70 mequiv. 100 g/cation exchange capacity. Serpentine and a mixed-layer chlorite—smectite are believed to be intermediate forms in the alteration of pyroxene—olivine parent rock to saponite. The glassy component of the tuff altered directly to the saponite.

All of the Swiss bentonites carry calcium as the major adsorbed cation.

Mineralogical studies. Samples 77 and 78 contain primarily a smectite which carries calcium and magnesium as exchangeable cations (Table 3.4A). The smectites are characterized by rather high magnesia in their chemical analyses in Table 3.4B. The chemical formula for the smectite 78 is calculated as:

$$[(Si_{3.82}Al_{0.18})(Al_{1.44}Fe^{3+}_{0.09}Mg_{0.46})O_{10}(OH)_2]M^{+}_{0.64}$$

Micas, kaolinite, quartz and feldspars are the common impurities in these samples. In addition, small amounts of cristobalite are suspected in these samples, as the 4.04 Å reflection of cristobalite is barely recognizable. The smectite particles in sample 77 occur mostly in two forms: Otay-type globular aggregates and compact lamellar aggregates. The smectites in the ash rock (No. 78) are mainly in the form of Cheto-type aggregates.

Turkey

Wayland (1971) lists an occurrence of bentonite of Cretaceous age in north central Turkey, but gives no further information concerning the

deposit. Deposits are reported at Eskisehir, Cankiri, and in Tokat Province.

Mineral analyses of a sample collected at Akpinar village, 11 km east of Rize in Northeast Turkey showed the presence of substantially pure montmorillonite.

Yugoslavia

Geological features. Bentonites are widely distributed in Yugoslavia, and material of excellent quality is produced commercially in many sections of the country. According to Lukas (1968), important layers of bentonite are found in Slovenia at Poljanskaluka, Kosovska Kamenic, Vrdnik, Kriva Palanka, Petrovac na Moru and Zolasak Gorica. The oldest deposit is at Petrovac na Moru and is from Triassic formations. The other deposits are Middle to Upper Tertiary in age. According to Rihtersic (1958), Oligocene andesite tuffs occur extensively in the basin of the Calje River in Slovenia and have altered to bentonite in many places, e.g., Blagovno and Sentjurij. Some of these latter bentonites contain cristobalite and zeolites and of interest is the statement by Drzaj and Kacjan (1968) that on acid activation the zeolite-bearing bentonites have relatively higher bleaching capacity for oils.

Nikolic and Obradovic (1963) describe a bentonite from Blace in Serbia which occurs within a lignite coal seam, and Trubelja (1966) describes a bentonite resulting from alteration of volcanic ash from Podhum village south of Livno. Stangatchilovitch (1963) described a bentonite in the marine cycle of the lignitic sequence in the Bogovina basin of Serbia.

Several deposits of bentonite commonly known as Ginovici clay are found near Kriva Palanka in Macedonia. The bentonite beds, up to 5 m thick, occur within brown gravelly loam of Upper Pliocene age. Small amounts of cristobalite are reported in the bentonite, but commonly the montmorillonite content reaches 85%. According to Sepesi and Hedjkezi (1966), this bentonite formed by the alteration of dacite tuffs in lacustrine water. In an earlier study of these deposits, Keramata (1957) pointed out that in some of them unaltered glassy dacitic tuff is interlaminated with beds of bentonite. Keramata (1957) emphasizes that magnesium was added in the formation of the bentonite from the ash. Konta et al. (1971) have described four microscopically distinct varieties of bentonite from the Ginovici locality.

Obradovic and Knezevic (1972) report bentonites at many places in the volcanic sedimentary series of Ladinian age in the Montenegrin littoral region of Yugoslavia. Various types of zeolite (clinoptilolite, analcime, leonardite), celadonite, and smectite are identified as diagenetic alteration products of volcanic glass. At places there is a gradual transition of tuffs to bentonite; elsewhere there is an alternation of bentonites and cherts. Clinoptilolite is described as an intermediate product in the alteration of the volcanic glass to smectite.

Currently bentonite production is reported near Pula in Istria, Kutina in Croatia, Laktasi in Bosnia, Kriva Palanka in Macedonia, and Petrovac in Montenegro (sample 79).

Mineralogical studies. The bentonite sample from Montenegro (79) contains a predominantly sodium montmorillonite (Table 3.4). The >10 μm fraction of the sample has at least 40% cristobalite but the fine fraction (—1 μm) only 5% cristobalite. The montmorillonite particles are mostly in the form of Cheto-type aggregates.

References

Austria

Janik, V., 1971. Chemical properties of the bentonite from Gossendorf, Styria. Mitt. Mus. Bergbau, Geol. Tech. Landesmus. "Joanneum", Graz, Abt. Mineral., (1—2): 51—52.

Kopetsky, G., 1961. Bentonit Lagerstätten am Gossendorf, Styria. Mitt. Mus. Bergbau, Geol. Paleontol., Graz, 43—53.

Paulitsch, P., 1953. Relict structure in Styrian bentonites. Mitt. Naturw. Ver. Steiermark, 83: 169—170.

Petrachek, W., 1940. Vulkanische Tuffe im Jungtertiär am Ostalpenrande. Akad. Wiss. Wien, 149: 145—154.

Bulgaria

Atanasov, G. and Goranov, A., 1963. Bentonitic clays from the region of Kurdjali. God. Sofiis Univ., Biol. Geol. Geogr. Fak., 50: 149—188.

Atanasov, G., Goranov, A. and Stefanov, D., 1972. Bentonite clays from the region south of Kurdjali and west of the Varvitza River. God. Sofiis Univ., Geol.-Geogr. Fak., 64(1): 202—223.

Cyprus

Anonymous, 1973. Bentonite in Europe. Ind. Miner., 64: 9—20.

Pantazis, T.M., 1967. Geology and mineral resources of the Pharmakas—Kalarasas area. Geol. Surv. Cyprus, Mem., 8: 190 pp.

Czechoslovakia

Anonymous, 1973. Bentonite in U.S.A. Appendix. Ind. Miner., 66: 15.

Gregor, M. and Pavlovic, J., 1962. The suitability of some East Slovakian Bentonites for the production of bleaching earths. Sb. Pr. Chem. Fak. SVST (Sloven. Vysokej, Skoly Tech), 1962(2): 67—72.

Konta, J., 1957. Clay Minerals of Czechoslovakia. Nakla. Cesosl. Akad., Praha, 200 pp.

Michalek, Z., 1956. Montmorillonite clays from Radzionkow, Upper Silesia. Zeszyty. Nauk. Akad. Gorn.-Hutn., Cracow, Rozpr., 39: 156 pp.

Mocik, S., Masar, G. and Sandor, H., 1968. Calculation of the formula of montmorillonite and its concentration in beneficiated bentonites. Acta Fac. Rerum. Nat. Univ. Comenianae, Chim., 12: 167—172.

England

Brammal, A., Leach, J.G.C. and Dunstall, W.J., 1940. Montmorillonite in Fuller's earth. Nutfield, Surrey. Geol. Mag., 77: 102—112.

Cowperthwaite, I.A., Fitch, F.J., Miller, J.A., Mitchell, J.C. and Robertson, R.H.S., 1972. Sedimentation, petrogenesis, and radioisotopic age of the Cretaceous Fuller's earth of Southern England. Clay Miner., 9: 309—327.

Grim, R.E., 1933. Petrography of the Fuller's earth deposits at Olmsted, Illinois. Econ. Geol., 28: 344—363.

Hallam, A. and Selwood, B.W., 1968. Origin of the Fuller's earth in the Mesozoic of Southern England. Nature (London), 220: 1193—1195.

Hallam, A. and Selwood, B.W., 1970. Montmorillonite and zeolite in Mesozoic and Tertiary beds of Southern England. Mineral Mag., 37: 945—952.

Newton, E.F., 1937. The petrography of some English Fuller's earth and the rocks associated with them. Proc. Geol. Assoc., 48: 174—197.

Poole, E.G., Kelk, B., Bain, J.A. and Morgan, D.J., 1971. Calcium montmorillonite (Fuller's earth) in the Lower Greensand of the Fernham area, Berkshire. Inst. Geol. Sci., London, Rep., 71: 64 pp.

Robertson, R.H.S., 1961. The origin of English Fuller's earths. Clay Miner. Bull., 4, 282—287.

Denmark

Unmack, A., 1949. X-ray investigation of some Danish clays. II. Montmorillonite clays. Yearb. R. Vet. Agric. Coll., Copenh., 1949: 192—204.

Faroe Islands (Denmark)

Bogvad, R., 1937. An investigation of "Bleaching Earths" from the Faroes. Dan. Geol. Foren., 9: 214—217.

Sabine, P.A., 1971. Bentonitic beidellite mud stone from the Faroe Islands. Clay Miner., 9: 97—106.

France

Charrin, V., 1951. Bentonite in Metropolitan France. Genie Civil, 123: 1011.

Damour, A.A. and Salvétat, O., 1847. L'analysis sur un hydrosilicate d'alumine trouvé à Montmorillon (Vienne). Ann. Chem. Phys., Ser. 3, 21: 376—383.

Déribéré, M. and Esme, A., 1951. Bentonite. Dunod, Paris, 3rd ed., 224 pp.

Germany

Antiorgitis, G., 1970. Bentonite from Rossberg near Darmstadt. Notizbl. Hess. Landesamtes Bodenforsch. Wiesbaden, 98: 206—211.

Fahn, R., 1965. The mining and preparation of bentonite. Interceram., 12: 119—122.

Güven, N., 1974. Lath-shaped units in fine-grained micas and smectites. Clays Clay Miner., 22: 385—390.

Schüller, A. and Köhler, R., 1953. Petrographic study and physical properties of bentonites formed from basalt at Steinberg near Ostritz. Z. Ges. Geol. Mineral., 2: 167—184.

Siegi, W., 1948. Glassy tuff in the Molasse of Upper Bavaria and its application in bleaching earths. Neues Jahrb. Mineral., Monatsh., Abt. A, 1948: 77—82.

Valeton, I., 1960. Volcanic tuff beds in the Upper Chalk of Northwestern Germany. Mitt. Geol. Staatsinst., Hamburg, 29: 26—41.

Greece

Franzini, M., Mazzouli, R., Pratesi, M. and Schiaffino, L., 1963. Mineral studies of some bentonites from Milos and Kimolos, Greece. Atti. Soc. Toscana Sci. Nat. Pisa, Mem. P.V., Ser. A, 70: 49—59.

Robertson, R.H.S., 1958. The earths of Theophrastos. The Classical Review, LXXII: 222—223.

Hungary

Barna, J., 1956. Basalt bentonite from Monostorapati. Banyasz. Kut. Intez. Kozl., 1: 97—103.

Barna, J., 1957. Cation exchange capacity of Hungarian bentonites and the exchange process when treated with soda. Acta Tech. Acad. Sci. Hung., 18: 325—338.

Nagy, K., 1854. Determination of the quantity and crystallographic formula of montmorillonite in Hungarian bentonites. Foldt. Kozl., 84: 3—15.

Szanto, F., Varkonyi, B., Gilde, N. and Balazs, J., 1967—1968. Colloidal chemical properties of Hungarian bentonites. Acta Phys. Chem., 13(12): 97—92 (1967); 13(3—4): 131—137 (1967); 14(3—4): 139—144 (1968).

Szeky-Fux, V., 1948. Bentonized rhyolitic tuff from Kobanya. Foldt. Kozl., 78: 185—196.

Szeky-Fux, V., 1957. The hydrothermal genesis of bentonites on the basis of studies in Komloska. Acta Geol. Acad. Sci. Hung., 4: 361—382.

Israel

Bentor, Y.K., 1966. The clays of Israel. Proc. Int. Clay Conf., Israel, pp. 23—48.

Weissbrod, T., 1962. Bentonite deposits, Makhtesh Ramon. Geol. Surv. Israel, Rep., A.P. 122/62.

Wolff, R. and Minkoff, I., 1962. Physical properties of Negev bentonite. Israel J. Technol., 10: 139—143.

Italy

Alietti, A. and Alietti, L., 1962. Diverse types of montmorillonite in bentonites from Gemmano (Forli). Period. Mineral., 31: 261—288.

Annedda, V., 1956. Deposits of bentonite in Sadali and Vallanova Tulo territories, Sardinia. Resoconti Assoc. Min. Sarda, 60: 5—9.

Cavinato, A., 1957. Geology and genesis of Italian bentonites. Atti Accad. Naz. Lincei, Ser. VIII, 23: 10 pp.

DeAngeles, G.C. and Novelli, G., 1957. Bentonite from Ponza. Geotecnica, 4: 1—7.

Güven, N. and Grim, R.E., 1972. X-ray diffraction and electron optical studies on smectite and α-cristobalite associations. Clays Clay Mineral., 20: 89—92.

Lupino, R., 1954. Bentonite from the Island of Ponza. Ricerca Sci., 24: 2316—2339.

Pietracaprina, A., Novelli, G. and Ranaldi, A., 1972. Bentonite deposits at Uri, Sardinia. Clay Miner., 9: 351—353.

Poppi, L., 1972. On some Italian bentonites. Int. Clay Conf., Spain, Abstr.

Prever, V.S. and Goria, C., 1941. Bentonite from the Publiesa district. Ind. Meccanica, 23(3): 92—96; (4) 131—133.

Savelli, F., 1938. Italina bentonite. Mat. prime.. Ital. Imp., 3: 129—137.

Savelli, F., 1943. Bentonite Colloidal Clay. Ubrico Hoepli, Milan, 537 pp.

Wayland, T.E., 1971. Geologic occurrence and evaluation of bentonite deposits. Trans Am. Inst. Min., Metall. Pet. Eng., 250(2): 120—132.

Zanettin, B., 1953. Montmorillonite clays from Campiglia and Tognazzo. Rend. Soc. Ital. Mineral. Petrol., 9: 219—236.

Poland

Alexandrowicz, S. and Parachoniak, W., 1958. Upper Cretaceous tuffogenic deposits in the Miechow syncline. Act. Geol. Pol., 8: 213—244.

Budkiewicz, M. and Tukarski, Z., 1971. Clay mineral raw material of Poland. Kwart. Geol., 15: 172—193.

Glogoczowski, J.J., 1958. Some properties of bentonites and bentonitic clays from Chmielnik. Ann. Soc. Geol. Pol., 27: 195—220.

Gucwa, J. and Koszarski, L., 1960. Bentonites in the Lower Krosno beds at Zagorz near Sanok. Kwart. Geol., 4: 181—193.
Heflik, W., 1959. Petrography of volcanic glass in bentonitic clays from Ciecierze near Chmielnik. Kwart. Geol., 3: 778—789.
Kamienski, M., 1965. Some remarks on bentonites of Poland. Arch. Min. Soc. Sci. Varsovie, 11: 113—121.
Krauss, E. and Rutkowski, J., 1962. Senonian bentonites in the Mikchow region. Rocz. Pol. Tow. Geol., 33, 131: 359—370.
Langier-Kuzniarowa, A., 1967. Miocene bentonites in the bore holes made in the Szydlow region. Bull., Inst. Geol., Warsaw, 207: 223—250.
Sikora, W. and Wieser, T., 1959. Occurrence of bentonites in the variegated shales of the Magura Nappe south of Grybow. Przegl. Geol., 7: 224—225.
Sujkowski, Z., 1934. The bentonite in Lower Sarmatian of Krzemieniec. Arch. Mineral. Soc. Sci. Varsovie, 10: 98—116.
Tokarski, J., 1948. On the genesis of bentonite from Podolia and Volhynia. Mém. Acad. Pol. Sci., Ser. B, Int., No. 143A: 48—58.
Tokarski, J., 1953. The genesis and systematic position of bentonites. Mém. Acad. Pol. Sci., Cl. 3, Ser. B, 1(6): 267—270.

Portugal

Galopim de Carvalho, A.M., 1969. On the occurrence of attapulgite in Portugal. Estud., Notas Trab. Serv. Fom. Min. (Port.) 18(3—4): 341—348.
Galopim de Carvalho, A.M., 1970. On the occurrence of bentonite in Portugal. Estud., Notas Trab. Serv. Fom. Min. (Port.), 19(3—4): 297—308.
Lapa, A.J.R., 1965. Bentonite. Bol. Minas, 2(4): 1—15.
Silva, D.J.R. and Neiva, J.M., 1948. Montmorillonite in granitic pegmatites and the problem of montmorillonitization. Publ. Mus. Lab. Mineral. Geol. Fac. Cienc. Porto, 53, 3 Ser.

Rumania

Cardew, J., 1952. Bentonite in Rumania's chemical industry. Chem. Age (London), 67: 862.
Dittler, E. and Kirnbauer, F., 1933. The bentonite occurrence at Tomesti, Rumania. Z. Prakt. Geol., 41: 121—127.
Felszeghy, E. and associates, 1963—1968. Colloidal clays of Rumania. Stud. Univ. Babes-Bolyai, Ser. Chem., vols. 8—12.
Ghergariu, L. and Mirza, I., 1961. Bentonite of Palazu. Mare (Dobrogea). Stud. Univ. Babes-Bolyai, Ser. 2, 1: 83—93.
Leonida-Zamfirescu, E., 1943. Study of Rumanian decolorizing earth. Inst. Geol. Rum., Ser. B, 22: 92 pp.
Neaesu, Gh., 1962. Bentonites from La Pirvova (Banat). Populara Romana Com. Geol., 46: 13—24 (1958—1959).
Nedelcu, F., 1968. Physical-chemical properties of Oarda bentonites. Com. Stat. Geol. Repub. Soc. Rom., 53(3): 323—339.
Popescu, I.C. and Mares, I., 1971. Mineralogic study of the bentonite rocks of Southern Dobrogea. An. Univ. Bucuresti, Geol., 19: 91—118.

Spain

Gutierrez-Rios, E., 1949. Spanish Bentonites. Consejo Superior Invest. Cient., 156 pp.
Gutierrez-Rios, E. and Hernando, L., 1947. Deposits of bentonite in Spanish Morocco. An. Edafol. Fisiol. Veg., 6: 53—77.
Güven, N., 1974. Lath-shaped units in fine-grained micas and smectites. Clays Clay Miner., 22: 385—390.

Linares, J., Huertas, F., Lachica, M. and Reyes, E., 1972. Geochemistry of trace elements during genesis of colored bentonites. Preprints, Int. Clay Conf., Madrid, 2: 415—419.
Martin-Vivaldi, J.L., 1949. Bentonites in Spain. Univ. Granada, Bol., 87: 14 pp.
Martin-Vivaldi, J.L., 1962. Bentonites of Cabo de Gata and the Guelaya Volcanic Province (North Morocco). Proc. Clay Conf., 11th, pp. 327—357.
Martin-Vivaldi, J.L. and Linares Gonzales, J., 1968/1969. The bentonites of Cabo de Gata. Bol. Geol. Min., 79(6): 605—611 (1968); 80(1): 74—80, 513—523, 605—611 (1969).
Martin-Vivaldi, J.L., Cano-Ruiz, J. and Fontboté, J.M., 1956. The bentonites from the volcanic region of Cabo de Gata (Almeria). U.S. Nat. Acad. Sci. Pub., 456: 181—184.

Switzerland
Hofmann, F., 1956. Petrographic and mineralogic investigations of the bentonites of Switzerland and Southwest Germany. Eclogae Geol. Helv., 49: 112—133.
Hofmann, F., 1958. The bentonite occurrence of LeLocla. Eclogae Geol. Helv., 51: 65—71.
Hofmann, F., 1959. Saponite as an alteration product of basaltic tuff at Karolihof. Schweiz. Mineral. Petrogr. Mitt., 39: 117—124.
Hofmann, F., Buchi, U.P., Iberg, R. and Peters, T.J., 1975. Occurrence, petrography, clay mineralogy and technical properties of bentonites in the Molasse basin of Switzerland. Beitr. Geol. Schweiz, Geotech. Ser., 54: 51 pp.

Turkey
Anonymous, 1973. Bentonite in Europe. Ind. Miner., 64: 9—20.
Wayland, T.A., 1971. Geologic occurrence and evaluation of bentonite deposits. Trans. Am. Inst. Min., Metall. Pet. Eng., 250: 120—132.

Yugoslavia
Anonymous, 1973. Bentonite in Europe. Ind. Miner., 64: 9—20.
Dragoslav, N. and Miroslav, Z., 1971. Bentonite of Sipovo, Bosnia. Glas. Prir. Muz. Beogradu, Ser. A, 26: 103—116.
Drzaj, B. and Kacjan, M., 1968. Bentonites from Zaloschk Mountain near Celje as raw material for chemically activated clays. Rud.-Metal. Zb., 1968(4): 405—521.
Ilic, M., 1969. Volcanogenic sedimentary facies of Neogene basins of Serbia and their economic significance. Bull., Inst. Geol. Geophys. Res., Belgrade, Ser. A, 26: 379—388.
Keramata, S., 1957. The origin of bentonites from Slaviste. Heidelb. Beitr. Mineral Petrogr., 4: 289—295.
Konta, J., Lardinski, B. and Velikov, D., 1971. Mineral and chemical composition of four varieties of bentonite from Ginovici, Yugoslavia. Acta Univ. Carol., Geol., 1971: 209—232.
Lukas, E., 1968. State of exploration of Zaluska Gorica bentonites in comparison with other Yugoslavian bentonites. Rud.-Metal. Zb., 1968(3): 277—286.
Nikolic, V. and Obradovic, J., 1963. Bentonite from Blace, Serbia. Geol. An. Balkan Poluostrva, 30: 125—128.
Obradovic, J. and Knezevic, V., 1972. Genesis of the bentonite from the volcanic sedimentary series in the Montenegrin littoral region (Yugoslavia). Proc. Int. Clay Conf., Madrid.
Rihtersic, J., 1958. Bentonite in the basin of Celje. Geol. Razpr. Porocila, 4: 193—196.
Sepesi, K. and Hedjkezi, T., 1966. Unpublished report referred to by J. Konta in Acta Univ. Carol., Geol., 1966(3): 209—232.
Stangatchilovitch, D., 1963. The formation of bentonite in the marine cycle of the lignitic basin of Bogovina, Serbia. C. R. Acad. Sci. Paris, 256: 4934—4935.
Stubican, V., Lisenko, N. and Wrischer, M., 1956. The morphology of montmorillonite

particles and the crystal form of free silica in some bentonites. Croat. Chem. Acta, 28: 239—248.
Trubelja, F., 1966. Montmorillonite from Podhum village south of Livno. Geol. Glas. (Sarajevo), 11: 347—350.

3.5. BENTONITES IN U.S.S.R., ASIA, AND THE SOUTHWEST PACIFIC

Bentonite deposits are widely distributed in the Soviet Union where they have been studied extensively, and where they are produced commercially in many areas. In Asian countries bentonites are best known in India, Phillipines, Japan and Pakistan with active commercial production in the former three countries. In the Southwest Pacific area bentonites are well known from several areas in Australia and New Zealand.

Australia

Numerous deposits of bentonite have been described in Australia. At Yarraman in Queensland, about 7 ft. of bentonite of Pliocene age occurs between bentonitic clays (Fig. 3.52). The bentonite has formed from a volcanic agglomerate and contains kaolinite in addition to smectite. The rock fragments of the agglomerate, largely composed of feldspar, have altered to kaolinite, whereas the matrix material has altered to smectite. The clays enclosing the bentonite contain relatively large amounts of kaolinite. The

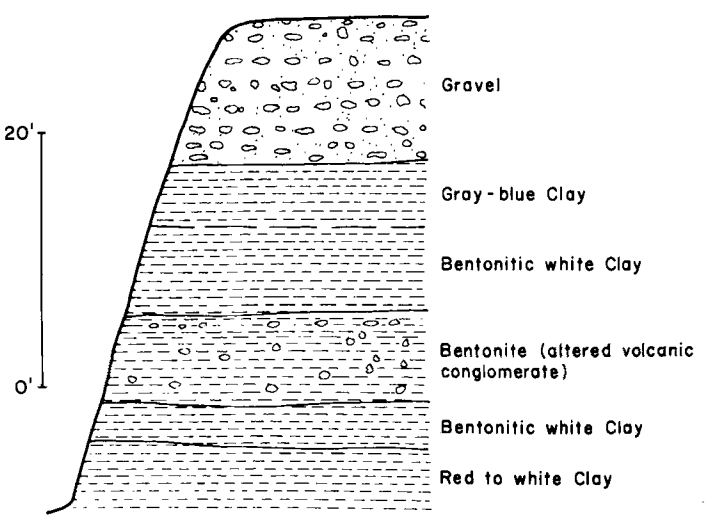

Fig. 3.52. Generalized section of Pliocene formations at Yarraman, Queensland, Australia.

bentonite contains foraminifera and other microfossils. There is no suggestion that weathering has been important in the formation of the bentonite, and it is concluded that the alteration took place in situ contemporaneous with accumulation of the volcanic debris, probably in a shallow marine environment.

At Marchagee in Western Australia, a thin bed of clay with an average thickness of 9 inches, called bentonite, is found in a dry desert pan underlain by 6 ft. of gypsiferous clay and then 15 ft. of brown clay. Particles of travertine are fairly abundant in all of the clays. The source of the bentonitic clay and its mode of origin is obscure, as no volcanic rocks occur in the district. Chemical analyses of the bentonite show a high content of magnesia (14.21%) and relatively low alumina (4.29%), suggesting that saponite is the smectite component.

The Permian—Triassic Coal Measures of New South Wales contain several beds of bentonite, varying in thickness from an inch to as much as 10 ft. Some of the bentonites are within coal seams, whereas others are interbedded with associated carbonaceous shale. The bentonite horizons in the Coal Measures do not show vertical variations in composition, and their contact with the coal or shale is abrupt. Although no clearly diagnostic textures are present in the clay, it seems probable that the bentonite has formed by the alteration of igneous material, and that the alteration was contemporaneous with the emplacement of the igneous material, which was probably ash. A few of these bentonites are relatively pure smectite, but most of them contain substantial amounts of mixed-layer illite—smectite, and in a few instances, kaolinite is also a significant component.

An interesting bentonite occurrence at Boggabri in New South Wales is associated with trachytes and andesites and appears to be the result of deuteric alteration. Still another deposit at Dubbo in New South Wales is reported in Upper Jurassic sandstone. Recently a bentonite formed from a tuff has been reported at Gillibrand in Victoria.

Burma

Samples of clay obtained from P.S. Keeling of the Burma Oil Company were found to be composed of smectite clay minerals and could be classed as bentonite. No information was obtained on the occurrence or location of the samples.

China

Bentonites are reported associated with coal at Nai-tsu-shan and at Manchou-kuo in Manchuria (Sakomoto, 1937, and Osaki, 1937). Wu and Lee (1948) report extensive beds of bentonite intercalated between rhyolite flows and overlying dacites in northern Chekiang.

India

Geological features. In the Barmer district of Rajasthan, bentonite is produced near Akli (sample 80) and Hathi-ki-Dhani (sample 81) from beds varying up to 10 ft. or more in thickness in a series of calcareous sands and conglomerates of Lower Tertiary age. The bentonite is quite pure smectite. Relict ash structures are not obvious in the clay. This fact and the absence of Tertiary volcanic activity in the area has caused Siddiquie and Bahl (1965) to rule out contemporaneous deposition and alteration of volcanic ash as the mode of origin, and to suggest that the clay formed by the weathering of Precambrian igneous and metamorphic rocks followed by transportation and deposition in the Barmer Embayment. It is difficult to believe that this mode of origin could produce the pure smectite clay of Akli. It is of interest that the same sequence of formations contain beds of substantially pure attapulgite which are produced as fuller's earth in the Barmer district.

Bentonites are also well known in the Bhimber and Kathau areas of Jammu and Kashmir where beds up to 4 ft. thick occur in a sequence of red clays and sandstones in the Upper Siwalik formations of Miocene age. Microscopic observations indicate that the clay has formed by the alteration of volcanic glass. In the Jhelum district of the Punjab, bentonite is reported in a marine sequence of Middle Siwalik age. Bentonites are also reported from numerous other localities in India, for example, near Gujarat, Karauli, Jaipur, and Madras, but there is little precise information concerning them.

Mineralogical studies. The X-ray data in Table 3.5A suggest the presence of a sodium montmorillonite with a basal spacing of 12.0 Å in the Akli bentonite. Its chemical formula is calculated from the data in Table 3.5B.

$$[(Si_{3.52}Al_{0.48})(Al_{1.48}Fe^{3+}_{0.39}Mg_{0.13})O_{10}(OH)_2]M^{+}_{0.62}$$

The smectite is distinguished by its high alumina and iron content. The extractable cations from the other bentonite (No. 81) are composed largely of sodium with some magnesium. The montmorillonites from this sample also carry large amounts of iron as indicated in Table 3.5B. Kaolinites are rather common in both of the samples, and they make up about 30% of the clay fraction in sample 81.

Irregular aggregates (Fig. 3.53) are the common forms of montmorillonites in the bentonite from Akli. As shown in the same figure, thin curled layers, like Cheto-type aggregates, and tiny platelets like Santa Rita aggregates are discernible in these aggregates. Lath-shaped mica units and their geometrically regular aggregations are frequently observed in the sample (Güven, 1974). The morphological features of the montmorillonites in sample 81 are very similar to those in the previous sample.

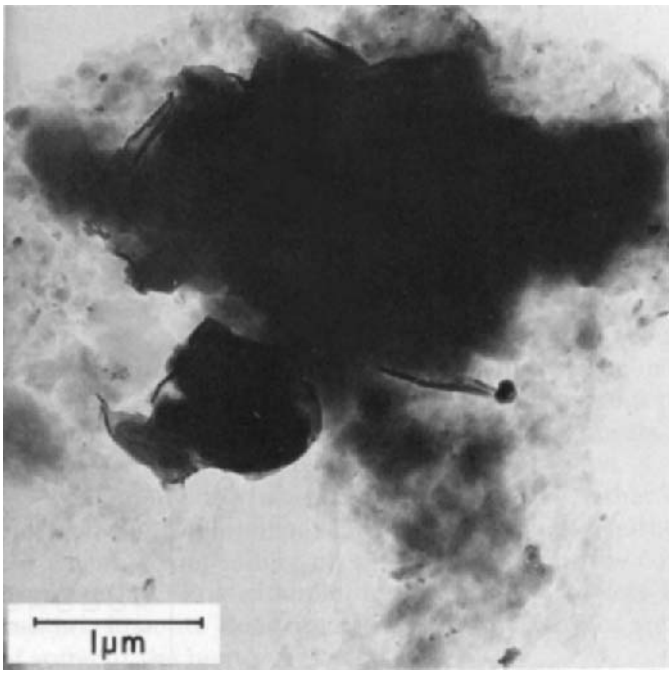

Fig. 3.53. Typical montmorillonite aggregates in bentonite from Akli, India.

Indonesia

Van Bemmelen (1970) in his volume on the mineral resources of Indonesia does not mention an occurrence of bentonite, but does mention the presence of pumice and of "trass" which is partially altered tuffaceous material. Earlier Harajosaestro (1953) noted clay grades of volcanic ash containing cristobalite.

Iran

An unpublished report by Henderson and Robertson (1958) states that a bleaching clay produced at Saveh near Ghom is for sale in the markets of Kermanshah and other Iranian cities.

Iraq

The Khawa clay in Mosul is reported by Hanna (1966) to be composed of dioctahedral montmorillonite.

TABLE 3.5A

Location, geological and mineralogical data on bentonites from India, Japan, and the U.S.S.R.

Sample no.	Location and formation	Geologic age	Smectite's spacings (Å)		MgO * (%)	Extractable cations (mequiv./100 g)					C.E.C. (mequiv./100 g)
			(001)	(06,33)		Mg	Ca	K	Na	total	
	India										
80	Rajasthan State, Sheo District, "Akli"	L. Tertiary	12.0		2.93						
81	Rajasthan State, Sheo District, "Hathi-ki-dhani"	L. Tertiary	13.2		1.49	23	4	2	79	108	80
	Japan										
82	Gumma Prefecture, Kwanto District, "Hojun"	U. Miocene	12.4	1.495	1.41	10	7	9	61	87	100
83	Gumma Prefecture, Kwanto District, "Hojun"	U. Miocene	12.3	1.495	1.30	7	9	8	57	81	153
84	Gumma Prefecture, Kwanto District, "Usui"	U. Miocene	12.1	1.496	0.70	6	10	10	41	67	79
	U.S.S.R.										
85	Askana, Georgia				4.60	nd	nd	nd	nd	nd	nd

* On ignited material from —1 μm fraction of clay stripped off exchangeable cations.

TABLE 3.5B

Chemical analyses of bentonites from India and Japan (on ignited material from —1 μm fractions of ammonium saturated clays)

Sample no.	SiO_2	Al_2O_3	Fe_2O_3	MgO	Li_2O	CaO	Na_2O	K_2O	Total	Impurities *
80	61.43	23.90	9.86	2.93	0.0	0.03	0.12	1.02	99.29	—
81	66.10	23.60	8.08	1.38	0.0	0.07	0.05	0.44	99.72	kaol(10)
82	79.07	16.84	1.46	1.41	0.0	0.01	0.02	0.04	98.85	crist(40)
83	76.64	19.39	1.89	1.30	0.0	0.01	0.02	0.04	99.29	crist(30)
84	79.86	16.86	1.61	0.70	0.0	0.03	0.14	1.03	100.23	crist(40)
85	67.57	21.44	5.60	4.60	0.0	0.01	0.08	0.50	99.80	—

* Impurities are semiquantitatively estimated from the X-ray diffraction data. (crist = cristobalite; kaol = kaolinite.)

Japan

Geological features. Bentonites as such were recognized in Japan about 1930, and have been actively produced commercially since 1938. However, bleaching clays, which in general could be designated as bentonites, have been produced since about 1890.

The more important deposits of bentonite are in Yamagata, Gumma Niigata, and Nagano Prefectures of northern Honshu and in Hokkaido. The deposits in Honshu have formed mostly from liparites and liparitic tuffs of Early Miocene age. In many instances the alteration has been essentially devitrification of ash, perhaps with contemporaneous deuteric alteration of tuffaceous glassy material. Such bentonites occur in horizontal to lenticular beds associated with bentonitic sands on mudstones frequently in a marine sequence. In other instances, the alteration appears to be by hydrothermal processes, and such deposits are irregular in shape.

Occasionally the alteration has produced other clay minerals, such as halloysite and allophane, rather than smectite, either alone or mixed with the smectite, depending on the parent rock or the composition of the agents of alteration. For example, in the absence of less than about 1% of magnesium, smectite does not tend to form. Zeolites are important components of some of the bentonites.

The deposits in the Prefectures of Honshu extend over large areas. For example, in the Gumma Prefecture, the bentonite zone is about 25 km long and 2 km wide. In the Usui (sample 84) and Hojun mines (samples 82 and 83) in the Kwanto district of the Gumma Prefecture several beds of bentonite totalling about 15 ft. thick are interbedded with brown mudstones of Upper Miocene age (Fig. 3.54). The bentonite beds are altered pumice and the pumice structure is retained in the clay. The mudstones are impure pumice and grade sharply into the bentonites. Non-clay mineral components of the bentonite are mostly feldspar, zeolite, opaline silica, and cristobalite, and these minerals are at places present in sufficient abundance to cause a sandy character and eliminate commercial use.

The deposits in Hokkaido have formed from Miocene—Pliocene tuffs by processes similar to those for the Honshu deposits.

Most, perhaps about all, of the so-called Japanese bleaching earth for decolorizing oils, are composed essentially of smectite. Japan produces in Yamagata and Niigata Prefectures, an "acid earth" for this purpose which contains cristobalite, allophane, and a zeolite in addition to the smectite. This earth has a relatively high silica to alumina ratio, a lower pH (5—6), and a smaller cation exchange capacity than bentonites generally. These earths are reportedly the result of the alteration of volcanic ash influenced greatly by weathering processes.

As would be expected from the volcanic character of the Japanese Islands, bentonite occurrences have been reported at a great many other places, for

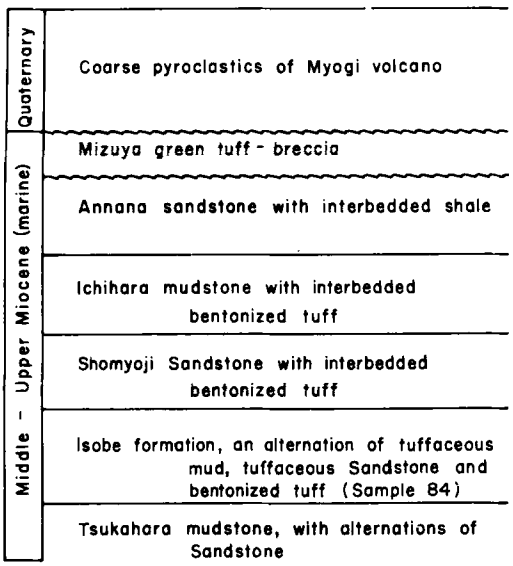

Fig. 3.54. Generalized section in the bentonite area of Usui, Gumma Prefecture, Japan (after Iwao, 1969).

example in the Fukuoka district (Sakamoto, 1970).

Japan contains many examples of soils formed by the weathering of volcanic ash, and consequently the weathering of volcanic ash has been studied extensively by Japanese geologists. The results of all these studies show that it is unlikely that weathering processes have been important in the formation of bentonites. In general, these studies show that weathering tends to produce a suite of clay minerals rather than a single one. Other clay minerals rather than smectite are likely to be most abundant, and/or there is a profile development, i.e. a vertical variation in clay mineral composition grading downward into the parent material. For example, Masui (1960) has described a weathering profile with montmorillonite in the upper horizon grading downward into halloysite and then ash. The Japanese investigations indicate that siliceous parent material relatively rich in magnesium favors the formation of smectite. Sudo et al. (1964) have made clay mineral analyses of about 600 samples of soil derived from volcanic ash and have reported allophane, hydrated halloysite, and a mixed-layer minerals as the major components. Although weathering is generally not the primary process in the formation of bentonites, superimposed superficial alteration may significantly influence the properties of bentonitic clay, e.g., the "acid earth".

Suzuki (1954) has described an interesting alteration of ash in the coal fields of Hokkaido. Alteration of the ash in marine water has yielded smectite and illite. In fresh water halloysite or kaolinite has formed.

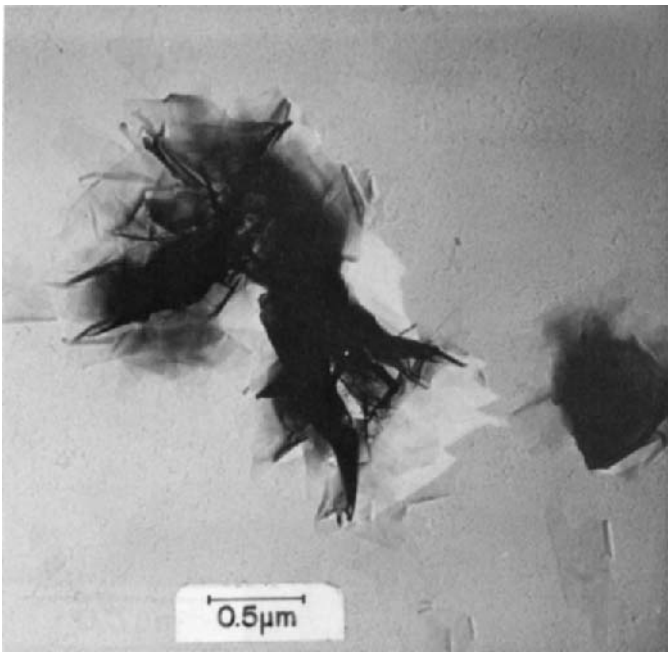

Fig. 3.55. Typical montmorillonite aggregates in bentonite from Hojun Mine (sample 82), Japan.

Mineralogical studies. The samples listed in Table 4.5A from Gumma Prefecture all contain large amounts of cristobalite—tridymite mixed layers. This free silica phase makes up about 30—40% of the bentonite in the above samples even of the fine fractions. Smectites in the samples have a basal spacing ranging from 12.1 to 12.4 Å, suggesting that sodium is the major interlayer cation in them. This is confirmed by extractable cations (Table 3.5A) from the samples. Furthermore, these samples are distinguished by rather low magnesia and iron contents (Table 3.5B) even after accounting for the free silica in them. They are very close to the montmorillonite—beidellite boundary.

Morphological features of smectites in the above sample are very similar. Smectites occur in the form of Wyoming-type (foliated) aggregates, S-, L- and E-type particles. The sample from Usui mine contains an appreciable amount of E-type lamellae. A typical foliated aggregate is shown in Fig. 3.55 from sample 82. In the latter sample the presence of extremely thin layers with large lateral dimensions is clearly discernible. Extensive folding and curling of these layers are commonly observed. The L-type particles are mostly formed by a backfolding of thin lamellae as recently described by Güven and Pease (1975). Backfolding of thin lamellae seem also to result in

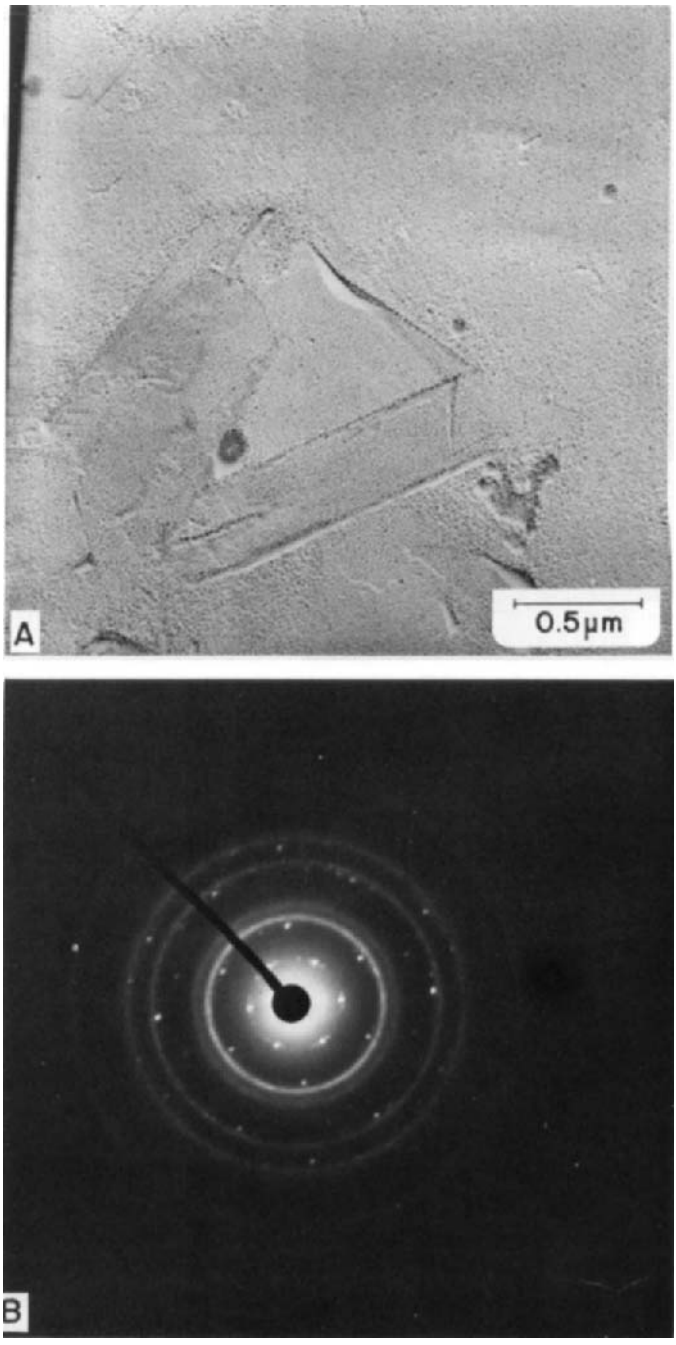

Fig. 3.56. A. Montmorillonite lamellae backfolded on itself into a triangular arrangement in bentonite from Hojun Mine (82), Japan. B. Its SAD pattern.

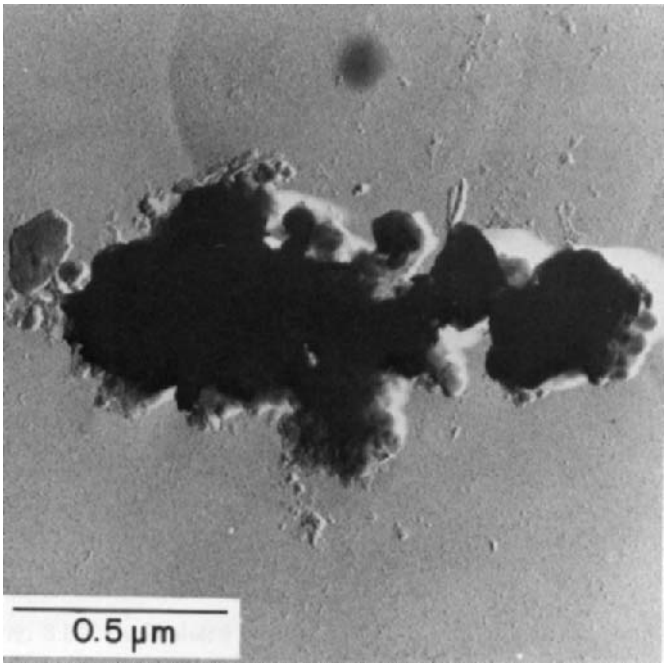

Fig. 3.57. A fine granular cristobalite aggregate in bentonite from Hojun Mine (82), Japan.

other regular geometrical forms, as shown in Fig. 3.56A. The particle in this figure consists of a triangular arrangement of three units. The SAD pattern of the particle (Fig. 3.56B) shows a predominant spot pattern, suggesting a crystallographically strict arrangement of these units.

The free silica phase (a cristobalite—tridymite mixed layer) occurs commonly in fine granular aggregates intergrown with smectites, as seen in Fig. 3.57 from sample 82. Fig. 3.58A, on the other hand, shows a lamellar aggregate of smectite, but its SAD pattern (Fig. 3.58B) has a distinct diffraction ring of 4.12 Å for cristobalite—tridymite mixed layer in addition to the 4.49 Å ring of smectite.

Korea

Bentonites are reported in the north Kyongsang Province of Korea, but no specific information could be found regarding their occurrence.

New Zealand

In view of the abundant volcanic activity in New Zealand, it is not surprising that bentonites have been reported in many areas. Fyfe (1934) reported

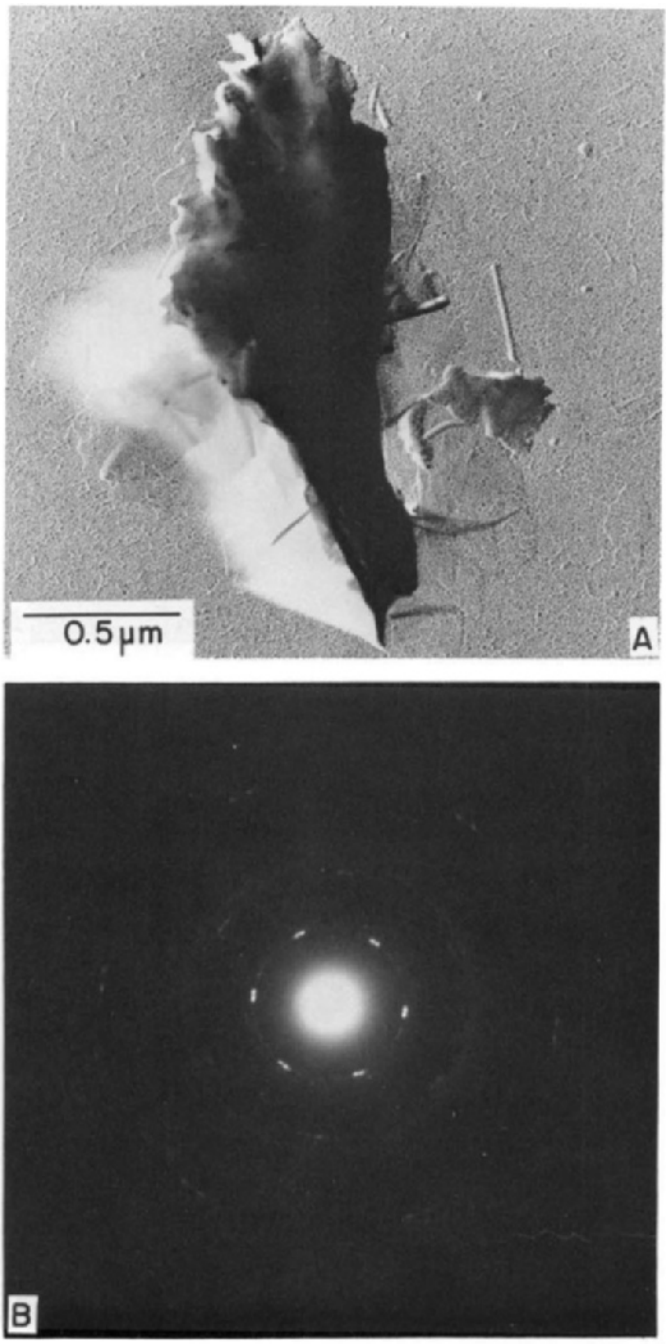

Fig. 3.58. A. Montmorillonite—cristobalite aggregate in the bentonite from Hojun Mine (82), Japan. B. Its SAD pattern.

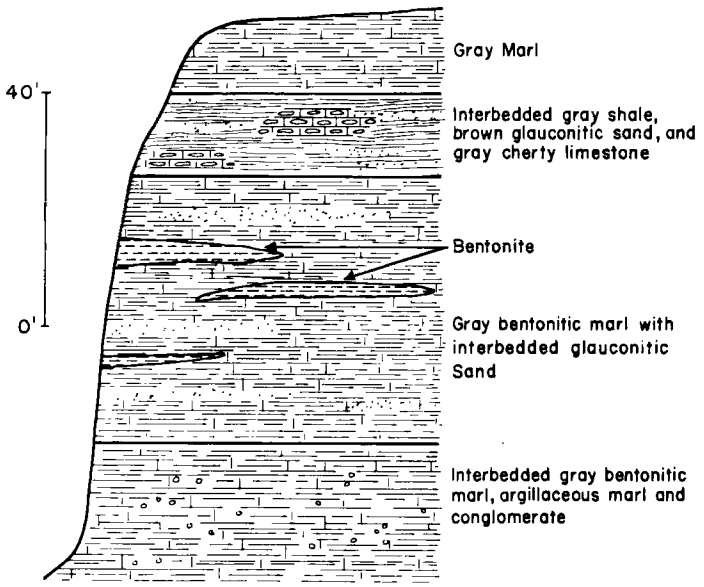

Fig. 3.59. Generalized section of Upper Senonian formations near Porangahau, New Zealand.

the wide distribution of bentonitic clays in the Gisborne-East Cape district of the North Island. The beds are post-Cretaceous and pre-Miocene in age, and they rest on highly folded Cretaceous strata and are accordant with overlying Miocene sediments.

In the Hawks Bay and Poverty Bay areas of the North Island, bentonites are described by Macpherson and Coventry (1941). Near Porangahau bentonitic shales with interbedded layers of relatively pure smectite 6—12 ft. thick occur in a section of shales, marls, and glauconitic sandstones. The section (Fig. 3.59) is Upper Senonian in age. The bentonites contain relict ash structures indicating an origin of altered volcanic ash. An interesting feature of these bentonites is the association of abundant impure bentonites, i.e. bentonitic shales, marls, etc., in which the ash material is mixed with illite, glauconite, calcite, quartz, etc. Even the relatively pure bentonites have appreciable quantities of non-smectite minerals. Nodules of barite and manganese oxide are commonly found scattered through the bentonite. It appears that the section containing the bentonite represents continuous deposition in a marine environment with the bentonite horizons indicating intervals of rapid accumulation of ash, so that the influx of detrital material was minimal. Bentonites of similar geologic age are reported by Fyfe (personal communication) in the north Auckland region of the North Island.

Macpherson (1952) has described bentonites from the Kekerangu and

Blue Slip areas of the South Island. There appear to be four bentonitic horizons in east Marlborough and north Canterbury: (1) Caro (Upper Senonian); (2) Waipara (Lower Eocene); (3) Benmore (Middle Eocene); and (4) Oxford (post-Whangaroan). The bentonites occur within bentonitic shales which are in turn associated with sands and conglomerates. Again, as in the case of some of the North Island bentonites, the material contains substantial amounts of non-smectite material.

Ritchie et al. (1969) reported bentonite in the Harper Hills about 25 miles west of Christchurch interstratified with basalt lava flows of probable Miocene age. The bentonite is associated with well-bedded tuffs containing well-preserved leaves from which accumulation in fresh water is inferred. Alteration of the parent basaltic tuff has yielded an iron-rich smectite.

Bentonite has been described by Wilson (1963) in the Lower Tertiary Dannevirke Series in the Waipara area north of Christchurch. The bentonite occurs at the base of a glauconitic calcareous mudstone sequence. In addition to the smectite, variable amounts of illite are also present along with fragments of amorphous material which may be glass shards.

Bentonite formed by the alteration of basaltic ash deposited in a fresh water lake has been described by Carlson and Rodgers (1974) from the Coalgate area west of Christchurch. Ferriferous beidellite is the dominant component. The ash is Upper Miocene in age. The alteration is believed to have occurred in a mildly alkaline environment in which initial reducing conditions became oxidizing.

The North Island has been the site of many ash showers in Recent times (Grange, 1931), and the weathering of this ash has been studied in considerable detail by Fields (1962, 1968). It is interesting that the volcanic glass in some instances has proven at least as resistant to weathering as the feldspars and other components of the ash. Various clay minerals have formed in the weathering process with smectite generally developing under conditions of poor drainage. In no instance has any material been reported in which there is a concentration of smectite that could be classed as bentonite.

Pakistan

Workable deposits of bentonite are reported (unpublished information from the Geological Survey of Pakistan) at Bhimbar in the Mirpur district of Kashmir, and at Rohtas and Ganda in the Jhelum district. The bentonites are of Miocene Siwalik age, and appear to be at about the same stratigraphic position as the bentonites in Kashmir in India. The beds have a maximum thickness of about 4 ft., but are commonly less than 2 ft. thick. They occur as layers in clays and sandstones, and vary in color from white to dark gray. Some of the Pakistan bentonites are very pure montmorillonite. Ali and Shah (1963) state that the Siwalik bentonites formed from volcanic ash that fell in estuarine or lagoonal environments. Recently, Alauddin et al. (1971)

have described montmorillonite clays from the Campbellpur District of Rawalpindi.

Philippines

Bentonites are produced commercially at Itilongos in northern Leyte. Several beds are reported from a sequence of marine shales and sands. X-ray diffraction analyses of several samples indicate quite pure smectite carrying calcium as the major exchangeable cation.

U.S.S.R.

Occurrences and geological features. Bentonites are found in many areas of the Soviet Union in formations of widely different geologic ages. The literature of the U.S.S.R. contains many hundreds of papers devoted to bentonites. The papers describe in great detail the mode of occurrence, the associated beds, and probable conditions of formation. The properties of the bentonites and their present and potential uses are also elaborated in a large number of publications. It is manifestly impossible to synthesize and summarize all of these data. All that is attempted herein is to briefly mention the largest and most important deposits, together with some of their salient characteristics.

Bentonite is known by a number of local names in the U.S.S.R.: gumbrin and askanite in Georhia, gilbai in Azerbaijan, olganite and gebelite in Turkmen, kil in Crimea, and nalchikin in Kazakhstan. Important areas of commercial production of bentonite in the Soviet Union are in Georgia, Azerbaijan, Armenia, the Ukraine, and in Middle Asia (Uzbekistan, Turkmenia, Tartar, etc.).

The bentonites in Azerbaidjia are in beds up to 4 ft. or more in thickness and range in age from Cretaceous to Tertiary Miocene. Important deposits are in the Kobystan and Kazakh regions. The bentonite has formed mostly by the diagenetic alteration of ash and tuff frequently in a marine environment. The bentonite layers are interbedded with limestone and shales. At places the alteration of the ash is incomplete, and, according to Seidov and Alizade (1970), the finer the grain of the associated rocks, the greater the intensity of alteration to the smectite. In general, the younger beds of ash show the least alteration. Both calcium and sodium varieties of smectite are reported, with the latter more prevalent in the Tertiary formations. Many of the bentonites show excellent shard structures.

Something over 100 deposits of bentonite are reported in Georgia, and they range in age from Jurassic to Tertiary. The best known deposits are in the Askana area where the so-called askanite is produced. These clays resulted from the alteration of pumice-like andesite—trachyte tuff. According to Belyankin and Petrov (1950), weathering has been the alteration pro-

cess. Rateev (1968), however, believes they are hydrothermal products resulting from five stages of alteration, and Manuilova et al. (1965) state that the alteration has taken place under conditions of subwater volcanism. The character of these bentonites, especially their relation to unaltered tuff, suggests that deuteric processes have also played an important role in their mode of origin.

Recently Dsotsenidze and Matchabely (1963) have provided the following additional data concerning the well-known bentonites of Georgia. The Gumbri bentonite northwest of Kutaissi occurs in beds up to 8 m thick in a section of limestones and glauconitic sands of Cretaceous Senomian and Turonian age. It was formed by the alteration of volcanic glass in a submarine environment. The underlying beds are silicified, indicating downward movement of silica.

The Askana deposits in the Makharadze area of Georgia are found in a series of Eocene tuffs and breccias ranging from trachyte to basalt in composition in a section of marine marls and shales. Two types of bentonite are produced: Askangel, the sodium variety from the lower part of the deposit, and Askangeline, the calcium variety from the upper part of the deposit. Cristobalite is present with the montmorillonite in the sodium variety. Various modes of origin including weathering and submarine alteration of ash have been suggested for the Askana deposit, but Dsotsenidze and Matchabely (1963) suggest that Askangel has formed by hydrothermal action, and that Askangeline has formed by the weathering of Askangel.

The so-called Akhaltsinkh bentonite deposits of Georgia range in age from Eocene to Pliocene. The deposits near Aspinksa occur in a calcareous sequence of Eocene age, and are said to have formed from ash and tuff by deep subaerial alteration. Other deposits in this area are interbedded with brown coals of Oligocene age. These latter deposits are relatively impure, and many contain substantial amounts of kaolinite and various detrital minerals in addition to the smectite. These clays are thought to be sediments derived from weathering crusts developed on Eocene and Oligocene rocks with later superimposed diagenetic alteration in an arid environment.

Armenia contains two well-known bentonite deposits. The Noemberyan deposits have formed from an acidic pumice tuff by diagenetic processes, and occur in a marine sequence. Both calcium and sodium smectites are reported. The Sarigyukh deposit is believed to have formed by hydrothermal alteration of porphyrites of andesite-basalt composition. The bentonite frequently contains relict structures of the porphyrite, and shows gradual transitions to unaltered porphyrite. Sulfide minerals are associated with the bentonite.

Numerous bentonite deposits are reported in the Ukraine ranging in age from Triassic to Tertiary. In the Donetz Basin, the Lower Triassic formations contain interlayers of strongly altered volcanic ash retaining good relict structures. In some of these bentonites, zeolite minerals and palygorskite are

reported with the smectite. The Gherkassy clay in the Ukraine is of special interest since it contains the first deposit of palygorskite (attapulgite) found in the U.S.S.R. The palygorskite with impurities of illite is overlain by a bed of pure smectite clay which is in turn overlain by a calcitic micaceous smectite clay. The palygorskite clay contains relicts of amphibole and perhaps was formed by the weathering of crystalline rocks with redeposition in a marine Lower Miocene basin.

In eastern Slovakia bentonites are reported that have formed probably by diagenetic—deuteric alteration of Tertiary rhyolitic—dacitic tuffs.

Bentonites are known from many other places in the Soviet Union, for example in the Volga region near Kuibyshev. In the Kazakhstan area in the vicinity of Alma-Ata, Miocene ash tuffs of andesitic composition have altered perhaps by a combination of hydrothermal and deuteric processes to bentonite. In the Balkash area of Turkmen Upper Pliocene ash tuffs have been altered to bentonite. According to Yurevich and Sokolova (1965) the intensity of the conversion of the ash to smectite is proportional to the magnesium content of the ash. According to Shabayeva (1964), palygorskite is a minor component of the Turkmen bentonites. In the Kuznetz Basin of Central Asia, Lower Permian dacites and andesite tuffs have altered to smectite clays. These bentonitic clays have formed in brackish waters, and are associated with coal seams. Other areas in which bentonites are reported are in Uzbekistan, Tatar, and Byelorussian S.S.R.

Tazhibayeva and Galiyev (1972) concluded that the bentonites from south Kazakhstan "resulted from erosion and redeposition of products of ancient crusts of weathering in a sea basin. Clay formation took place in basins with an alkaline and deoxidizing environment under arid climatic conditions during Paleocene time. The original clay was composed of hydromica which was altered through an intermediate mixed-layer stage to smectite during transportation and deposition under the influence of an alkaline marine medium".

Mineralogical studies on Askana bentonite. The name "Askanite" refers to the smectite occurring as the major clay mineral in Askana bentonite. It has a composition of:

$$[(Si_{3.90}Al_{0.10})(Al_{1.36}Fe^{3+}_{0.24}Mg_{0.40})O_{10}(OH)_2]M^{+}_{0.50}$$

The bulk chemical composition of the smectite, therefore, corresponds to that of a montmorillonite. Morphological features of the Askanite particles have been recently described by Pease et al. (1974). According to them, the E-, L- and S-type single crystallites make up one half of the sample. The remainder is formed by Wyoming-type (foliated) aggregates and compact lamellar aggregates. The foliated aggregates are designated by the letter *F* in Fig. 3.60, in which typical compact aggregates (*C*) and S-type lamellae are

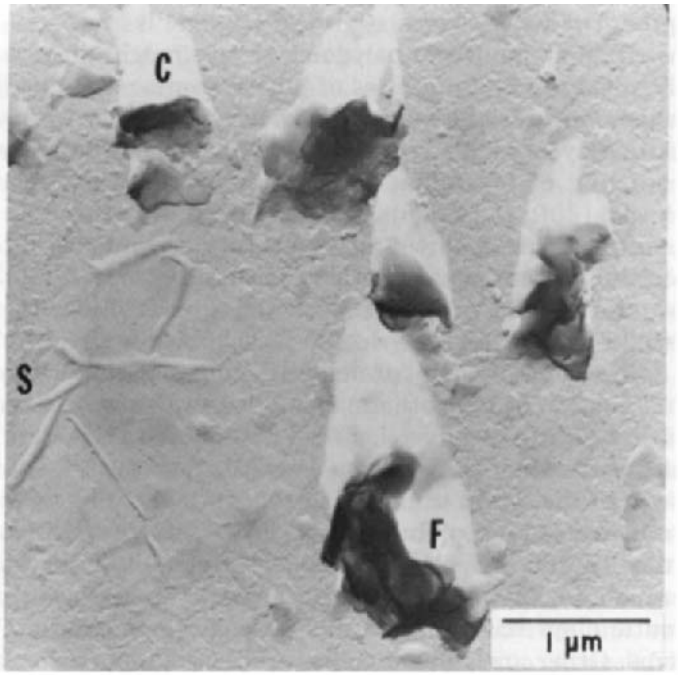

Fig. 3.60. The S-type crystallites (designated by the letter *S*) and compact lamellae (*C*) and foliated aggregates (*F*) in Askana bentonite.

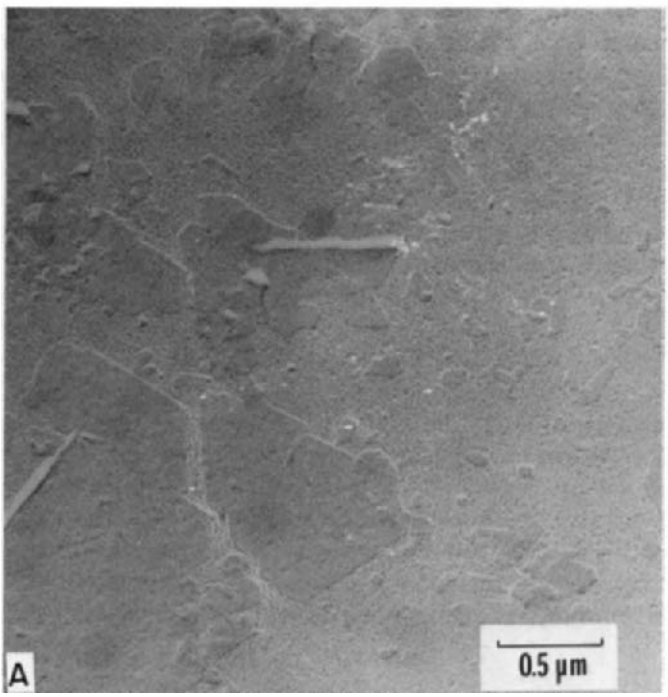

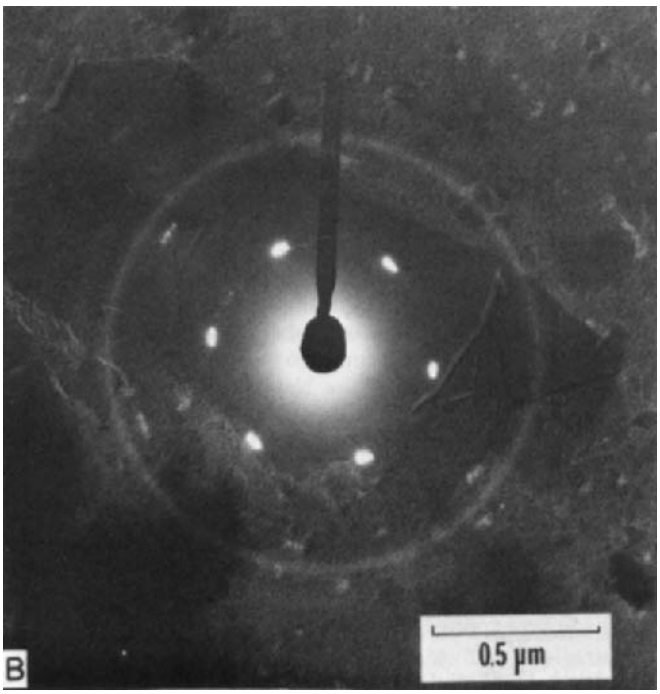

Fig. 3.61. Askana montmorillonite particles with extremely regular morphological features. A. The E- and S-type lamellae. B. An L-type particle with its superimposed SAD pattern.

also seen. The euhedral lamellae (E-type) are shown in Fig. 3.61A, and L-type particle in Fig. 3.61B. The lateral dimensions of the E-type particles in Fig. 3.61A range from 0.1 to about 1 μm. The thicknesses of these particles range from 60 to 200 Å. The L-type particle in Fig. 3.61B has lateral dimensions of 1.0 $\times$ 2.0 μm and a thickness of 80 Å. The superimposed SAD pattern shows the predominance of 01, 11, and $1\bar{1}$ reflections which are equally strong in intensity. This hexagonal symmetry of spots suggests a random stacking sequence of layers in the particle. The SAD data on Askanite particles with different morphologies do not, however, indicate any significant differences in the *b*-dimensions of these particles. The E-, L-, and S-type particles have an average *b*-dimension of 8.94 $\pm$ 0.03 Å, whereas the foliated aggregates have an average *b*-dimension of 8.96 $\pm$ 0.03 Å.

References

Australia

Bowen, K.G., 1970. Further report on Bentonite at Gellibrand. Min. Geol. J., 11: 33—39.

Cameron, J.B., 1963. Occurrence of montmorillonite clays, Malabar, Rosewood Coal Field. Queensland Gov. Min. J., 64: 458—541.

Darragh, P.J. and Bowen, K.G., 1965. The occurrence of bentonite at Gellibrand. Min. Geol. J., 6: 32—36.
Fisher, N.F., 1946. Bentonite and Fuller's earth. Aust. Bur. Miner. Resour., Geol. Geophys., Rep., 30: 21 pp.
Graham, J., 1953. An examination of clays from Marchagee and Cardabia. J. R. Soc. West. Aust., 37: 91—95.
Loughnan, F.C. and See, G.T., 1959. Bentonite and Fuller's deposits of New South Wales. Australasian Inst. Min. Metall. Proc., 190: 85—104.

China
Osaki, H., 1937. A new locality of bentonite and white tuffaceous shale in the Nai-tsu-shan coal fields. Geol. Inst. South Manchuria Railroad, Bull., 8—9: 31—37.
Sakomoto, T., 1937a. A *new mineral bentonite in Man-chou-kuo*. Geol. Inst. South Manchuria Railroad, Bull., 8—9: 1—18.
Sakomoto, T., 1937b. A bentonite and acid earth in the Nai-tsu-shan coal field. Geol. Inst. South Manchuria Railroad, Bull., 8—9: 45—59.
Wu, P. and Lee, M.T., 1948. Bentonite in Northern Chekiang. Contrib. Nat. Res. Inst. Geol., Acad. Sin., 7: 1015.

India
Bhola, L., 1947. Bentonite in India. Q. J. Geol., Min. Metall. Soc. India, 19: 55—77.
Guha, S.K., Das, S.R. and Sudhir, Sen, 1973. Physicochemical properties of bentonites from Gujarat, Jammu and Kashmir. Trans. Indian Ceram. Soc., 32: 11—15.
Güven, N., 1974. Lath-shaped units in fine-grained micas and smectites. Clays Clay Miner., 22: 385—390.
Siddiquie, N.N. and Bahl, D.P., 1965. Geology of the bentonite deposits of the Barmer District, Rajasthan. Mem. Geol. Surv. India, 96: 36 pp.
Talati, D.J., 1970. On the origin and classification of Bhavnagar bentonite, Gujaret State. Mineral Wealth (Gujarat Div. Geol. Min.), 6: 15—18.

Indonesia
Harajosaestro, R.R., 1953. Preliminary note on cristobalite in clay grade *volcanics*. Indones. J. Nat. Sci., 3: 116—122.
Van Bemmelen, R.W., 1970. Geology of Indonesia. 2. Economic Geology. Martinus Nijhoff, The Hague, 265 pp.

Iran
Henderson, S.G. and Robertson, R.H.S., 1958. A Mineralogical Reconnaissance in West Iran. Resource Use Limited, Glasgow, 150 pp.

Iraq
Hanna, A.B., 1966. Dioctahedral montmorillonite of Iraq. Arab. Sci. Conf., 5th, Bagdad, pp. 199—208.

Japan
Güven, N. and Pease, R.W., 1975. Electron-optical investigations on montmorillonites. II. Morphological variations in the intermediate members of the montmorillonite/beidellite series. Clays Clay Miner., 23: 187—191.
Hayashi, H. and Sudo, T., 1957. Zeolite-bearing bentonites. Mineral. J., 2: 191—199.
Iwao, S., 1969. The clays of Japan. Geol. Survey of Japan.
Lee, D.E., 1951. Bentonite and bleaching clays in Japan. Nat. Res. Sect. Gen. Hdg. Supreme Command for Allied Powers, Rep., 139: 31 pp.

Masui, J., 1960. On montmorillonite in a volcanic ash soil. J. Jap. Assoc. Mineral., 49: 263—271.
Masui, J. and Shoji, S., 1970. Formations of clay minerals from pumice in volcanic ash soils of Japan. Nendo Kagaku, 9(3—4): 29—33.
Mitsuda, T., 1960. On 'acid clays' and cristobalite from Itoigawa. Kobutsugaku Zasshi (J. Miner. Soc. Jap., 4: 335—362.
Sakamoto, M., 1970. Bentonite from the Fukuoka District. Nendo Kagaku, 10: 39—51.
Sudo, T., Kurabayashi, S., Tsuchiya, T. and Kaneko, S., 1964. Mineralogy and geology of Japanese volcanic ash soils. Int. Cong. Soil Sci., 8th, 3: 1095—1104.
Suzuki, K., 1954. Studies of clay minerals found in the coal measures of the coal fields of Hokkaido. Shigen Kagaku Kenkyusho Iho (Misc. Rep.) Res. Inst. Nat. Resour., 34: 58—59; 35: 71—81.
Uchida, M., 1946. Bojondo (Bentonite). Hokuryukan, Tokyo, 190 pp.
Utida, M., 1937. Studies of Yamagata bentonite. J. Jap. Ceram. Soc., 45: 800—807, 873—880.

Korea

Anonymous, 1973. Bentonite. Ind. Miner., 66: 9—15.
Kim, M.S., 1972. Improvement of the adsorption by chemical treatment of Ysong-II bentonite. Daehan Hwahak Hwoejee, 16(4): 241—248.
Moon, T.J. and Kwan, O.K., 1972. Grease from Korean bentonites. Daehan Hwahak Hwoejee, 16(3): 193—199.

New Zealand

Anonymous, 1973. Bentonite in the U.S.A. Appendix. Ind. Miner., 66: 15.
Carlson, J.R. and Rodgers, K.A., 1974. The Coalgate bentonite. Clays Clay Miner., 10: 153—172.
Fields, M., 1962. The nature of the active fraction of soils. N.Z. Dep. Sci. Ind. Res., Soil Bur., Publ., 227: 19 pp.
Fields, M., 1968. Mineralogy of New Zealand Soils. N.Z. Dep. Sci. Ind. Res., Soil Bur., Bull., 168(26): 22—39.
Fyfe, H.E., 1934. Bentonite and its occurrence in N. Zealand. N.Z. J. Sci. Technol., 15: 386—394.
Grange, L.I., 1931. Volcanic ash showers. N.Z. J. Sci. Technol., 12: 228—240.
Ker, D.S., 1969. Bentonite on Parehaka Station, East Coast, New Zealand. Dep. Sci. Ind. Res., Ser. 63: 67—75.
Macpherson, E.O., 1952. The stratigraphy and bentonitic shale deposits of Kekerangu and Blue Slip, Marlborough. N.Z. J. Sci. Technol., Ser. B, 33(4): 258—286.
Macpherson, E.O. and Coventry, R.G., 1941. Bentonite in Southern Hawks Bay, New Zealand. N.Z. J. Sci. Technol., 22: 265—275.
Ritchie, J.A., Gregg, D.R. and Ewart, A., 1969. Bentonites in Canterbury. N.Z. J. Geol. Geophys., 12(4): 583—608.
Wilson, D.D., 1963. Geology of the Wiapara Subdivision. N.Z. Geol. Surv. Bull., 64: 122 pp.

Pakistan

Alauddin, M., Qaiser, M.A., Akhter, S.M. and Khan, A.H., 1971. Mineralogy and chemistry of Dherikot clays from Campbellpur District, Rawalpindi Division. Sci. Ind. (Karachi), 8(3—4): 343—346.
Ali, S.T. and Shah, I., 1963. Bentonite resources of Pakistan. Symp. Industrial Rocks and Minerals, Lahore, pp. 153—160.

U.S.S.R.

Avakyan, G.S., 1968. Formation condition of the Sarigyukh bentonite clay deposit. Izv. Akad. Nauk Arm. SSR, 21(5): 45—52.

Belyankin, D.S. and Petrov, V.P., 1950. Petrographic composition and origin of Askana clays. Bull. Acad. Sci. USSR, Ser. Geol., 1950(2): 33—44.
Budnikov, V.I. and Kazanskii, Y.P., 1960. Detection of bentonite in the Kuznetz Basin. Dokl. Akad. Nauk SSSR, 131: 1417—1419.
Chukhrov, F.V., 1968. Some results of the study of clay minerals in the U.S.S.R. Clays Clay Miner., 16: 3—14.
Dsotsenidze, G.S. and Matchabely, G.A., 1963. The genesis of bentonites of Georgian SSR. Proc. Int. Clay Conf., Stockholm, 2: 203—210.
Kopkin, R., 1965. Eastern Slovakian bentonites. Tr. Ukr. Ghekh. Konf. Bentonitham Uzghorod, Ukr. SSR, 1965: 16—21.
Kovalenko, D.N. and Slutzkaya, R.K., 1958. Mineral composition of bentonite clays in the Cherkassy region deposit. Gliny Ukr. Akad. Nauk, Ukr. Sb., 1958(2): 14—22.
Kukorskii, E.G. and Ostrovskaya, A.B., 1962. X-ray study of bentonite clays of the Cherkassy deposit. Sov. Min. Ukr. SSR, Pervogo Vses. Soveshch, Kiev, 1962: 67—74.
Manuilova, N.S., Sukhanova, S.M. and Varlomov, V.P., 1965. Swelling of bentonites. Nauchn. Issled. Mekh. Stroit. Mater. Konstr., 1965(5): 68—85.
Merabishvili, M.S., 1962. Bentonite clays. Gosgeoltekhizdat, Moscow, 128 pp.
Ovcharenko, F.D., 1958. Ukrainian Bentonite. Izd. Akad. Nauk Ukr. SSR, Kiev, 100 pp.
Ovcharenko, F.D., Kirichenko, N.G., Ostrovskaya, A.B. and Forgii, M.G., 1966. Cherkassy deposit of bentonite and palygorskite clays. Nauk Dumka, Kiev.
Pease, R.W., Güven, N. and Grim, R.E., 1974. Electron-optical observations on Askanite particles. Estud. Geol. (Madrid), 30: 309—314.
Petrosov, I.L.M. and Tsameryan, P.P., 1964. Petrography and mineralogy of bentonite clays in the Noemberyan deposit. Izv. Akad. Nauk Arm. SSR, 22(4): 50—59.
Rateev, M.A., 1967. Sequence of hydrothermal alteration of volcanic rocks into bentonitic clays of the Askana deposit in the Georgian S.S.R. Dokl. Akd. Nauk SSSR, 175(3): 675—678.
Rateev, M.A., 1968. Authigenic clay formation in volcanic-sedimentary formations. Izv. Akad. Nauk Kazan. SSR, 1968: 88—94.
Sabitov, A.A., 1968. Mineral composition of bentonites from the Smyshlyaersk deposits. Tr. Inst. Geol. Nauk, Akad. Nauk Kaz. SSR, 1968(19): 149—155.
Seidov, A.G. and Alizade, K.A., 1966. The formation and mineralogy of bentonites from Azerbaidjia. Clay Miner., 6: 157—166.
Seidov, A.G. and Alizade, K.A., 1970. Mineralogy and origin of the bentonite clays of Azerbaidjia. Izd. Akad. Nauk Azerb. SSR, Baku, 190 pp.
Shabayeva, Y.Y., 1964. Palygorskite from Paleogene beds of Southeast Turkmenia. Dokl. Acad. Sci. U.S.S.R., Earth-Sci. Sect., 143: 94—97.
Sokolova, G.U., 1965. Triassic tuffaceous formations in the Donetz Basin. Geol. Zh., Akad. Nauk. Ukr. SSR, 25(4): 90—94.
Tazhibayeva, P.T. and Galiyev, M.S., 1972. Genetic features of South Kazakhstan bentonites. Int. Clay Conf., Madrid.
Yurevich, A.L. and Sokolova, A.L., 1965. Formation of fine-grain fraction minerals in the Upper Pliocene ash tuffs of the Balkash area in Turkmenia. Litol. Polezn. Iskop., 1965: 34—53.

3.6. ORIGIN OF BENTONITES

As stated in Chapter I, the clay to which the name bentonite was first applied was formed by the alteration of volcanic ash, and early definitions of bentonite indicated this mode of origin. Recent studies have shown that

some clays designated as bentonite on the basis of their composition and properties have had other modes of origin. Consideration of the various ways in which bentonites are formed make it convenient to discuss their origin under the following headings:

(a) Alteration of volcanic ash or tuff essentially in situ.

(b) Hydrothermal alteration generally of igneous rocks.

(c) Deuteric alteration of igneous material.

(d) Miscellaneous and uncertain modes of origin including instances where no precise mode of origin can be established.

Alteration of volcanic ash or tuff essentially in situ

This mode of origin is established by the presence of shards and other relict structures of the parent ash or tuff which can be seen in microscopic examinations, by the character of the nonclay minerals, and, at times, by transitions to associated beds of ash or tuff. Alteration in situ is indicated by the high concentration of clay minerals, by the absence of detrital minerals, by the association with adjacent beds, and by the transition to ash or tuff (Hagner, 1939). There are instances, in Patagonia in Argentina (Bordas, 1943), where the altered ash has been transported a short distance and then deposited without substantial contamination by detrital impurities. There are also many instances, such as in the Orange Free State of South Africa, where origin by the alteration of volcanic ash or tuff cannot be established unequivocally, but where composition and general considerations make it likely. In some instances, there is no evidence of any volcanic activity in the area at the proper geologic interval.

Alteration of ash or tuff in situ is by far the commonest mode of origin of bentonites. The bentonites in the formations of Cretaceous age in Wyoming and Montana of the U.S.A. are the classic examples of this mode of origin. In the United States, bentonites in Mississippi, Texas, Arizona and California also have originated in this way. It is not feasible or necessary to list exhaustively all bentonites that have formed by the alteration of volcanic ash or tuff, but examples are to be found in England, Germany, U.S.S.R., Hungary, Yugoslavia, Japan, Morocco, Argentina, New Zealand, South Africa, etc. Such bentonites can exhibit substantial variations in type of component smectite, in chemical composition, in abundance of nondetrital nonclay minerals, e.g., zeolites and cristobalites, and, consequently, to a limited extent in physical properties. The amount of swelling and rheology can vary substantially.

It is clear that there are no narrowly restricted conditions necessary for the formation of bentonites from volcanic ash or tuff. That the environment in which the alteration took place can vary widely is indicated by the wide range of associated sedimentary beds. Alteration in a shallow marine environment is most common, as illustrated by the bentonites in Wyoming,

Texas, and Mississippi of the U.S.A., those of England and Germany, and some of those in the U.S.S.R. Some of the bentonites in Canada, Czechoslovakia, Rumania, New Zealand, Switzerland, and Yugoslavia appear to have been formed in fresh water. Estuaries and lagoons are reported as the site of formation of the bentonites in Egypt and Pakistan. The bentonite from Marchagee, Australia seems to have formed in a desert pan. Bentonites interbedded with coal in Australia and Canada indicate that the alteration of the ash or tuff also can take place in a coal-forming environment. In some areas, notably Argentina and Canada, the bentonites are found in sections containing both marine and nonmarine sediments, again illustrating that the nature of the environment in which the alteration took place is not critical.

An aqueous environment is undoubtedly helpful in providing the necessary water for the hydration of the ash or tuff to the smectite. Only a few instances are known in which ash falling on land has altered to bentonite (Bordas, 1943; Hofmann, 1949). There seems to be no reason why a particularly wet ash falling on land should not alter to a smectite clay.

Bentonites have formed from volcanic ash varying in composition from rhyolitic to basaltic (Konta, 1957; Hofmann and Jager, 1959; Ritchie and Gregg, 1965). However, most bentonites have formed from ash ranging from rhyolitic to dacitic in composition, with latitic ash being most prevalent (Slaughter and Early, 1965). It appears that a high silica content (70%) does not favor the alteration process (Ross and Hendricks, 1945), and that a moderate magnesia content (5—10%) does. The composition of the ash is important in controlling the composition of the smectite that forms. Thus, Hofmann and Jager (1959) record the formation of saponite from basaltic ash, and Patterson (1955) has shown that the exchangeable cation composition of some Wyoming bentonites is related to the composition of the ash. A fairly high magnesium content appears to favor alteration, and Yurevich and Sokolova (1965) concluded that the intensity of the conversion of volcanic ash to smectite is proportional to the magnesium content of the ash.

Volcanic ash does not always alter to bentonite. This is vividly shown in instances where there is an alternation of ash and bentonite as in Argentina and the Cheto area of Arizona, and by the presence of unaltered ash in the geologic column (Swineford et al., 1955). X-ray diffraction analyses of such ash frequently show that some alteration has taken place. Certainly where the ash and bentonite are interlayered, the unaltered ash and the altered ash must have had the same source, and the data indicate that the composition was about the same and the ashes accumulated in the same environment. A possible explanation is that some ash falls were relatively wet and had a high gaseous content, and that such ash altered to the smectite. There is considerable evidence that a wet ash favors the formation of bentonite (Hofmann, 1956). An alternative explanation is that the ash fell on land with superficial alteration of the ash beds. In most instances the very extensive uniform thickness of the interlayered beds and the absence of transitions vertically is against the alternative mode of origin.

The alteration process is essentially devitrification of the ash, hydration, and crystallization of the smectite around many nuclei. In some instances, there is evidence of a loss of alkalies during the alteration. Also, the silicification of some beds underlying some bentonites indicates downward migration of silica. In some cases, there is evidence that leaching accompanied the alteration. In other cases there is no evidence of any leaching.

Many authors, for example Martin-Vivaldi and Pino Vasquez (1956) have pointed out that bentonites often have a higher magnesium content than the probable parent material. Clearly in some instances magnesium appears to have been added in the alteration process, and magnesium-rich waters moving through the ash have been postulated. The source of the magnesium is a problem, but then the high magnesium content in many sedimentary rocks is difficult to understand (Ross and Hendricks, 1945; Patterson, 1955; Keramata, 1957).

Several authors, Ghergariu et al. (1964), have concluded that sometimes the transformation of the tuff took place under the action of a strong circulation of infiltrated waters which caused the hydrolysis of the volcanic mass. This may have been a factor for some bentonites, but there is no evidence that this was a factor for other bentonites.

In general, the alteration of the ash or tuff to the smectite was probably contemporaneous with the accumulation of the igneous material, and once the smectite was formed, there was little further alteration. Evidence for the contemporaneous alteration of the ash or tuff can be found in many deposits, for example, the Cherry Lease deposits of Texas contain dikes of loose sand from the overlying formation, which show a gradational contact with the bentonite. In Mississippi a bentonite grades upward into a glauconitic sand which contains nodules of bentonite, again indicating rapid alteration of the ash. The interlamination of bentonite and ash or shales, as has been noted, favors the contemporaneous alteration of ash to smectite.

Detailed studies in Wyoming of calcium and sodium bentonites indicate that the particular exchangeable cation composition developed at the time of formation of the smectite, and not in a later process (Patterson, 1955). There are a few exceptions to this conclusion. The hydrogen bentonite in the Pembina area of Canada was formed when the oxidation of pyrites in overlying shales produced acid which in turn produced the hydrogen bentonite.

The detrification process generally took place in water, and cannot be considered to be the result of superficial weathering processes. The evidence for the absence of weathering is the vertical uniformity of the mineral composition, i.e. the absence of any soil profile development. It is well known that smectite minerals may form by the weathering process under certain conditions of climate, topography, drainage, etc., from some types of parent rocks. Generally, the weathering processes do not lead to the formation of a single clay mineral, and, hence, not to a material with the properties of bentonite. There are some exceptions to the foregoing statements, and some of

the Argentine and possibly the Austrian bentonites may have formed by weathering processes. In some cases, e.g., the Japanese acid earths, the calcium bentonites of Azerbaidjian, and the Pembina, Canada bentonites, secondary superficial alteration superimposed on the devitrification process has affected the character of the bentonite.

The available evidence suggests that the cristobalite present in some bentonites formed from the glassy ash, and was not a crystalline component of the ash. Based on oxygen-isotope studies, Henderson et al. (1971) have shown that the cristobalite in the Helms bentonite of Texas was formed at about 25°C. These authors concluded that the cristobalite crystallized at about this temperature from amorphous silica released during the devitrification of the glass. Based on the isotope content of the oxygen in the smectite of this bentonite, they concluded that the smectite also crystallized at about this temperature. Flörke (1955) earlier had concluded that the cristobalite in bentonites had formed at a low temperature because of its defective lattice. It probably should not be concluded that the cristobalite in bentonites has always formed at such a low temperature. Gruner (1940) earlier concluded that this mineral in Wyoming bentonites formed in the devitrification of the volcanic glass. Reynolds and Anderson (1967) have described an association of cristobalite-containing bentonites with coal in the Colville Group of Upper Cretaceous age in northern Alaska. This association led them to suggest that the presence of humic acid favors the formation of cristobalite during the devitrification of the ash. It is interesting that cristobalite is extremely rare in bentonites older than the Cretaceous.

The zeolites found in some bentonites also appear to be products of the devitrification of the glass, and numerous authors (Kerr, 1931; Kerr and Cameron, 1936; Bramlette and Posnjak, 1932) have suggested that the zeolites are intermediate components formed from the glass which then altered to smectite. Kizaki (1965) has described instances where the cores of ash shards are composed of clinoptilolite and the outer rim is smectite. Sudo et al. (1960) have emphasized that zeolite structures are readily developed from volcanic glass. It has been shown by Deffeyes (1959) that a highly saline environment favors the formation of zeolites from volcanic ash. An ash rich in alkalies and under conditions where there is no leaching, so that these components remain in the environment, would be expected to lead to the formation of zeolites. Reynolds and Anderson (1967) have presented evidence that the composition of the ash rather than the environment is responsible for the formation of clinoptilolite in the Alaskan bentonites investigated by them.

Microscopic studies show that nonvitreous components of the parent ash may be altered to smectite. Thus particles of feldspar frequently show distinct alteration to smectite. It is of interest that flakes of biotite commonly present in bentonites generally appear to be completely unaltered.

There are many problems remaining for an understanding of the

devitrification process. Why, for example, are the smectite units relatively large and thin as they are in some of the Wyoming bentonites? Why are they more granular in many other bentonites? Why in some instances are kaolinite minerals formed in the devitrification process?

Hydrothermal alteration generally of igneous rocks

Hydrothermal alteration appears to have been the mode of origin of many bentonites with the character of the parent rock showing wide variations. Frequently the texture of the parent rock is retained in the bentonite, e.g., Algeria, Spain, Greece, Hungary, etc. Commonly, smectite is the sole alteration product, but in some instances other clay minerals in small quantities are also present; such as, halloysite in some of the Algerian bentonites, and halloysite and allophane in some of the bentonites from Japan.

It is well established that the various types of clay minerals can form by hydrothermal alteration processes acting on metamorphic, igneous, or sedimentary rocks. Clay minerals are being formed in this way at the present time in hot springs areas in Yellowstone National Park in Wyoming, U.S.A. (Fenner, 1936), in Iceland (Correns, 1962), in New Zealand (Steiner, 1953), and elsewhere. Numerous occurrences of clay minerals found in this way are associated with ore deposits, for example, at Butte, Montana, U.S.A. (Sales and Meyers, 1948). Usually the hydrothermal alteration processes produce a suite of clay minerals in a given occurrence. Frequently there is a sequence of clay minerals away from the source as illustrated in the base metal deposit at Butte, Montana, and in the hot springs of New Zealand. Sometimes, essentially a single clay mineral has developed replacing a large mass of host rock, usually igneous but at times sedimentary. At Eureka, Utah, U.S.A., halloysite has developed in place of a carbonate rock. At Cornwall, England, the alteration of a granite has been essentially to kaolinite. There are many places, as noted below, where the sole alteration product is smectite, and in these instances, the clay is referred to as bentonite. There seems to be no particular type of smectite that characterizes bentonites of this mode of origin.

Many examples of bentonites produced by hydrothermal alteration could be given, but the following will suffice to illustrate their general character, composition, and type of parent material. At Lalla Maghnis near Oran in Algeria, Sadran et al. (1955) have described the alteration of a rhyolite plug to a smectite. Kaolinite in the amount of about 20% is also present in the alteration product. The hydrothermal alteration is believed to have been followed by the circulation of magnesium-rich water, possibly meteoric, which added magnesium and leached silica and alkalies. The rhyolite structure is perfectly retained in the alteration product and the volume is unchanged.

One of the early descriptions of a hydrothermal bentonite deposit was the one at Tomesti in Rumania by Dittler and Kirnbauer (1933). Here the parent

material is a liparite, and the depth of alteration is given as evidence for the hydrothermal origin. The original texture of the liparite is preserved.

Avakyan (1968) described an Armenian bentonite produced by hydrothermal alteration of porphyrites of andesite-basalt composition. The bentonite contains relicts of the porphyrites, and at places shows transitions to the parent rock. It is concluded that the hydrothermal solutions must have been alkaline to favor the formation of the smectite.

Rateev (1967) attributed the origin of the well-known Askana bentonite clays of Georgia, U.S.S.R., to hydrothermal alteration of pyroclastic rocks, and in some instances the simple devitrification of ash and tuff was probably accompanied by processes that could be classed as hydrothermal.

Some of the bentonites near Almeria on the Mediterranean coast of Spain are hydrothermally altered trachyte. Again, the texture of the parent rock is preserved and the depth of alteration is significant.

Andreatta (1952) has pointed out that some Italian bentonites have been formed by hydrothermal alteration, and commonly the most altered material is in the center of the alteration zone.

The well-known Italian bentonite from the Island of Ponza has been described by Lupino (1954) as being a consequence of the alteration of rhyolitic glassy tuff by hydrothermal processes associated with the closing stages of volcanic activity. Study by one of us (REG) could detect no definite evidence of hydrothermal alteration, and devitrification of the tuff seems to be the dominant process, although some deuteric alteration superimposed on hydrothermal alteration is possible. The underlying silicified zone indicates that the alteration process was accompanied by the downward movement of silica.

Atanasov and Goranov (1963) describe the Kurdjali bentonite in Bulgaria as resulting from hydrothermal alteration superimposed on the devitrification of tuffs and lavas which range from rhyolitic to basaltic in composition. A zonal distribution of the alteration products indicates the hydrothermal action.

It is clear that in some instances the alteration process is a fairly straightforward chemical reaction, as is the case with the hectorite at Hector, California, where siliceous, lithium, and flourine bearing agents have reacted with carbonates to form the clay mineral. In other instances, the altering agents have seeped through the parent rock, transforming it by complex reactions to a mass of smectite without substantial leaching, and with the preservation of the original rock texture. The process has been one of hydration and frequently the addition of magnesium. As indicated previously, hydrothermal alteration processes, in many cases, may have been superimposed on devitrification processes; the bentonites of the Amargosa Valley in Nevada appear to be such an example.

The depth of alteration, the absence of vertical variations in composition, and the absence of any suggestion of a soil profile are definite evidences that

surficial weathering processes have not played a significant role in the formation of these bentonites.

Deuteric alteration of igneous material

Deuteric is used here to indicate changes taking place in an igneous rock immediately following its implacement as a consequence of the reaction of gases and vapors included within the igneous mass and its other components. Admittedly, there is no sharp demarkation between deuteric alteration and hydrothermal processes or, for that matter, devitrification. Certainly for the origin of bentonites, all of these processes have operated. There are some bentonites, however, for which deuteric alteration seems to be the sole or at least the dominant mode of origin.

An interesting example of deuteric alteration is found in a glassy perlitic rhyolitic lava in a volcanic sequence near the top of the Stormberg Series of the Karoo System of Liassic age, and which extends from Mozambique southward into Zululand of the Natal State of the Union of South Africa. The alteration of the perlite to smectite is extremely irregular. At some places the alteration is complete, and there are huge masses of bentonite tens of feet thick. At other places, the smectite is scattered through the glass, or the perlite is unaltered. Frequently, there are smectite nodules within the perlite. There is no suggestion of any relationship with fractures or the penetration of hydrothermal agents from an outside source. It seems clear that the alteration took place as a consequence of gases and vapors included within the parent igneous rock, and was concentrated where the gases and vapors were most abundant. Of special interest are occurrences in Zululand in which the resulting clay mineral is kaolinite. One can find specimens altered both to smectite or to kaolinite; which mineral forming probably depended on the composition of the gases and vapors and/or on the chance migration and local removal of alkalies and alkaline earths.

Cavinato (1957) considers many Italian bentonites to have been formed by the intrusion of a very wet magma followed quickly on cooling by the action of gases and vapors present in the intruded rock.

Schüller and Köhler (1953) describe a German occurrence in which the lower part of a nepheline basanite has been altered apparently by deuteric reactions to a bentonite. This occurrence indicates that the deuteric mode of origin is not restricted to acidic igneous rocks, although it is probably most common in such material.

Miscellaneous and uncertain modes of origin

In the following occurrences of bentonites various modes of origin have been suggested. In many instances, the absence of associated volcanic activity or igneous material, and the absence of a texture indicating ash, tuffs, or

any igneous material has been taken as evidence of an origin unrelated to igneous activity. Such negative evidence really carries little weight, and often the alternative suggested modes of origin are not very convincing. For example, several authors (Belyankin, 1950; Heflik, 1959) have suggested an origin due to weathering for some bentonites, and although weathering processes in some few cases may have been superimposed on bentonites, there are only a very few examples where this seems to have played any role whatsoever in the origin of bentonites. One of the cases in which weathering has played a role has been described by Bordas (1943) from Argentina. Here, in sections consisting of an alternation of ash and bentonite, the upper part of some of the ash beds are altered to smectite. Another example is described by Sudo et al. (1960) from Japan in which the surface of tuffs of Tertiary Age has been uniformly altered to smectite. Masui and Shoji (1970) has emphasized that such weathering products in Japan usually are composed of a variety of clay minerals. Hayashi (1971) has shown that halloysite rather than smectite is the common weathering product of volcanic ash in Japan.

Siddiquie and Bahl (1965), in their study of the extensive deposits of bentonite of Tertiary Age in the Barmer District of Rajasthan, India, ruled out alteration of volcanic material as a mode of origin because of the absence of volcanic activity in the Tertiary interval in this area. They suggest that the clays formed by weathering of Precambrian igneous and metamorphic rocks in a humid climate with later transportation and deposition in the Barmer Embayment. Certainly very unusual circumstances would be required for a clay as pure as the Barmer bentonites to have been formed in this way. There are instances, for example, in Argentina (Bordas, 1943) and Czechoslovakia (Michalek, 1965) in which altered ash bentonites have been transported short distances and redeposited without substantial contamination by detrital material.

Kopetsky (personal communication) suggested a unique mode of origin for some Austrian bentonites. According to him, they are derived from trachy-andesites containing abundant feldspar which were altered by solutions of silica and sulfate bearing waters to the so-called "Austrian Trass" which is mainly an aggregate of opal and alunite. Finally, weathering destroyed the "Trass", during which hydrous sulfate solutions led to the formation of smectite.

An interesting occurrence of bentonite is reported from Marchagee in Western Australia by Graham (1953). Two beds of bentonite, each about 12 inches thick, separated by gypsiferious clays, form clay pans in the bed of a lake depression in a desert area. A somewhat similar occurrence has been described by Gindy and Badra (1968) from Egypt. In neither instance is there any associated volcanic activity and the precise mode of origin is obscure.

Papke (1969) has recently concluded that some of the bentonites in Nevada, U.S.A., were formed by partial leaching and alteration of glassy

rhyolitic rocks by ground waters. Bramlette (see Ross and Hendricks, 1945) earlier presented evidence implying that ground water brought about the alteration of volcanic ash to montmorillonite in the Santa Monica area near Los Angeles. A consideration of bentonite deposits in general strongly suggest that ground water rarely played a significant role in the formation of bentonites. However, such water may have been important in supplying the additional magnesium which seems to have accompanied the formation of some bentonites.

A large amount of research (for a summary, see Grim, 1968) has shown that the various clay minerals, including smectites, can be synthesized at ordinary conditions of temperature and pressure from mixtures of their constituent oxides and hydroxides. Recently, Harder (1972) has shown that the presence of magnesium in the starting material favors the formation of smectites. Small amounts of magnesium, of the order of 6% MgO, lead to the development of smectites.

Millot (1970) has pointed out that smectite may be formed directly (neoformation) in certain sedimentary environments. Chamley and Millot (1972) have described the neoformation of montmorillonite, illite, and chlorite in sediments in the Santorin volcanic archipelago. Diatoms supplied the silica, and the aluminum was derived from the hydrolysis of pumice under marine conditions.

Neoformation of smectite in a sedimentary environment is certainly a possible mode of origin for some occurrences, for example, in Marchagee, Western Australia, where there is no evidence of any related volcanic activity.

References

Andreatta, C., 1952. On the origin of montmorillonite clays by hydrothermal action in Italy. Int. Geol. Congr., Proc., 18: 149—161.

Atanasov, G. and Goranov, A., 1963. Bentonitic clays from the region of Kurdjali. Ann. Univ. Sofia, 56: 149—188.

Avakyan, G.S., 1968. Formation conditions of the Sarigyukh bentonitic clay. Izv. Akad. Nauk, Arm. SSR, Nauki Zemle, 21: 45—52.

Belyankin, D.S., 1950. Petrographic study of Askan clay. Izv. Akad. Nauk SSSR, Ser. Geol., 2: 33—44.

Bordas, A.F., 1943. Contribution to the knowledge of bentonites in Argentina. Serv. Geol. Min., Estud. Espec., 15, 60 pp.

Bramlette, M.N. and Posnjak, E., 1932. Zeolitic alteration of pyroclastics. Am. Mineral., 18: 167—173.

Cavinato, A., 1957. Geology and genesis of some Italian bentonites. Accad. Nazionale dei Lincei, Rome, 23: 10 pp.

Chamley, H. and Millot, G., 1972. Neoformation of montmorillonite from diatom and ashes in the marine sediments of Santorin. C. R. Acad. Sci., Ser. D, 274(8): 1132—1134.

Correns, C.W., 1962. Formation and transformation of clay minerals during decomposition of basalts. Colloq. Int. C.N.R.S., 105: 109—121.

Deffeyes, K.S., 1959. Zeolites in sedimentary rocks. J. Sediment. Petrol., 29: 602—609.

Dittler, E. and Kirnbauer, F., 1933. The bentonite occurrence at Tomesti, Rumania. Z. Prakt. Geol., 41: 121—127.
Fenner, C.N., 1936. Bore hole investigations in Yellowstone Park. J. Geol., 44: 225—315.
Flörke, O.W., 1955. The problem of the existence of high modification cristobalite in opals, bentonites and glasses. Neues Jahrb. Mineral., Monatsh., 10: 217—223.
Ghergariu, L., Mirza, I. and Ionescu, G., 1964. Geological and mineralogical study of bentonite from Acna Mures. Stud. Univ. Babes-Bolyai, Ser. Geol.-Geogr., 1: 23—37.
Gindy, A.R. and Badra, A., 1968. Bentonite-like clays and marls in the northwest desert of Egypt. Proc. Egypt Acad. Sci., 21: 11—36.
Graham, J., 1953. An examination of clays from Marchagee and Cardabia Western Australia. J. R. Soc. West. Austr., 37: 91—95.
Grim, R.E., 1968. Clay Mineralogy. McGraw-Hill, New York, N.Y., 2nd ed., 596 pp.
Gruner, J.W., 1940. Abundance and significance of cristobalite in bentonite and Fuller's earths. Econ. Geol., 35: 867—875.
Hagner, A.F., 1939. Adsorptive clays of the Texas Gulf Coast. Am. Mineral., 24: 67—108.
Harder, M., 1972. Role of magnesium in the formation of smectite minerals. Chem. Geol., 10: 31—39.
Hayashi, T., 1971. Weathering of volcanic ash and clay minerals of the volcanic ash from Mt. Ta-tun-shan (Taiwan). Nendo Kagaku, 11(3): 109—113.
Heflik, W., 1959. Petrography of volcanic glass in bentonite clays from Ciecierze, Poland. Kwart. Geol., 3: 778—789.
Henderson, J.H., Jackson, M.L., Syers, J.K., Clayton, R.N. and Rex, R.W., 1971. Cristobalite authigenic origin in relation to montmorillonite and quartz origin in bentonites. Clays Clay Miner., 19: 229—238.
Hofmann, F., 1949. Montmorillonite in the molasse of Eastern Switzerland. Schweiz. Mineral. Petrogr. Mitt., 29: 43—49.
Hofmann, F., 1956. Petrographic and clay mineral studies of the bentonites of Switzerland and Southwest Germany. Eclogae Geol. Helv., 49: 113—133.
Hofmann, F. and Jager, E., 1959. Saponite as an alteration production of basaltic tuff at Karlihof. Schweiz. Mineral. Petrogr. Mitt., 39: 117—124.
Keramata, S., 1957. The origin of bentonites of Slaviste. Heidelb. Beitr. Mineral. Petrogr., 4: 289—295.
Kerr, P.F., 1931. Bentonite from Ventura, California. Econ. Geol., 26: 153—168.
Kerr, P.F. and Cameron, E.N., 1936. Fuller's earth of bentonite origin from Tehachapi, California. Am. Mineral., 21: 230—237.
Kizaki, Y., 1965. Diagenic alteration of Tertiary tuffs of Southern Gumma Prefecture, Gumma Daigaku Kiyo, Shizenkagaku-Hen, 13: 153—203.
Konta, J., 1957. Clay Minerals of Czechoslovakia. Nakladatelstvi Ceskoslovenske Akademie Ved, Prague, 200 pp.
Lupino, R., 1954. A bentonite from the Island of Ponza. Ric. Sci. Rome, 1954: 2326—2339.
Mathieu-Sicaud, A., Méring, J. and Perrin-Bonnet, I., 1951. Electron microscopic study of montmorillonite and hectorite saturated with different cations. Bull. Soc. Fr. Mineral. Cristallogr., 14: 439—455.
Martin-Vivaldi, J.L. and Del Pino Vazquez, C., 1956. Conditions of formation of montmorillonite in nature. Trab. Reunion Int. Reactividad Solidos, Madrid, 2: 481—503.
Masui, J. and Shoji, S., 1970. Formations of clay minerals from pumice in volcanic ash soils of Japan. Nendo Kagaku, 9 (3—4): 29—33.
Michalek, Z., 1965. Montmorillonite clays from Radzionkow, Upper Silesia. Zesz. Nauk. Akad. Krakowie, 39: 156 pp.
Millot, G., 1970. Geology of Clays. Springer, New York, N.Y., 429 pp.
Papke, K.G., 1969. Montmorillonite deposits in Nevada. Clays Clay Miner., 17: 221—222.

Patterson, S.H., 1955. Geology of the Northern Black Hills Bentonite Mining District. Ph.D. Thesis, Univ. Illinois, 137 pp.
Rateev, M.A., 1967. Sequence of hydrothermal alteration of volcanic rocks into bentonitic clays of the Askana deposit in the Georgian S.S.R. Dokl. Akad. Nauk SSSR, 175: 675—678.
Reynolds, R.C. and Anderson, D.M., 1967. Cristobalite and clinoptilolite in bentonite beds of the Colville Group of Northern Alaska. J. Sediment. Petrol., 22: 966—969.
Ritchie, J.A. and Gregg, D.R., 1965. Bentonites of Canterbury. Proc. Commonw. Min. Congr., Wellington, 208: 1—2.
Ross, C.S. and Hendricks, S.B., 1945. Minerals of the montmorillonite group. U.S. Geol. Surv., Prof. Pap., 205B: 23—79.
Sadran, G., Millot, G. and Bonifas, M., 1955. The origin of the bentonite deposits of Lalla Maghnia (Oran). Bull. Serv. Carte Geol. Alger., 5: 213—234.
Sales, R. and Meyers, C., 1948. Wall-rock alteration at Butte Montana. Am. Inst. Min. Metall. Eng., Tech. Publ., 2400.
Schüller, A. and Köhler, R., 1953. Physical properties of bentonite formed from basalt at Steinberg near Ostritz (Lausitz). Geologie (Berlin), 2: 167—184.
Siddiquie, N.N. and Bahl, D.P., 1965. Geology of the bentonite deposits of the Barmer District, Rajasthan. Mem. Geol. Surv. India, 96: 1—96.
Slaughter, M. and Early, J.W., 1965. Mineralogy and significance of Mowry bentonites, Wyoming. Geol. Soc. Am., Spec. Pap., 116 pp.
Sudo, T., Hayashi, H. and Matsuoka, M., 1960. Zeolites in glassy tuffs and bentonites in Japan. Proc. Int. Geol. Congr., Copenhagen.
Steiner, A., 1953. Hydrothermal rock alteration at Wairaki, New Zealand. Econ. Geol., 48: 1—13.
Swineford, A., Frye, J.C. and Leonard, A.B., 1955. Petrography of the Late Tertiary ash falls in the Central Great Plains. J. Sediment. Petrogr., 25: 243—261.
Yurevich, A.L. and Sokolova, A.L., 1965. Formation of fine-grained fraction minerals in the Upper Pliocene ash and tuffs of the Balkhash area in Turkmenia. Litol. Polezn. Iskop., 1965: 34—53.

3.7. CRYSTAL GROWTH ASPECTS OF SMECTITE MORPHOLOGY

In order to properly interpret morphological variations in smectite crystallites and in its crystalline aggregates, some understanding is necessary concerning the crystal-growth mechanisms and the factors affecting crystal morphology. These factors and the related growth mechanisms will be briefly described in this section with emphasis on mica-type layer silicates. Crystallization may be described as a result of two processes: nucleation and crystal growth. The relationship between nucleation rate and growth rate, both of which are directly related to the degree of supersaturation, determines whether the final crystalline product will be an aggregate or a single crystal. Crystalline aggregates are more common for smectites than the single crystallite. Morphological features of these smectite aggregates will be interpreted in terms of crystal growth mechanisms after discussing the factors affecting morphology of single smectite crystallites.

In this regard, a distinction should be made between internal (structural) and external factors. The internal factors are related to the crystal structure and to its imperfections such as dislocations. The major external factors are temperature, pressure (hydrostatic), degree of disequilibrium (supersaturation, concentration, and diffusion gradients), viscosity of the medium, and the presence of impurities. During the crystallization of layer silicates the internal factors seem to be strongly effective, leading to the prominence of lamellar forms.

The correlation between structure and morphology of a crystal has been expressed by the generalized principle of Bravais (Donnay and Harker, 1937) and by its extension (Donnay and Donnay, 1961). This principle, developed on empirical grounds, reveals that the importance of a crystal form (i.e. frequency of occurrence and regular surface area) decreases with decreasing interplanar spacing d_{hkl}, provided due considerations are given to space group symmetry or pseudosymmetry operations.

The established crystal forms for a related layer silicate (muscovite) but with much better crystallinity were given by Peacock and Ferguson (1943) along with the interplanar spacings as:

hkl:	(002)	(020)	(110)	($\bar{1}$11)	(021)	(111)	($\bar{1}$12)	(022)	(112)
d (Å):	10.00	4.51	4.51	4.47	4.42	4.29	4.25	4.12	3.99
form:	{001}	{010}	{110}	{$\bar{1}$11}	{021}	{111}	{$\bar{1}$12}	{011}	{122}

As pointed out by the above investigators, the observed forms of muscovite are in good agreement with the Bravais principle. The common habits of smectite single crystallites were depicted in p. 10 (Chapter 2) with their predominant forms. As mentioned there, the euhedral smectite crystallites occur in hexagonal platelets, rhombs, laths and sometimes in fibers. They exhibit, therefore, only the first three forms {001}, {010}, and {110} with basal forms predominating. It is expected from the Bravais principle that the {010} and {110} forms will be equally developed and this will lead to the development of a hexagonal platelet. The existence of rhombs and laths cannot be readily explained from the Bravais principle. For this purpose the physical basis of the Bravais principle needs to be further examined. The physical basis of the generalized Bravais principle was sought in the arrangement of strong bonds in the structure by Hartman and Perdok (1955), and by Hartman (1972). These investigators consider the crystal growth, to a first approximation, as the formation of strong bonds between crystallizing particles (atoms, ions, molecules). The morphology is then directly related to the directions of strong first coordination bonds formed during, or prior to, the crystallization. An uninterrupted chain of such strong bonds between the building units is called a "periodic bond chain" (PBC). A crystal can be considered as an array of slices with thickness d_{hkl} and parallel to the crystal

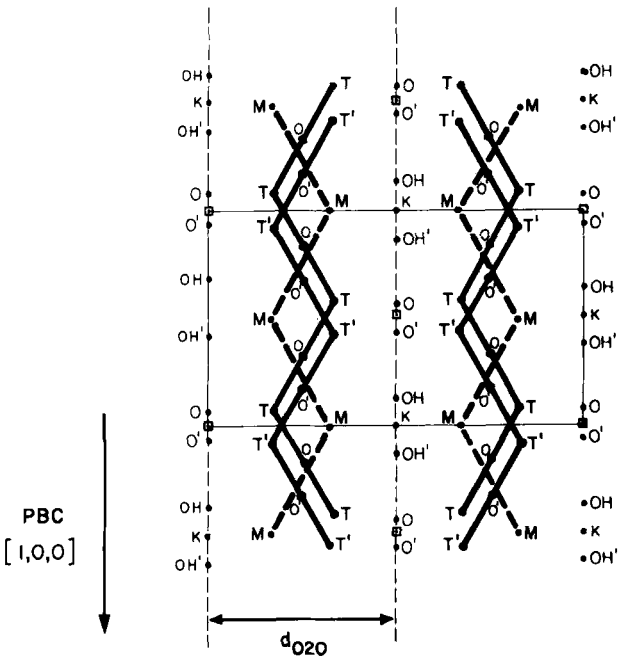

Fig. 3.62. Periodic bond chains along the [100] direction in a dioctahedral 1 *M* mica (*T*—*O*—*T*: tetrahedral silica chains, *M*—*O*—*M*: octahedral metal-oxygen chain).

faces. Using this concept, three classes of faces can be distinguished depending on how many coplanar PBC's are present in a slice of d_{hkl}. Accordingly, the so-called *flat* faces contain two or more PBC's in a slice of d_{hkl}, the *stepped* faces only one PBC, and the *kinked* faces no PBC's at all. Growth rates of the faces are considered to be proportional to the attachment energies of building blocks to the faces. The periodic bond chains in a dioctahedral 1 *M* mica structure consist of chains of tetrahedra and those of octahedra. In the original description of PBC's these chains must have the same stoichiometric composition as the crystal. In a complex structure like a mica, one cannot impose this condition on the periodic bond chains in the structure. The tetrahedral and octahedral chains form PBC vectors along the directions [100], [$\bar{1}$10], and [$\bar{1}\bar{1}$0]. A slice of d_{020} containing two tetrahedral and one octahedral chains is shown in Fig. 3.62; all these chains form the same PBC vector [1,0,0]. The slice of d_{110} containing tetrahedral and octahedral chains with the [$\frac{1}{2}$,$\frac{1}{2}$,0] PBC vector is similarly depicted in Fig. 3.63. Since the attachment energies of building units to the tetrahedral and octahedral chains are the same in the [100], [$\bar{1}$10], and [$\bar{1}\bar{1}$0] directions, a mica crystal is expected to grow equally fast along these directions. The basal faces, (001), being parallel to these three PBC vectors are the *flat* faces

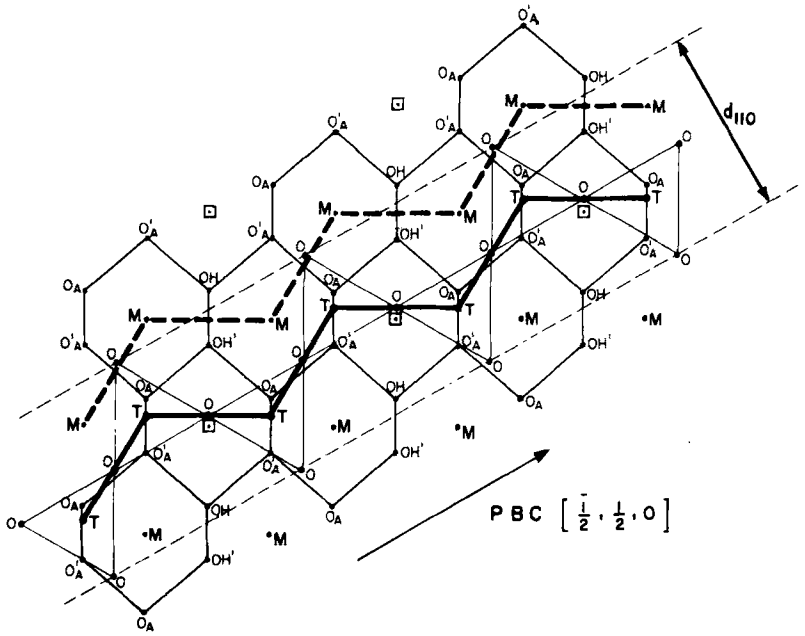

Fig. 3.63. Periodic bond chains along the [110] direction in a dioctahedral mica (*T—O—T*: tetrahedral silica chains, *M—O—M*: octahedral metal-oxygen chain).

in Hartman and Perdok's terminology. Thus, the {001} is the most important form for the layer silicates. The (010) and (110) faces, being parallel to one PBC vector each, are expected to have equal importance, i.e., to be equally developed. The arrangement of PBC vectors suggest that the {010} and {110} are the second most important forms for a mica. It is, therefore, expected that mica crystals will develop hexagonal platelets when they grow slowly in equilibrium without any external interferences. As pointed out by Hartman (1969), deviations from the expected morphology suggest that the interference by external factors has taken place during the crystal growth. The d_{010} and d_{110} (or $d_{1\bar{1}0}$) slices of mica may behave differently under external effects such as solvent and impurity effects. As seen in Figs. 3.62 and 3.63, the arrangement of oxygens and hydroxyls (which form attachment sites between slices) is different along the edges of the d_{020} slice than from those along the edges of d_{110} and the $d_{1\bar{1}0}$ slices. The hydroxyl and oxygen atoms along the edges of the d_{020} slice are coplanar and arranged into a more uniform surface. The oxygens and hydroxyls along the edges of the d_{110} and $d_{1\bar{1}0}$ slices form a "kinked" surface. The uniform surfaces of the d_{020} slices can easily adsorb impurities in the form of a protective layer. The latter may impede the growth rate of the {010} form, leading to the predominance of this form over the {110} form. Consequently, hexagonal platelets may

degenerate into laths, and finally fibers. The reverse situation, i.e. because of impurities or other external factors, preferential growth along the PBC vectors in the $[\bar{1}10]$ and $[1\bar{1}0]$ directions may lead to the predominance of {110} form over the {010}, and subsequently to the formation of diamond-shaped platelets.

For the subhedral lamellae (S- and H-type particles) the growth in the $\langle hk0 \rangle$ directions seems to be rather irregular, so that no $\{hk0\}$ forms develop, but only {001} forms are developed. The subhedral lamellae may also be formed by irregular tearing or breaking of larger lamellae. In the thicker subhedral lamellae (H-type particles) the successive layers do not have a strict crystallographic order of a single crystal. They are intermediate in complexity between a single crystal and crystalline aggregate. The PBC concept of Hartman and Perdok (1955) seems to explain the morphological variations for the smectite single crystals. In order to understand the morphological features of the polycrystalline aggregates of the same material, we need to briefly review the crystal growth mechanisms.

Crystal-growth mechanisms

As schematically shown in Fig. 3.64, there are basically two modes of crystal growth (Cabrera and Coleman, 1963): (1) layer-after-layer growth, and (2) dendritic growth. In general, layer-after-layer growth occurs at low crystallization rates, whereas dendritic growth is favored at high crystallization rates. During the layer-after-layer growth, the growing surface requires a source of steps. This growth surface is said to be "singular". The steps are provided on growing surface either by a two-dimensional nucleation or by a screw dislocation. Dendritic growth has a growth front with tree-like branchings, and does not require a source of steps. In this case, the growth surface

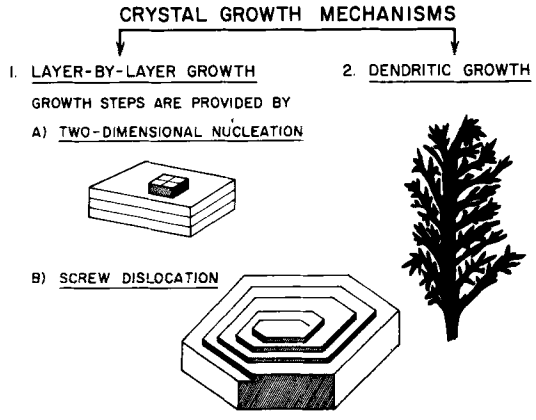

Fig. 3.64. Crystal-growth mechanisms.

is said to be "nonsingular". The dendrites leave a lot of interstitial spaces where solutions, gases, and amorphous materials may easily be entrapped. The branches of a dendrite may be crystalline needles or lamellae. The connections of these branches to the dendrite are rather delicate, and can break up easily; this results in separate needles and lamellae.

The dendrites are classified according to the spatial relationships between their branches. A rather complete classification of dendrites was presented by Saratovkin (1959). The following forms of dendrites seem to be of special interest to the morphological features of smectite aggregates:

(a) Irregular dendrites: there are no geometrical relationships between secondary, tertiary, and higher order branches of such dendrites.

(b) Cellular dendrites: these dendrites resemble a honeycomb in which the branches have strictly defined orientations.

(c) Foliated or layered dendrites: the branches are developed laterally in form of thin layers which are often folded.

(d) Spherulites: these consist of a bundle of radiating needles or lamellae.

Typical smectite dendrites were shown in Figs. 3.24A and 3.34, where the branchings of the growth front are clearly visible. It is also interesting to note that the limbs of the dendrite in these aggregates seem to end in the form of regular lamellae. In fact, some of these lamellae develop into small rhombs as seen in Fig. 3.34. These lamellae are probably developed during the later stages of crystal growth at slower crystallization rates.

With the above background, we may now relate the morphological features of smectite aggregates to the possible crystal growth mechanisms. Cheto-type aggregates (Fig. 3.7) are similar to irregular dendrites in which the branchings look like fibers due to the intensive curling and folding of extremely thin layers. Reticulated lamellar aggregates (Santa Rita-type, Fig. 3.12A) and compact lamellar aggregates (Fig. 3.4A) seem to be compatible with a layer-after-layer growth mechanism. In foliated aggregates (Wyoming-type, Figs. 3.4B and 3.5) one can see the characteristics of both crystal growth mechanisms. The globular aggregates (Otay-type, Fig. 3.8A and B, and Fig. 3.15A) represent a high nucleation rate followed by a high growth rate. This does not leave time for the individual crystallites to develop any forms. These tiny crystallites, mostly oval shaped and with diameters of 150—200 Å are clustered.

Finally, it must be said that in some cases the morphological features of the aggregate may be inherited from the parent volcanic glass, with the devitrification process altering the mineralogy but not the texture.

References

Cabrera, N. and Coleman, R.V., 1963. Theory of crystal growth from the vapor. In: J.J. Gilman (Editor), The Art and Science of Growing Crystals. Wiley, New York, N.Y., pp. 3—28.

Donnay, J.D.H. and Harker, D., 1937. A new law of crystal morphology extending the law of Bravais. Am. Mineral., 22: 446—467.
Donnay, J.D.H. and Donnay, G., 1961. Assemblage liaisons et structure crystalline. C. R. Acad. Sci., 252: 908—909.
Hartman, P., 1969. The dependence of crystal morphology on crystal structure. In: N.N. Sheftal (Editor), Growth of Crystals. Consultants Bureau, New York, N.Y., 7: 3—24.
Hartman, P., 1972. Structure and morphology: In: P. Hartman (Editor), Crystal Growth — An Introduction. North-Holland, Amsterdam, pp. 367—402.
Hartman, P. and Perdok, W.G., 1955. On the relations between structure and morphology of crystals. Acta Crystallogr., 8: (I) 49—52; (II) 521—524; (III) 525—529.
Peacock, M.A. and Ferguson, R.B., 1943. The morphology of muscovite in relation to the crystal lattice. Univ. Toronto, Geol. Ser., 48: 65—82.
Saratovkin, D.D., 1959. Dendritic Crystallization. Consultants Bureau, New York, N.Y.

3.8. CHEMICAL VARIATIONS IN THE MONTMORILLONITE—BEIDELLITE SERIES

Although foundations of modern clay mineralogy were based on chemical grounds, the interest in the chemistry of clay minerals has not kept up with that in X-ray diffraction and electron-optical investigations of these minerals. Recently, a timely monograph by Weaver and Pollard (1973) presented a comprehensive account of this subject. In the following, some of the problems related to the chemistry of dioctahedral aluminous smectites are discussed; specifically considered are the main source of variance and the nature of correlations between the major elements, as well as methods of formula calculations. A large number of good chemical analyses is available in the literature on smectites; 152 of these analyses are compiled in this monograph (Table 3.6). On the basis of such a large number of data, one expects to obtain statistically significant information on the variations in the chemistry of the dioctahedral smectites. For this purpose, factor analysis (Harman, 1960; Lawley and Maxwell, 1962; Klovan, 1975) seems to provide a rather promising approach. The results of such a factorial analysis using principal component solution are described in the following discussion.

Description of the chemical data in the literature

Chemical data for 152 samples have been compiled in Table 3.6 with special emphasis on the quality of the analysis and the presence of impurities. Samples for which more than 5% crystalline or amorphous impurities were reported have been omitted. For smaller amounts of impurities, the original data have been corrected before including in Table 3.6. The data for samples 14, 17, 39, 46, 64, 84, 99, 102, 113, 117, 118, and 135 have been corrected after Foster (1951, and 1953). The data for samples 9, 11, 39, 40, 41, 55, 57, 61, 62, 65, 70, 71, 72, 73, 81, 82, and 88 are similarly corrected for impurities as reported by Schultz (1969). Pretreatments which samples received prior to the analysis are also listed in Table 3.6 except for samples of Grim

TABLE 3.6

Chemical data on dioctahedral smectites (see text for the description of the data)

SAMPLE #	SIO2	AL2O3	FE2O3	FEO	MGO	MNO	LI2O	CAO	NA2O	K2O	TOTAL
1	55.99	18.92	3.38	0.0	3.08	0.0	0.0	1.61	0.0	0.08	83.06
2	49.91	17.20	2.17	0.26	3.45	0.04	0.0	2.31	0.14	0.28	75.76
3	61.16	20.38	3.66	0.0	4.52	0.03	0.0	0.14	3.70	0.04	93.63
4	61.77	19.85	1.95	0.0	5.56	0.0	0.0	1.89	0.07	0.09	91.18
5	51.40	15.40	1.50	0.04	5.00	0.17	0.0	2.30	0.30	0.12	76.23
6	55.20	17.00	1.60	0.20	5.00	0.0	0.0	0.09	3.10	0.26	82.45
7	67.77	21.17	1.86	0.0	5.20	0.0	0.0	0.18	3.74	0.08	100.00
8	67.49	21.36	1.89	0.0	5.21	0.0	0.0	0.14	3.84	0.07	100.00
9	44.60	20.00	5.20	0.16	2.20	0.04	0.0	2.08	0.56	0.65	75.49
10	51.69	18.65	4.00	0.23	1.64	0.0	0.0	0.29	0.08	0.17	76.75
11	58.69	22.40	5.67	0.0	1.87	0.0	0.0	0.0	2.50	0.13	91.26
12	45.12	28.24	4.12	0.0	2.32	0.0	0.0	0.88	0.0	0.0	80.68
13	45.52	27.52	2.80	0.0	3.00	0.0	0.0	0.52	0.0	0.0	79.36
14	54.58	16.36	2.59	0.11	4.58	0.0	0.0	0.72	3.02	0.91	82.77
15	55.80	28.60	0.41	0.0	2.03	0.0	0.0	2.23	2.09	0.48	91.64
16	49.70	22.10	2.12	0.0	2.85	0.0	0.0	1.08	1.17	0.0	79.02
17	53.02	18.35	2.33	0.13	3.92	0.0	0.0	0.80	3.80	0.16	82.51
18	50.28	20.00	4.00	0.0	4.60	0.0	0.0	1.08	0.0	0.0	79.96
19	50.33	16.42	2.42	0.0	4.10	0.0	0.0	1.39	0.12	1.00	75.78
20	50.30	15.96	0.86	0.0	6.53	0.0	0.0	1.24	1.19	0.45	76.53
21	49.56	15.08	3.44	0.0	7.84	0.01	0.0	1.08	0.0	0.0	77.01
22	63.04	18.44	1.20	0.0	7.30	0.01	0.0	0.08	3.40	0.02	93.49
23	51.29	15.53	1.78	0.0	4.34	0.0	0.0	3.24	0.35	0.0	76.53
24	62.23	21.03	1.75	0.48	5.70	0.0	0.0	0.0	0.65	0.0	91.84
25	50.64	15.73	1.60	0.0	5.37	0.0	0.0	3.34	0.25	0.0	76.93
26	50.03	16.75	5.83	0.47	2.78	0.01	0.0	1.20	0.26	0.60	77.93
27	56.69	18.61	2.41	0.16	5.14	0.01	0.0	0.55	1.43	0.47	85.47
28	50.06	21.32	0.22	0.0	4.42	0.13	0.0	1.26	0.33	0.19	77.93
29	50.72	22.14	0.78	0.71	4.28	0.11	0.0	1.56	0.0	0.0	80.30
30	53.96	15.44	1.12	0.0	6.99	0.0	0.0	0.80	0.94	0.54	79.79
31	53.88	11.66	4.60	0.0	8.61	0.18	0.0	1.56	0.15	0.39	81.03
32	47.28	20.27	8.68	0.0	0.70	0.0	0.0	2.75	0.97	0.0	80.65
33	54.46	16.84	3.36	0.0	4.84	0.0	0.0	3.20	0.0	0.0	82.70
34	48.30	16.98	4.04	0.0	3.74	0.0	0.0	2.90	0.30	1.25	77.51
35	61.40	25.03	2.52	0.23	3.26	0.0	0.0	0.33	0.62	0.0	93.39
36	51.20	22.14	0.0	0.0	3.53	0.18	0.0	3.72	0.28	0.28	81.33
37	49.55	17.78	6.61	0.0	3.24	0.0	0.0	0.0	0.0	0.0	77.18
38	59.30	36.11	0.50	0.0	0.10	0.0	0.0	0.02	3.98	0.11	100.12
39	52.28	20.69	0.24	0.0	2.76	0.0	0.02	3.18	0.04	0.04	79.25
40	49.52	17.15	5.65	0.32	2.80	0.0	0.0	0.92	0.15	0.85	77.36
41	59.30	20.40	5.74	0.0	2.40	0.07	0.0	0.03	2.52	0.66	91.12
42	59.73	24.30	5.54	0.37	2.10	0.0	0.0	0.0	0.80	0.22	93.06
43	59.01	27.17	3.78	0.27	2.20	0.0	0.0	0.0	0.28	0.22	92.93
44	50.53	19.31	7.25	0.0	2.60	0.02	0.0	0.72	0.41	0.34	81.18
45	51.18	16.30	2.20	0.23	4.41	0.01	0.0	2.12	0.17	0.38	77.00
46	50.37	17.11	2.68	0.20	3.80	0.0	0.0	1.23	0.56	0.09	76.04
47	50.39	17.37	2.84	0.0	4.56	0.0	0.0	1.29	0.46	0.04	76.95
48	49.48	17.75	3.33	0.15	4.42	0.0	0.0	0.16	0.06	0.06	75.41
49	47.64	17.79	3.35	0.32	2.63	0.0	0.0	1.23	0.12	0.26	73.34
50	50.20	16.19	4.13	0.0	4.12	0.0	0.0	2.18	0.17	0.16	77.15
51	50.95	16.54	1.36	0.26	4.65	0.01	0.0	2.26	0.17	0.47	76.67
52	63.42	19.44	1.87	0.0	5.00	0.0	0.0	0.11	3.46	0.08	93.38
53	65.00	22.80	3.07	0.40	3.90	0.0	0.0	0.05	0.17	0.13	95.52
54	46.95	27.26	2.26	0.32	1.39	0.01	0.0	0.0	0.20	0.36	78.75
55	50.70	19.40	0.05	0.20	3.60	0.01	0.0	2.60	0.06	0.0	76.62
56	45.32	27.84	0.80	0.0	0.16	0.0	0.0	2.75	0.10	0.12	77.10
57	47.78	19.88	0.83	0.0	3.20	0.0	0.0	2.30	0.06	0.0	74.05
58	51.37	15.41	0.78	0.14	6.22	0.0	0.0	0.0	0.79	0.46	75.17
59	48.24	22.32	0.36	0.0	6.64	0.0	0.0	2.04	0.0	0.0	79.60
60	52.30	14.43	2.00	0.0	6.15	0.05	0.0	2.12	0.50	0.52	78.07
61	60.21	19.13	1.07	0.0	4.57	0.03	0.0	0.04	3.90	0.14	89.09
62	50.11	15.56	0.94	0.13	4.37	0.05	0.0	2.21	0.13	0.10	73.60
63	54.90	19.50	1.60	0.0	3.10	0.01	0.0	0.11	0.09	0.22	79.53
64	51.64	18.03	1.24	1.40	3.25	0.0	0.0	2.18	2.09	0.12	79.95

TABLE 3.6 (continued)

SAMPLE #	SIO2	AL203	FE203	FEO	MGO	MNO	LI2O	CAO	NA2O	K2O	TOTAL
65	54.53	19.61	3.10	0.13	2.65	0.0	0.0	0.25	1.68	0.31	82.26
66	61.12	23.10	4.37	0.0	2.50	0.0	0.0	0.24	2.90	0.04	94.27
67	56.80	21.32	4.07	0.0	2.31	0.0	0.0	0.07	3.06	0.11	87.74
68	54.70	19.90	2.50	0.96	2.40	0.0	0.0	0.07	3.80	0.05	84.38
69	54.90	19.80	3.70	0.0	3.00	0.01	0.0	0.09	0.12	0.16	81.78
70	52.30	16.99	3.70	0.84	4.02	0.02	0.0	1.40	0.30	0.01	79.58
71	56.67	18.86	3.29	0.80	2.37	0.07	0.0	1.47	1.52	0.55	85.60
72	53.90	17.40	2.30	0.0	4.20	0.0	0.0	0.70	0.26	0.44	79.20
73	52.39	20.21	1.82	0.27	2.47	0.02	0.0	1.84	0.19	0.0	79.21
74	66.97	21.51	5.74	0.0	2.90	0.0	0.0	0.19	2.57	0.11	99.99
75	66.79	21.55	5.95	0.0	2.92	0.0	0.0	0.17	2.55	0.07	100.00
76	66.74	21.41	5.90	0.0	3.11	0.0	0.0	0.13	2.64	0.08	100.01
77	51.74	22.81	0.39	0.0	3.32	0.0	0.0	0.0	0.17	0.26	78.69
78	52.08	18.20	2.88	0.0	4.48	0.0	0.0	2.28	0.0	0.0	79.92
79	51.87	26.80	1.42	0.0	4.42	0.0	0.0	1.90	0.03	0.09	86.53
80	46.04	22.60	5.48	0.25	1.85	0.0	0.0	1.26	0.0	2.25	79.73
81	47.20	18.50	5.80	0.0	3.30	0.0	0.0	1.00	2.50	1.30	79.60
82	57.60	20.64	4.89	0.0	4.00	0.03	0.0	0.64	3.00	0.07	90.87
83	54.25	17.60	4.31	0.0	3.88	0.02	0.0	1.06	2.16	0.12	83.40
84	50.50	16.53	2.36	0.0	3.39	0.0	0.0	2.40	0.0	0.25	75.53
85	44.23	31.30	5.77	0.0	0.18	0.0	0.0	0.45	0.19	0.95	83.07
86	49.48	16.30	3.12	0.0	4.69	0.05	0.0	2.15	0.03	0.36	76.18
87	53.50	21.20	3.74	0.0	2.27	0.0	0.0	0.71	1.75	0.20	83.37
88	59.47	22.17	4.32	0.0	2.73	0.0	0.0	0.14	3.18	0.03	92.04
89	54.90	20.30	3.70	0.0	2.40	0.0	0.0	0.17	2.79	0.08	84.34
90	54.34	19.92	1.11	2.17	2.21	0.01	0.0	0.33	2.65	0.45	83.19
91	54.62	20.08	2.36	1.03	2.15	0.35	0.0	0.40	2.26	0.35	83.60
92	54.34	20.12	1.13	2.06	2.02	0.01	0.0	0.53	2.44	0.49	83.14
93	54.07	20.24	2.45	0.74	1.92	0.01	0.0	0.55	2.35	0.40	82.73
94	62.75	22.12	3.94	0.0	2.64	0.0	0.0	0.29	0.20	0.06	92.00
95	62.30	23.50	3.35	0.37	1.95	0.0	0.0	0.31	0.40	0.03	92.21
96	65.60	23.22	6.11	0.0	2.73	0.0	0.0	0.11	2.12	0.10	99.99
97	66.42	22.11	6.69	0.0	2.59	0.0	0.0	0.06	2.12	0.02	100.01
98	64.66	22.71	7.13	0.0	2.96	0.0	0.0	0.06	2.48	0.02	100.02
99	45.89	17.60	1.60	0.0	5.08	0.0	0.0	1.52	0.0	0.0	71.69
100	54.90	20.30	1.90	1.60	2.40	0.0	0.0	0.10	3.40	0.13	84.73
101	53.50	21.57	3.28	0.0	1.89	0.0	0.0	1.25	1.94	1.04	84.47
102	53.46	20.14	3.67	0.30	2.49	0.0	0.0	0.50	2.75	0.60	83.91
103	57.49	20.27	2.92	0.19	3.18	0.0	0.0	0.23	1.32	0.28	85.88
104	64.55	25.44	4.55	0.0	2.74	0.0	0.0	0.18	2.43	0.11	100.00
105	64.71	25.06	4.72	0.0	2.55	0.0	0.0	0.12	2.81	0.02	99.99
106	63.33	25.20	5.22	0.0	3.19	0.0	0.0	0.11	2.91	0.02	99.98
107	60.20	26.20	3.76	0.34	1.92	0.0	0.0	0.04	0.34	0.02	92.82
108	61.30	22.40	3.55	0.39	2.81	0.0	0.0	0.0	2.71	0.04	93.20
109	69.10	23.50	3.81	0.0	3.87	0.0	0.0	0.08	0.19	0.38	100.93
110	64.80	24.60	4.25	0.21	2.83	0.0	0.0	0.0	3.15	0.04	99.88
111	54.88	19.92	4.10	0.22	2.83	0.0	0.0	2.22	1.75	0.26	86.18
112	61.63	24.92	0.70	0.78	4.51	0.0	0.0	0.0	0.37	0.0	92.91
113	50.44	16.26	5.38	0.0	2.95	0.0	0.0	0.72	0.0	0.0	75.75
114	50.20	16.70	5.00	0.10	4.00	0.01	0.0	0.95	0.58	0.38	77.92
115	52.90	17.90	4.80	0.20	2.90	0.0	0.0	0.12	2.90	0.27	81.99
116	49.34	22.88	2.36	0.0	1.67	0.0	0.0	2.66	0.0	0.0	78.91
117	51.50	19.34	0.10	0.0	3.46	0.0	0.0	0.48	0.20	0.0	75.08
118	52.09	17.68	0.06	0.0	3.54	0.06	0.0	3.28	0.0	0.0	76.71
119	44.02	28.90	5.15	0.33	0.50	0.0	0.0	0.68	0.17	0.50	80.25
120	60.76	23.08	6.10	0.0	1.44	0.0	0.0	0.17	0.13	0.21	91.89
121	60.22	23.67	6.28	0.0	1.46	0.0	0.0	0.13	0.09	0.19	92.04
122	62.00	23.42	3.74	0.32	0.93	0.0	0.0	0.68	0.72	2.63	94.44
123	58.67	27.34	3.64	0.38	2.00	0.0	0.0	0.0	0.62	0.18	92.83
124	60.90	20.71	2.06	0.36	6.84	0.0	0.0	0.30	0.23	0.0	91.40
125	61.55	20.44	2.02	0.38	6.06	0.0	0.0	0.0	0.30	0.0	90.75
126	59.91	21.97	6.72	0.0	2.15	0.0	0.0	0.34	0.09	0.11	91.29
127	52.43	15.95	1.42	0.10	5.02	0.0	0.0	2.97	0.0	0.0	77.89
128	64.70	18.60	8.12	0.25	4.32	0.0	0.0	0.0	3.30	0.04	99.33
129	50.30	14.86	8.86	0.35	3.06	0.0	0.0	2.07	0.0	0.04	79.54
130	52.70	14.20	10.40	0.88	2.20	0.0	0.0	0.10	3.20	0.16	83.84
131	50.86	18.76	2.07	0.0	3.48	0.0	0.0	1.76	0.37	0.0	77.30

TABLE 3.6 (continued)

SAMPLE #	SIO2	AL2O3	FE2O3	FEO	MGO	MNO	LI2O	CAO	NA2O	K2O	TOTAL
132	51.14	19.76	0.83	0.0	3.22	0.0	0.0	1.62	0.04	0.11	76.72
133	48.60	20.03	1.25	0.0	5.24	0.16	0.0	1.72	0.0	0.0	77.00
134	60.16	23.24	0.98	0.0	3.79	0.0	0.0	1.91	0.04	0.13	90.25
135	54.28	17.92	3.88	0.0	3.24	0.0	0.0	1.80	0.10	0.25	81.47
136	64.00	29.00	0.21	0.0	3.03	0.0	0.0	0.0	3.98	0.05	100.27
137	49.21	22.61	0.43	0.0	2.13	0.0	0.0	1.95	0.45	0.0	76.78
138	50.01	19.36	2.36	0.70	4.40	0.0	0.0	1.20	1.09	0.35	79.47
139	50.72	18.12	2.41	1.02	4.29	0.0	0.0	0.80	3.00	0.62	80.98
140	66.11	25.48	0.52	0.0	4.07	0.0	0.0	3.75	0.07	0.0	100.00
141	51.95	18.02	0.21	0.0	5.10	0.0	0.0	2.09	0.04	0.0	77.41
142	60.62	22.18	2.06	0.0	4.80	0.0	0.0	0.38	0.06	0.03	90.13
143	63.37	23.37	3.82	0.47	3.22	0.0	0.0	0.0	0.63	0.0	94.88
144	60.70	20.28	4.07	0.0	3.98	0.0	0.0	0.75	0.62	0.17	90.57
145	66.32	22.42	3.30	0.0	4.07	0.0	0.0	0.03	3.68	0.06	99.88
146	61.56	22.99	2.23	0.0	4.48	0.0	0.0	0.30	0.12	0.17	91.85
147	47.38	21.27	10.66	0.0	0.42	0.0	0.0	0.78	0.12	0.08	80.71
148	62.70	22.20	4.62	0.48	2.00	0.0	0.0	0.58	0.01	0.12	92.71
149	48.24	20.30	2.29	0.11	2.06	0.0	0.0	2.10	0.36	0.05	75.51
150	48.60	18.40	1.21	0.07	1.88	0.0	0.0	2.25	0.35	0.28	73.04
151	60.00	19.70	6.70	0.56	1.33	0.0	0.0	2.60	0.53	0.06	91.48
152	61.60	30.58	3.73	0.10	1.93	0.0	0.0	1.09	0.35	0.60	99.98

SAMPLE #	SAMPLE LOCATION AND SOURCE
1	UMIAT, ALASKA; ANDERSON AND REYNOLDS (1966)
2	CHAMBERS, ARIZONA; A.P.I. 23, KERR ET AL.(1951)
3	CHAMBERS, ARIZONA; EARLEY ET AL.(1953)
4	CHETO, ARIZONA; GRIM AND KULBICKI, NO. 1 (1961)
5	SANDERS,ARIZONA;SCHULTZ(1969),NO. 36 (SAME LOCALITY AS CHETO,CHAMBERS)
6	SANDERS,ARIZONA; SCHULTZ(1969),NO. 37
7	CHAMBERS,ARIZONA;ROBERSON ET AL.(1968),0.1-0.5 MICRONS,NA-CLAY
8	CHAMBERS,ARIZONA;ROBERSON ET AL.(1968),0.05-0.1 MICRONS,NA-CLAY
9	JOSEPH CITY, ARIZONA; SCHULTZ(1969), NO. 73
10	LITTLE ROCK, ARKANSAS; A.P.I. 28, KERR ET AL.(1951)
11	LITTLE ROCK,ARKANSAS;EARLEY ET AL.(1953)
12	NASHVILLE, ARKANSAS; ROSS AND HENDRICKS (1945), NO. 51
13	NASHVILLE, ARKANSAS; ROSS AND HENDRICKS (1945), NO. 52
14	AMARGOSA VALLEY, CALIFORNIA; ROSS AND HENDRICKS (1945), NO. 3
15	CASTLE MOUNTAIN,IVANPAH,CALIFORNIA;HEYSTECK (1952)
16	CLAIRMONT, CALIFORNIA; ROSS AND HENDRICKS (1945), NO. 40
17	HECTOR, CALIFORNIA; ROSS AND HENDRICKS (1945), NO. 14
18	LOS ANGELES, CALIFORNIA; ROSS AND HENDRICKS (1945), NO. 43
19	MARICOPA,CALIFORNIA; ROSS AND HENDRICKS (1945), NO. 7
20	OTAY, CALIFORNIA; ROSS AND HENDRICKS (1945), NO. 15
21	OTAY, CALIFORNIA; ROSS AND HENDRICKS (1945), NO. 32
22	OTAY, CALIFORNIA; EARLEY ET AL.(1953)
23	OTAY,CALIFORNIA;KELLEY (1945), CA-CLAY,-1 MICRON FRACTION
24	OTAY, CALIFORNIA; GRIM AND KULBICKI (1961), NO. 2
25	NEWBERRY,CALIFORNIA;KELLEY (1945),CA-CLAY,-1 MICRON FRACTION
26	SANTA MONICA, CALIFORNIA; ROSS AND HENDRICKS (1945), NO. 26
27	SHOSHONE, AMARGOSA VALLEY, CALIFORNIA; SCHULTZ(1969), NO. 52
28	PALA, CALIFORNIA; ROSS AND HENDRICKS (1945), NO. 36
29	PALA, CALIFORNIA; ROSS AND HENDRICKS (1945), NO. 42
30	SAN DIEGO COUNTY, CALIFORNIA; ROSS AND HENDRICKS (1945), NO. 9
31	TEHACHPI, CALIFORNIA; ROSS AND HENDRICKS (1945), NO. 4
32	BEIDELL, COLORADO; ROSS AND HENDRICKS (1945), NO. 44
33	CONEJOS QUADRANGLE, COLORADO; ROSS AND HENDRICKS (1945), NO. 8
34	DENVER BASIN,COLORADO;WEAVER AND POLLARD (1973), NO. 10
35	GRAND JUNCTION, COLORADO; GRIM AND KULBICKI (1961), NO. 26
36	BRANCHVILLE, CONNECTICUT; ROSS AND HENDRICKS (1945), NO. 33
37	TWIN FALLS, IDAHO; ROSS AND HENDRICKS (1945), NO. 35
38	BLACK JACK MINE, IDAHO; WEIR AND GREENE-KELLY (1962)
39	GREENWOOD, MAINE; ROSS AND HENDRICKS (1945), NO. 28
40	AMORY, MISSISSIPPI; A.P.I. 22, KERR ET AL.(1951)
41	AMORY, MISSISSIPPI; EARLEY ET AL.(1953)
42	AMORY, MISSISSIPPI; GRIM AND KULBICKI (1961), NO. 12
43	AMORY, MISSISSIPPI; GRIM AND KULBICKI (1961), NO. 34

TABLE 3.6 (continued)

SAMPLE #	SAMPLE LOCATION AND SOURCE
44	BOONEVILLE, MISSISSIPPI; ROSS AND HENDRICKS (1945), NO. 38
45	BURNS, MISSISSIPPI; A.P.I. 21, KERR ET AL.(1951)
46	LEMON, MISSISSIPPI; ROSS AND HENDRICKS (1945), NO. 20
47	LEMON, MISSISSIPPI; ROSS AND HENDRICKS (1945), NO. 23
48	LEMON, MISSISSIPPI; ROSS AND HENDRICKS (1945), NO. 31
49	LORENA, MISSISSIPPI; A.P.I. 20, KERR ET AL.(1951)
50	POLKVILLE, MISSISSIPPI; ROSS AND HENDRICKS (1945), NO. 14
51	POLKVILLE, MISSISSIPPI; A.P.I. 19,KERR ET AL.(1951)
52	POLKVILLE, MISSISSIPPI; EARLEY ET AL.(1953)
53	POLKVILLE, MISSISSIPPI; GRIM AND KULBICKI (1961), NO. 25
54	PONTOTOC, MISSISSIPPI; ROSS AND HENDRICKS (1945), NO. 50
55	APRIL FOOL HILL, MANHATTAN, NEVADA; SCHULTZ(1969), NO. 29
56	CARSON DISTRICT, NEVADA; ROSS AND HENDRICKS (1945), NO. 49
57	ELY, NEVADA; SCHULTZ(1969), NO. 30
58	DIXON, NEW MEXICO; ROSS AND HENDRICKS (1945), NO. 5
59	EMBUDO, NEW MEXICO; ROSS AND HENDRICKS (1945), NO. 45
60	SANTA CRUZ, NEW MEXICO; ROSS AND HENDRICKS (1945), NO. 1
61	SANTA RITA, NEW MEXICO; EARLEY ET AL.(1953)
62	SANTA RITA, NEW MEXICO; A.P.I. 30, KERR ET AL.(1951)
63	WALHALLA, CAVALIER COUNTY, NORTH DAKOTA; SCHULTZ(1969), NO. 60
64	ARDMORE, SOUTH DAKOTA; ROSS AND HENDRICKS (1945), NO. 12
65	BELLE FOURCHE, SOUTH DAKOTA; A.P.I. 27, KERR ET AL.(1951)
66	BELLE FOURCHE, SOUTH DAKOTA; EARLEY ET AL.(1953)
67	BELLE FOURCHE, SOUTH DAKOTA; OSTHAUS (1955), NA-CLAY, 0.2-0.05 MICRONS
68	BELLE FOURCHE, SOUTH DAKOTA; SCHULTZ(1969), NO. 10
69	ELK CREEK, EAST OF PIEDMONT, SOUTH DAKOTA; SCHULTZ(1969), NO. 61
70	INDIAN CREEK(NORTH), BUTTE COUNTY, SOUTH DAKOTA; SCHULTZ(1969), NO. 55
71	OAHE DAM(WEST END), HUGHES COUNTY, SOUTH DAKOTA; SCHULTZ(1969), NO. 18
72	NIOBRARA FORMATION, CROOK COUNTY, SOUTH DAKOTA; SCHULTZ(1969), NO. 44
73	WHEELER BRIDGE, GREGORY COUNTY, SOUTH DAKOTA; SCHULTZ(1969), NO. 20
74	FAYETTE COUNTY,TEXAS;ROBERSON ET AL.(1968),0.1-0.5 MICRONS,NA-CLAY
75	FAYETTE COUNTY,TEXAS;ROBERSON ET AL.(1968),0.05-0.1 MICRONS,NA-CLAY
76	FAYETTE COUNTY,TEXAS;ROBERSON ET AL.(1968),-0.05 MICRONS, NA-CLAY
77	LEAKEY, TEXAS; ROSS AND HENDRICKS (1945), NO. 34
78	SAN ANTONIO,TEXAS; ROSS AND HENDRICKS (1945), NO. 27
79	SOUTH BOSQUE, TEXAS; ROSS AND HENDRICKS (1945), NO. 49
80	FAIRVIEW, UTAH; ROSS AND HENDRICKS (1945), NO. 46
81	PARIA, UTAH; SCHULTZ(1969), NO. 74
82	PLYMOUTH, UTAH; EARLEY ET AL.(1953)
83	PLYMOUTH, UTAH; OSTHAUS (1955), NA-CLAY, 0.2-0.05 MICRONS
84	IRISH CREEK, VIRGINIA; ROSS AND HENDRICKS (1945), NO. 13
85	ROSELAND, VIRGINIA; ROSS AND HENDRICKS (1945), NO. 54
86	SPOKANE, WASHINGTON; ROSS AND HENDRICKS (1945), NO. 21
87	BATES PARK, NEAR CASPER, WYOMING; SCHULTZ(1969), NO. 13
88	CLAY SPUR, WYOMING; EARLEY ET AL.(1953)
89	CLAY SPUR, WYOMING; OSTHAUS (1955), NA-CLAY, 0.2-0.05 MICRONS
90	CLAY SPUR,WYOMING(BLUISH-GRAY);KNECHTEL AND PATTERSON (1962)
91	CLAY SPUR,WYOMING(OLIVE-GREEN);KNECHTEL AND PATTERSON (1962)
92	CLAY SPUR,WYOMING(BLUISH-GRAY);KNECHTEL AND PATTERSON (1962)
93	CLAY SPUR,WYOMING(OLIVE-GREEN);KNECHTEL AND PATTERSON (1962)
94	COLONY,WYOMING;GRIM AND KULBICKI NO. 33
95	CROOK COUNTY, WYOMING; GRIM AND KULBICKI (1961), NO. 10
96	CROOK COUNTY,WYOMING;ROBERSON ET AL.(1968),0.1-0.5 MICRONS,NA-CLAY
97	CROOK COUNTY,WYOMING;ROBERSON ET AL.(1968),0.05-0.1 MICRONS,NA-CLAY
98	CROOK COUNTY,WYOMING;ROBERSON ET AL.(1968),-0.05 MICRONS, NA-CLAY
99	FORT STEEL, WYOMING; ROSS AND HENDRICKS (1945), NO. 29
100	MOORCROFT (10 MILES NE),WYOMING; SCHULTZ(1969), NO. 12
101	OSAGE, WYOMING; ROSS AND HENDRICKS (1945), NO. 30
102	UPTON, WYOMING; ROSS AND HENDRICKS (1945), NO. 19
103	UPTON, WYOMING; A.P.I. 258, KERR ET AL.(1951)
104	UPTON,WYOMING;ROBERSON ET AL.(1968),0.1-0.5 MICRONS, NA-CLAY
105	UPTON,WYOMING;ROBERSON ET AL.(1968),0.05-0.1 MICRONS,NA-CLAY
106	UPTON,WYOMING;ROBERSON ET AL.(1968),-0.05 MICRONS,NA-CLAY
107	WESTON COUNTY, WYOMING; GRIM AND KULBICKI (1961), NO. 35
108	VOLCLAY,WYOMING;BRINDLEY AND ERTEM(1971), -1 MICRON FRACTION,NA-CLAY
109	WYOMING; ROSS AND MORTLAND (1966)

TABLE 3.6 (continued)

SAMPLE #	SAMPLE LOCATION AND SOURCE
110	WYOMING; WEIR (1965), NA-CLAY, -2 MICRONS
111	ROSEDALE, ALBERTA, CANADA; ROSS AND HENDRICKS (1945), NO. 25
112	PEMBINA, MANITOBA, CANADA; GRIM AND KULBICKI (1961), NO. 24
113	ATZCAPOZALCO, MEXICO; ROSS AND HENDRICKS (1945), NO. 22
114	ATZCAPOZALCO,MEXICO;SCHULTZ(1969),NO. 65
115	ATZCAPOZALCO, MEXICO; SCHULTZ(1969), NO. 66 (AFTER IRON REMOVAL)
116	MANIQUIPI, MEXICO; ROSS AND HENDRICKS (1945), NO. 39
117	SANTA ROSA, MEXICO; ROSS AND HENDRICKS (1945), NO. 24
118	TATATILA, MEXICO; ROSS AND HENDRICKS (1945), NO. 6
119	ANCON,CANAL ZONE,PANAMA;ROSS AND HENDRICKS (1945),NO. 53
120	SAN GABRIEL,POTRERILLOS,MENDOZA,ARGENTINA;GRIM AND KULBICKI NO.14
121	SANTA ELENA,POTRERILLOS,MENDOZA,ARGENTINA;GRIM AND KULBICKI NO.13
122	TALA, HERAS, MENDOZA, ARGENTINA; GRIM AND KULBICKI (1961), NO. 9
123	SIN PROCEDENCIA, ARGENTINA; GRIM AND KULBICKI (1961), NO. 16
124	MARIO DON FERNANDO,RETAMITO,ARGENTINA; GRIM AND KULBICKI (1961), NO. 5
125	EL RETAMITO,RETAMITO,SAN JUAN,ARGENTINA;GRIM AND KULBICKI (1961), NO. 4
126	EMILIA,CALINGASTA,SAN JUAN,ARGENTINA;GRIM AND KULBICKI NO.15
127	STYRIA,AUSTRIA;ROSS AND HENDRICKS (1945),NO.2
128	REDHILL, ENGLAND; WEIR (1965), NA-CLAY, -2 MICRONS
129	WOBURN, BEDFORDSHIRE, ENGLAND; SCHULTZ(1969), NO. 63
130	WOBURN,ENGLAND; SCHULTZ(1969) NO. 64, -.25 MICRON FRACTION
131	ANGLAR, FRANCE; ROSS AND HENDRICKS (1945), NO. 17
132	MONTMORILLON, FRANCE; ROSS AND HENDRICKS (1945), NO. 18
133	MONTMORILLON, FRANCE; ROSS AND HENDRICKS (1945), NO. 37
134	MONTMORILLON, FRANCE; GRIM AND KULBICKI (1961), NO. 31
135	NIEDER-BAYERN, GERMANY; ROSS AND HENDRICKS (1945), NO. 10
136	UNTERRUPSROTH, GERMANY; WEIR (1965), NA-CLAY, -2 MICRONS
137	RHON, GERMANY; SCHULTZ(1969), NO. 32
138	GEMMANO,ITALY;WEAVER AND POLLARD (1973) NO. 16
139	GEMMANO,ITALY;WEAVER AND POLLARD (1973) NO. 17
140	SKYRVEDALEN,NORWAY;WEIR (1965)
141	SELONGIN DAURA,U.S.S.R.;WEAVER AND POLLARD (1973) NO. 3
142	MARNIA,ALGERIA;GRIM AND KULBICKI NO. 29
143	MARNIA, ALGERIA; GRIM AND KULBICKI (1961), NO. 30
144	FADLI,MOSTAGANEM,ALGERIA;GRIM AND KULBICKI NO.27
145	CAMP-BERTEAU, MOROCCO; WEIR (1965), NA-CLAY, -2 MICRONS
146	TAOURIRT,MOROCCO; GRIM AND KULBICKI NO.28
147	ROPP,NIGERIA;WEAVER AND POLLARD (1973) NO. 9
148	ROKKAKU, YAMAGATA PREFECTURE, JAPAN; GRIM AND KULBICKI (1961), NO. 11
149	TOTTORI,JAPAN;WEAVER AND POLLARD (1973) NO. 4
150	TOTTORI,JAPAN;WEAVER AND POLLARD (1973) NO. 6
151	HUMBER RIVER,NEW SOUTH WALES,AUSTRALIA;GRIM AND KULBICKI (1961), NO. 36
152	SWANSEA, NEW SOUTH WALES; HAMILTON (1971), -1 MICRON

and Kulbicki (1961). The latter consisted of the <2 μm fraction of H-clays, i.e., exchangeable cations were replaced by hydrogen. Samples 1—110 are from the bentonite deposits in the United States of America; these are listed in alphabetical order by States. This allows one to easily make a comparison of the chemical data for smectites from a given deposit or locality. This does not imply that exactly the same sample was analyzed by various workers, but rather samples from different locations within a given occurrence. Samples 111—152 are related to the bentonite deposits in other parts of the world. Only ten major oxides are considered. TiO_2 has not been included as it is not certain whether it occurs in the smectite structure or as a separate phase in the samples. The percentage values of oxides in Table 3.6 refer to sample weights at different temperatures (110°C, room temperature, or

1000°C-ignition). Accordingly, the total of the analyses varies, since the dehydration losses are not included in the table. This will induce extra variance in the statistical analysis of the data. To avoid this situation, structural formulae were calculated from the data in Table 3.6 and statistical analyses were carried out on these formulae rather than on the raw data. There is, however, more than one method available for the derivation of chemical formulae for dioctahedral smectites, and this is briefly discussed in the next section.

Methods for calculating structure formulae for the dioctahedral smectites

Structural formulae for minerals can be derived from their chemical analyses under the assumption of fixed anionic charges, or that of fixed cationic numbers. These two methods will be briefly described with respect to the formulae calculations for dioctahedral smectites.

(1) *Method of fixed anionic charges.* This method was proposed by Marshal (1935, 1949) and slightly modified by Ross and Hendricks (1945). The formula calculation is based on the assumption that 22 anionic charges, in form of $O_{10}(OH,F)_2$, are present in the unit formula. In this method, the gram-equivalents of cationic constituents are first obtained by dividing the percent oxide of the constituent by its molecular weight, and then multiplying by the cationic charges in the molecule (e.g., for Al_2O_3 the molecular weight is 101.94 and the cationic charges are $3 \times 2 = 6$). The numbers of cations are calculated by setting the sum of gram-equivalents of cationic constituents equal to 22 (anionic charges). Ross and Hendricks (1945) modified slightly the above method in that they assigned 0.33 charges to the exchangeable cations, irrespective of the observed base-exchange values. They pointed out that the uncertainties involved in determining exchangeable cations forced them to assign an average value (0.33) to them.

(2) *Method of "fixed cationic numbers".* The sum of tetrahedral and octahedral cations in the formula is ideally 6.00 for the dioctahedral smectites. The first step is to calculate the atomic proportions by dividing the oxide percent of the constituent by its molecular weight and by multiplying the result by the number of constituent atoms in the oxide molecule. The sum of the atomic proportions of the tetrahedral and octahedral cations can be set equal to 6.00, and the formula can be calculated. This method is based on a perfect cationic occupation as opposed to the perfect anionic framework assumed in method 1.

The method of "fixed cationic numbers" would appear to have two advantages over the other method: (a) The requirement of a perfect anionic framework for the clay minerals is probably much less realistic than the requirement of a perfect cationic occupation. It is suspected that these layer silicates have larger hydroxyl content, often in form of silanol (Si—OH) groups. (b) The method does not require an accurate analysis of exchange-

TABLE 3.7

Chemical formulae for smectites calculated (1) after the method of fixed anionic charges and (2) after the method of fixed cationic numbers

Sample no.	Method	Tetrahedral cations		Octahedral cations						Total oct. cations	Interlayer cations		
		Si	Al	Al	Fe^{3+}	Fe^{2+}	Mg	Mn	Li		Ca	Na	K
7	(1)	3.99	0.01	1.46	0.08	0.00	0.46	0.00	0.00	2.00	0.01	0.43	0.01
	(2)	3.99	0.01	1.46	0.08	0.00	0.46	0.00	0.00				
12	(1)	3.33	0.67	1.78	0.23	0.00	0.25	0.00	0.00	2.26	0.07	0.0	0.0
	(2)	3.19	0.81	1.54	0.22	0.00	0.24	0.00	0.00				
151	(1)	3.92	0.08	1.44	0.33	0.03	0.13	0.00	0.00	1.93	0.18	0.07	0.01
	(2)	3.97	0.03	1.50	0.33	0.03	0.13	0.00	0.00				
mean (for 152 analyses)	(1)	3.84	0.16	1.53	0.17	0.01	0.36	0.00	0.00	2.05	0.08	0.15	0.02
	(2)	3.80	0.20	1.47	0.17	0.01	0.36	0.00	0.00				

able interlayer cations. The exact amount of interlayer cations in smectites is very difficult to obtain and the inclusion of the interlayer cations into the formula calculation is prone to introduce errors.

Differences in structural formulae obtained by the above two methods are demonstrated in a few examples in Table 3.7. Same chemical formulae are obtained by both methods for sample 7 for obvious reasons. For an extreme case as in sample 12, the method of fixed anionic charges gives a total octahedral occupancy of 2.26. Consequently, the layer charge of the smectite is greatly reduced to −0.14. The method of fixed cationic numbers gives a formula with unlikely high layer charges (−1.05). Thus, both methods seem to give rather unrealistic formulae for this sample. Such formulae with large excess or deficiency in octahedral occupancy often indicate complications, or the presence of undetected impurities. For instance, Foster (1951) examined ten of the samples with excess octahedral occupancies reported by Ross and Hendricks (1945). She found a significant part of magnesium to be exchangeable, and after correcting for it, the total octahedral occupancy was reduced to 1.99—2.01 for these ten samples. Sample 151 in Table 3.7 illustrates the reverse situation, in which the method of fixed anionic charges leads to a deficient octahedral occupancy. The layer charge of the smectite is consequently increased, whereas, the method of fixed anionic numbers results in a relatively smaller layer charge. The actual formula may well lie somewhere between them.

The mean values for the chemical formulae obtained by both methods are given at the bottom of Table 3.7. They are rather close to each other, as the mean value of the total octahedral occupancy is 2.05 for the method of fixed anionic charges. In summary, the method of fixed cationic numbers seems to give equally good results for the dioctahedral smectites as long as the impurities do not appreciably complicate the chemical data.

Factorial analysis of the chemical data

As mentioned earlier, the clays were subjected almost arbitrarily to various pretreatments such as saturations with H^+, Na^+, or Ca^+ prior to the analysis. This makes the distribution of interlayer cations (Ca^{2+}, Na^+, K^+) meaningless for a statistical analysis. We confined the statistical analysis to the variations in tetrahedral (Si^{4+}, Al^{3+}) and octahedral (Al^{3+}, Fe^{3+}, Fe^{2+}, Mg^{2+}, Mn^{2+}, and Li^+) ions. To eliminate the effects of interlayer cations completely, the chemical formulae for the clays in Table 3.6 are calculated on the basis of fixed cationic numbers. The raw chemical data in Table 3.6 consist of oxides, and they were transformed into another matrix with eight variables representing directly the numbers of tetrahedral and octahedral ions in the structure. This 8×152 matrix has been subjected to an R-mode factor analysis. This procedure begins with the calculations of the correlation coefficients (r_{ij}) between the variables (tetrahedral and octahedral cations in our

TABLE 3.8

The correlation matrix of tetrahedral and octahedral cations in dioctahedral smectites

	Si	Al-tet.	Al-oct.	Fe^{3+}	Fe^{2+}	Mg	Mn	Li
Si	1.00							
Al-tet.	−0.99	1.00						
Al-oct.	−0.18	0.18	1.00					
Fe^{3+}	−0.11	0.11	−0.31	1.00				
Fe^{2+}	0.10	−0.10	0.05	−0.05	1.00			
Mg	0.24	−0.24	−0.76	−0.37	−0.14	1.00		
Mn	−0.04	0.04	−0.09	−0.14	0.09	0.16	1.00	
Li	0.04	−0.04	0.11	−0.12	−0.04	−0.03	−0.02	1.00

case). The so-obtained correlation matrix is given in Table 3.8. In this correlation matrix we are confronted with the well-known problem of "the constant-sum" of geochemistry (Chayes, 1960). Composition data, regardless whether they are expressed in percentages or in real numbers of a chemical formula, are drawn from matrices with constant row-sums. Correlations between such "closed variables" may partly be related to the constant-sum constraint. Our 8×152 data matrix consists of eight variables and 152 observations for each of them; five of these variables have comparable variances as indicated by the following standard deviations: s(Si) = 0.166; s(Al-tet.) = 0.165; s(Al-oct.) = 0.158; $s(Fe^{3+})$ = 0.111; $s(Fe^{2+})$ = 0.021; s(Mg) = 0.163; s(Mn) = 0.003; and s(Li) = 0.001. Under these conditions, the effect of the constant sum is not expected to be so strong as to invalidate our analysis. Nevertheless, we must confine our attention to strong negative correlations and to large factor loadings. Examination of the correlation matrix in Table 3.8 shows that a high negative correlation (−0.99) between tetrahedral aluminum and silicon, and a significant negative correlation (−0.76) between octahedral aluminum and magnesium. The former correlation is a trivial one and it is an example of the constant-sum constraint since the sum of tetrahedral aluminum and silicon is a constant. It is difficult to draw any other conclusions directly from this correlation matrix. *R-mode* factor analysis provides a more powerful method to describe a correlation matrix and to find underlying relationships between the variables. Our correlation matrix has been subjected to such an analysis using *principal factoring with iterations*. The latter method and the related computer programs are described by Nie et al. (1975). *Principal factoring with iterations* replaces the main diagonal of the correlation matrix with initial estimates of *communalities*, and employs an iteration to improve the initial estimates. *Communalities*, designated by h_j^2's, are that portion of variances of the variables that is due to the correlations between the variables. Since the variables are standardized, the variance of a variable is unity. Thus $1 - h_j^2$ represents the portion of the vari-

TABLE 3.9

Factor matrix using principal factors with iterations

Variable	Factor 1	Factor 2	Factor 3	Factor 4	Factor 5	Factor 6
Si	0.85	0.46	0.18	−0.13	0.03	−0.01
Al-tet.	−0.85	−0.46	−0.18	0.13	−0.03	0.00
Al-oct.	−0.58	0.74	−0.27	−0.20	0.02	−0.03
Fe^{3+}	−0.21	−0.24	0.95	0.00	0.06	0.01
Fe^{2+}	0.04	0.37	0.05	0.91	−0.08	0.01
Mg	0.70	−0.60	−0.38	0.07	−0.08	−0.01
Mn	0.06	−0.11	−0.19	0.19	0.45	0.01
Li	−0.00	0.10	−0.10	−0.09	−0.03	0.19

	communality	factor	eigenvalue	% variance	cumulative % variance
Si	0.993	1	2.332	37.0	37.0
Al-tet.	0.993	2	1.542	24.4	61.4
Al-oct.	1.000	3	1.233	19.5	81.0
Fe^{3+}	0.999	4	0.946	15.0	96.0
Fe^{2+}	0.972	5	0.216	3.4	99.4
Mg	1.000	6	0.039	0.6	100.0
Mn	0.286				
Li	0.065				

ance of a variable that is not caused by its correlations to other variables, and it is called the *unique* variance of the variable. The results of the factor analysis are given in Table 3.9. At the top of the table is the matrix of *loadings* of eight variables on six factors. The latter are the *eigenvectors* of the correlation matrix as modified by *communalities.* These new factors are orthogonal, i.e., independent of each other. At the bottom of Table 3.9 *communalities* of variables, *eigenvalues* of factors, and percentage of variance represented by the factors, are shown. Accordingly, 95% of the total variance in the data is accounted for by four independent factors. The *communalities* of the variables indicate that almost all of the variance in Si, tetrahedral Al, octahedral Al, Fe^{3+}, Fe^{2+}, and Mg is related to the correlations between these variables. The *communalities* of Mn and Li, on the other hand, indicate that the variances related to these ions are unique, and not related to other ions. In order to interpret the factors in a more meaningful way, the factors are rotated using *varimax* criterion, which maximizes the variance represented by each factor. The new factor matrix is given in Table 3.10. An examination of this matrix shows that tetrahedral aluminum and silicon load very heavily on *factor 1*, and loadings of all other variables on this factor are almost negligible. Thus, *factor 1* represents the tetrahedral composition (specifically tetrahedral Si and Al). The loadings of tetrahedral Al and Si are of

TABLE 3.10

Varimax rotated factor matrix

Variable	Factor 1	Factor 2	Factor 3	Factor 4	Factor 5	Factor 6
Si	0.99	−0.10	−0.04	0.04	−0.04	0.05
Al-tet.	−0.99	0.11	0.04	−0.04	0.04	−0.06
Al-oct.	−0.11	0.92	−0.31	−0.01	−0.08	0.21
Fe^{3+}	−0.06	0.01	0.95	−0.04	−0.15	−0.24
Fe^{2+}	0.07	0.08	−0.03	0.97	0.09	−0.09
Mg	0.14	−0.90	−0.36	−0.12	0.14	−0.05
Mn	−0.04	−0.08	−0.07	0.05	0.52	−0.03
Li	0.03	0.05	−0.06	−0.03	−0.02	0.24

opposite sign, and this makes *factor 1* a bipolar one. Similarly, octahedral Al and Mg load very heavily on *factor 2*. Since the loadings of other variables are very small, this factor represents octahedral Al and Mg. *Factor 2* is again bipolar, as the loadings of Al and Mg are of opposite sign. Only trivalent iron (Fe^{3+}) loads very heavily on *factor 3*, whereas only divalent (Fe^{2+}) has a high loading on *factor 4*. The loadings of the variables on the remaining *factors 5* and *6* are negligible. The following conclusions can now be drawn from the above results of the factorial analysis:

(1) The total variance in chemical composition of the smectites in Table 3.6 is represented by four independent factors.

(2) *Factors 1* and *2* represent 61.4% of the total variance in the data. Since these factors are independent of each other, tetrahedral composition of the smectite is not correlated with its octahedral composition.

(3) *Factors 3* and *4*, which together account for 34.5% of the total variance, represent Fe^{3+} and Fe^{2+}, respectively. Again, since all the factors are orthogonal to each other, the two states of iron are not correlated with each other, nor are they correlated to other cations in the structure.

References

Anderson, D.M. and Reynolds, R.C., 1966. Umiate bentonite: an unusual montmorillonite from Umiat, Alaska. Am. Mineral., 51: 1443—1456.

Brindley, G.W. and Ertem, G., 1971. Preparation and solvation properties of some variable charge montmorillonites. Clays Clay Miner., 19: 400.

Chayes, F., 1960. On correlation between variables of constant sum. J. Geophys. Res., 65: 4185—4192.

Earley, J.W., Osthaus, B.B. and Milne, I.H., 1953. Purification and properties of montmorillonite. Am. Mineral., 38: 707—724.

Foster, M.D., 1951. The importance of exchangeable magnesium and cation exchange capacity in the study of montmorillonite clays. Am. Mineral., 36: 717—730.

Foster, M.D., 1953. Geochemical studies of clay minerals. III. The determination of free silica and free alumina in montmorillonites. Geochim. Cosmochim. Acta, 3: 142—154.

Grim, R.E. and Kulbicki, G., 1961. Montmorillonite: high temperature reactions and classification. Am. Mineral., 46: 1329—1369.
Hamilton, J.D., 1971. Beidellitic montmorillonite from Swansea, New South Wales. Clay Miner., 9: 114.
Harman, H.H., 1960. Modern Factor Analysis. University of Chicago Press, Chicago, Ill.
Heysteck, H., 1962. Hydrothermal rhyolitic alteration in the Castle Mountains, California. Clays Clay Miner., 11: 158—168.
Kerr, P.F., Hamilton, P.K., Pill, R.J., Wheeler, G.V., Lewis, D.R., Burchardt, W., Reno, D., Taylor, G.L., Mielenz, R.L., King, M.E. and Schieltz, N.C., 1951. American Petroleum Institute Research Project 49, Analytical data on reference clay materials — Prelim. Rep., 7, Columbia Univ., New York, N.Y.
Klovan, J.E., 1975. R- and Q-mode factor analysis. In: R.B. McCammon (Editor), Concepts in Geostatistics. Springer, Berlin—Heidelberg—New York, pp. 21—69.
Knechtel, M.M. and Patterson, S.H., 1962. Bentonite deposits of the northern Black Hills district, Wyoming, Montana, and South Dakota. U.S. Geol. Surv. Bull., 1082-M: 893—1030.
Lawley, D.N. and Maxwell, A.E., 1962. Factor Analysis as a Statistical Method. Butterworths, London.
Marshall, C.E., 1935. Layer lattice and base-exchange clays. Z. Kristallogr., 91: 433—449.
Marshall, C.E., 1949. The Colloid Chemistry of Silicate Minerals. Academic Press, New York, N.Y.
Nie, N.H., Hull, C.H., Jenkins, J.G., Steinbrenner, K. and Bent, D.H., 1975. Statistical Package for the Social Sciences. McGraw-Hill, New York, N.Y., pp. 468—514.
Osthaus, B.B., 1955. Kinetic studies on montmorillonite and nontronite. Clays Clay Miner., 4: 301—310.
Robertson, H.E., Weir, A.H. and Wood, R.D., 1968. Morphology of particles in size fractionated Na-montmorillonites. Clays Clay Miner., 16: 239—247.
Ross, C.S. and Hendricks, S.B., 1945. Minerals of the montmorillonite group. U.S. Geol. Surv., Prof. Pap., 205-B: 79 pp.
Ross, G.J. and Mortland, M.M., 1965. A soil beidellite. Soil Sci. Soc. Am. Proc., 30: 337—343.
Schultz, L.G., 1969. Lithium and potassium absorption, dehydroxylation temperature, and structural water content of aluminous smectites. Clays Clay Miner., 17: 115—149.
Weaver, C.E. and Pollard, L.D., 1973. The Chemistry of Clay Minerals. Elsevier, Amsterdam, 213 pp.
Weir, A.H., 1965. Potassium retention in montmorillonites. Clay Miner., 6: 18—19.
Weir, A.H. and Greene-Kelly, R., 1962. Beidellite. Am. Mineral., 17: 137—146.

3.9. SUMMARY OF GEOLOGY AND MINERALOGY OF BENTONITES

Geological features of bentonites

Bentonites are reported associated with and intercalated with all types of sediments including conglomerates. However, they are most often found associated with beds which are marine in origin. These marine formations may be glauconitic sands (Mississippi, Poland), limestone (Israel), shales (Wyoming, U.S.A.), or calcareous fossiliferous sands and marls (England, Morocco). The associated beds may also be non-marine in origin, such as fresh-water limestones (Brazil, Canada, Czechoslovakia, Rumania, Switzer-

land, Yugoslavia), carbonaceous shale (Australia), or beds of coal (Australia, Canada, Yugoslavia, U.S.S.R.). The associated beds may be bentonitic in character, for example, shales in New Zealand and Poland; clays in Australia and New Zealand; sands in Japan; and silts in Algeria. Radiolarian chert is found with bentonites in Cyprus, and diatomaceous earth is associated with bentonites in many areas (Algeria, Peru, etc.). Microscopic thin-section studies of some bentonites (e.g. Canada) reveal fragments of diatoms altered to smectite. In many instances it is difficult to distinguish pseudomorphs of diatom fragments from those of glass shards.

Unaltered ash beds are intercalated with bentonite layers in several countries. In the U.S.A. and Argentina sections have been found which show a repetition of bentonite—ash—bentonite—ash—bentonite— etc., with each bed being a matter of inches in thickness. Commonly, the ash horizons show slight alteration at their tops, and a sharp break with the overlying bentonite.

A few bentonites are reported to be fossiliferous; for example, there are marine fossils in some of the bentonites in Israel, and both marine and nonmarine fossils in various bentonites in Argentina. Silicified wood and bone are found in some bentonites in Colorado, U.S.A.

It follows from the foregoing statements that the strata immediately overlying and underlying bentonites in a sedimentary sequence may be of any type. In a few instances the underlying beds are silicified downward for a distance of one to three feet, apparently by downward movement of silica from the bentonite (Wyoming, Italy, Mexico, U.S.S.R.). The thickness of the silicified zone is related to the thickness of the bentonite layer; the thickness increasing as the bentonite beds become thicker. Analyses indicate that only a small amount of silica has been added to the underlying sediment in the silicification process. In Germany there has been silicification of underlying beds of sand with the amount of added silica being so slight that the sands are not cemented.

There appears to be no correlation between the character of the adsorbed cation in the smectite of the bentonites (i.e. sodium versus calcium) and the character of the enclosing formations.

In general, the basal contact of bentonite with underlying beds is sharp, whereas there is a gradational contact with the overlying beds. The overlying contact may be an interlayering of beds or a gradual transition of the bentonite to shale, sand, etc. In some cases (e.g. Mississippi) overlying beds of sand contain nodular masses of bentonite sharply separated from the sand. There are almost no cases where the uppermost portion of a bentonite layer shows any indication of weathering, and there is no suggestion of a profile of weathering at the top of bentonite horizons.

While bentonites vary in color from black to white, and may be of any color, most bentonites are gray, blueish gray, light yellow or green. Frequently the bentonite is blue-green when fresh and becomes yellow upon weathering. Many light colored bentonites have a speckled appearance due to

the presence of many minute particles of oxides of manganese, biotite, etc., that are disseminated through the clay. Such particles tend to be absent or at least not visible in dark colored bentonites.

Individual beds of bentonite may be laminated or massive. The massive variety frequently breaks along irregular curved surfaces that have been described as "jigsaw puzzle" fractures. Because of expansion and contraction on wetting and drying, bentonite outcrops frequently have a "popcorn" appearance. Some bentonites, for example, those in Wyoming and Germany, contain distinct nodular masses of spheroidally laminated blue bentonite. These so-called "blue eggs" are relatively pure smectite, but seem to have lower colloidal properties than the massive bentonite. It is well known that weathering at an outcrop tends to increase the colloidal properties of bentonites.

Sometimes a given geologic unit will contain as many as twenty individual bentonite beds separated by nonbentonitic material. The Cretaceous formations of Wyoming and Montana in the U.S.A., and the Tertiary formations of the U.S.S.R. and Argentina are examples of the multiplicity of bentonite layers. On the other hand, there may be a single or at most, two or three bentonite horizons in a given geologic formation, as for example in the Karoo System in South Africa, and in the Tertiary formations of India and California.

Bentonites vary in thickness from an inch or less to twenty feet or more. Often the thicker beds seem to be composites of several layers. Difference in color and variations in properties vertically through a bentonite horizon suggest the composite character. In general, bentonites tend to be lenticular, i.e., they tend to thin out horizontally and merge with the enclosing formations. However, the areal extent may be quite large — a matter of tens of square miles in the Wyoming area.

Some bentonites are not found in a sequence of sedimentary formations, but are associated with igneous rocks of a wide variety of types. This is often true for bentonites which have been formed by hydrothermal or deuteric processes. Although the associated igneous material may be of any type and either effusive or intrusive, intrusive masses of acidic types are most common. In such occurrences of bentonite there may be irregular masses of almost pure smectite surrounded by igneous material, there may be scattered masses of clay disseminated within the igneous mass, or there may be an intimate mixture of the two materials. The contact of the clay and the igneous mass is usually gradational. A common feature of such bentonites is that the texture of the parent igneous rock is preserved in the clay. There is no evidence of shrinkage or any change of volume in the transition of the igneous rock to the smectite clay.

Clays that can be classed as bentonites on the basis of composition and properties are found in formations ranging in age from Upper Paleozoic to Pleistocene or possibly Recent. The Permian—Triassic coals of Australia con-

tain bentonites. Triassic formations of Argentina, the Ukraine in the U.S.S.R., and Yogoslavia contain bentonites. Some of the South African bentonites are Triassic in age, and the Jurassic formations in Israel, England, and the U.S.S.R. contain bentonites. By far most of the bentonites world wide are in formations of Cretaceous age, usually Upper Cretaceous age. Bentonites are so common in the Upper Cretaceous that it is worth while to look for them in any sequence of formations of that age. Bentonites are very abundant in Tertiary formations, particularly in those of Miocene age. Some of the Japanese bentonites, and possibly some of those in Nevada, are Pleistocene or possibly Recent in age.

So-called metabentonites are reported in many formations of Paleozoic age. In general, these materials are composed of illite—smectite mixed-layer minerals, so that the material does not have the physical properties of bentonites. The metabentonites have been looked upon essentially as altered volcanic ash to which potassium has been added later, giving rise to the illite component and the loss of bentonite properties.

Mineralogical features of bentonites

Smectites form the major mineralogical component in bentonites. Members of the montmorillonite—beidellite series are by far the common smectites in bentonites. No beidellite end-member has been found among the samples studied. Nor is any nontronite end-member observed. Several end-member montmorillonites have, however, been observed. These end-member montmorillonites are found, for instance, in the samples from Cheto, Otay, Santa Rita, Tatatilla (Mexico), Mostaganem (Algeria), Ramblon (Argentina), Surrey (England, samples 60 and 61). Smectite in the well-known Wyoming bentonite falls rather closely to the montmorillonite—beidellite boundary line. The chemical data suggest that there are an appreciable number of montmorillonites at around this boundary line. A few of them such as samples from Challao and Las Heras (both Argentina), Usui (Japan), and Natal Province (Union of South Africa), have very low magnesia content suggesting that they may be at the beidellite side of the montmorillonite—beidellite series. Smectites of the saponite—hectorite series have been found in a few samples. Again the end-member hectorite has been so far reported in the Hector deposit of California.

The data on extractable cations indicate that Na and Ca are the most common interlayer cations in the above samples. Mg is extracted only from a few samples in appreciable quantities. The variations in basal spacings seem to directly correlate with the interlayer population. The (06, 33) spacings indicate that dioctahedral smectites occur in all the samples studied with the exception of smectites from Nevada (samples 13—16).

The chemical data were obtained on the ignited samples where the smectites were stripped of their interlayer cations by NH_4^+ saturation. Conse-

quently the composition of tetrahedral and octahedral sheets was directly obtained. The total variance in the chemical data was simply reduced to SiO_2, Al_2O_3, Fe_2O_3, and MgO for the dioctahedral smectites. The magnesia content of these smectites forms an important parameter with respect to the position of a sample in montmorillonite—beidellite series. For the montmorillonite end-member MgO content can vary from 3.0% at the minimum layer charge of $z = 0.25$ to 7.2% at the maximum layer charge of $z = 0.6$ (on the basis of $MgO + Al_2O_3 + SiO_2 = 100$). Magnesia content of the above dioctahedral samples ranges from about 2.0% to 6.0% after due considerations for the impurities in the samples. Iron content (as Fe_2O_3) ranges on the other hand from about 1.0% to 11.7% with a few exceptions (Tables 3.1B to 3.5B). The smectite from Tatatilla, Mexico (sample 43) is distinguished by practically the absence of iron. The variance in alumina and silica values for the samples is mainly caused by the associated free silica (cristobalite and quartz) in the samples. Some of the bentonites contain up to 50—60% cristobalite even in the -1 μm fractions.

The morphological features of smectite aggregates in the montmorillonite—beidellite series show the following variations: Wyoming-type lamellar aggregates are found in about 35 of about 80 samples examined. Cheto-type mossy aggregates occur in 27 samples. In a few samples both Cheto- and Wyoming-type aggregates are found in the same sample. Reticulated aggregates (Santa Rita-type) are observed in 8 samples. In these samples Cheto-type aggregates also occur to a smaller extent. Again in only 8 samples globular aggregates (Otay-type) are found with small amounts of Wyoming- and Cheto-type aggregates. Smectite single crystallites (S-, E- and H-type particles) occur in all samples but with varying amounts. The samples carrying Wyoming-type aggregates seem to contain large amounts (up to 50%) of these single crystallites. Those samples with Cheto-type aggregates contain small amounts (5—20%) single crystallites in form of S-, E-, and H-type particles, Smectite laths occur only in some samples.

In order to properly interpret the morphological variations in smectite particles, we need to consider the nature of factors controlling the crystal-growth mechanisms during their crystallization. In this regard a distinction should be made between internal (structural), and external factors such as temperature, degree of supersaturation, viscosity, and the impurities. Factors affecting morphological features of the crystals are rather complex. It is therefore rather difficult to assign some geological significance to a specific morphological feature. Morphological features of Wyoming- and Cheto-type aggregates are compatible with a dendritic (tree-like) crystallization, whereas the single smectite crystallites seem to form by a layer-after-layer growth mechanism. In general, dendritic growth is favored at high crystallization rates under nonequilibrium conditions, whereas the layer-after-layer mechanism occurs at low crystallization rates under equilibrium conditions. The smectite aggregates are therefore expected to form at the early stages of crys-

tal growth under high supersaturation, and the single crystallites are probably developed during the later stages of crystallization.

Free silica minerals, cristobalite and tridymite, are important components of some bentonites. The characteristic 4.04 Å X-ray reflection of α-cristobalite in bentonites is often broadened toward the lower angle suggesting the presence of stacking disorder in the structure of this mineral. The low temperature (α-) tridymite is characterized, on the other hand, by the strong 4.11 Å reflection. The broad reflection with maxima at 4.11 and 4.04 Å found in some samples is interpreted as indicating cristobalite—tridymite mixed-layering. Structurally, these two forms of silica are very similar, namely cristobalite displays ABC... stacking sequence of (SiO_4) sheets, and tridymite on ABAB... stacking sequence.

Quartz, feldspars, kaolinite, mica, illite, gypsum, calcite, and accessories (heavy minerals) are the minor components in bentonites; they are concentrated in the coarser fractions (>10 μm). Zeolites seem to occur rarely in bentonites. Micas and kaolinite occur in both fine and coarse fractions, and they are often in the form of hexagonal platelets. Feldspars consist of sanidine, orthoclase, microcline, and plagioclases. Plagioclases are often intensively altered, and have an anorthite content from An_{10} to An_{30}. For the zeolites, analcite has been found in large amounts in one sample (No. 32), whereas clinoptilolite occur as accessory minerals in a few samples. Heavy minerals with a density above 2.90 were separated and optically identified. Zircon, opaque minerals (mainly magnetite), apatite, magnesite, and pyroxenes were found in most of the samples. No systematic analysis of heavy minerals was made. Biotite in large euhedral flakes is a very common component of bentonites.

Chapter 4

SELECTED AREA ELECTRON DIFFRACTION STUDIES ON MUSCOVITE, BEIDELLITE, AND MONTMORILLONITE

Members of the montmorillonite—beidellite series form the smectites commonly occurring in bentonites. The wide range of applications of bentonite in science and technology is related to the structural, chemical, and morphological (particle habit, size, and mode of aggregations) properties of smectite particles in these clays. Electron optics probably provide the most powerful methods for precise analyses of the above properties of smectite particles. In this chapter we will first evaluate the major factors affecting the diffraction of electrons by the mica-type layer silicates. This will be done in two sections: (1) interference function, and (2) selected area electron diffraction on muscovite. These two sections should provide the background necessary to understand the transmission and diffraction images formed by electrons from smectite particles. Subsequently the crystal structures of montmorillonite and beidellite will be examined in Sections 4.3 and 4.4.

4.1. INTERFERENCE FUNCTION

In electron optics the image contrast and the diffraction effects of a crystalline solid are defined by the so-called interference function. The function expresses the total interference between the waves which are formed by the scattering of electrons from the content of each unit cell in the solid. Thus the function is the heart of the matter for understanding the image contrast and diffraction effects from a solid. Therefore, the properties of the interference function will be first discussed for a normal (undeformed) and then for a bent lattice.

Properties of the interference function for undeformed lattices

The interference function (S) for an undeformed and orthogonal lattice may be expressed as:

$$S = \sum_{m=0}^{M-1} \exp[2\pi i m\boldsymbol{s} \cdot \boldsymbol{a}] \sum_{n=0}^{N-1} \exp[2\pi i n\boldsymbol{s} \cdot \boldsymbol{b}] \sum_{p=0}^{P-1} \exp[2\pi i p\boldsymbol{s} \cdot \boldsymbol{c}] \qquad (1)$$

where the reciprocal lattice vector $|\boldsymbol{s}| = 2 \sin \theta/\lambda$, and M, N, P are the number of the unit cells along the $\boldsymbol{a}$, $\boldsymbol{b}$, and $\boldsymbol{c}$ directions. These three summations have a common form. Therefore, the properties for one of them, sometimes called the one-dimensional interference function, will be described in the following instead of the total interference function. Each of the above summations can be reduced as:

$$S = \sum_{m=0}^{M-1} \exp[2\pi i m\boldsymbol{a} \cdot \boldsymbol{s}] = \frac{\sin \pi M\boldsymbol{a} \cdot \boldsymbol{s}}{\sin \pi \boldsymbol{a} \cdot \boldsymbol{s}} \cdot \exp[ni(M-1)\boldsymbol{a} \cdot \boldsymbol{s}] \tag{2}$$

For intensity calculations, the function $|S|^2$ is needed. The exponential term $\exp[\pi i(M-1)\,\boldsymbol{a} \cdot \boldsymbol{s}]$ can then be disregarded as it has the unit modulus. The function $|S|^2$ can be further simplified by expressing $\boldsymbol{s}$ in units of $\boldsymbol{a}^*$:

$$\boldsymbol{s} = u \cdot \boldsymbol{a}^*$$

$$\boldsymbol{a} \cdot \boldsymbol{s} = u \cdot \boldsymbol{a}^* \cdot \boldsymbol{a} = u$$

$$|S|^2 = \frac{\sin^2 \pi M u}{\sin^2 \pi u} \tag{3}$$

The interference function in this form becomes perfectly general, and it is independent of any cell parameter (real and reciprocal). It needs to be evaluated but once, and then can be used for any other crystal. The argument (u) of the function represents a fraction of the distance between two consecutive reciprocal lattice points in any direction. This is considered in increments of one-hundredths of the reciprocal spacing. The function (S^2) has been exactly evaluated and normalized (i.e. S^2/M^2) for $M = 2$ to 100. For larger values of M, the crystal can be considered as "infinite". The numerical values of the normalized interference function have been listed in Table 4.1. These values can now be used for any other crystal. For the special case $M = 1$, the function is always unity and it is not listed in the table. The normalized interference function (S^2/M^2) has also been plotted in Fig. 4.1 for M values of 1, 2, 3, 4, 5, and 10 in order to show the properties of this function. The function for an undeformed lattice is symmetrical at the origin and at $u = \frac{1}{2}$, i.e. $f(u) = f(-u)$ and $f(\frac{1}{2} + u) = f(\frac{1}{2} - u)$. It is therefore completely sufficient to list the values of the function in the interval $u = 0.00$ to 0.50. The interference function has zero values at all the points with $u = n/m$ and has maxima for $u = (n + \frac{1}{2})(1/M)$, where n is an integer but u remains a fractional number. The elongation of a diffraction spot is usually given by the width of the first maxima, which is equal to $u = (1/M)$. In other words, the elongation of a reflection is simply determined by the reciprocal of the number of unit-cells in that direction. It is also important to realize that there are additional subsidiary maxima for $u = (n + \frac{1}{2})(1/M)$ as long as the

TABLE 4.1

Numerical values for the normalized interference function $(S^2/M^2)\ 10^4$ for the crystal thickness of 2 to 100 unit-cells. The u values are given in fractions of the distance between two consecutive reciprocal lattice points.

U	M=2	M=3	M=4	M=5	M=6	M=7	M=8	M=9	M=10	M=11	M=12	M=13	M=14	M=15	M=16	M=17	M=18	M=19	M=20
0.0	10000	10000	10000	10000	10000	10000	10000	10000	10000	10000	10000	10000	10000	10000	10000	10000	10000	10000	10000
0.01	9990	9974	9951	9921	9885	9843	9794	9740	9678	9611	9538	9459	9375	9284	9189	9088	8981	8870	8754
0.02	9961	9895	9804	9688	9548	9384	9198	8990	8763	8517	8254	7975	7683	7378	7063	6739	6409	6074	5735
0.03	9911	9765	9563	9309	9005	8656	8267	7843	7390	6914	6420	5915	5405	4896	4393	3903	3430	2979	2553
0.04	9843	9585	9234	8798	8287	7713	7091	6434	5758	5076	4403	3752	3134	2559	2036	1570	1167	826	550
0.05	9755	9358	8824	8173	7429	6621	5775	4921	4086	3295	2567	1920	1365	908	551	291	120	28	0
0.06	9649	9086	8341	7456	6477	5453	4433	3461	2576	1807	1174	685	337	121	17	4	54	143	246
0.07	9524	8771	7798	6673	5476	4284	3168	2185	1375	760	339	97	4	23	111	230	345	431	475
0.08	9382	8419	7204	5850	4474	3184	2068	1185	559	181	18	15	112	248	375	458	482	446	366
0.09	9222	8032	6574	5013	3513	2208	1192	501	123	1	55	197	348	453	484	441	343	222	111
0.10	9045	7616	5920	4189	2631	1399	565	123	0	83	251	406	483	465	370	237	112	28	0
0.11	8853	7174	5256	3401	1859	778	185	1	83	271	431	491	438	308	160	48	1	19	75
0.12	8645	6713	4594	2670	1217	350	18	56	255	435	494	421	268	113	18	4	53	121	167
0.13	8423	6236	3947	2013	716	101	16	203	415	499	425	257	93	7	15	82	150	174	143
0.14	8187	5750	3327	1444	356	4	117	362	499	449	273	94	4	23	101	165	170	117	48
0.15	7939	5259	2743	970	129	24	262	476	485	318	116	7	24	108	171	164	98	28	0
0.16	7679	4769	2205	595	19	119	400	513	390	167	19	16	103	173	162	89	18	2	37
0.17	7409	4284	1719	318	4	249	494	472	253	50	4	86	170	167	90	15	4	47	87
0.18	7129	3809	1292	133	60	378	525	372	120	1	56	158	177	101	18	4	50	91	79
0.19	6841	3350	927	31	159	479	493	244	30	20	130	186	124	29	2	48	92	78	27
0.20	6545	2909	625	0	278	534	409	123	0	83	182	155	51	0	39	91	81	28	0
0.21	6243	2491	386	26	393	538	297	36	25	150	184	89	5	24	85	88	33	0	23
0.22	5937	2100	208	94	487	494	180	1	85	191	140	26	8	72	96	45	1	20	56
0.23	5627	1738	88	189	549	413	83	13	150	187	74	0	47	99	64	6	13	53	52
0.24	5314	1408	21	295	572	310	21	61	193	144	20	17	89	86	19	5	47	57	18
0.25	5000	1111	0	400	556	204	0	123	200	83	0	59	102	44	0	35	62	28	0
0.26	4686	850	18	493	504	110	18	178	170	28	18	96	79	8	17	61	41	2	16
0.27	4373	624	69	564	427	42	64	209	116	1	58	105	37	2	49	57	10	8	40
0.28	4063	434	143	609	334	5	123	207	58	9	96	82	5	26	66	27	1	33	38
0.29	3757	281	232	625	236	3	178	175	15	42	111	41	3	57	51	3	20	44	14
0.30	3455	162	330	611	147	30	216	123	0	83	96	9	27	68	21	5	43	28	0
0.31	3159	77	428	570	74	77	228	68	14	111	60	1	57	52	1	28	42	5	13
0.32	2871	24	520	508	24	134	211	23	48	115	23	19	71	22	7	47	20	2	32
0.33	2591	1	601	429	1	188	173	1	88	94	1	50	60	1	31	41	1	21	31
0.34	2321	6	666	341	6	230	121	6	118	57	6	72	31	6	49	18	5	36	11
0.35	2061	34	712	252	33	251	68	32	126	21	30	73	6	28	45	1	25	28	0
0.36	1813	84	737	169	79	248	26	71	110	2	60	52	1	49	22	6	38	8	11
0.37	1577	151	739	98	134	223	3	109	78	5	80	22	17	51	3	26	28	0	27
0.38	1355	233	720	44	191	181	3	134	40	27	78	2	42	34	3	39	8	13	26
0.39	1147	325	681	11	241	130	24	139	11	58	56	3	57	10	21	33	0	29	10
0.40	955	424	625	0	278	78	60	123	0	83	27	23	51	0	39	13	12	28	0
0.41	778	527	555	11	296	35	101	92	10	90	5	48	29	10	41	0	29	11	9
0.42	618	629	475	41	295	8	136	53	37	76	1	62	7	31	25	7	32	0	24
0.43	476	728	390	87	274	0	158	20	69	49	17	57	0	46	6	25	17	8	24
0.44	351	821	304	143	236	13	161	2	94	20	43	36	12	42	1	36	2	24	9
0.45	245	904	221	205	186	43	145	3	103	2	64	13	34	23	14	28	3	28	0
0.46	157	976	147	266	132	84	113	23	92	3	70	0	50	4	32	10	19	15	9
0.47	89	1034	85	320	80	129	74	54	66	22	57	7	48	1	39	0	31	1	23
0.48	39	1076	39	363	38	168	36	88	35	49	33	28	30	15	28	8	25	4	23
0.49	10	1102	10	391	10	195	10	114	10	73	9	50	9	35	9	26	9	19	9
0.50	0	1111	0	400	0	204	0	123	0	83	0	59	0	44	0	35	0	28	0

TABLE 4.1 (continued)

U	M=21	M=22	M=23	M=24	M=25	M=26	M=27	M=28	M=29	M=30	M=31	M=32	M=33	M=34	M=35	M=36	M=37	M=38	M=39	M=40
0.0	10000	10000	10000	10000	10000	10000	10000	10000	10000	10000	10000	10000	10000	10000	10000	10000	10000	10000	10000	10000
0.01	8634	8509	8379	8246	8108	7967	7823	7675	7524	7371	7215	7056	6895	6733	6568	6403	6236	6068	5899	5730
0.02	5396	5056	4719	4386	4058	3737	3425	3122	2829	2549	2282	2028	1789	1564	1355	1162	985	823	678	548
0.03	2157	1791	1460	1164	903	679	489	334	212	120	56	17	1	4	23	54	95	142	192	244
0.04	335	178	74	17	0	15	54	110	176	244	310	369	417	451	470	474	463	439	404	360
0.05	23	81	159	245	327	396	445	471	474	454	415	361	298	231	167	109	62	27	7	0
0.06	343	419	465	477	456	407	338	259	180	109	54	17	1	4	22	51	85	117	144	161
0.07	472	427	352	260	168	89	33	4	2	22	57	96	132	157	167	162	142	112	78	45
0.08	261	157	71	17	0	15	51	97	137	162	168	152	122	83	46	17	2	2	14	35
0.09	33	1	12	52	103	146	168	163	135	93	50	17	1	4	22	46	70	83	84	73
0.10	23	75	130	164	168	140	94	46	12	0	10	35	63	82	85	73	50	25	7	0
0.11	135	169	163	124	70	23	1	7	33	63	84	85	67	40	15	1	3	17	36	49
0.12	167	125	65	17	0	15	47	77	87	74	46	17	1	4	21	41	52	49	35	16
0.13	81	24	0	15	51	81	87	66	33	7	1	14	36	51	50	35	15	2	2	14
0.14	4	7	42	78	88	67	31	4	2	21	44	54	44	22	4	1	12	27	36	31
0.15	23	66	89	76	39	7	2	21	46	54	40	16	1	4	20	34	35	22	7	0
0.16	80	89	58	17	0	15	42	55	42	17	1	6	23	36	32	16	2	2	13	24
0.17	83	42	6	4	31	54	49	23	2	4	23	36	31	14	1	4	18	26	21	8
0.18	32	1	12	43	56	37	9	1	17	35	34	16	1	4	19	27	20	6	0	8
0.19	0	19	50	53	25	2	7	29	38	23	4	2	16	27	21	6	0	9	19	18
0.20	23	54	49	17	0	15	36	33	12	0	10	26	24	9	0	8	19	18	7	0
0.21	56	48	13	1	21	39	27	5	2	19	28	15	1	4	17	20	9	0	6	15
0.22	48	12	2	25	39	22	1	7	25	25	7	0	12	21	13	1	3	14	15	5
0.23	13	2	27	40	18	0	12	28	20	2	4	18	19	6	0	10	17	8	0	5
0.24	1	26	40	17	0	15	29	16	0	8	21	15	1	4	16	13	2	2	11	12
0.25	23	41	19	0	16	30	14	0	12	22	10	0	9	17	8	0	7	14	7	0
0.26	42	23	0	15	30	13	0	14	22	7	1	13	16	4	1	12	12	2	2	11
0.27	30	1	13	31	14	0	15	22	5	2	16	14	1	4	14	8	0	7	12	4
0.28	5	8	31	17	0	15	22	5	3	17	12	0	7	15	5	1	10	10	1	4
0.29	3	29	22	0	13	23	6	3	18	12	0	9	14	3	3	12	7	0	7	9
0.30	23	29	3	9	24	8	2	18	12	0	10	13	1	5	12	4	1	10	7	0
0.31	33	9	4	24	12	1	17	13	0	11	13	1	6	12	2	3	11	4	1	8
0.32	19	0	22	17	0	15	16	0	10	14	1	6	12	2	4	11	2	2	9	3
0.33	1	15	24	1	11	19	1	8	15	1	6	13	1	5	11	1	4	9	1	3
0.34	5	27	7	5	21	4	5	17	3	5	13	2	5	11	1	5	9	1	5	7
0.35	23	17	1	20	10	2	17	6	3	14	3	4	11	1	5	9	0	6	7	0
0.36	27	2	14	17	0	15	10	1	14	5	3	12	2	5	9	0	6	6	0	7
0.37	12	4	22	3	9	15	0	12	8	1	12	3	4	10	0	7	6	0	7	3
0.38	0	20	12	3	19	2	8	12	0	12	5	3	10	1	6	6	0	8	2	2
0.39	8	22	0	16	9	3	15	1	9	8	1	11	2	5	7	0	8	2	3	6
0.40	23	8	7	17	0	15	5	5	12	0	10	4	4	9	0	8	3	3	7	0
0.41	22	0	20	4	9	12	1	14	1	8	7	1	10	0	7	4	2	7	0	6
0.42	7	10	15	1	17	1	11	6	4	11	0	10	2	5	6	1	8	0	6	2
0.43	0	21	2	13	8	4	13	0	12	1	8	5	3	8	0	8	1	6	3	2
0.44	11	15	3	17	0	15	2	9	6	4	9	1	9	0	8	2	4	4	2	6
0.45	23	2	15	6	8	10	3	12	0	11	0	9	2	6	4	3	6	1	7	0
0.46	18	3	18	0	16	0	13	2	9	4	6	6	3	7	1	8	0	7	0	6
0.47	4	16	6	10	8	6	9	3	10	1	10	0	9	0	8	0	7	1	5	2
0.48	1	20	0	17	0	15	0	12	1	10	1	8	2	6	3	5	3	3	4	2
0.49	14	8	11	8	8	8	6	8	4	7	3	7	2	7	2	6	1	6	1	6
0.50	23	0	19	0	16	0	14	0	12	0	10	0	9	0	8	0	7	0	7	0

U	M=41	M=42	M=43	M=44	M=45	M=46	M=47	M=48	M=49	M=50	M=51	M=52	M=53	M=54	M=55	M=56	M=57	M=58	M=59	M=60
0.0	10000	10000	10000	10000	10000	10000	10000	10000	10000	10000	10000	10000	10000	10000	10000	10000	10000	10000	10000	10000
0.01	9560	9390	9221	9051	8883	8715	8548	8382	8217	8054	7893	7734	7576	7421	7269	7118	6971	6827	6685	6547
0.02	433	334	249	178	120	74	40	17	4	0	4	15	32	54	80	110	142	175	209	243
0.03	294	340	381	416	443	461	471	473	466	452	430	403	371	335	296	257	217	178	142	108
0.04	310	257	204	154	109	70	39	17	4	0	4	15	31	51	73	95	116	136	150	160
0.05	6	22	46	73	101	126	147	160	166	163	153	137	115	92	68	45	26	12	3	0
0.06	167	161	145	120	92	63	37	17	4	0	4	14	29	46	62	74	82	84	81	72
0.07	20	4	0	7	21	40	59	75	83	84	77	64	47	29	14	4	0	2	10	20
0.08	57	75	84	83	72	54	34	16	4	0	4	14	27	40	48	51	48	39	28	16
0.09	52	30	11	1	2	11	25	40	49	51	46	34	20	8	1	1	6	16	25	32
0.10	6	21	37	49	52	45	31	16	4	0	4	13	24	32	35	30	21	11	3	0
0.11	52	43	27	10	1	1	10	22	32	35	30	19	8	1	1	6	15	22	25	22
0.12	3	1	9	23	33	35	27	15	4	0	4	13	22	25	22	14	5	0	1	7
0.13	28	35	32	19	6	0	3	13	22	25	21	11	3	0	4	12	18	19	13	6
0.14	17	4	0	7	18	25	23	14	4	0	4	12	18	18	12	4	0	2	8	14
0.15	6	18	26	23	12	2	1	7	16	19	15	6	0	2	8	14	15	9	3	0
0.16	25	15	3	0	7	17	19	13	4	0	4	11	15	12	5	0	2	8	12	11
0.17	0	4	14	20	15	5	0	4	12	15	11	3	0	4	10	12	8	2	0	4
0.18	16	19	10	1	2	10	16	12	4	0	4	11	12	7	1	1	6	10	9	3
0.19	7	0	4	13	15	8	1	2	9	13	8	2	1	6	10	8	3	0	3	8
0.20	6	15	14	5	0	5	12	11	4	0	4	10	9	3	0	3	8	8	3	0
0.21	14	4	0	6	13	10	2	1	7	11	6	1	1	7	9	4	0	2	7	7
0.22	0	7	13	9	1	2	9	10	4	0	4	9	7	1	1	6	7	3	0	2
0.23	13	10	1	2	9	10	3	0	5	9	5	0	3	7	6	1	1	5	6	2
0.24	3	1	8	11	4	0	6	9	4	0	4	8	5	0	2	7	5	0	1	5
0.25	0	11	5	0	5	9	5	0	4	8	4	0	4	7	3	0	3	6	3	0
0.26	9	1	3	9	6	0	3	8	4	0	4	7	3	0	4	6	2	0	4	5
0.27	1	8	9	1	2	8	6	0	3	7	3	0	4	6	1	1	5	4	0	2
0.28	10	4	0	6	8	1	2	7	4	0	4	6	1	1	5	4	0	2	5	2
0.29	1	3	9	4	0	6	6	0	3	6	2	0	5	4	0	2	5	1	1	4
0.30	6	8	1	3	8	2	1	6	4	0	4	5	1	2	5	2	0	4	3	0
0.31	5	0	6	6	0	4	6	1	2	6	2	1	5	3	0	4	3	0	3	4
0.32	1	8	4	0	6	4	0	5	4	0	4	4	0	3	4	0	2	4	1	1
0.33	8	1	2	7	1	2	6	1	1	5	1	1	5	1	1	4	1	1	4	1
0.34	0	4	6	0	4	5	0	4	4	0	4	3	0	4	3	0	3	2	0	3
0.35	6	5	0	6	3	1	6	2	1	5	1	2	4	0	2	4	0	2	3	0
0.36	3	1	7	1	2	6	0	3	4	0	4	3	0	4	1	1	4	0	2	3
0.37	2	7	1	4	5	0	5	2	1	5	1	2	4	0	3	2	0	3	1	1
0.38	6	0	5	4	1	5	1	2	4	0	4	2	1	4	0	2	3	0	3	1
0.39	0	6	3	1	5	0	4	3	1	5	0	2	3	0	4	1	2	3	0	3
0.40	6	2	2	5	0	5	2	2	4	0	4	1	1	3	0	3	1	1	3	0
0.41	2	2	5	0	5	1	3	3	0	4	0	3	2	1	3	0	3	1	1	3
0.42	3	5	0	5	1	4	3	1	4	0	4	1	2	3	0	3	0	3	1	1
0.43	5	0	6	0	4	2	2	4	0	4	0	3	1	1	3	0	3	0	3	1
0.44	0	6	0	4	2	2	3	1	4	0	4	1	3	2	1	3	0	3	0	3
0.45	6	1	4	2	3	3	1	4	0	4	0	3	1	2	2	1	3	0	3	0
0.46	1	4	2	2	3	1	4	0	4	0	4	0	3	1	2	2	1	2	1	3
0.47	3	3	2	4	1	4	0	4	0	4	0	4	0	3	1	2	1	2	2	1
0.48	4	1	4	1	4	0	4	0	4	0	4	0	3	0	3	0	3	1	2	1
0.49	0	5	0	5	0	5	0	4	0	4	0	4	0	3	0	3	0	3	0	3
0.50	6	0	5	0	5	0	5	0	4	0	4	0	4	0	3	0	3	0	3	0

TABLE 4.1 (continued)

U	M=61	M=62	M=63	M=64	M=65	M=66	M=67	M=68	M=69	M=70	M=71	M=72	M=73	M=74	M=75	M=76	M=77	M=78	M=79	M=80
0.0	10000	10000	10000	10000	10000	10000	10000	10000	10000	10000	10000	10000	10000	10000	10000	10000	10000	10000	10000	10000
0.01	2411	2279	2151	2026	1904	1787	1673	1563	1456	1354	1255	1161	1070	984	901	822	748	677	610	547
0.02	277	309	340	368	393	415	434	449	461	468	472	472	468	461	451	437	421	402	381	358
0.03	79	53	33	17	7	1	0	4	11	22	35	51	67	84	100	116	130	143	152	160
0.04	165	165	160	150	136	120	101	82	63	45	29	17	7	2	0	2	7	14	24	34
0.05	3	10	21	34	48	61	72	80	84	83	79	71	61	49	36	24	14	6	2	0
0.06	39	44	29	16	6	1	0	4	11	20	30	39	46	50	51	48	42	33	24	15
0.07	32	42	49	51	49	42	32	21	11	4	0	1	5	11	19	26	31	34	33	30
0.08	6	1	1	5	13	22	29	34	34	30	23	15	7	2	0	2	6	12	18	23
0.09	34	31	24	15	6	1	0	4	10	17	23	25	23	18	11	5	1	0	2	7
0.10	3	9	17	23	25	22	15	8	2	0	2	7	13	17	19	16	12	6	2	0
0.11	15	7	1	0	4	11	16	19	17	12	5	1	0	3	8	12	15	13	10	5
0.12	14	19	18	13	6	1	0	4	9	14	15	12	8	2	0	2	6	10	12	10
0.13	1	1	5	11	15	14	9	3	0	1	5	10	12	10	6	1	0	2	6	9
0.14	15	10	4	0	1	8	11	12	9	4	0	1	4	8	10	8	4	1	0	3
0.15	3	8	12	11	6	1	0	4	8	10	8	3	0	1	4	8	8	5	2	0
0.16	5	1	1	5	9	10	6	1	0	3	7	8	6	2	0	2	5	7	6	2
0.17	9	10	6	1	0	4	8	8	5	1	0	3	7	7	3	0	1	3	6	5
0.18	0	2	7	8	5	1	0	4	7	6	3	0	1	5	6	4	1	0	2	5
0.19	8	3	0	2	6	7	4	0	1	4	6	4	1	0	3	5	4	1	0	2
0.20	3	7	7	2	0	2	6	6	2	0	2	5	5	2	0	2	4	4	2	0
0.21	2	0	3	6	5	1	0	3	6	4	0	1	4	5	2	0	1	4	4	1
0.22	6	5	1	0	4	6	3	0	1	5	4	1	0	3	4	3	0	1	3	3
0.23	0	3	6	3	0	2	5	4	1	0	3	4	2	0	2	4	2	0	1	3
0.24	5	1	1	4	5	1	0	3	4	2	0	2	4	2	0	2	4	2	0	1
0.25	3	5	3	0	2	5	2	0	2	4	2	0	2	4	2	0	2	3	2	0
0.26	1	1	4	4	0	1	4	3	0	1	4	2	0	2	3	2	0	2	3	1
0.27	5	2	0	3	4	1	0	3	3	0	1	3	2	0	2	3	1	0	2	3
0.28	0	4	3	0	1	4	2	0	3	3	0	1	3	2	0	2	3	1	0	2
0.29	3	0	2	4	1	1	3	2	0	2	3	0	1	3	1	0	2	2	0	1
0.30	3	4	0	1	4	1	0	3	2	0	2	3	0	1	3	1	0	2	2	0
0.31	0	2	4	1	1	3	1	0	3	2	0	2	2	0	1	2	0	1	2	1
0.32	4	1	1	3	1	0	3	1	0	3	2	0	2	2	0	2	2	0	1	2
0.33	1	3	1	0	3	1	0	3	1	0	3	1	0	2	1	0	2	1	0	2
0.34	2	0	3	1	0	3	1	0	3	1	0	3	1	1	2	1	1	2	0	1
0.35	3	2	0	3	1	0	3	1	1	3	1	1	2	0	1	2	0	1	2	0
0.36	0	2	2	0	3	1	0	3	1	1	2	0	1	2	0	2	1	0	2	1
0.37	3	0	2	2	0	3	1	1	2	0	1	2	0	2	1	0	2	0	1	2
0.38	1	3	0	2	2	0	3	1	1	2	0	2	1	0	2	0	1	2	0	2
0.39	1	1	3	0	2	1	0	2	0	2	2	0	2	0	1	2	0	2	1	1
0.40	3	1	1	2	0	2	1	1	2	0	2	1	1	2	0	2	1	1	2	0
0.41	0	3	1	1	2	0	2	0	1	1	0	2	0	2	1	0	2	0	2	1
0.42	2	0	3	0	2	1	0	2	0	2	1	1	2	0	2	0	1	1	0	2
0.43	1	2	0	3	0	2	1	1	2	0	2	0	2	1	1	1	0	2	0	1
0.44	1	2	2	1	2	0	2	0	2	1	1	1	0	2	0	2	0	1	1	1
0.45	3	0	2	1	1	2	0	2	0	2	0	2	0	1	1	1	1	0	2	0
0.46	0	3	0	2	0	2	1	1	1	1	2	0	2	0	2	0	2	0	1	1
0.47	2	0	2	0	2	0	2	0	2	0	2	0	1	1	1	1	1	1	0	1
0.48	2	1	1	1	1	2	1	2	0	2	0	2	0	2	0	2	0	2	0	1
0.49	0	2	0	2	0	2	1	2	1	1	1	1	1	1	1	1	1	1	1	1
0.50	3	0	3	0	2	0	2	0	2	0	2	0	2	0	2	0	2	0	2	0

U	M=81	M=82	M=83	M=84	M=85	M=86	M=87	M=88	M=89	M=90	M=91	M=92	M=93	M=94	M=95	M=96	M=97	M=98	M=99
0.0	10000	10000	10000	10000	10000	10000	10000	10000	10000	10000	10000	10000	10000	10000	10000	10000	10000	10000	10000
0.01	488	433	381	333	289	248	211	177	147	119	95	74	56	40	27	17	10	4	1
0.02	334	309	283	256	230	204	178	153	130	108	88	70	53	39	27	17	9	4	1
0.03	164	165	164	159	152	143	132	119	106	91	77	63	49	37	26	17	9	4	1
0.04	45	56	66	74	80	83	84	82	78	71	63	54	44	34	24	16	9	4	1
0.05	2	6	12	20	28	36	43	48	50	50	48	44	38	30	23	15	9	4	1
0.06	8	3	0	1	4	9	15	22	28	32	34	34	31	26	21	14	9	4	1
0.07	24	17	10	4	1	0	2	6	12	17	21	24	24	22	18	14	8	4	1
0.08	25	23	19	14	8	3	0	0	3	7	12	16	18	18	16	13	8	4	1
0.09	12	17	18	18	14	9	4	1	0	2	5	9	13	14	14	11	8	4	1
0.10	2	5	10	13	14	13	9	5	1	0	1	4	8	11	12	10	7	4	1
0.11	1	0	2	6	10	12	11	8	4	1	0	1	4	8	9	9	7	4	1
0.12	7	3	0	1	4	7	9	9	7	3	1	0	2	5	7	8	6	4	1
0.13	10	7	3	1	0	2	6	8	8	5	2	0	1	3	6	7	6	4	1
0.14	6	8	7	4	1	0	2	5	7	6	4	1	0	1	4	6	6	3	1
0.15	2	5	7	6	3	1	0	2	5	6	5	2	0	1	3	5	5	3	1
0.16	0	1	4	6	5	3	0	0	3	5	5	3	1	0	2	4	5	3	1
0.17	3	0	1	3	5	5	2	0	1	3	5	4	1	0	1	3	4	3	1
0.18	5	2	0	1	3	5	4	1	0	1	4	4	2	0	0	2	4	3	1
0.19	4	4	2	0	1	3	4	2	0	0	2	4	3	1	0	2	3	3	1
0.20	2	4	4	1	0	1	3	3	1	0	1	3	3	1	0	1	3	3	1
0.21	0	2	4	3	1	0	2	3	2	0	0	2	3	2	0	1	2	3	1
0.22	1	0	2	3	2	0	1	3	3	1	0	1	3	2	0	0	2	2	1
0.23	3	1	0	2	3	1	0	1	3	2	0	1	2	2	1	0	2	2	1
0.24	3	2	0	1	3	2	0	0	2	2	1	0	2	2	1	0	1	2	1
0.25	2	3	1	0	1	3	1	0	1	2	1	0	1	2	1	0	1	2	1
0.26	0	2	3	1	0	2	2	0	0	2	2	0	1	2	1	0	1	2	1
0.27	0	0	2	2	0	1	2	1	0	1	2	0	0	2	2	0	1	2	1
0.28	2	0	1	2	1	0	2	2	0	1	2	1	0	1	2	0	0	2	1
0.29	2	1	0	2	2	0	1	2	1	0	2	1	0	1	2	0	0	2	1
0.30	2	2	0	1	2	1	0	2	1	0	1	2	0	1	2	1	0	1	1
0.31	0	2	1	0	2	2	0	1	2	0	1	2	0	0	2	1	0	1	1
0.32	0	1	2	0	1	2	0	0	2	1	0	2	1	0	1	1	0	1	1
0.33	1	0	2	1	0	2	1	0	1	1	0	1	1	0	1	1	0	1	1
0.34	2	0	1	2	0	1	2	0	1	1	0	1	1	0	1	1	0	1	1
0.35	2	1	0	2	1	0	2	1	0	2	0	1	1	0	1	1	0	1	1
0.36	0	2	0	1	2	0	1	1	0	1	1	0	1	0	0	1	0	1	1
0.37	0	1	1	0	2	0	0	1	0	1	1	0	1	1	0	1	0	1	1
0.38	1	0	2	0	1	1	0	1	0	0	1	0	1	1	0	1	0	1	1
0.39	2	0	1	1	0	2	0	1	1	0	1	0	1	1	0	1	0	0	1
0.40	2	1	1	1	0	1	1	0	1	0	1	0	0	1	0	1	0	0	1
0.41	1	1	0	1	0	1	1	0	1	0	1	1	0	1	0	1	1	0	1
0.42	0	2	0	1	1	0	1	0	1	0	1	1	0	1	0	1	1	0	1
0.43	0	1	1	0	1	0	1	0	1	1	0	1	0	1	0	1	1	0	1
0.44	1	0	1	0	1	0	1	1	0	1	0	1	0	1	0	1	1	0	1
0.45	2	0	1	1	1	1	0	1	0	1	0	1	0	1	1	0	1	0	1
0.46	1	1	0	1	0	1	0	1	0	1	0	1	0	1	1	0	1	0	1
0.47	0	1	0	1	0	1	0	1	0	1	1	1	0	1	0	1	0	1	1
0.48	0	1	0	1	0	1	1	1	1	0	1	0	1	0	1	0	1	0	1
0.49	1	0	1	0	1	0	1	0	1	0	1	0	1	0	1	0	1	0	1
0.50	2	0	1	0	1	0	1	0	1	0	1	0	1	0	1	0	1	0	1

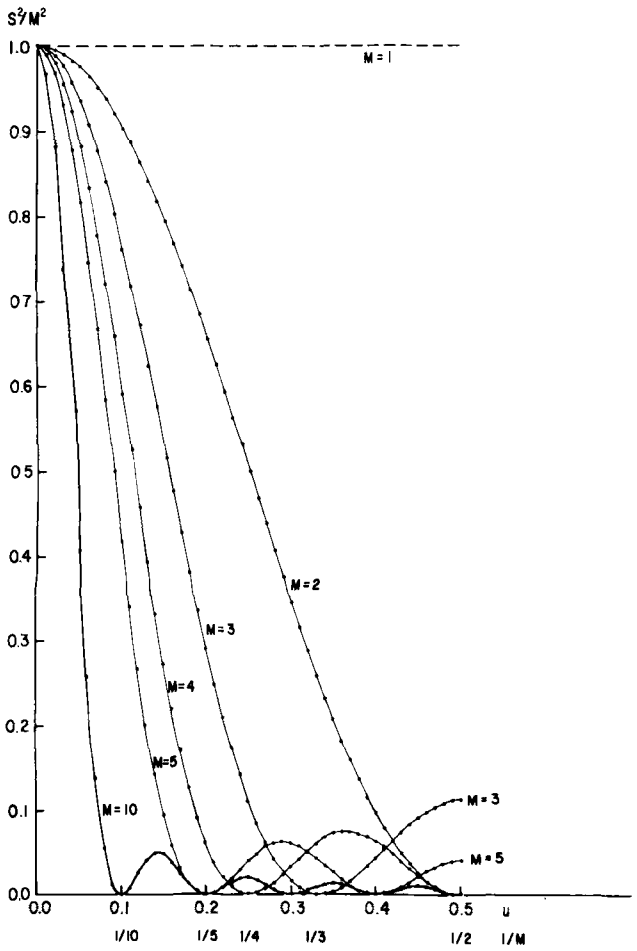

Fig. 4.1. Normalized interference function (S^2/M^2) for the M values 1, 2, 3, 4, 5, and 10.

quotient u is a fractional number. A strong reflection may have effects farther away on the reciprocal lattice row.

For a crystal of uniform thickness the "interference function" affects all the reciprocal lattice points to the same extent as defined by M, the number of unit-cells in a given crystal. If the crystal is not uniform, e.g. wedge-shaped, the interference function will affect each reciprocal lattice point corresponding to M values in each direction.

Properties of the interference function for bent lattices

In transmission electron microscopy and diffraction, the samples are in the form of very thin films. They may be easily bent by the mechanical

instability of the supporting substrates. The bending of some solids may well be an inherent structural property. A special case of bending (cylindrical one) was the subject of the investigations by Blackman (1951), Whittaker (1955 and the references given there), Waser (1955), and Kunze (1956). A more general approach to bending effects was proposed by Cowley (1961), and by Mitra and Battacherjee (1975). Unlike the simple method described in the following, the formulations in these previous studies are either mathematically complex or do not lend themselves readily to a systematic evaluation of bending effects on diffraction intensities. Evaluation of bending effects on the image contrast and on the diffraction pattern can be done in terms of the interference function. For this purpose the above interference function for undeformed lattices will be reformulated for bent lattices. When a crystal lattice is bent, in general, the lattice points will be randomly displaced. This will then give rise to a randomness between the phases of their scattering, and in this sense the scattering from such a collection of unit cells becomes non-coherent. For sake of simplicity, an orthogonal crystal with one atom per unit cell will be considered. For an undeformed and orthogonal lattice the interference function (S) of eq. 1 can be rewritten as:

$$S = \sum_{m=0}^{M-1} \sum_{n=0}^{N-1} \sum_{p=0}^{P-1} \exp[2\pi i \boldsymbol{s} \cdot \boldsymbol{R}_{mnp}] \tag{4a}$$

$$\boldsymbol{R}_{mnp} = m\boldsymbol{a} + n\boldsymbol{b} = p\boldsymbol{c} \tag{4b}$$

where the position vector $\boldsymbol{R}_{mnp}$ defines the location of each lattice point with respect to a common origin. After bending, however, the position vector needs to be redefined for each unit cell. We will first consider two special cases of bending: spherical and cylindrical. Any other mode of bending may well be expressed by combining these special cases. The position vectors will be first defined for each mode of bending and the interference function will then be expressed in terms of these new position vectors.

Spherically bent lattice

In Fig. 4.2A a spherically bent lattice plane is shown. The plane was coincident to the XY-plane before the deformation. Each lattice point after the bending can be defined by the spherical coordinates r, Φ, and θ. From these, r is the radius of the sphere and also the radius of the curvature for the bending. For a three-dimensional case, one can consider several such concentric spheres with radii $r_p = r + p \cdot c$, where p is the number of unit cells in the Z-direction and c is the cell parameter in that direction. The spherical coordinates can be transformed to the original XYZ cartesian coordinates via

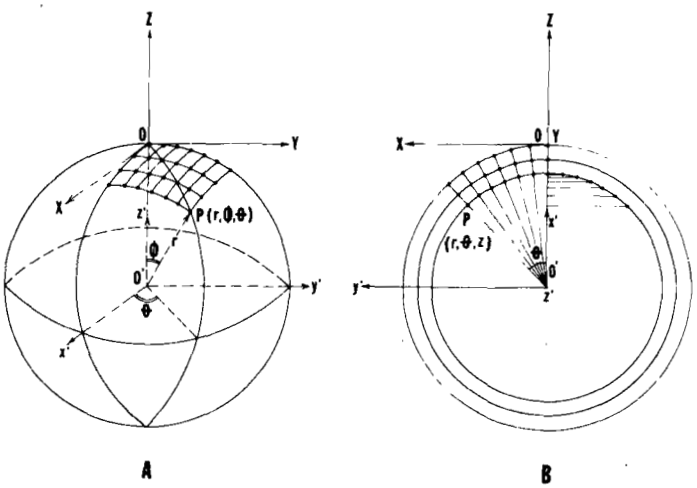

Fig. 4.2. Bending models with their curvilinear and rectangular coordinate systems. A. Spherically bent lattice where r, ϕ, and θ are the spherical coordinates of the lattice point P. B. Cylindrically bent lattice where r, θ, and z' are the cylindrical coordinates of the lattice point P.

the other cartesian coordinate system $x'y'z'$ (Fig. 4.2A):

$$X = x' = r_p \sin\phi \cos\theta$$

$$Y = y' = r_p \sin\phi \sin\theta$$

$$Z = z' - r_p = r_p(\cos\phi - 1.0)$$

The angles ϕ and θ may be computed in radians as:

$$\phi = (m^2a^2 + n^2b^2)^{1/2}/r_p \tag{5}$$

$$\theta = \tan^{-1}(nb/ma) \tag{6}$$

The position vector of any lattice point may now be given by:

$$\boldsymbol{R} = \boldsymbol{j}_x X + \boldsymbol{j}_y Y + \boldsymbol{j}_z Z$$

where $\boldsymbol{j}_x$, $\boldsymbol{j}_y$, and $\boldsymbol{j}_z$ are unit vectors along the X, Y, and Z directions. The interference function can be rewritten:

$$S = \sum_{m=0}^{M-1} \sum_{n=0}^{N-1} \sum_{p=0}^{P-1} \exp\{2\pi i\boldsymbol{s} \cdot [\boldsymbol{j}_x r_p \sin\phi \cos\theta + \boldsymbol{j}_y r_p \sin\phi \sin\theta$$

$$+ \boldsymbol{j}_z r_p(\cos\phi - 1.0)]\}$$

remembering $s = h'a^* + k'b^* + l'c^*$, where h', k', and l' are not only integers but continuous variables:

$$S = \sum_{m=0}^{M-1} \sum_{n=0}^{N-1} \sum_{p=0}^{P-1} \exp\left\{2\pi i r_p \left[\frac{h'}{a} \sin\phi \cos\theta + \frac{k'}{b} \sin\phi \sin\theta + \frac{l'}{c}(\cos\phi - 1)\right]\right\} \quad (7)$$

The Φ and θ angles actually possess subscripts of (m, n, p) as defined by eqs. 5 and 6. These subscripts have been dropped for simplicity of expression.

Cylindrically bent lattice

The model for cylindrically bent crystal is given in Fig. 4.2B. The stack of lattice planes parallel to XY becomes, after deformation, cylindrical surfaces with a radius r_p around a common cylinder axis. The radius of any one of the cylinders is given by $r_P = r + p \cdot c$, where p is the number of lattice planes and c is the spacing between them. The lattice points may now be first defined by cylindrical coordinates r, θ, z' (Fig. 4.2B). The XYZ cartesian coordinates may be obtained from these cylindrical coordinates via the other orthogonal coordinate system $x'y'z'$ shown in the same figure:

$$X = y' = r_p \sin\theta$$

$$Y = z' = nb$$

$$Z = x' - r_p = r_p(\cos\theta - 1.0)$$

As in the case for spherical bending, the interference function may be written for a cylindrical lattice:

$$S = \sum_{m=0}^{M-1} \sum_{n=0}^{N-1} \sum_{p=0}^{P-1} \exp\left\{2\pi i \left[r_p \frac{h'}{a} \sin\theta + r_p \frac{l'}{c}(\cos\theta - 1.0) + k'n\right]\right\}$$

or:

$$S = \sum_{m=0}^{M-1} \sum_{p=0}^{P-1} \exp\left\{2\pi i \left[r_p \frac{h'}{a} \sin\theta + r_p \frac{l'}{c}(\cos\theta - 1.0)\right]\right\} \cdot \sum_{n=0}^{N-1} \exp(2\pi i k'n) \quad (8)$$

where $\theta = ma/r_p$ (in radians) and all the other symbols have the same meaning as in the spherical case.

We can conclude from the above derivations that the interference function for a bent lattice is specifically defined by the lattice parameters of the

crystal, and it must be calculated separately for each bent crystal. This is in contrast to the interference function for undeformed lattices. The new interference function for a bent lattice does not refer to the reciprocal space with the curvelinear coordinates, but with its natural coordinates h', k', and l'.

Diffraction effects of bending on the single crystal reflections

The interference functions, as reformulated, have been computed for several sets of parameters. An orthogonal lattice with parameters $a = 5.2$ Å, $b = 9.0$ Å, and $c = 10.0$ Å (similar to those of a mica) but with a single atom per unit cell * has been considered. We chose hypothetical crystals in the form of a square in the X—Y plane, with an edge (A) of 135 Å, 270 Å, 540 Å, and 1080 Å in order to demonstrate the typical bending effects. Larger linear dimensions require hours of computing time. These small crystallite sizes may be helpful for considering deformation of clay crystallites and mosaic blocks in real crystals. In large crystals the bending may well be accommodated by a smaller deformation of mosaic blocks rather than a uniform deformation of the whole crystal.

In the Z direction the thickness of the crystal has been varied between 10 Å (a single lattice plane) to 100 Å (ten lattice planes). Several radii of curvature ($r = 4000$, 2000, 1000, 500, and 250 Å) have been considered in order to cover a wide range of bending angles. The bending angle is defined as $\alpha = A/r$ (in radians). The interference function has been computed for each combination of A and r and it has been normalized so that its maximum value is 1.0 corresponding to that of an undeformed lattice. For bending angles of 0.04 radians or larger, it was found that the number of lattice planes in the Z direction does not cause any appreciable differences in the values of the interference function. In fact, for a bending angle of 0.135 radians for $A = 135$ Å and $r = 1000$ Å, the value of the normalized interference function for ten lattice planes is about 1% different from that of the function for a single lattice plane. The graphs of the interference function given here are for a two-dimensional lattice plane.

It is important to note the deviations of the normalized interference function from the normalized interference function of an undeformed lattice. This deviation describes the diffraction effects of bending in a rather simple and graphical manner. The interference function for an undeformed two-dimensional lattice (i.e. with a single unit-cell thickness) is always unity along the c^* direction of hk reciprocal lattice rows, as shown with dashed

* If the cell contains more than one atom, then the bending will also cause displacements of the atoms within the unit cell. The above formulation will remain valid provided the new positions of the displaced atoms within the unit cell are used for the structure factor calculations. Thus, the bending of the unit cell can be accounted for in the structure factor without any modification in the above interference functions.

lines in Figs. 4.3—4.6. Deviation of the interference function from this horizontal line, gives directly the effects of bending on the intensity and the profile of the reflections. For a three-dimensional lattice with multiple lattice planes in the Z-direction, the interference function for unbent crystal will be symmetrical peak centered around the dotted lines at the integer values of l' in Figs. 4.3—4.6. These dotted lines represent the normalized interference function for an infinitely thick crystal. As mentioned above there is very little difference in the values of the normalized interference functions for bent two- and three-dimensional lattices. The curves for bent two-dimensional lattices may also be used to a very close approximation for bent three-dimensional lattices. The deviations of these curves from the symmetrical profiles centered at the reciprocal lattice nodes give the diffraction effects of bending in the case of bent three-dimensional lattices. Following this simple approach, the interference function has been plotted for different orders and classes of reflections under various conditions of bending. It has been found that the bending models considered do not modify diffraction profiles and intensities along the $[hk0]^*$ directions but along the c^* direction. The properties of interference function are described in the c^* direction for hk and $00l$ reflections in the following paragraphs.

hk reflections from spherically bent crystal

All the hk reflections are similarly affected by the spherical bending of the crystal. As an example, these effects are described for three orders of $0k$ reflections; these are 02, 04, and 06 reflections with increasing Bragg angles. The bending effects can be typically studied for a radius of curvature of 1000 Å in crystallites with linear dimensions A = 135, 270, 540, and 1080 Å. The profiles of the interference functions for these examples are given in Fig. 4.3. For a crystallite with a linear dimension A = 135 Å and with a radius of curvature of 1000 Å (α = 0.135 rad.), the interference function has values very close to unity at the positions l' = 0.0 along the hk rows. The interference function shows, however, appreciable deviations from the dashed lines at other l' positions for all three reflections 02, 04, and 06. There is an asymmetrical broadening of the profile for these reflections. For a crystallite with A = 270 Å, the interference function shows a significant reduction from the value of 1.0. This reduction is about 12% for the 02 reflection, 37% for the 04 reflection, and 65% for the 06 reflection. The profile of the interference function becomes broad and asymmetrical for all these reflections in increasing amount with the order of diffraction. Furthermore, the peak positions shift from their normal positions for the higher order reflections. In fact, the maximum for the 04 reflection shifts from l' = 0 to l' = 0.1 and similarly the peak for the 06 reflection appears at l' = 0.3. For a crystallite with a linear dimension of 540 Å, the 02 reflection has lost 80% of its normal intensity. In addition, the profile of the inter-

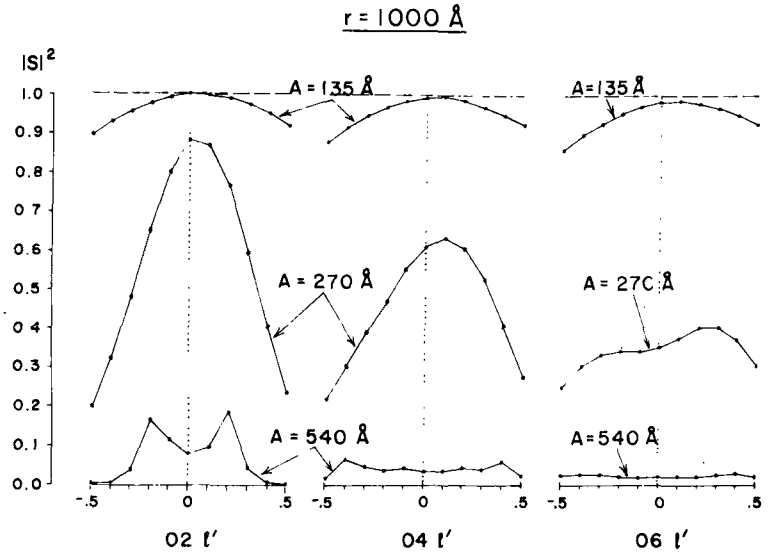

Fig. 4.3. Profiles of the interference function for a spherically bent crystallite with various linear dimensions (A) and for radius of curvature of 1000 Å. Dashed lines give the interference function for an unbent two-dimensional crystal, whereas the dotted line represents the interference function for a three-dimensional crystal with infinite thickness.

ference function displays now two maxima at $l' = -0.2$ and $l = 0.2$. The interference function shows about 96% and 97% reductions in intensity for the reflections 04 and 06 correspondingly. Therefore, these reflections will practically disappear. For a crystallite with a linear dimension of 1080 Å, the function has a value close to zero, even for the 02 reflection; for this reason, it has not been plotted. There will be virtually no more coherent scattering from this crystallite.

hk reflections from cylindrically bent crystal

As seen from eq. 8 and also from the geometry of the cylindrical bending, all *hk* reflections are not affected in the same manner by the deformation. Specifically, the reflections from the set of planes perpendicular to the cylinder axis behave differently from the others. In our model, where the cylinder axis is parallel to the *b*-axis of the crystal, 0*k* reflections form such special reflections. Therefore, the profile of the interference function will be discussed separately for 0*k* and *hk* reflections. The effects of the bending are typically displayed in Fig. 4.4 for the crystallites with linear dimensions of 135 Å, 270 Å, and 540 Å, and with a radius of curvature of 1000 Å.

The profile of the interference function for 02, 04, and 06 reflections are exactly the same. The profile is symmetrical and changes in width only with

the linear dimension of the crystallite (Fig. 4.4). The peak position of the interference function appears exactly at $l' = 0$ or an integer as expected also from an undeformed lattice. The only difference between the diffraction profiles of a bent and unbent crystal is the following: for an unbent two-dimensional lattice the interference function has always the value of unity in the c^* direction of the hk rod. The interference function for a two-dimensional bent lattice, however, behaves as though there are several unit cells in the c^* direction. This is due to the fact that bending of a two-dimensional lattice generates a sequence of several layers.

Other hk reflections behave similar to the 11, 22, and 33 reflections which the interference function is plotted in Fig. 4.4. For a crystallite with a linear dimension of 135 Å, all three orders show very small reductions in their intensities. A crystallite size of 270 Å, on the other hand, displays the effects of bending rather clearly. The values of the interference function drop to 0.97 for the 11 reflection, 0.88 for the 22 reflection and 0.76 for the 33 reflection. The profiles for all these reflections are asymmetrically broadened and peak positions are displaced to $l' = 0.1$ for the 22 and 33 reflections. For a crystalline size of 540 Å, the effects of bending on the above reflections are rather drastic. The profile of the 11 reflection displays two maxima at $l' = 0.2$ and $l' = -0.2$ with an average loss of 55% from its normal intensity. The 22 reflection displays three maxima at $l' = -0.3$, $l' = 0.0$, and $l' = 0.3$ with a loss of intensity of about 60%. The profile of the 33 reflection becomes rather broad and irregular, with about 90% loss of intensity.

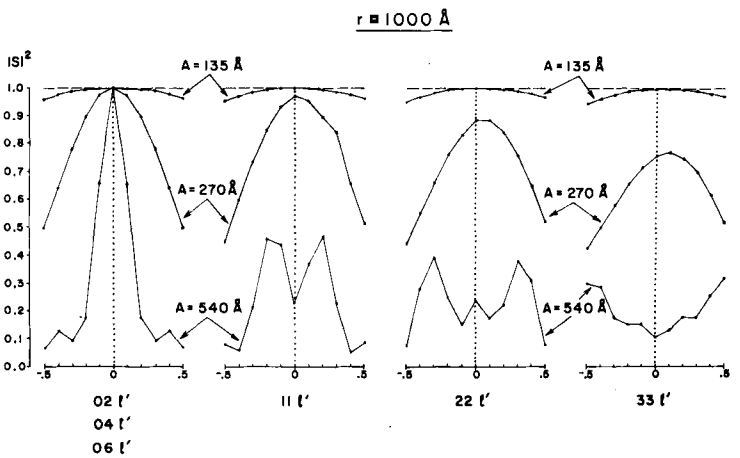

Fig. 4.4. Profiles of the interference function for cylindrically bent crystallite with various linear dimensions (A) and for a radius of curvature of 1000 Å. The dashed line gives the interference function for an unbent two-dimensional crystal, whereas the dotted lines represent the same function for a three-dimensional crystal with infinite thickness.

Effects of bending on 00l reflections

This special class of 00*l* reflections undergoes much larger intensity losses and distortions in their profiles for the bending models considered above. The continuous profile of the interference function in the range of $l' = 0.5$ to 4.0 has been plotted in Fig. 4.5 for a spherically bent crystal. Cylindrical bending also gives a similar profile for the interference function in the same range. Various radii of curvature (250, 500, 1000, 2000, and 4000 Å) have been considered for a crystallite size of 135 Å. The profile shows a continuous decrease in the value of the interference function with the increasing l' index of the reflection. This reduction is increasing drastically with decreasing radius of curvature, i.e. with increasing amount of bending. Thus, the behavior of the interference function predicts anomalous intensity ratios for the different orders of 00*l* reflections and higher background intensity for the bent crystallites. This suggests some caution in interpreting the inten-

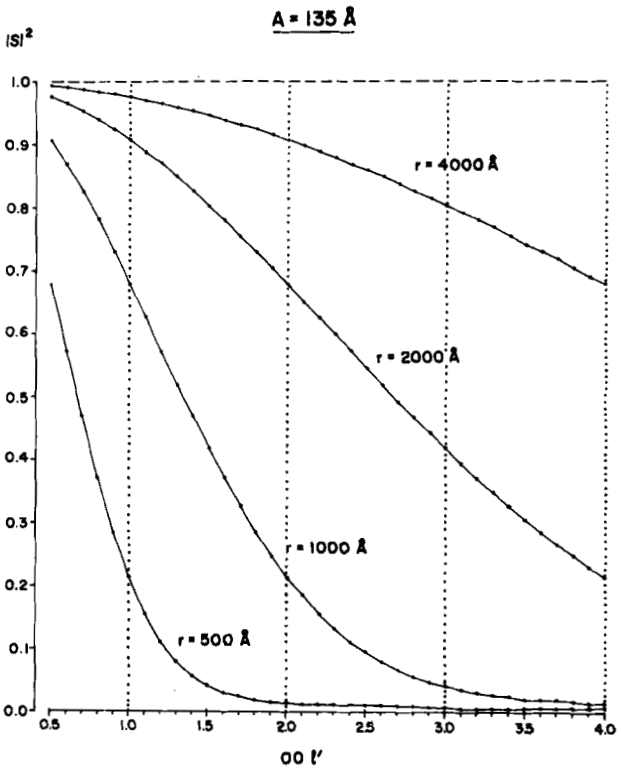

Fig. 4.5. The interference function for the 00*l* reflections from a spherically bent crystallite with a linear dimension of 135 Å and with different radii of curvature. The dashed and dotted lines represent the same quantities as in the Fig. 4.4.

sities of basal reflections especially for clay minerals whose diffraction data are often limited to this special class of reflections. Why these reflections undergo so much distortion and loss of intensity can be easily inferred from Fig. 4.2B. As seen on the upper right quadrant of the circle in this figure, bending of this model generates a series of lattice planes parallel to $00l$ but with an irregular spacing and hence random phasal relationships between them.

The parameters of bending

A few comments should be made on the question of how bending can be defined. The apparent parameters of the bending are the linear dimension (A) of the crystallite and the radius of curvature (r). The ratio (α) of these two parameters is defined as the bending angle (i.e. $\alpha = A/r$). The question arises as to whether this ratio can be used for evaluating the diffraction

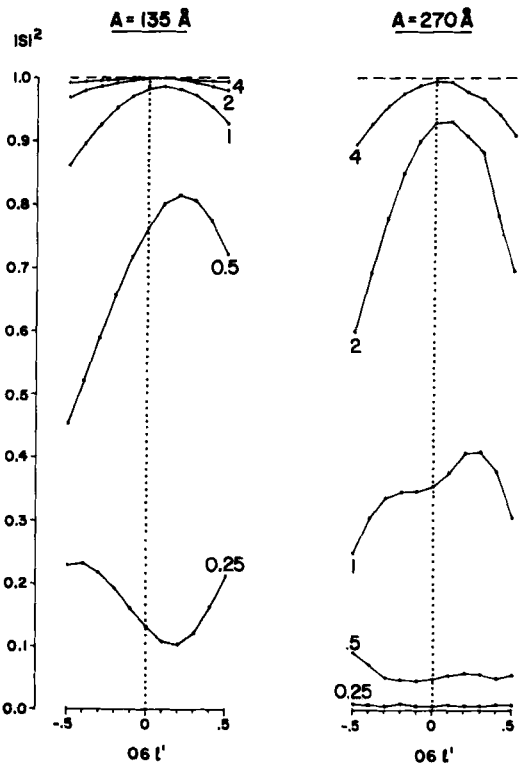

Fig. 4.6. The variations in interference function for the 06 reflection for different sets of A/r values. Numbers next to the curves give the radii of curvature in thousands of Ångstroms. The dashed and dotted lines represent the same quantities as in the Fig. 4.4.

effects of bending, instead of using two parameters A and r. If such a relationship can be derived, this obviously will reduce the computations to a marked degree. In order to explore this possibility, the interference function has been evaluated for several sets of A/r values. The results for crystallite sizes of 135 Å and 270 Å for the spherical bending are plotted in Fig. 4.6. By doubling the edge of a two-dimensional square crystallite, the number of lattice points will be increased four times. Therefore it is expected that the interference functions would show some similarity for the sets 135/1000 and 270/4000; 135/500 and 270/2000; and 135/250 and 270/1000. In fact, Fig. 4.6 shows that the interference function has similar, but not identical, profiles for the cases 135/1000 and 270/4000; and for 135/500 and 270/2000. The maximum values of the interference function are distinctly different for the above sets. This similarity, however, breaks down when the bending angle is increased. In fact, the pair 135/250 and 270/1000 show completely different profiles for the interference function. Thus the bending must be defined by the two parameters A and r, and not simply by their ratio, i.e. with the bending angle (α). This also the case for cylindrical bending.

4.2. SELECTED AREA ELECTRON DIFFRACTION ON MUSCOVITE

In an electron microscope the first image of an object is formed at the image plane of the objective lens simultaneously with its diffraction pattern being formed at the back focal plane of the same lens. In modern electron microscopes an aperture (area selecting) can be inserted in the image plane of the objective lens. This will restrict scattered electrons to the area selected by the aperture to reach the subsequent lenses (intermediate and projector). An electron microscope equipped with an area selecting aperture allows one to obtain diffraction patterns from areas as small as 0.2 μm in diameter. By changing the strength of the intermediate lens, one can observe the image or the diffraction pattern. Thus the transmission electron image of the same area can be superimposed on the diffraction pattern. Selected area diffraction (SAD) combined with transmission electron microscopy probably form the most powerful method for providing information about the structure and morphology of minute crystallites such as clay minerals. It seems rather important to evaluate the major factors affecting the SAD patterns. The general theory of electron diffraction in kinematical terms is well developed as given in the several standard textbooks by Pinsker (1953), Vainshtein (1964), Cowley (1967), Murr (1970), Rymer (1970), Beeston et al. (1973), among others. Geometrical theory of electron diffraction has been thoroughly treated by Gard (1971) with particular emphasis on layer silicates. In the following, the factors specifically affecting the intensities of selected area electron diffraction patterns of micas will be discussed as recently described by Güven (1974). These factors are related to: (1) lattice properties of

micas; (2) properties of the Ewald sphere for electron diffraction; (3) finite crystal thickness; (4) orientation of the crystal with respect to the incident electron beam (tilt and bending); and (5) objective lens properties. These factors will be described in terms of the kinematical theory of electron diffraction which assumes single (instead of multiple) scattering of electrons from a thin crystalline film.

Lattice properties of micas

The reciprocal lattice plane (a^*c^*) of a hypothetical mica single layer is shown in Fig. 4.7A, where the c^*-direction is taken parallel to the electron beam. The magnitude of a reciprocal lattice vector H_{hkl} and that of its projection on a reference plane passing through the origin and parallel to the

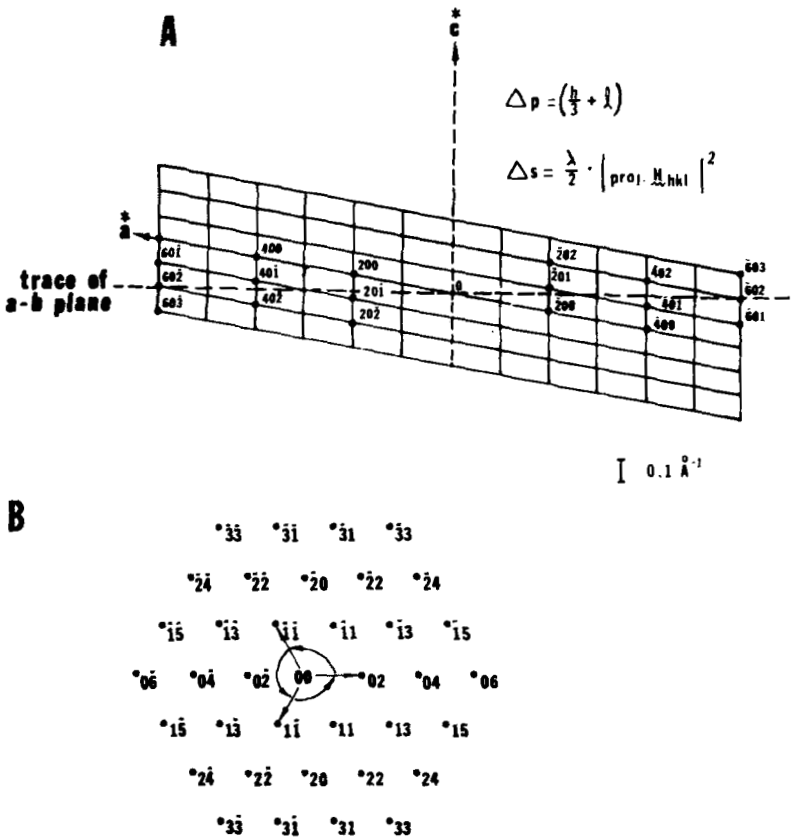

Fig. 4.7. Two projections of the reciprocal lattice of a mica single layer. A. The a^* c^* reciprocal lattice plane and reciprocal lattice points close to the Ewald sphere, which almost coincides with the a—b (reference) plane. B. The projection of the hk lattice rows onto the a—b (reference) plane of mica layer.

a—b plane can be calculated from the following relationships for a monoclinic crystal:

$$|H_{hkl}|^2 = h^2a^{*2} + k^2b^{*2} + l^2c^{*2} + 2lhc^*a^* \cos\beta^*$$

$$|\text{proj. } H_{hkl}|^2 = h^2a^{*2} \sin^2\beta^* + k^{*2}b^{*2}$$

The distance $(\Delta p)_{hk}$ of a reciprocal lattice point above the reference plane is given by the relationship:

$$(\Delta p_{hkl})^2 = |H_{hkl}|^2 - |\text{proj. } H_{hkl}|^2$$

$$= (ha^* \cos\beta^* + lc^*)^2$$

replacing $\cos\beta^* = c^*/3a^*$ and expressing Δp_{hkl} in terms of c^*:

$$\Delta p_{hkl} = \left(\frac{h}{3} + l\right)$$

This relationship tells us that all the reciprocal lattice points lying exactly on the reference plane have h and l indices with $[(h/3) + l] = 0$. Other reciprocal lattice points have a distance defined by Δp_{hkl} from that plane.

Stacking sequences in micas. Another feature of mica lattices is related to the fact that micas and other silicates may form modifications with different stacking sequences. SAD patterns can reflect the appropriate symmetry if the "finite" thickness of the crystal has an integral multiple of the number of layers in a stacking sequence. For instance, for a $3T$ mica, a deviation from hexagonal symmetry may be expected if the number of layers is not $3n$. Similarly for the $2M_1$ muscovite, the stacking sequence creates a glide plane which will show up as a mirror plane in the SAD pattern of this mica. If there is an odd number, such as 3 or 5 layers, deviation from this mirror plane may be seen on the pattern.

A completely random stacking sequence for a mica may give a hexagonal symmetry as the (hk) reciprocal lattice rows will superimpose on each other in the manner shown in Fig. 4.7B. The calculation of the intensity variations caused by stacking disorder is rather complicated. There are rather extensive treatments of this problem in the literature by Hendricks and Teller (1942), Wilson (1948), Guinier (1963), and Warren (1969).

Properties of the Ewald sphere for electron diffraction

It is well known that the Ewald sphere approximates rather closely a plane for electron diffraction, and that this plane is often considered to coincide with

the above reference plane in the vicinity of the origin. The intensity of a reflection is a maximum at the exact Bragg condition, and it falls sharply as it deviates slightly from this position. It is significant to know how much the Ewald sphere deviates from a plane, i.e. the curvature of the Ewald sphere. The amount of this deviation (Δs) is given by the following relationship:

$$\Delta s = |\text{proj. } \boldsymbol{H}_{hkl}| \tan \theta_{hkl}$$

$$\tan \theta_{hkl} \simeq \frac{|\text{proj. } \boldsymbol{H}_{hkl}|}{2/\lambda}$$

$$\Delta s \simeq \frac{\lambda}{2} |\text{proj. } \boldsymbol{H}_{hkl}|^2 = \frac{\lambda}{2}\left[\frac{h^2}{a^2} + \frac{k^2}{b^2}\right]$$

for an accelerating voltage of 80 keV, λ is 0.0418 Å and:

$$\Delta s \simeq 0.02 \times |\text{proj. } \boldsymbol{H}_{hkl}|^2$$

As long as we limit our observations to the part of the reciprocal space with $|\boldsymbol{H}_{hkl}| \leqslant 1.0$ Å^{-1}, the maximum deviation of the sphere from the reference plane will be about 0.02 Å^{-1}. For the {11} and {02} type reflections of a mica, this deviation will be about 0.001 Å^{-1}. It is more practical to give the deviation Δs in fractions of reciprocal lattice parameters in this direction: $\Delta s' = \Delta s/c^*$. Now we can give the formula for the exact distance of a reciprocal lattice point to the sphere of reflection as $\zeta_{hkl} = \Delta p - \Delta s'$. Note that the ζ_{hkl} is given in fractions of reciprocal cell parameters. This distance is also referred to as the "excitation error".

In the above discussion, the spread of electron energies due to fluctuations in the acceleration voltage has been considered to be negligible, as is the case for the modern electron microscope. It may, however, be worthwhile to mention the effect of the beam divergence on the Ewald sphere: the incident beam on the specimen consists of a narrow cone defined by the radius of the condenser aperture and the focal length of the condenser lens. In modern instruments, the minimum angle of this convergence varies between $1—2 \cdot 10^{-3}$ radians.

Finite thickness of crystal

In selected area electron diffraction of the layer silicates the lateral (x, y) dimensions of the crystal (i.e. in the directions perpendicular to the incident beam) can be considered "infinite", whereas the third dimension of the crystal (i.e. in the direction along the incident beam) is a "finite" quantity. Intensity calculations from a crystal with "finite" dimension (t) require the

exact evaluation of the interference function (S). For an incident electron beam with an intensity J_0 per unit area, the kinematically diffracted beam intensity (I) at a distance r from the specimen is given by the following equation (Vainshtein, 1964, with some modifications of symbols):

$$I = (J_0/r^2) \cdot |F_{hkl}|^2 \cdot |S|^2$$

where F_{hkl} is the structure amplitude and S is the interference function. The intensity, integrated over the x and y directions of the screen can be expressed as:

$$I_{hkl'} = J_0 \cdot (A_1 \cdot A_2) \cdot \lambda^2 \cdot (|F_{hkl'}|^2/V^2) \cdot (\sin^2 \pi A_3 u_3)/(\pi u_3)^2 \qquad (10)$$

where h, k are regular integer indices but l' is a real number so that one can follow the intensity variations in the c^* direction continuously. By definition the product $J_0 \cdot (A_1 \cdot A_2)$ is the incident beam intensity (I_0) received by the area ($A_1 \cdot A_2$) of the crystal whose linear dimensions are represented by A_1, A_2, and A_3. The symbol V is the unit-cell volume and u_3 gives the distance from a reciprocal lattice point hk in the c^* direction. At the exact Laue condition, $u_3 = 0$ and l' becomes an integer l. The last trigonometric term is then equal to t^2 with t being the thickness of the crystal:

$$I_{hkl}/I_0 = \lambda^2 \cdot |F_{hkl}|^2 \cdot t^2/V^2$$

The critical thickness of the crystal is defined by the relationship $I_{hkl}/I_0 = 1$. Thus the critical thickness (t_c), above which the scattering becomes dynamic, can be calculated from the following relationship:

$$t_c = V/(\lambda \cdot |F_{hkl}|)$$

The critical thickness of muscovite has been found to be 363 Å for the strongest reflection $F_{33\bar{1}} = 61.5$ at the accelerating voltage 80 kV. Crystals with thicknesses far below the critical thickness should be considered in order to carry out the intensity calculations in terms of the kinematical theory.

The last term in eq. 10 is an approximation to represent the variations of the interference function along the c^* direction of the crystal. This term can be given in the exact form as $\sin^2 \pi Pu/\sin^2 \pi u$ by expressing u in fractions of c^*, and P as the number of unit cells in this direction:

$$I_{hkl'} = |F_{hkl'}|^2 \cdot (\sin^2 \pi Pu)/P^2 \sin^2 \pi u \qquad (11)$$

The factor P^2 in the denominator normalized the interference function in order to compare directly the intensities of the crystals with different thicknesses.

For the above intensity equations one assumes an ideally imperfect crystal in which the mosaic blocks have misorientations in the order of a maximum few minutes of arc. If, however, the angular spread in mosaic orientations becomes large, e.g., in the order of few degrees, the intensity must be corrected for this "secondary extinction" texture. In this case Vainshtein (1964) modifies the relative intensities for electron diffraction with a factor of d_{hkl}:

$$I_{hkl} = |F_{hkl}|^2 \cdot d_{hkl} \tag{12}$$

This implies, of course, a drastic intensity reduction with increasing order of diffraction. It is, however, to be considered only for large angular misorientations of mosaic blocks.

Orientation of the crystal: tilt and bending

The elongation of reciprocal lattice points due to shape-transform gives rise to the so-called relaxation of the Laue condition of diffraction. There may be a range of orientation of the crystal for which observable intensity may be present. The half angle ($\frac{1}{2}\Delta\alpha$) of the tilt of the crystal is defined by the thickness (t) and the magnitude of the reciprocal lattice vector $|H|$ by a simple relationship:

$$\tfrac{1}{2}\Delta\alpha \simeq \frac{1/t}{|H|} = \frac{d}{t}$$

For a mica of 100 Å thickness and for the 11, 02 type reflections with d = 4.50 Å, $\frac{1}{2}\Delta\alpha \simeq 0.045$ radians, i.e. 2.5°. This means a 11 or 02 type reflection will be observed over a range of tilt of ±2.5°. The range of tilt, similarly calculated, is found to be 1.3° for the 04 type reflections and 0.65° for the 06 type reflections.

Bending of the mica flakes is rather common, and its diffraction effects have been discussed in the previous section. Bending may also be observed directly by the presence of extinction contours in the electron transmission images.

Objective lens properties

The following properties of the objective lens directly affect the selected area electron diffraction patterns: depth of field, focal length variations, and spherical aberrations.

Depth of the field (D_{f_i}) of the objective lens is defined by the expression: $D_{f_i} = 2r/\alpha_0$, where r is the radius of the disc of confusion (i.e. the resolution limit), and α_0 is the objective aperture angle. For instance, for r = 10 Å and

$\alpha_0 = 10^{-3}$ radian, depth of field is about 2 μm for a transmission electron image. In the diffraction mode, the objective aperture is removed, and the depth of the field is expected to reduce more than one order in magnitude. As a result of that, the focusing conditions become more critical for the diffraction pattern than for the transmission image. The focusing conditions established on the image may be off-focus for the diffraction pattern.

Variations in focal length of the objective lens can appreciably modify the SAD pattern. These effects can readily be demonstrated by deliberately changing the objective lens current. The intensities of the spots and hence the symmetry of the SAD patterns may undergo unexpected changes due to focusing conditions.

Spherical aberrations of the objective lens give rise to certain errors between the area selected for diffraction and the actual area contributing to the diffraction. The latter does not correspond exactly to the area defined by the field limiting aperture in the image plane of the objective lens due (a) to the spherical aberrations, and (b) to incorrect focusing conditions. These errors have been discussed by Agar (1960) and by Riecke (1961). According to them, the displacement (y_s) of the image, with respect to the actual specimen, is in the direction of the diffraction vector, and is given by:

$$y_s = C_s \cdot \theta^3$$

where C_s is the spherical aberration coefficient of the objective lens and is equal to 2—3 mm, and θ is the Bragg angle of reflection in radians. For the reflections 40, 26, and at an operating voltage of 80 kV ($\lambda = 0.0418$ Å), α is approximately 0.016 radians, ($\sin\theta/\lambda = 0.39$), and the y_s displacement due to spherical aberration is 130 Å. With high-order reflections this error becomes much larger as it is proportional to the third power of the diffraction angle. We will therefore, analyze the SAD patterns of mica-type layer silicates up to $\sin\theta/\lambda = 0.40$. Furthermore, the errors in focusing conditions cause a displacement (y_f) between the image and the object planes, and this displacement is expressed simply as:

$$y_f = D \cdot \theta$$

where D is the error in focusing, and it is positive for over-focusing and negative for underfocusing. The total displacement (y) is then the sum or difference of the same displacements depending on the focusing conditions:

$$y = C_s\theta^3 \pm D\theta$$

In general, one may expect rather erroneous diffraction effects if the area selected is less than 0.5 μm in diameter. One has to pay attention to the proper dispersion of the particles on the microscope grid.

Comparison between experimental and theoretical intensity variations of SAD patterns of $2M_1$ muscovite

In the previous sections the factors which may affect intensities in the SAD patterns of micas have been described. Now the intensities for the *hk* spots of a $2M_1$ muscovite flake about 100 Å thick ($M = 5$) will be calculated and compared to the observed ones. Because of the very small c^* parameter of the crystal, we may consider for each *hk* spot the three reciprocal lattice points close to the Ewald sphere (Fig. 4.7A). We may call this part of the *hk* row the "excitation region" for the (*hk*) reflection on SAD patterns. These three reflections have been listed in Table 4.2 with their excitation errors (ζ) and intensities (I_{hkl}). The reciprocal lattice points are plotted in Fig. 4.8 with respect to a reference axis $\zeta = 0$, which indicates exactly where the Ewald sphere intersects each (*hk*) row. The l' integer or fractional index of each *hk* row at the intersection has been also listed in the same table. Continuous intensity variations along each (*hk*) row has been plotted in the excitation region from $\zeta = -1.0$ to $\zeta = 1.0$. For this purpose, structure factors have been calculated using l' indices, where l' varies with increments $\Delta l = 0.1$. Similarly, the interference function has been evaluated for each point defined by the l' values along an *hk* row. The intensities have been calculated using the eq. 11. The results are plotted in Fig. 4.8. For symmetrical rows, e.g. 11 and $\bar{1}1$ rows for $2M_1$ muscovite, the intensity distribution has been computed for one of the rows, and the other is derived from it by the symmetry. Atomic and cell parameters reported by Güven (1971) have been used for the structure factor calculations. Atomic scattering factors for electrons (f_e) have been plotted for the major atoms in layer silicates in Fig. 4.9. These values were taken from Ibers and Vainshtein (1968), and they are corrected for the relativistic effects $m/m_0 = (1 - v^2/c^2)^{-1/2} = 1.1566$ at the accelerating voltage 80 kV. These scattering factors are for the free atoms, and they may have very large errors in the angular range below $\sin\theta/\lambda \leqslant 0.1$ Å^{-1}, but they are reliable above 0.3 Å^{-1} to about 10% (Hirsch et al., 1965). The $\sin\theta/\lambda$ values of the major diffraction spots are also shown in the same figure. In ordinary SAD patterns of micas the recorded region of most practical value is below $\sin\theta/\lambda = 0.4$ Å^{-1}. The differences in scattering powers of Si and Al are rather small. Different structural models related to the Al, Si distributions are not expected to show noticeable changes in calculated intensities on the basis of the scattering power. Fig. 4.10A gives a SAD pattern of a properly focused 100 Å (five unit-cell) thick muscovite. The observed intensities of the spots within the range of $\sin\theta/\lambda < 0.40$ have been visually estimated and are listed in Table 4.2. The expected intensities have been calculated under two assumptions:

(a) The SAD patterns represent the point intersection at $\zeta = 0$ of the Ewald sphere with each *hk*-row. The intensities at this point intersection are designated as $I_{hkl'}$ and they are given together with the l' indices in the same

TABLE 4.2

Important data for the three reciprocal lattice (r.l.) points in close approximity to Ewald sphere for the hk spots on the SAD patterns with c^* being parallel to the incident electron beam. (The excitation error, ζ, is in units of c^*; I_{hkl} and $I_{hkl'}$ are normalized to $I_{060} = 100$ and $I_{\Delta\zeta}$ is normalized to $I_{\Delta\zeta}$ for 06 = 100; $I_{hkl'}$ and $I_{\Delta\zeta}$ values are for a 5 unit-cell thickness of mica)

Indices of r.l. points	ζ	I_{hkl}	hk spot on SAD	l' index at $\zeta = 0$	$I_{hkl'}$ at $\zeta = 0$	Observed I_0	Integrated $I_{\Delta\zeta}$
021	0.98	5	02	0.0	5	10	8
020	−0.02	5					
02$\bar{1}$	−1.02	5					
111	1.31	12	11	−0.3	4	60	59
110	0.31	16					
11$\bar{1}$	−0.69	42					
$\bar{1}$11	0.65	42	$\bar{1}$1	0.3	1	60	54
$\bar{1}$10	−0.35	16					
$\bar{1}$1$\bar{1}$	−1.35	12					
201	1.61	0	20	−0.6	0	40	48
200	0.61	42					
20$\bar{1}$	−0.39	0					
131	1.27	94	13	−0.3	1	45	55
130	0.27	5					
13$\bar{1}$	−0.73	42					
$\bar{1}$31	0.61	42	$\bar{1}$3	0.4	0	40	52
$\bar{1}$30	−0.39	5					
$\bar{1}$3$\bar{1}$	−1.39	94					
041	0.92	6	04	0.1	3	5	11
040	−0.08	3					
04$\bar{1}$	−1.08	6					
220	0.59	7	22	−0.6	0	25	20
22$\bar{1}$	−0.41	14					
22$\bar{2}$	−1.41	0					
$\bar{2}$22	1.25	0	$\bar{2}$2	0.7	0	30	21
$\bar{2}$21	0.25	14					
$\bar{2}$20	−0.75	7					
240	0.53	7	24	−0.5	0	20	7
24$\bar{1}$	−0.47	1					
24$\bar{2}$	−1.47	0					
$\bar{2}$42	1.20	0	$\bar{2}$4	0.8	0	15	9
$\bar{2}$41	0.20	1					
$\bar{2}$40	−0.80	7					
310	0.86	0	31	−0.9	0	5	1
31$\bar{1}$	−0.14	0					
31$\bar{2}$	−1.14	2					

TABLE 4.2 (continued)

Indices of r.l. points	ζ	I_{hkl}	hk spot on SAD	l' index at $\zeta = 0$	$I_{hkl'}$ at $\zeta = 0$	Observed I_0	Integrated $I_{\Delta\zeta}$
$\bar{3}12$	0.86	2	$\bar{3}1$	1.1	0	5	2
$\bar{3}11$	−0.14	0					
$\bar{3}10$	−1.14	0					
151	1.20	2	15	−0.2	0	10	3
150	0.20	2					
$15\bar{1}$	−0.80	1					
$\bar{1}51$	0.53	1	$\bar{1}5$	0.5	0	10	3
$\bar{1}50$	−0.47	2					
$\bar{1}5\bar{1}$	−1.47	2					
061	0.82	5	06	0.2	0	100	100
060	−0.18	100					
$06\bar{1}$	−1.18	5					
$33\bar{2}$	−1.18	1	33	−0.8	0	100	102
$33\bar{1}$	−0.18	105					
330	0.82	1					
$\bar{3}30$	−1.18	1	$\bar{3}3$	1.2	0	100	102
$\bar{3}31$	−0.18	105					
$\bar{3}32$	0.82	1					
400	1.10	37	40	−1.1	1	50	37
$40\bar{1}$	0.10	0					
$40\bar{2}$	−0.90	32					
260	0.43	26	26	−0.4	0	35	34
$26\bar{1}$	−0.57	7					
$26\bar{2}$	−1.57	35					
$\bar{2}62$	1.10	35	$\bar{2}6$	0.9	1	35	39
$\bar{2}61$	0.10	7					
$\bar{2}60$	−0.90	26					

table. Under this assumption, there is no agreement between the observed and calculated SAD intensities.

(b) The expected intensities have been calculated by integrating over an interval from $\zeta = -1.0$ to $\zeta = 1.0$ (i.e. corresponding to an interval of 0.10 $Å^{-1}$) for each hk spot. Thus we assume that the scattered electrons originate from a "finite" vertical portion of each hk row. The integrated intensities ($I_{\Delta\zeta}$) seem to give an acceptable agreement between the observed and calculated SAD intensities. Let us examine the nature of this integration: if we consider the intensity of the 11 spot, the observed intensity is much stronger than the intensity at the intersection point corresponding to

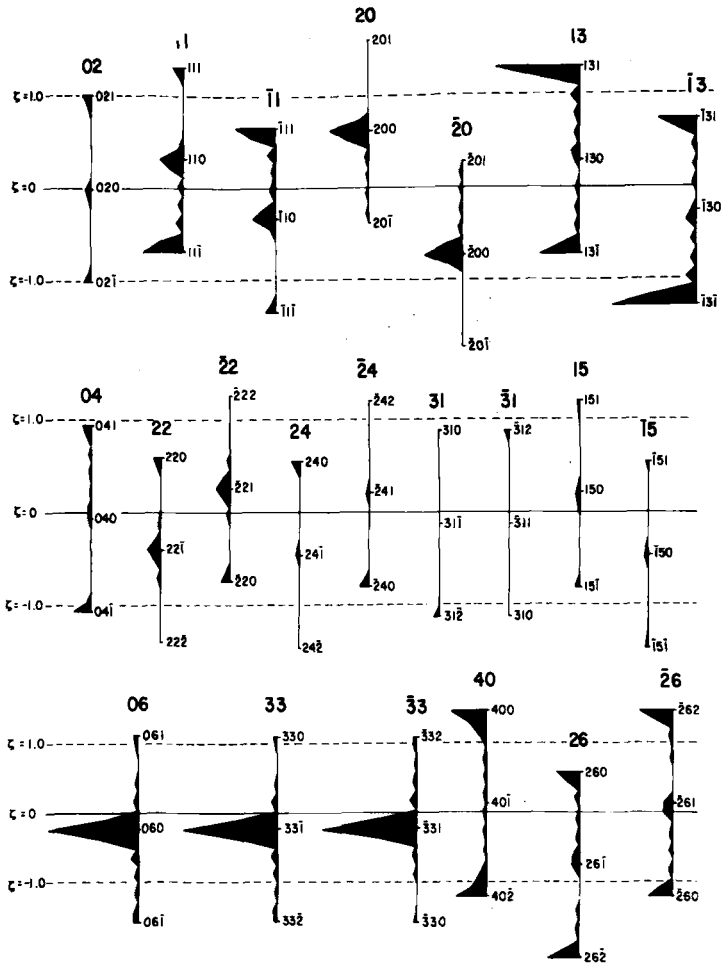

Fig. 4.8. SAD intensity variations along the *hk* rows in the "excitation region" for $2M_1$ muscovite of 100 Å thickness (see text).

the $l' = -0.3$. If, however, the intensity is calculated by integrating from $l' = 1.3$ to $l' = -0.7$, it is rather close to the observed one. For the same integration interval, l' values of other *hk* spots can be determined similarly. Since these l' values are different for each reflection, it may be more practical to refer to this integral in terms of ζ-values. Considering the three reflections (111, 110, $11\bar{1}$) in the close vicinity of the Ewald sphere, one has to assume that the $11\bar{1}$ spot fully contributes to the intensity in order to account for the strong intensity of the 11 spot. The "excitation error" of the $11\bar{1}$ reciprocal lattice point is, however, -0.69 (c^*), and its elongation in terms of kinematical theory is $u = 0.2$ (c^*). Therefore, its contribution to the

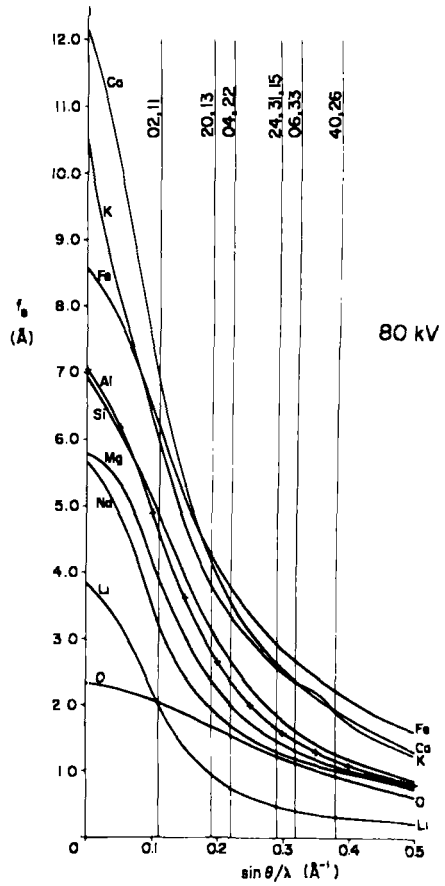

Fig. 4.9. Scattering factors for electrons for the common atoms in mica-type layer silicates.

observed intensity cannot be simply related to this elongation. However, other factors such as tilting or bending, and the spread of mosaic orientations within a crystallite may bring a reciprocal lattice point with $\zeta \neq 0$ into the reflecting position. Fig. 4.10B schematically explains how a segment of a reciprocal lattice row can be excited simultaneously, even though the simple geometrical theory of diffraction limits the intersection between the diffraction vector CH_0 (referred to Fig. 4.10B) and the Ewald sphere to a point P_0 with $\zeta = 0$. The reciprocal lattice point P_1 on the drawing has an excitation error ζ_1 but it can be brought onto the Ewald sphere by the rotation ϵ_1 due to the above factors. Similarly ϵ_2 rotation will bring the reciprocal lattice point P_2 with the excitation error ζ_2 onto the sphere of reflection. Thus the entire segment P_1P_2 of the reciprocal lattice row will be excited at the same time resulting in the H_1CH_2 cone of the diffracted

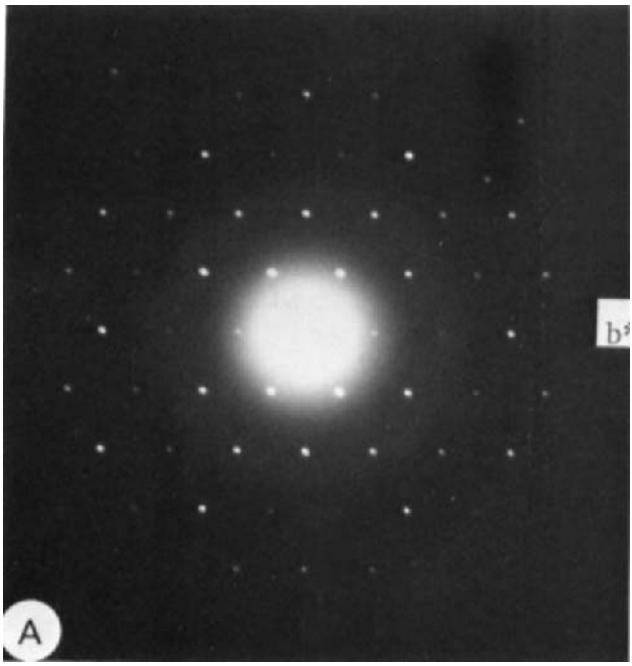

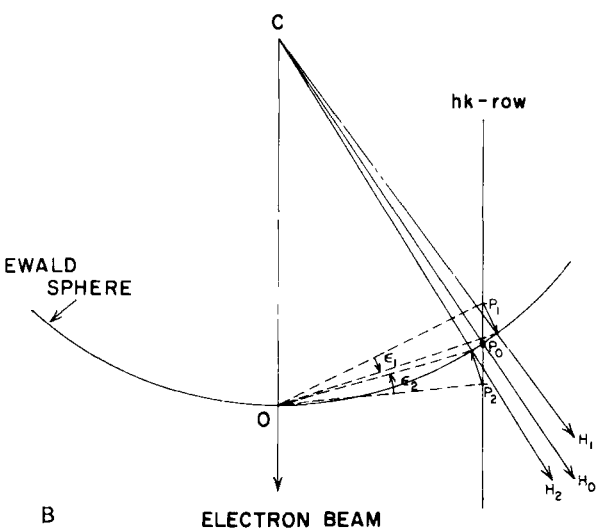

Fig. 4.10A. SAD pattern of a mica-flake with a thickness of 100 Å. B. Simultaneous excitation of a segment (P_1P_2) of the reciprocal lattice row *hk* caused by the rotations ϵ_1 and ϵ_2. (The scale of the drawing is exaggerated.)

beams. An integration over the P_1P_2 segment (i.e. over the interval $\Delta\zeta$) is obviously needed in order to account for the observed intensities.

Another interesting feature of $2M_1$ muscovite is the fact that the 02 and $0\bar{2}$ reflections are significantly weaker that the {11} reflections. Even changing focusing conditions and having considerable tilt (up to 2.5° for 100 Å thickness) does not cause any appreciable changes in the intensities of {02} reflections. This is not true for other micas, and for other type layer silicates. These reflections form diagnostic criterion for $2M_1$ type dioctahedral layer silicates on the SAD pattern.

Discrepancies between SAD symmetry and crystal symmetry

As it was derived by Vainshtein (1964), only six different plane point groups may be observed on the SAD patterns. These are 2, $2mm$, 4, $4mm$, 6, and $6mm$. Physical, geometrical, and instrumental factors may sometimes give rise to deviations in SAD patterns from these symmetries. We will consider only the deviations caused by the factors discussed in this section. In general, the symmetry related reciprocal lattice points are expected to have equal intensities on a SAD pattern if their excitation errors, i.e., their distances from the Ewald sphere, are equal. This may not always be true for crystals with monoclinic and triclinic symmetry, even under ideal focusing conditions without any tilt or bending. In such instances we need to have a certain amount of tilt to observe the symmetry. In monoclinic crystals, only the symmetrical reciprocal lattice points with $\Delta p = 0$, i.e. $[(h/3) + l] = 0$ such as 020 and $0\bar{2}0$ have equal distances to the Ewald sphere. The well-known relationship (Friedel's law) in diffraction symmetry $I_{hk} = I_{\bar{h}\bar{k}}$ may not be observed because of different ζ values of the centrosymmetrical reciprocal lattice points. Under non-ideal conditions, (i.e. with the objective lens off-focus, the presence of tilt or bending, and nonuniform thickness), SAD symmetry will deviate from the crystal symmetry as discussed above. The plane point group $2mm$ of $2M_1$ muscovite may then be reduced to the all possible subgroup symmetries such as m, 2, $\bar{1}$, and 1. The deviation from the actual symmetry would be more pronounced for the spots with larger indices as the difference in excitation errors (ζ) for the symmetrical reflections may become larger.

4.3. CRYSTAL STRUCTURE OF BEIDELLITE

Electron-optical data on beidellites have been previously reported by Nixon and Weir (1957), Weir and Green-Kelly (1962), and Méring and Oberlin (1971), among others. It was shown that beidellites have better developed crystal forms than montmorillonites. The beidellite sample from the Black Jack Mine (Idaho, U.S.A. with U.S. National Museum No. R4762) shows

exceptionally high degree of crystallinity for a smectite in the above series. In fact, the investigations by Weir and Greene-Kelly (1962) on this sample clarified the dispute on the definition of beidellite. They gave the chemical formula of the Na-saturated sample as:

$$[(Al_{1.98}Fe^{3+}_{0.02}Mg_{0.01})(Si_{3.48}Al_{0.52})O_{9.98}(OH)_2](Na_{0.45}K_{0.01})$$

Because of its better crystallinity, beidellite may provide us with the background to understand the SAD patterns of other smectites in this series. Among the previous investigations, Méring and Oberlin (1971) reported that the SAD patterns of Unterrupsroth beidellite are approximately hexagonal. Besson and Tchoubar (1972), on the other hand, proposed the plane group $c1m1$ (corresponding to the space group $C2$) for another beidellite from Unterrupsroth (Germany).

Beidellite particles were found on the electron micrographs to be predominantly in the form of lath-shaped units and ribbons ranging in length from 0.1 to 30 μm. A typical beidellite ribbon with backfolding is seen in Fig. 4.11. This bright-field image of the particle shows, aside from few small wrinkles on its surface, an unusually well-developed morphology for a smectite.

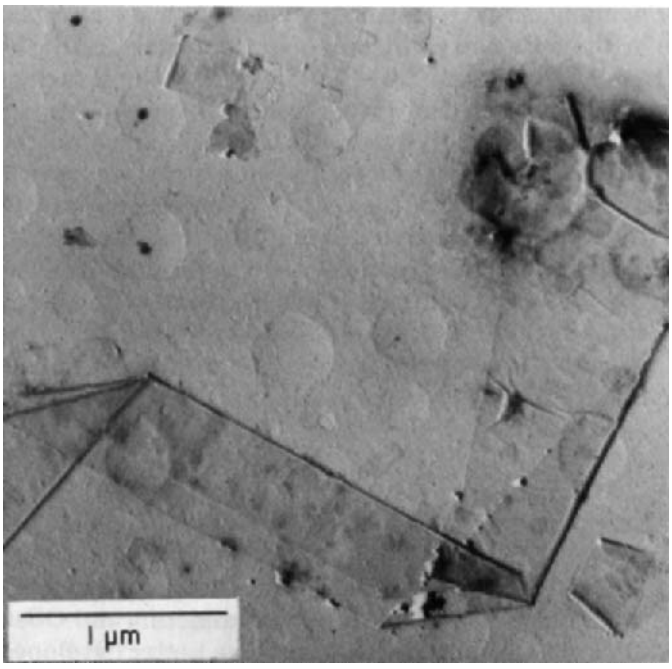

Fig. 4.11. Electron micrograph of a typical beidellite ribbon in the Black Jack Mine sample.

Structural models for beidellite with different octahedral configurations

Three models have been considered for beidellite crystal structure. These models are based on different octahedral configurations. For all models the distribution of the tetrahedral cations (Si, Al) has been assumed to be disordered. The scattering factors of these atoms for electrons are so close to each other that it would not be feasible to differentiate between structures with different (Si, Al) distribution. The situation is different for various octahedral ordering schemes involving vacancies and occupied sites. In the structure of a 1*M* mica-type layer silicate there are three octahedral sites in the asymmetric part of the unit cell. One of them (*M*1) is distinct from two others (*M*2's) and has, ideally, a site symmetry of 2/*m*. This site is vacant in the *C*2/*m* space group for a 1*M* dioctahedral mica and this is the first model (Fig. 4.12A) to be considered. If, however, the *M*1 and one of the *M*2 are occupied and the other *M*2 site is left vacant, then the symmetry is reduced to *C*2 (Fig. 4.12B). This model was first proposed by Méring and Oberlin (1971). Thus, there is a strict octahedral ordering in both of the models, We can now derive hypothetically another model by assuming a disorder in

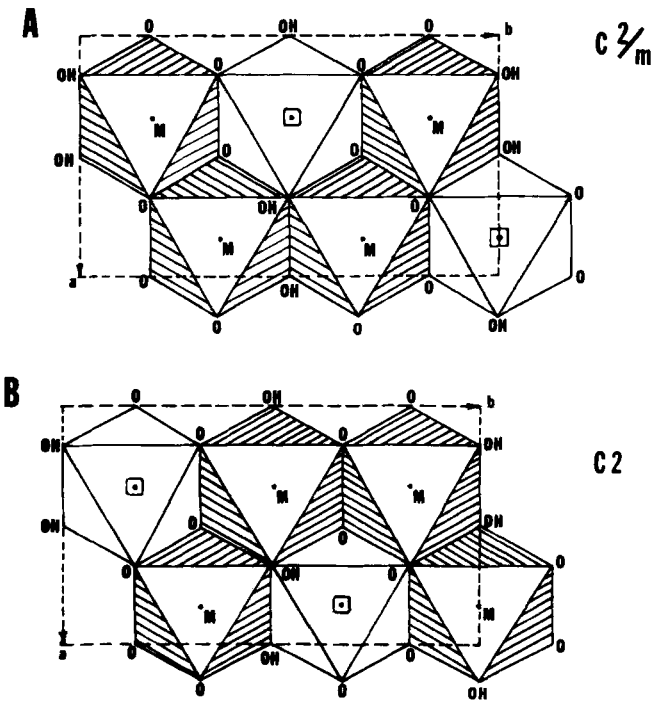

Fig. 4.12. The two possible octahedral configurations for a dioctahedral mica layer with the symmetries indicated next to them.

occupancy of $M1$ and $M2$ sites. This model, designated by the letter D, has also $C2/m$ symmetry, but $M1$ and $M2$ sites have an occupancy of 0.67. From crystal chemical considerations such an octahedral disorder is expected to be rather unstable, for it will locally result in a trioctahedral arrangement of the aluminum ions. The octahedral disorder may take place in real crystals in terms of antiphase domains having individually $C2/m$ symmetry but related to each other by 120° rotations.

The atomic coordinates for the above models are derived from those of the $1M$ phlogopite structure (Steinfink, 1962). The model with space group $C2/m$ has the atoms listed in Table 4.3 in its asymmetric unit. The model $C2$ has the additional atoms listed in the same table. No correction has been made for the thermal vibrations of atoms. Some investigators (Méring and Oberlin, 1971; Besson and Tchoubar, 1972) use the two-dimensional plane groups $c2mm$ and $c1m1$ instead of the three-dimensional space groups $C2/m$ and $C2$ for the intensity calculations. This implies that the z-coordinates of atoms are ignored. If the SAD patterns were representing only $hk0$ reflections, the two-dimensional plane groups will give the same intensities as the corresponding three-dimensional space groups. As discussed previously in Section 4.2, the SAD pattern of a layer silicate with c^* parallel to the incident beam does not represent the $hk0$ reciprocal lattice plane, but a section of each hk row at different l' value. Intensities for the above models have been calculated with the eq. 11 of Section 4.2 for thicknesses ranging from one up to ten layers ($P = 1$ to 10). The structure amplitude $F_{hkl'}$ has been calculated varying l' values continuously by increments of 0.1. The so-obtained intensity variations along the hk rows of the most common reflections are plotted in Fig. 4.13 for a single layer of beidellite with $C2/m$ and $C2$ symmetries.

TABLE 4.3

Atomic coordinates of beidellite for the models $C2/m$ and $C2$ (see text)

Model	Atom	x	y	z
$C2/m$	Na	0.0	0.0	0.0
	Al($M2$)	0.0	0.167	0.5
	OH	0.135	0.0	0.396
	O-1	0.496	0.0	0.170
	O-2A	0.834	0.223	0.169
	O-3A	0.627	0.168	0.390
	Si-A	0.577	0.168	0.226
$C2$	In addition to the above atoms:			
	Al($M1$)	0.0	0.5	0.5
	O-2B	0.834	0.777	0.169
	O-3B	0.627	0.832	0.390
	Si-B	0.577	0.832	0.226

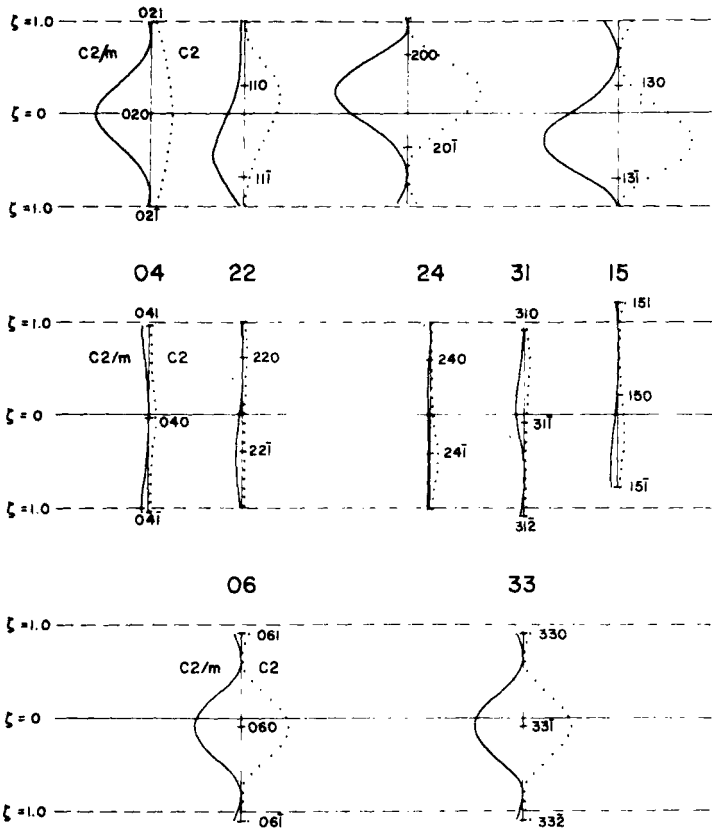

Fig. 4.13. Intensity variations along the hk rows in the c^* direction for a single layer of beidellite with $C2/m$ and $C2$ (dotted line) symmetries.

An examination of Fig. 4.13 shows that all the reflections have similar intensities except the 02 and 11 reflections. The intensities of these reflections are very sensitive to the structural changes considered in the above models. Fortunately, these reflections, compared to other reflections, are least affected by factors such as bending and tilting of the crystallites. The diagnostic value of them was earlier pointed out by Méring and Oberlin (1971). We plotted only intensity variations along the 02 and 11 rows in Fig. 4.14 for single beidellite layers of the above three models. In Fig. 4.14, ζ-axis refers to the "excitation error" of each reciprocal lattice point along a given hk row. The coordinate $\zeta = 0$ defines the intersection point of the Ewald sphere with each reciprocal lattice row. Theoretically, the interference region at this intersection (i.e. at $\zeta = 0$) is responsible for the observed intensity of 02 and 11 spots. As seen in Fig. 4.14, the 020 reciprocal lattice point has an "excitation error" very close to zero. The 110 reciprocal

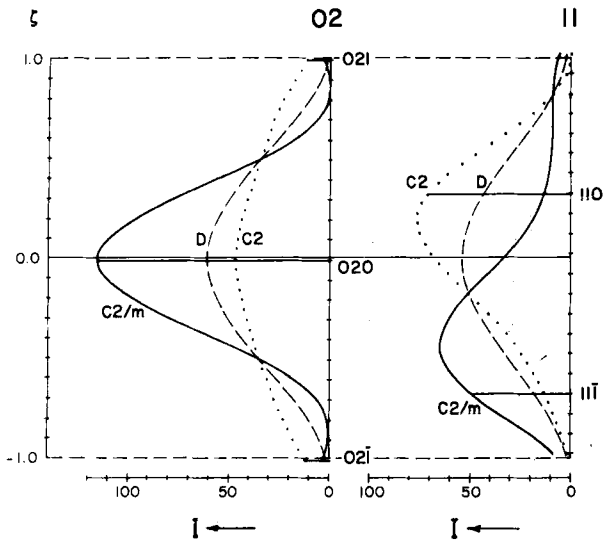

Fig. 4.14. Intensity variations along the 02 and 11 rods for single beidellite layers with different octahedral configurations. The ζ coordinate gives the "excitation errors" for each point along the *hk* rod and $\zeta = 0$ indicates the intersection point of the Ewald sphere with each *hk* rod.

lattice point, on the other hand, has an "excitation error" of 0.32 (in units of c^*) and, the $l' = -0.3$ section of the 11 rod lies exactly on the Ewald sphere. The expected intensity ratios (I_{02}/I_{11}) at $\zeta = 0$ are 3.4 for the $C2/m$ symmetry, 1.1 for the D model, and 0.7 for the $C2$ space group. These intensity ratios may easily differentiate between the beidellite single layers with the above structures. They also show that the above octahedral disorder greatly affects the intensities of {11} reflections. Unfortunately, we were not able to find a beidellite crystal with a single unit cell thickness among more than a few hundred extremely thin flakes examined under the electron microscope. We were able, however, to make observations on crystals with two or more layers in their thicknesses. These will be described in the next section, and the choice of the model for beidellite crystal structure was made using these SAD patterns.

SAD patterns of beidellite crystals with multiple layers in thickness

A series of SAD patterns were obtained from beidellites with different thicknesses. The thicknesses of the crystals were measured by using the shadows cast by carbon/platinum coating. The thicknesses were found to be 2, 3, 4, 5, 6, 7, and more layers. From these, the SAD patterns are shown in Fig. 4.15 for thicknesses of 3, 4, 5, and 7 layers. These SAD patterns may

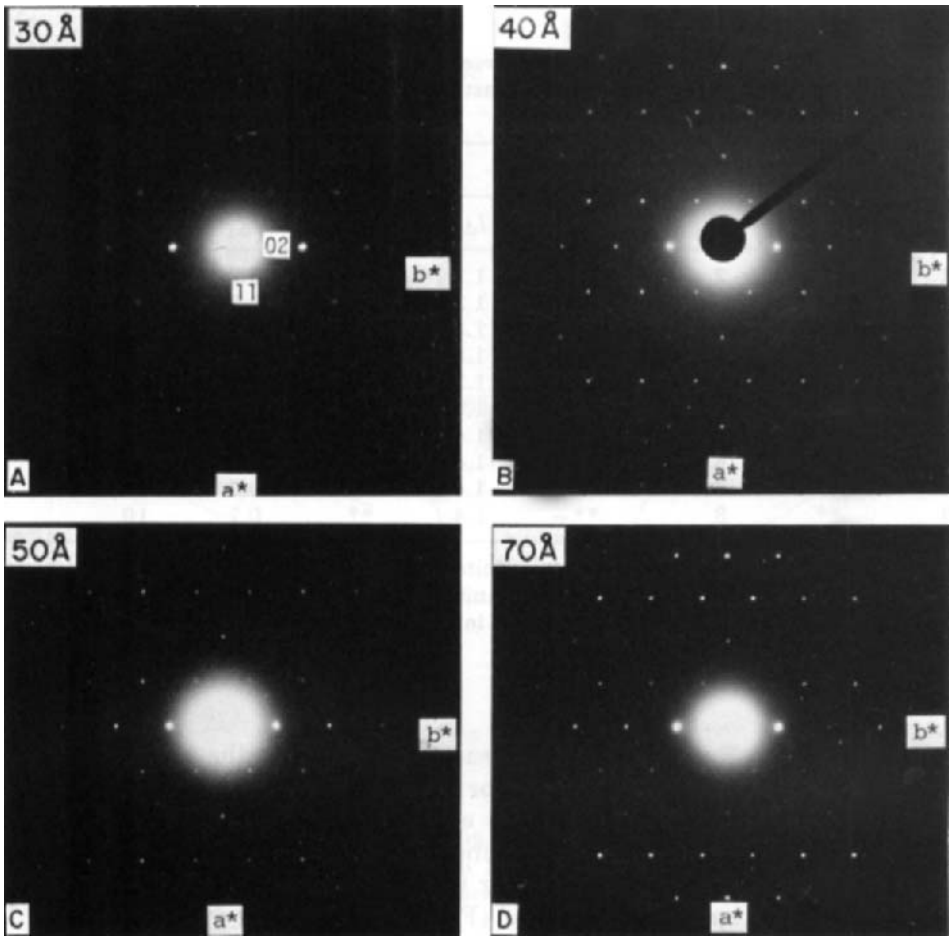

Fig. 4.15. Selected area electron diffraction patterns of beidellite crystallites coated with C/Pt with thicknesses indicated on the figures.
(The a^* direction marked on the patterns is not the actual but the projected a^* direction on the a—b plane of beidellite.)

show experimentally how the thickness affects the intensity of the spots. They probably represent the first experimental data obtained since the theory of shape transform was formulated. The expected intensities for 02 and 11 spots were calculated according to eq. 11 and they are listed in Table 4.4 in form of the ratios of the 02/11 reflections for different beidellite models and thicknesses. The observed intensity ratios from Fig. 4.15 are also given in Table 4.4. The intensity variations along 02 and 11 rows are plotted in Fig. 4.16 for thicknesses of 1, 2, 3, 4, 5, and 10 layers for $C2/m$ model. First we may assume that the interference region at $\zeta = 0$, i.e. at the exact intersec-

TABLE 4.4

Calculated intensity ratios (I_{02}/I_{11}) for different models with consideration of thickness variations (P) from one to ten layers. The last column gives the observed intensity ratios (I_{02}/I_{11}) obs.

$C2/m$			D		$C2$		(I_{02}/I_{11})obs.
P	I_ζ	$I^*_{\Delta\zeta}$	I_ζ	$I_{\Delta\zeta}$	I_ζ	$I_{\Delta\zeta}$	
1	3	2	1	1.1	0.7	0.7	
2	11	4	3	1.3	2	0.7	10
3	116	5	61	1.3	47	0.7	5
4	116	6	31	1.3	24	0.7	5
5	58	7	20	1.3	12	0.7	5
6	**	7	61	1.3	47	0.7	7
7	**	6	**	1.4	**	0.7	10
8	116	6	61	1.4	24	0.7	
9	**	7	61	1.4	47	0.7	
10	**	8	**	1.4	**	0.7	10

* The intensity ($I_{\Delta\zeta}$) is integrated over a finite section ($\Delta\zeta$) of hk rod in the vicinity of the Ewald sphere from $\zeta = -0.5$ to 0.5 (in units of c^*). In the previous column the intensity (I_ζ) is calculated exactly at the point of intersection of hk rod with the Ewald sphere i.e. at $\zeta = 0.0$.

** Refers to the case where I_{11} is zero.

tion point of the Ewald sphere with each hk rod giving the intensity (I_ζ) of the spot. The expected intensities for this case (Table 4.4) shows drastic changes with thickness variations for each model. The observed SAD patterns in Fig. 4.15, however, do not indicate any large changes in intensity with variations in the thicknesses. For instance, the expected intensity ratio for 02/11 reflections of $C2/m$ model (Fig. 4.16 and Table 4.4) is about 3 : 1 for a single layer, 11 : 1 for two layers, and 116 : 1 for three and four layers in thickness. Other models have similar ratios for intensities (I_ζ) calculated at $\zeta = 0.0$. In fact, for a beidellite crystal of 10 or more layers in thickness, only the 02, $0\bar{2}$ reflections are expected to have observable intensities at $\zeta = 0$ for all the models considered. In practice, beidellite crystals with 10 or more layers in thickness display more reflections. If, however, one assumes that the interference region has a "finite" depth, e.g. from $\zeta = -0.5$ to +0.5 (in units of c^*), then the intensities integrated ($I_{\Delta\zeta}$) over the interval ($\Delta\zeta$) seem to be compatible with the observed data. This suggests that a "finite" section of each hk row contributes to the observed intensity. Table 4.4 shows that the integrated intensity ratios for 02/11 reflections for the $C2/m$ model vary between 4 : 1 to 8 : 1 for the thicknesses of 2 to 10 layers. These intensity ratios are in the same order of magnitude as the observed intensity ratios ranging 5 : 1 to 10 : 1. As seen in the same table, the expected integrated intensity ($I_{\Delta\zeta}$) ratios for 02/11 reflections for the above thickness

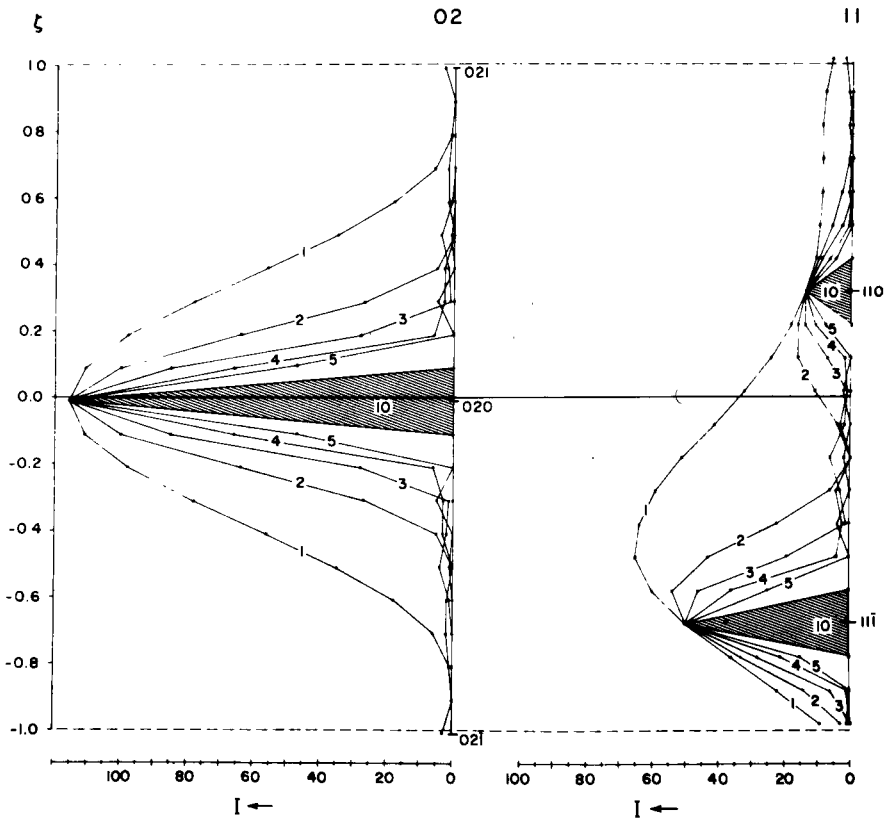

Fig. 4.16. Intensity variations along the 02 and 11 reciprocal lattice rods of beidellite crystallites with $C2/m$ symmetry, but with 1, 2, 3, 4, 5, or 10 layers in their thicknesses. The number of layers is indicated on the curves.

series range between 1.3 : 1 and 1.4 : 1 for the model D with octahedral disorder. These intensity ratios are about 0.7 for the $C2$ model. The observed 02/11 intensity ratios are much closer to those calculated for the $C2/m$ model than for $C2$ and D models. This indicates that the beidellite has a structure close to $C2/m$ model with the $M1$ octahedral sites being left vacant.

Having established the model on the basis of 02 and 11 reflections for the crystal structure of beidellite, we will now study in detail the observed and calculated intensities of SAD patterns. The observed intensities are visually estimated on the scale 5—100 as there was no densitometer available. The expected intensities are computed by integrating over the previously mentioned interval, and they are listed in Table 4.5. Comparison of the observed and calculated intensities shows several anomalies which are briefly described in the following pages.

TABLE 4.5

Calculated ($I_{\Delta\zeta}$) and observed (I_0) intensities for beidellite with $C2/m$ symmetry and with the P number of layers in its thickness. (The index l' gives the intersection of the Ewald sphere with each hk row.)

hk	l'	$P = 3$		$P = 4$		$P = 5$		$P = 7$	
		$I_{\Delta\zeta}$	I_0	$I_{\Delta\zeta}$	I_0	$I_{\Delta\zeta}$	I_0	$I_{\Delta\zeta}$	I_0
02	0.0	118	100	117	100	117	100	116	100
11	−0.3	25	20	20	20	18	20	18	10
$\bar{1}1$	0.4	25	20	20	20	18	20	18	5
20	−0.6	54	30	42	30	38	25	37	15
13	−0.3	55	35	44	30	39	35	38	15
$\bar{1}3$	0.4	55	30	44	30	39	35	38	15
04	0.0	2	25	1	25	2	45	1	25
22	−0.6	12	0	12	5	12	5	12	5
$\bar{2}2$	0.7	13	0	13	5	12	5	12	5
24	−0.6	6	0	5	0	5	0	5	10
$\bar{2}4$	0.7	6	0	5	0	5	0	5	15
31	−0.9	15	10	15	25	15	30	15	35
$\bar{3}1$	1.0	15	10	16	25	15	30	15	35
15	−0.3	3	15	3	15	3	15	2	20
$\bar{1}5$	0.4	9	10	7	15	6	10	4	15
06	0.1	100	10	100	15	100	20	100	30
33	−0.9	103	20	103	30	103	40	103	40
$\bar{3}3$	1.0	103	20	103	30	104	40	103	40
40	−1.2	38	15	37	30	7	25	34	45
26	−0.6	48	0	44	10	42	5	39	15
$\bar{2}6$	0.8	40	5	39	5	38	10	36	10

Effects of bending on SAD patterns of beidellites. As seen in Figs. 4.15A—D, the higher orders of reflections have undergone markedly larger reductions in intensity than the lower orders, regardless of the thicknesses of the beidellite crystallites. This is shown clearly for the 33 and 06 spots as well as for other reflections. The 06 and 33 reflections are about three to ten times weaker than their calculated values. Other layer silicates such as micas, kaolinite, and chlorites under the same experimental conditions do not show such an intensity reduction with the increasing diffraction angle. The question still arises as to whether sample preparations and metal coating may have such an effect specifically for the beidellite. Two other sample preparation techniques are tested. Specimen grids are prepared by floating a thin formvar film on top of a dilute beidellite suspension in distilled water without addition of tertiary butylamine. Charged polymer films such as that of formvar are found to easily pick up beidellite particles from the suspension. Subsequently, these particles were not coated by any metal. The SAD pattern from uncoated beidellite particles in Fig. 4.17 are very similar to

those patterns in Fig. 4.15 obtained from particles that were coated with carbon/platinum. Samples were also mounted on holey carbon films where beidellite particles may occur over the holes in the supporting film. The SAD pattern from these beidellite particles without a substrate and without a metal coating are also similar to those described above. After the above three sample preparation techniques, beidellite particles give very similar SAD patterns. It must also be noted that gold-coating of the particles causes a drastic reduction of the intensities for higher order reflections. From gold-coated beidellite particles one often observed only 02 and 11 reflections. The observed intensity reduction with increasing diffraction angle is most likely due to the bending effects as discussed in detail in the first section of this chapter. In fact, the SAD patterns in Figs. 4.15 and 4.17 show features similar to those described for the spherical bending of the crystallites with the linear dimensions of 270 Å and 540 Å that are bent to a radius of curvature of 1000 Å in Fig. 4.3 (Section 4.1). Although the intensity reductions in Figs. 4.15 and 4.17 are larger along the b^* than along the other directions, we may still consider a spherical bending for the beidellite crystallites in order to give a qualitative explanation for the observed data. The calculated intensity ratios of the 02/06 and 02/33 reflections for an undeformed beidellite crystallite are both about 6 : 5, whereas the observed ratios for the 02/06 reflections range between 3 : 1 and 5 : 1 in Figs. 4.17A and B. In the SAD pattern in Fig. 4.17C, all the reflections except 02 are very weak or missing. The large reductions in intensity or the total loss of reflections were shown in Fig. 4.3 for the interference functions of crystallites with the linear dimensions of 270 Å and 540 Å, and bent to a radius of curvature of 1000 Å. The dimensions of the beidellite crystallite are much larger and beidellites have more atoms per unit cell than the models used in Fig. 4.3. It would be prohibitively time consuming to calculate the exact corrections for bending effects on the beidellites. The above explanation is, therefore, to be considered as strictly qualitative.

Anomalies in the SAD patterns of beidellite.

(a) Some reflections, particularly 04 and 15, display much stronger intensities as compared to the expected ones. Since the beidellite crystallites, giving rise to the SAD patterns in Fig. 4.15, have a thickness far below the critical one, dynamical effects cannot be responsible for this situation. Other layer silicates, e.g. kaolinite or micas, do not show such strong 04 and 15 reflections.

(b) In few of the SAD patterns, reflections related by the mirror symmetry and hence with equal "excitation errors" such as 11 and $1\bar{1}$, do not have equal intensities. This is demonstrated in Fig. 4.5D, where the intensities of the other symmetry related reflections do not indicate possible orientation errors (tilting) in the specimen. This may be interpreted that some of the beidellite crystallites have actually a triclinic symmetry, or that

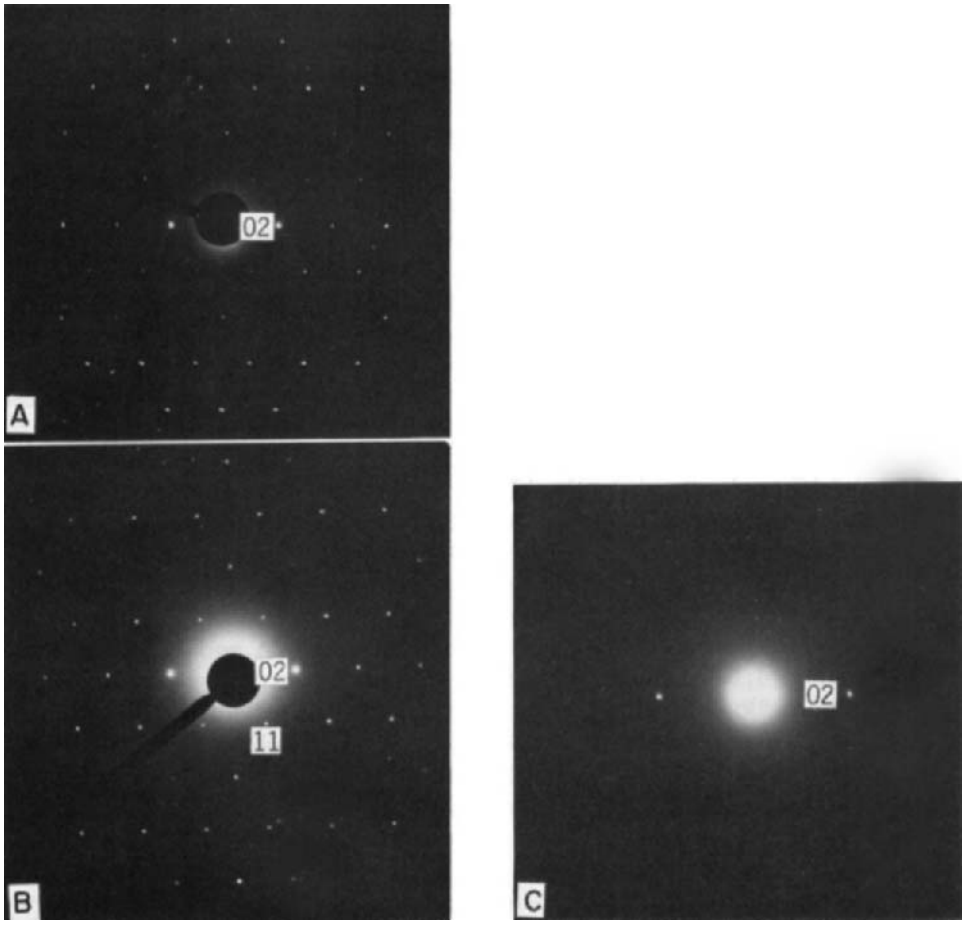

Fig. 4.17. SAD patterns of beidellites displaying various degrees of bending. A, B. Uncoated samples. C. Carbon—platinum coated sample.

the arrangement of domains in them may be responsible for such a symmetry in SAD patterns.

(c) Other anomalous features of beidellite SAD patterns consist of streaks and extra spots between the normal Bragg reflections. The streaks are commonly observed after a long exposure and are confined to the directions parallel to ⟨11⟩ and ⟨02⟩. The extra spots appear rarely but distinctly. These features of beidellite SAD patterns are discussed by Güven et al. (1977) elsewhere.

4.4. CRYSTAL STRUCTURE OF MONTMORILLONITE

Previous studies

Zvyagin and Pinsker (1949), using the "oblique texture" method on the polycrystalline specimens, proposed the space group $C2/m$ for montmorillonite (askanite). This is the ideal symmetry of a mica-type layer silicate. They did not make any deductions regarding the details of the structure.

Cowley and Goswami (1961) published SAD patterns with hexagonal symmetry for montmorillonite from Clay Spur (Wyoming), Little Rock (Arkansas), and from a sample from New South Wales. One of the SAD patterns (Type B) given by Cowley and Goswami is very similar to those of mica impurities, and it is possibly not from a montmorillonite. These investigators explained the hexagonal symmetry in terms of 20—50 degrees bending of montmorillonite layers. Cowley and Goswami assumed that the montmorillonite flakes were bent about X- and Y-axes with the incident beam being parallel to the Z-axis. Under these circumstances, they give the intensity of $hk0$-type reflections by the following expression, which is slightly modified from the original equation (Cowley, 1961; equation 7):

$$I(s) = \sum\sum f_i f_j \exp(2\pi i \boldsymbol{s} \cdot \boldsymbol{r}_{ij}) \cdot \exp\{-(\pi^2/\sigma^2) \cdot (s^2 \cdot r_{ij}^2 \cdot \cos^2\alpha)\} \qquad (1)$$

where σ is the average amount of bending, $\boldsymbol{r}_{ij}$ is the inter-atomic vector, $\boldsymbol{s}$ the reciprocal lattice vector, and α is the angle between the vector $\boldsymbol{r}_{ij}$ and the Z-axis. Because $r_{ij} \cos\alpha = \Delta z_{ij}$ (the difference between z-coordinates of the pairs of atoms), the second exponential may be written simply as $e^{-\Delta}ij$ with:

$$e^{-\Delta}ij = \exp-(\pi^2/\sigma^2)(s^2 \cdot \Delta z_{ij}^2) \qquad (2)$$

Cowley (1961) gives the following interpretation to eq. 2: In this equation the exponential term expresses the correction in regard to the contribution from a pair of atoms in the bent crystal. Obviously, this contribution depends on the variable z_{ij} for a given bending (σ = constant) and for a given reflection (s = constant). While $\Delta_{ij} = 0$ represents the unbent crystal, $\Delta_{ij} = \pi^2$ (i.e. $\Delta z_{ij} = \sigma/s$) reduces the contribution from the above pair of atoms to about zero. Such pairs of atoms may be considered as contributing practically nothing to diffraction intensity, i.e., scattering non-coherently. Therefore, one can estimate the range of coherency in the Z-direction for a given amount of bending. After having estimated this range, the bent crystal is divided into coherently diffracting slabs in this direction. Total diffraction intensity for a bent crystal is then calculated by adding the intensities from such slabs.

For the bending angles of 20—50°, Cowley and Goswami (1961) calculated the range of coherency in the Z-direction to be about 3 Å for mont-

morillonite. They assumed that the octahedral and the tetrahedral networks scatter independently within the bent montmorillonite layer, which then explains the observed hexagonal symmetry. Cowley and Goswami's interpretation seems to be questionable in that Δz_{ij}, the quantity defining the coherency range in the Z-direction, refers to the difference between the z-coordinates of the pairs of atoms after the bending. Since this quantity Δz_{ij} is equal to $r_{ij} \cdot \cos \alpha$, it is determined by the r_{ij} distance between the atoms before the bending and on the α angle between the r_{ij} vector and the Z-axis after the deformation. Atoms on the same plane before the bending may have large Δz_{ij} values after the bending and, therefore, scatter non-coherently. Similarly, atoms in different z-levels before the bending may have smaller Δz_{ij} values after the deformation. In other words, the above slabs of 3 Å in bent crystal do not correspond to tetrahedral and octahedral sheets of the unbent crystal. It is not justifiable to assume that tetrahedral and octahedral networks scatter independently in the bent crystal.

Méring and Oberlin (1971) obtained SAD patterns in the following way: they separated fine fractions from the Na-saturated montmorillonite samples of Wyoming and Camp-Berteaux. The specimen grids used for electron diffraction were unshadowed and thin particles were, therefore, invisible in the bright-field mode of imaging. They obtained SAD patterns with hexagonal symmetry from the Camp-Berteaux montmorillonite. These hexagonal patterns were interpreted by them as edge-to-edge associations of montmorillonite crystallites arranged with about 60° orientations. For the Wyoming montmorillonite they obtained a monoclinic spot pattern with the plane point group $2mm$. From this pattern, Méring and Oberlin (1971) concluded that the pattern is from a monolayer and the Wyoming montmorillonite single layer has the non-centrosymmetrical plane group $c1m1$ (corresponding to space group $C2$). They also suggested that the structure may exhibit certain deviations from the ideal scheme similar to those observed in muscovite. The symmetry of montmorillonite will be discussed in terms of more familiar space group notations instead of plane groups. This also makes it unnecessary to consider the projections of the structures. The space group $C2$ presents certain rather unusual crystal-chemical features for a layer silicate. The two configurations of octahedral networks for dioctahedral micas were shown in Figs. 4.12A and B in Section 4.3. The Fig. 4.12A represents the common configuration with the ideal symmetry of $C2/m$ for space group (i.e. $C2mm$ for plane group) where the mirror plane passes through OH's and vacant octahedral sites. This configuration is observed in all the well-studied dioctahedral micas in which distortions and order-disorder may reduce this symmetry to its subgroups $C2$, $C\bar{1}$, etc. The other configuration, shown in Fig. 4.12B has the $C2$ space group where the mirror plane is destroyed by the choice of vacant octahedral sites. An unusual feature of this configuration is the fact that the OH—OH edges shown on the unshaded faces of the octahedra, are not shared between octahedral cations.

There is an asymmetric distribution of anions around the vacant site. Such a hydroxyl configuration has not yet been observed in another dioctahedral layer silicate. Thus, the space group $C2$, if correct, gives rather unusual properties to the montmorillonite single layers as compared to the other dioctahedral mica-type layers.

Roberson and Towe (1972) reported SAD spot patterns with a triclinic symmetry for Wyoming (Upton) and Camp-Bertreaux montmorillonites. The images of the particles giving rise to the diffraction patterns were not recorded. They assumed that the $-0.05\ \mu m$ fraction of the samples (from which the above SAD patterns were obtained) contained only montmorillonite particles. Furthermore, both Roberson and Towe (1972) and Méring and Oberlin (1971) assumed that a spot SAD pattern would only be obtained from a single montmorillonite layer because of the turbostratic structure of the latter. These assumptions were questioned by Güven (1972), and the same sample from Wyoming (kindly furnished by Dr. Towe) has been reexamined. It was found that this fine fraction ($-0.05\ \mu m$) of the Upton sample contains a large number of subhedral lamellae of montmorillonite, a few aggregates, and a few lath-shaped crystallites. Mica impurities were also observed. Such a mica is shown in Fig. 4.18A and its SAD pattern in Fig. 4.18B. The latter has a plane point symmetry $2mm$ and some doubling of spots. The morphology of mica particles is, however, similar to that of subhedral smectite lamellae in this sample. It is, therefore, not possible to distinguish micas and montmorillonite particles on the basis of morphology. The SAD patterns of micas have, however, much sharper spots with stronger intensities than those of montmorillonites observed by us. The b-dimensions of subhedral montmorillonite lamellae vary within the values 9.00 ± 0.02 Å. The subhedral lamellae of montmorillonite crystallites are found to give SAD patterns similar to the pattern previously reported by Roberson and Towe (1972). It is therefore, expected that the latter SAD pattern is also from a montmorillonite crystallite. The thickness of these crystallites giving rise to the SAD spot patterns, goes up to 50 Å. Therefore, a spot SAD pattern does not necessarily imply the presence of single montmorillonite layer, as assumed by the above investigators.

Characteristic features of the SAD spot patterns from montmorillonite crystallites

Typical SAD spot patterns and the images of montmorillonite crystallites giving rise to them are shown in the following figures:

Fig. 4.19: (A) A subhedral lamella of at least 40 Å thickness in Ponza montmorillonite (No. 70), and (B) its SAD pattern.

Fig. 4.20: (A) A subhedral lamellar particle of about 30 Å thickness from the Wyoming (Upton) montmorillonite, and (B) its SAD pattern.

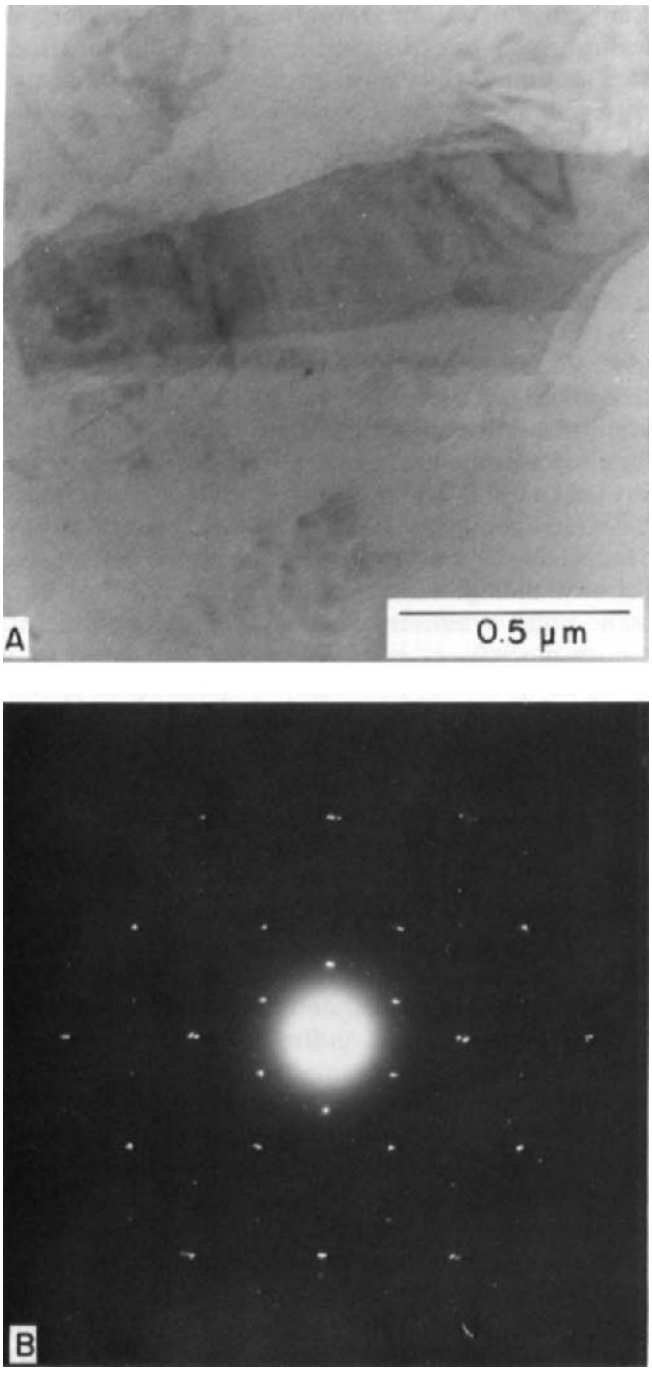

Fig. 4.18. A. A typical mica flake in Wyoming bentonite from Upton County. B. Its SAD pattern.

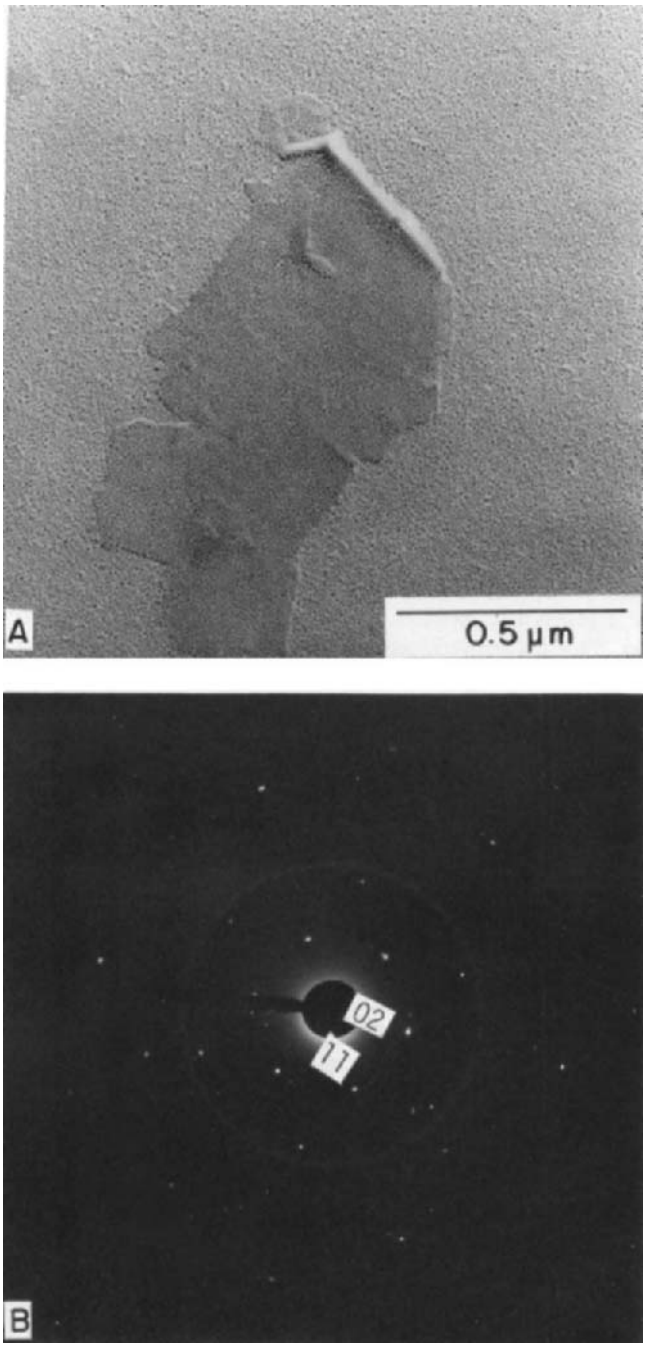

Fig. 4.19. A. Typical S-type particle of Ponza montmorillonite (sample 70). B. Its SAD pattern.

Fig. 4.21: (A) A subhedral lamella of at least 50 Å thickness in Tatatilla montmorillonite, and (B) its SAD pattern.

Fig. 4.22: (A) A euhedral lamella of 50 Å thickness in Camp-Berteaux montmorillonite, and (B) its SAD pattern.

Fig. 4.23: (A) A subhedral lamella of 30 Å thickness in Wyoming montmorillonite (Weston), and (B) its SAD pattern.

Because of the irregular shadows and the unfavorable shadow directions, the thickness for montmorillonite crystallites from the Tatatilla and Ponza samples could not be measured precisely.

The SAD patterns in Figs. 4.19B, 4.20B, and 4.21B from Ponza, Upton and Tatatilla montmorillonites are remarkably similar to one another. On these patterns there is one set of strong spots which may be originating from a large crystallite. In addition, there are several weak spots especially observable along the 11, 02 ring. These weak spots may be caused by a number of very small crystallites associated with the large one. In fact, in Fig. 4.21A one can see several tiny crystallites on top or around the large one. Nevertheless, the main set of spots can be analyzed separately. The diagnostic 02, 11, and $\bar{1}1$ reflections (and those related centrosymmetrically to them) are of equal intensity in all of the three SAD patterns. The 06, 33, and $\bar{3}3$ reflections are equal or somewhat weaker in intensity than the 02 reflections on the same patterns. The 04 spot is stronger in intensity than the 22 and $\bar{2}2$ reflections, thereby indicating a monoclinic symmetry (the plane point group $2mm$) for these patterns. However, there are several weak reflections in these patterns which violate the mirror symmetry. Specifically the intensities of the pair of reflections (31, $3\bar{1}$), (13, $1\bar{3}$), (42, $4\bar{2}$), ($\bar{3}1$, $\bar{3}\bar{1}$), and ($\bar{4}2$, $\bar{4}\bar{2}$) do not follow the mirror symmetry as indicated more clearly by Roberson and Towe (1972). Similarly, the pairs of reflections (13, $1\bar{3}$), ($\bar{1}3$, $\bar{1}\bar{3}$), (15, $1\bar{5}$) and ($\bar{1}5$, $\bar{1}\bar{5}$) do not follow the mirror symmetry in Fig. 4.19 from Ponza montmorillonite. These SAD patterns have, strictly speaking, the plane point symmetry 2, and on this basis Roberson and Towe (1972) suggested a triclinic symmetry for the crystal structure of montmorillonite. The absence of the mirror plane is not obvious in the other SAD patterns in Figs. 4.22 and 4.23. The SAD patterns of the montmorillonite crystallite from Tatatilla (Fig. 4.21B) show that the reflections with higher indices can be very weak or missing. In fact, only the 02, 11, and $\bar{1}1$ reflections are observable in the SAD patterns of the montmorillonite crystallites from Camp-Berteaux (Fig. 4.22B) and Wyoming (Fig. 4.23B). This may well be caused by a slight bending of these lamellae as previously discussed for the beidellite in Section 4.3. The 02, 11, and $\bar{1}1$ spots, however, have equally strong intensities in all the above SAD patterns except the one particle from the Wyoming (Weston) sample (Fig. 4.23B). In the latter pattern the 02 spots are a little stronger in intensity than the 11 and $\bar{1}1$ spots. In the same sample (Weston, Wyoming) the other montmorillonite particles show almost always equally strong 02, 11, and $\bar{1}1$ spots as is the case for the other samples.

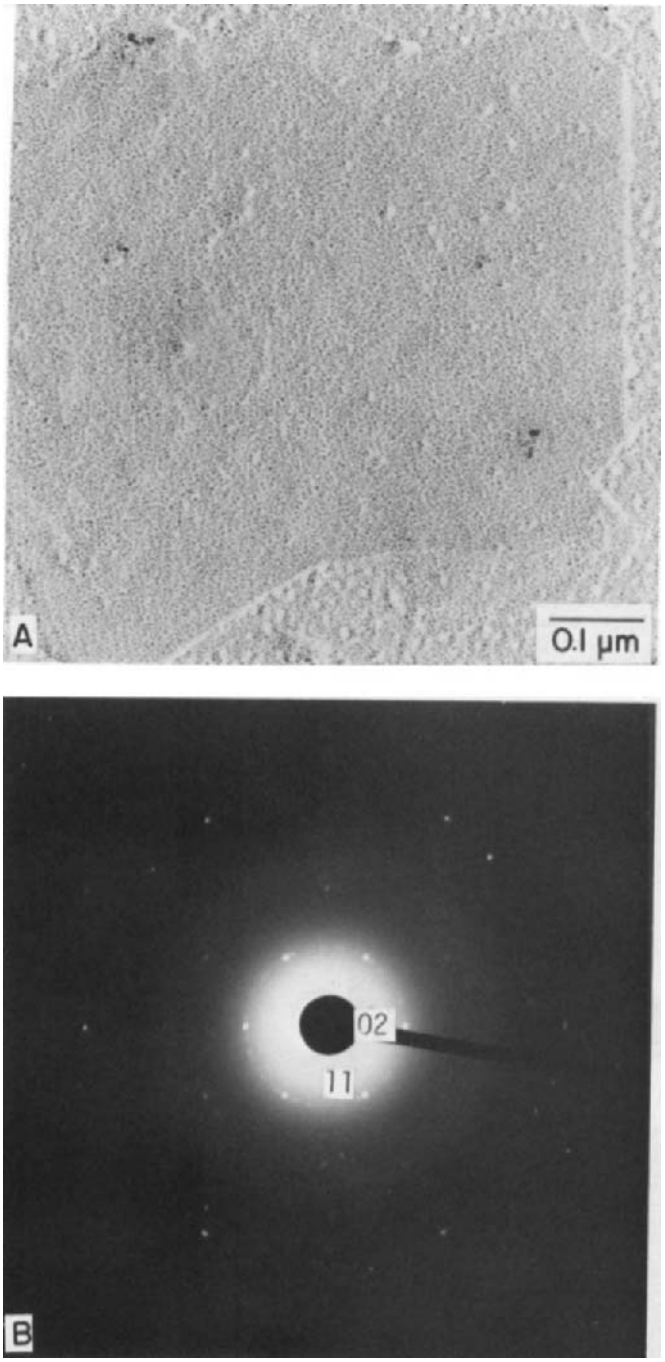

Fig. 4.20. A. S-type crystallite of Wyoming montmorillonite (Upton County). B. Its SAD pattern.

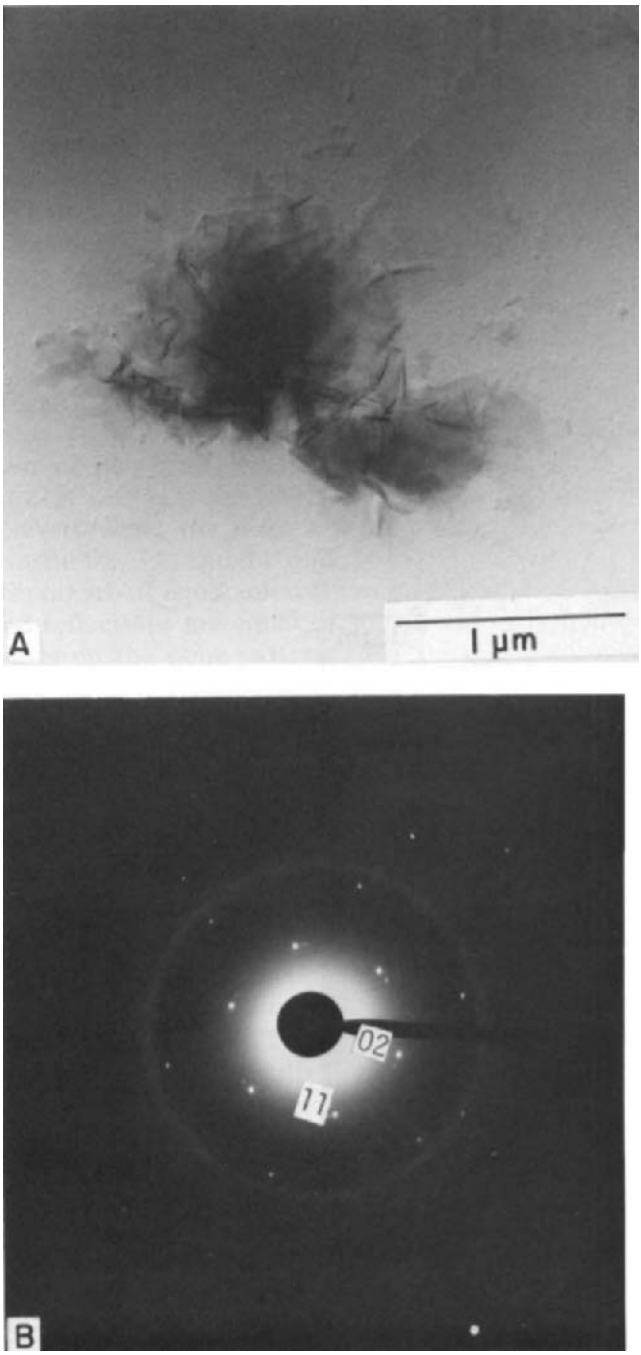

Fig. 4.21. A. S-type montmorillonite crystallite (in the upper right part of the figure) together with a layered aggregate in Tatatilla montmorillonite. B. The SAD pattern of the S-type lamella.

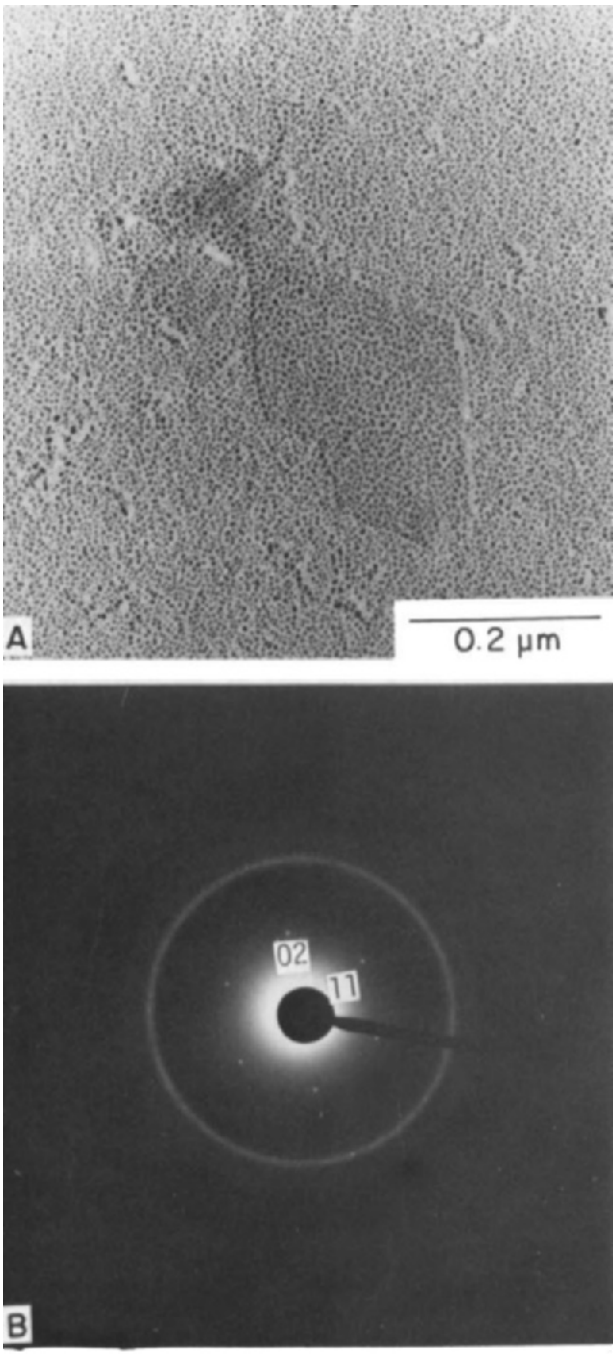

Fig. 4.22. A. E-type lamellae in Camp-Berteaux montmorillonite. B. Its SAD pattern displaying only 02, 11, and $1\bar{1}$ spots.

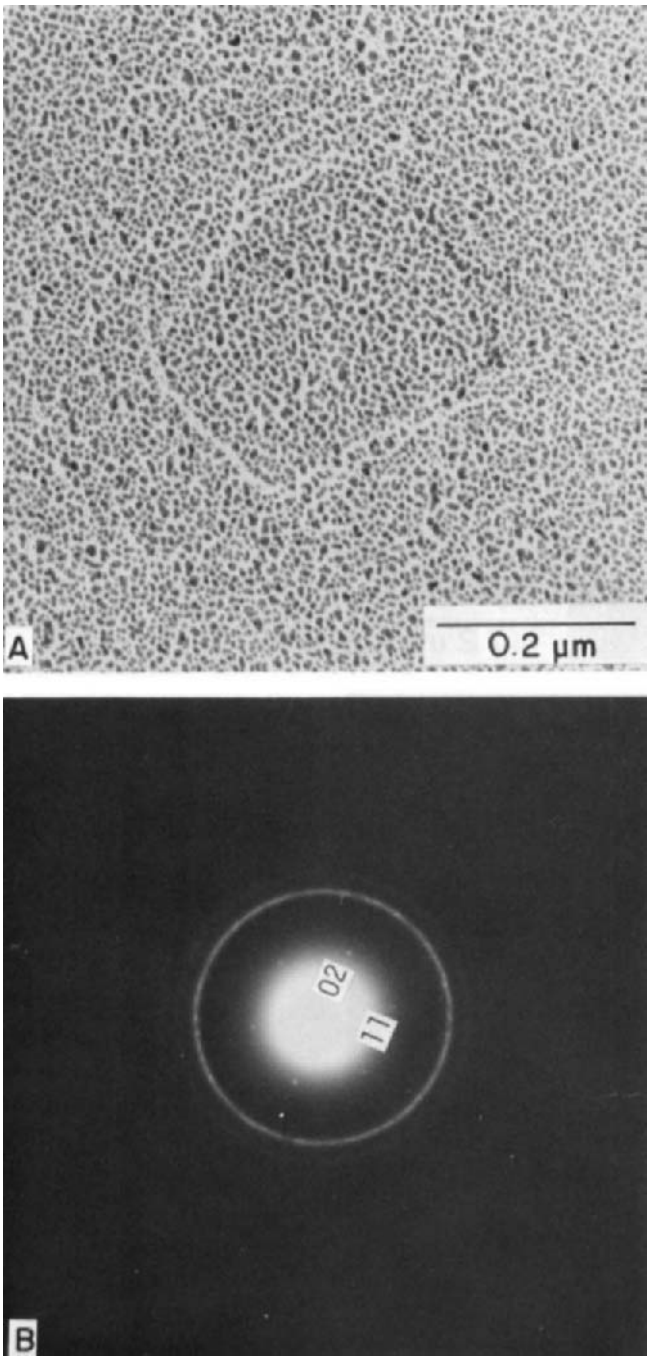

Fig. 4.23. A. S-type lamellae of Wyoming montmorillonite (Weston) with a thickness of 30 Å. B. Its SAD patterns (the rings belong to the gold-coating).

Interpretation of the SAD patterns and conclusions

Structural models under consideration for the montmorillonite are those ($C2/m$, $C2$, and D) described in the Section 4.3 for the beidellite. Since the differences in scattering power of the atoms involved in the substitutions for beidellite—montmorillonite series are negligibly small, the displacements in atomic positions related to these substitutions may cause only small changes in intensities. Therefore, the expected intensities for the above models of montmorillonite will be very close to those computed for the beidellite models. Because of the limited data obtained form the SAD patterns, we will be concerned only with the question of which one of the above models represents more closely the montmorillonite structure not with the details of it.

It was shown (in Section 4.3) that the intensities of the 02, 11, and $1\bar{1}$ reflections are very important for distinguishing between the above models, whereas the other reflections are expected to have similar intensities. Table 4.4 (in Section 4.3) indicates that the expected 02/11 (integrated) intensity ratio is about 0.7 for the model $C2$ with the thicknesses of 1—10 layers, the ratio is 1.3 for the D model with thicknesses of 1—10 layers. The commonly observed SAD patterns with equally strong 02, 11, and $1\bar{1}$ reflections do not provide conclusive evidence for any of the above models of montmorillonite crystal structure. In the only SAD pattern with $I_{02}/I_{11} \neq 1$ (Fig. 4.23) the observed intensity ratio (02/11) is about 1.2—1.3, and is compatible with the model D. The latter model has to be considered as a domain structure for the reasons mentioned in the previous section. The two possible ways of generating equally strong 02, 11 and $1\bar{1}$ reflections are:

(a) A random stacking sequence between the montmorillonite single layers: in this case regardless of whether the single layer has $C2/m$ or $C2$ symmetry, the SAD pattern is expected to show a hexagonal symmetry, and equally strong 02, 11, and $1\bar{1}$ spots.

(b) A domain structure where the domains with $C2$ or $C2/m$ symmetries are arranged with 60 or 120 degrees rotations with respect to each other. Again the SAD pattern is expected to show a hexagonal symmetry and equally strong 02, 11, and $1\bar{1}$ spots.

The question of whether the triclinic symmetry, as inferred from the intensities of rather weak reflections with higher order indices, is a valid one or not remains to be answered. Intensities of these weak reflections can be easily affected by experimental factors. A triclinic symmetry resulting from small variations, such as distortions in the $C2/m$ and $C2$ models, cannot account for the presence of equally strong 02, 11, $1\bar{1}$ spots while affecting the intensities of the weak higher order reflections. Thus, no concrete evidence is obtained from the SAD spot patterns of montmorillonites to propose modifications to the $C2/m$ symmetry for montmorillonites as inferred by Zvyagin and Pinsker (1949) from the oblique texture electron diffraction data.

REFERENCES

Agar, A.W., 1960. Accuracy of selected-area microdiffraction in the electron microscope. Br. J. Appl. Phys., 11: 185—189.

Beeston, B.E.P., Horne, R.W. and Markham, R., 1973. Electron Diffraction and Optical Diffraction Techniques. North-Holland, Amsterdam, 251 pp.

Besson, G. and Tchoubar, C., 1972. Détermination du groupe de symétry du feuillet élementaire de la beidellite. C. R. Acad. Sci. Paris, Sér. D, 275: 633—636.

Blackman, M., 1951. Diffraction from a bent crystal. Proc. Phys. Soc. (London), Sect. B, 64: 625—637.

Bradley, D.E., 1959. High resolution shadow-casting technique using simultaneous evaporation of platinum and carbon. Br. J. Appl. Phys., 10: 198—203.

Cowley, J.M., 1961. Diffraction intensities from bent crystals. Acta Crystallogr., 14: 920—927.

Cowley, J.M., 1967. Crystal structure determination by electron diffraction. Progr. Mater. Sci., 13: 269—321.

Cowley, J.M. and Goswami, A., 1961. Electron diffraction patterns of montmorillonite. Acta Crystallogr., 14: 1071—1079.

Gard, J.A., 1971. Interpretation of electron micrographs and electron-diffraction patterns. In: J.A. Gard (Editor), The Electron-Optical Investigations of Clays. Mineral. Soc., Monogr., 3: 27—78.

Greene-Kelly, R., 1953. The identification of montmorillonoids in clay. J. Soil Sci., 4: 233—237.

Guinier, A., 1963. X-ray diffraction. Freeman, San Fransisco, Calif.

Güven, N., 1971. The crystal structure of $2M_1$ phengite and $2M_1$ muscovite. Z. Kristallogr., 134: 196—212.

Güven, N., 1974. Factors affecting selected area electron diffraction patterns of micas. Clays Clay Miner., 22: 97—106.

Güven, N., 1975. Evaluation of bending effects on diffraction intensities. Clays Clay Miner., 23: 272—277.

Güven, N. and Pease, R.W., 1975. Selected area electron diffraction studies on beidellite. Clay Miner., 10: 427—436.

Güven, N., Pease, R.W. and Murr, L.E., 1977. Fine structure in the selected area diffraction patterns of beidellite, and its dark-field images. Clay Miner., 12: 67—74.

Hendricks, S. and Teller, E., 1942. X-ray interference in partically ordered layer lattices. J. Chem. Phys., 10: 147—167.

Hirsch, P.B., Howie, A., Nicholson, R.B., Pashley, D.W., Wheland, M.J., 1965. Electron Microscopy of Thin Crystals. Plenum Press, New York, N.Y., pp. 90—91.

Ibers, J.A. and Vainshtein, B.K., 1968. In: K. Lonsdale (Editor), International Crystallographic Tables. Vol. III, Tables 3.3.3.a (1). Kynoch Press, Birmingham, pp. 218—219.

Kunze, G., 1956. Zür Röntgenstreuung an unvollständigen zylindrischen Gittern — I and II. Acta Crystallogr., 9: 841—854.

Méring, J. and Oberlin, A., 1971. The smectites. In: J.A. Gard (Editor), The Electron-Optical Investigations of Clays. Mineral. Soc. Monogr., 3: 193—229.

Mitra, G.B. and Battacharjee, S., 1975. The structure of halloysite. Acta Crystallogr., 31B: 2851—2857.

Murr, L.E., 1970. Electron Optical Applications in Materials Science. McGraw-Hill, New York, N.Y., 544 pp.

Nixon, H.L. and Weir, A.H., 1957. The morphology of Unter-Rupsroth montmorillonite. Mineral. Mag., 31: 413—416.

Pinsker, Z.G., 1953. Electron Diffraction. Butterworth, London.

Riecke, W.D., 1961. Über die Genauigkeit der Übereinstimmung von ausgewähltem und beugendem Bereich bei der Feinbereichs-Elektronenbeugung im Le Pooleschen Strahlengang. Optik, 18(6): 278—293.
Roberson, H.E. and Towe, K.M., 1972. Montmorillonite: electron diffraction from two-dimensional single crystals. Science, 176: 908—909.
Rymer, T.B., 1970. Electron Diffraction. Methuen, London.
Steinfink, H., 1962. Crystal structure of a trioctahedral mica: phlogopite. Am. Mineral., 47: 886—896.
Vainshtein, B.K., 1964. Structure Analysis by Electron Diffraction. Pergamon, New York, N.Y.
Warren, B.E., 1969. X-Ray Diffraction. Addison-Wesley, London.
Waser, J., 1955. Fourier transforms and scattering intensities of tubular objects. Acta Crystallogr., 8: 142—150.
Weir, A.H. and Greene-Kelly, R., 1962. Beidellite. Am. Mineral., 17: 137—146.
Whittaker, E.J.W., 1955. The diffraction of X-rays by a cylindrical lattice-II and III. Acta Crystallogr., 8: 261—271.
Wilson, A.J.C., 1948. X-Ray Optics. Methuen, London.
Zvyagin, B.B. and Pinsker, F.G., 1949. Structure of montmorillonite. Dokl. Akad. Nauk SSSR, 68: 65—67, 505—508.

This Page Intentionally Left Blank

Chapter 5

PROPERTIES AND USES OF BENTONITE

Bentonites have a wide variety of uses in many different industries. They are components in many commercial products. Also the presence of a bentonite component in clays and soils may significantly affect the properties of such materials, and hence be of importance in agriculture, construction engineering, ceramics, etc. The use of bentonites depends on their properties, hence it is desirable to consider uses and properties together.

5.1. GENERAL STATEMENT

The properties of bentonites are contingent upon the fact that they are composed of smectite clay minerals, and the properties of the smectite in turn are contingent upon its chemical composition, atomic structure, and morphology. As discussed in detail elsewhere in this volume, smectites have unique structural attributes. The mineral is composed of silica and alumina sheet-like units arranged in such a way that smectites are essentially books of sheets or laths, or bundles of needles. The individual sheets or laths or needles are loosely tied together — in fact water can enter between the sheets, laths, or needles separating them. As a consequence, smectite clays are readily dispersed in water into extremely small particles.

Because of the structure of the flat surfaces of the individual particles, the water adsorbed on these surfaces has distinctive properties. The water immediately on the surface is composed of oriented water molecules, and hence does not have the properties of liquid water (Grim, 1968). The orientation of the water molecules decreases outward from the surfaces. The composition of the smectite is always such as to leave it unbalanced with a net negative charge which is balanced by an adsorbed cation such as sodium, calcium, etc. These balancing cations are found on the surfaces of the smectite units and determine to a large extent the ease of separation, i.e. the dispersion of the mineral and the character and thickness of the adsorbed water layer.

The foregoing attributes of smectites determine their properties in water systems, for example, viscosity, thixotropy, plasticity, shrinkage, bonding

strength, shear strength, water impedance, etc. Further, it follows that these properties will not be the same for all smectites. They will vary depending on the identity of the adsorbed balancing cations. Since the balancing cations can be changed by simple mechanical treatment, some of the properties of smectite clays can be manipulated as desired. Or the properties can be altered inadvertently sometimes with disastrous results.

Organic as well as inorganic cations may serve to balance the negative charge on the smectite units. Further, the structure of the surface permits the adsorption of many nonionic organic compounds, for example, various polar organic molecules. The organic compounds may coat the surfaces of the smectite units thereby destroying their water adsorbing capacity and making them hydrophobic and oleophyllic. Such smectite-organic complexes have interesting properties and industrial uses. The properties of the adsorbed organic compounds may be changed, i.e. the clay may have a catalytic effect on the organic compound which opens up areas of industrial use, for example, in decolorizing oils and in the preparation of catalysts.

As noted elsewhere (pp. 143—145), the chemical composition of smectites varies, and the smectite particles occur in a variety of habit and modes of aggregation. Some properties and hence some uses are contingent on the habit of the particles, thus the sheet-like units are desired for water impedance. The phases formed when smectites are heated to elevated temperatures are related primarily to the chemical composition, and hence certain ceramic uses are related to the chemical composition of the smectites.

Because of all the foregoing characteristics, some properties of bentonites will vary from sample to sample even in a given deposit. Also some of the properties may vary as a consequence of processing, e.g. on the amount of drying and grinding. Thus, the figures and values given in the following discussion for the various properties must be considered only in general terms.

5.2. PROPERTIES RELATED TO CERAMICS

Plasticity

Plasticity may be defined as the property of a material which permits it to be deformed under stress without rupturing and to retain the shape produced after the stress is removed. Clay materials develop plasticity when mixed with relatively small amounts of water. In general, three ways to approach the measurement of plasticity have been followed. One is to determine the amount of water necessary to develop optimum plasticity or the range of water contents in which plasticity is demonstrated. Determinations of the Water of Plasticity and the Atterberg (1911, 1912) values of Plastic Limit, Liquid Limit, and Plasticity Index would be placed in this category. A second method is to determine the amount of penetration of a needle or

some type of plunger into a plastic mass of clay under a given load or rate of loading (Whittemore, 1935). A third way is to determine the stress necessary to deform the clay, and the maximum deformation the clay will undergo before rupture — at different moisture contents and with varying rates of stress application.

Water of Plasticity (Table 5.1) of a clay is the percent water, determined on a dry weight basis, usually at about 105°C, necessary to develop optimum plasticity. The optimum point is an arbitrary matter, but usually this is readily determinable. Each clay mineral will show a range of values for Water of Plasticity since particle size, crystallinity of the clay mineral, and exchangeable cation composition also exert an influence. In the case of smectites, the Water of Plasticity varies greatly with the nature of the exchangeable cation with sodium giving especially high values. Because of the pronounced thixotropy of many smectite clays, the value for Water of Plasticity may be difficult to measure.

In the Atterberg method, the range of moisture contents from that value just adequate for powdered clay to form a coherent mass (Plastic Limit) to that value where an extremely small stress causes deformation (Liquid Limit) is determined (Table 5.2). The difference between the Liquid Limit and the Plastic Limit is the Plasticity Index. Smectites show a wide range of values, especially Liquid Limits, with smectites carrying sodium being extremely high.

Stress—strain values (Graham and Sullivan, 1939) show that smectites in general require more water than the other clay minerals to develop plastic properties, less force to yield, and less force to yield continuously. Further, values for smectite vary with the nature of the exchangeable cation, and the effect of a particular cation may be different from that for the other clay minerals.

Green strength

Green strength is measured as a transverse breaking strength of a test bar suspended between two narrow supports (Table 5.3). It varies tremendously with small variations in water content. The strength with water equal to the Water of Plasticity is in general lower than the maximum value.

The maximum green strength of smectites is greater, by a factor of about

TABLE 5.1

Water of plasticity in percent by weight (after White, 1947)

Kaolinite	9— 56
Illite	17— 39
Smectite	83—250

TABLE 5.2

Atterberg Limit values, modified after Fendius and Endell, (1935)

	Plastic limit	Liquid limit
Kaolinite	35—45	50—75
Ca-smectite	90	160
Na-smectite	75	500

2, than that of the other clay minerals. However, at Water of Plasticity values, the green strength of smectites is likely to be less than that of the other clay minerals, by a factor of about 2, as a consequence of the considerably higher Water of Plasticity values for smectites.

Small amounts of nonclay minerals may actually increase the green strength of clay bodies because they permit a more uniform texture to be developed. The permissible amount of nonclay material causing an increase in strength would be expected to be higher for smectites than for the other clay minerals.

Drying shrinkage

Drying shrinkage (Table 5.4) is the reduction in length or volume of a mass of shaped clay that takes place when the mass is dried at 105°C for at least 5 h. The measurement is made normally on bodies prepared at Water of Plasticity values.

Drying shrinkage tends to increase with decreasing particle size, and decreasing crystallinity. Regarding exchangeable cations, sodium smectites show relatively high drying shrinkage. The presence of nonclay in a ceramic body tends to reduce drying shrinkage. In the absence of a substantial (25%) of nonclay minerals, smectite clays are difficult to dry without developing cracks and planes of weakness because of the high shrinkage.

Dry strength

Dry strength is a measure of the transverse breaking strength of a test piece after drying at 105°C for about 5 h. The dry strength of all the clay

TABLE 5.3

Maximum green strength (after Hofmann, 1956)

Kaolinite	0.35—3 kg/cm^2
Illite	0.35—3 kg/cm^2
Smectite	5+ kg/cm^2

TABLE 5.4

Linear drying shrinkage (after White, 1947)

Kaolinite	3—10 percent of dry length
Illite	4—11 percent of dry length
Smectite	12—13 percent of dry length

minerals show a tremendous range (10—1000 lb/inch^2) depending on particle size, perfection of crystallinity, and, especially for the smectites, the nature of the exchangeable cations. Measurements made on test pieces containing considerable nonclay granular material yield somewhat different results than those of the pure clay minerals, especially for smectites. The addition of a small amount of smectite to a clay body with other clay minerals may greatly increase the strength. Thus the addition of 5% of smectite to a kaolinite body increased the strength from about 280 to 730 psi (Grim, 1962).

Firing properties

Shrinkage and pore water is lost on heating clay bodies to 100—150°C. Smectites lose the expanding property of their lattice on heating to 100—300°C with the precise temperature depending on the chemical composition and the nature of the exchangeable cation (Grim, 1962). Between about 450 and 700°C, the hydroxyl water is lost from the smectite lattice, again with the exact temperature depending on the chemical composition and the nature of the exchangeable cations. In the case of dioctahedral smectites, the loss of hydroxyls is not accompanied by loss of structure and there is substantially no shrinkage. In the case of the trioctahedral smectites, the structure tends to be lost with the removal of the hydroxyls and there may be some accompanying shrinkage.

In the case of dioctahedral smectites, the structure is lost at about 900°C. Above this temperature, smectites develop a variety of new crystalline phases depending on their structure and chemical composition. For many smectites there is an initial phase depending on structure with later phases developing at higher temperatures where chemical composition is the major control. Grim (1962) has summarized the phases developed at high temperatures by the various clay minerals, and his work should be consulted for details.

The formation of high temperature phases is accompanied by vitrification and shrinkage which may be as much as 20% for pure smectites. Fusion temperature ranges from about 1000°C for iron-rich smectites to 1500°C for those low in iron. For the iron-rich varieties fusion follows loss of structure quickly with little or no intermediate crystalline phase formation. Many, but

not all, smectites contain sufficient iron to produce a red to brown firing color.

General statement

Because of the high water of plasticity and hence shrinkage properties, smectite clays would not be expected to be prime ceramic raw materials. However, small amounts of smectite, especially the low iron varieties, may be very valuable ingredients to ceramic bodies as small amounts give valuable strength and in some cases shrinkage and vitrification properties. Also, the property of dispersing in water to provide slips with good suspension characters makes them valuable in slip casting processes, and in porcelain enamel formulations.

5.3. PROPERTIES RELATED TO USES IN FOUNDRY MOLDING SANDS

Molding sands, which are composed of sand and clay, are used extensively in the metallurgical industry in shaping metal by the casting process. The clay provides bonding strength and plasticity to the sand—clay mixture. A small amount of water, called tempering water, must be added to the mixture to make it somewhat plastic and cohesive so that it can be molded around a pattern, and to give it sufficient strength to maintain the cavity after the pattern is removed and while hot metal is poured into it. These properties vary greatly with the amount of tempering water. The hot metal may be cast in molding sands with the tempering water (green state), or after drying to remove the tempering water (dry state). Thus, both green and dry strength are important properties of molding sands. Flowability and hot strength are also important characteristics of molding sands.

Green compression strength

Green compression strength is the compressive force necessary to cause failure in a test specimen containing tempering water and compacted by ramming a specific amount. Tests are made with varying amounts of tempering water. The Temper Point at which a sand—clay mixture has optimum molding properties is generally at a higher water content than that required for maximum strength. At maximum green strength, the mixture is generally too brittle and insufficiently plastic to use. The following data are largely from Grim (1962) and Grim and Cuthbert (1945).

As shown in Fig. 5.1, there is considerable variation in green strength for various smectite clays. Figs. 5.2 and 5.3 show the relation of amount of tempering water and amount of clay to the green compression strength of a sodium and a calcium bentonite. Fig. 5.4 shows the maximum green com-

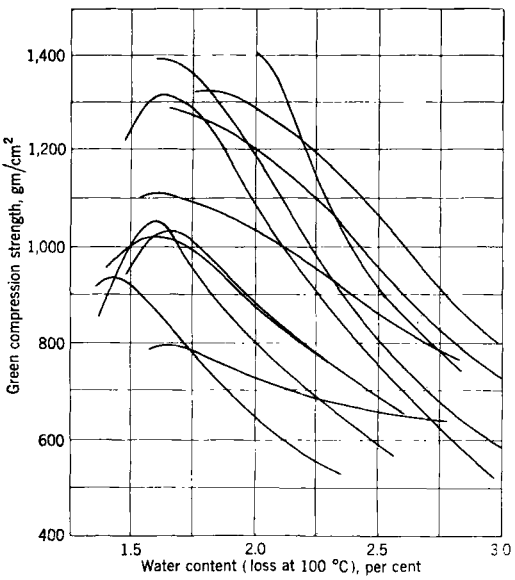

Fig. 5.1. Green compression strength of various bentonites (after Hofmann, 1956).

pression strength for varying amounts, up to 15%, of several types of clay. The calcium bentonites have the highest green strength as compared to sodium bentonite, halloysite, illite and kaolinite clays.

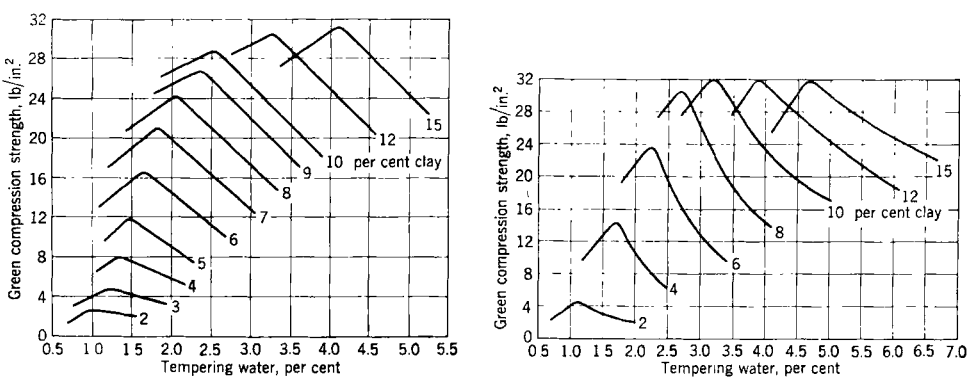

Fig. 5.2. Green compression strength versus amount of tempering water in sands bonded with varying amounts of a sodium bentonite.

Fig. 5.3. Green compression strength versus amount of tempering water in sands bonded with varying amounts of a calcium bentonite.

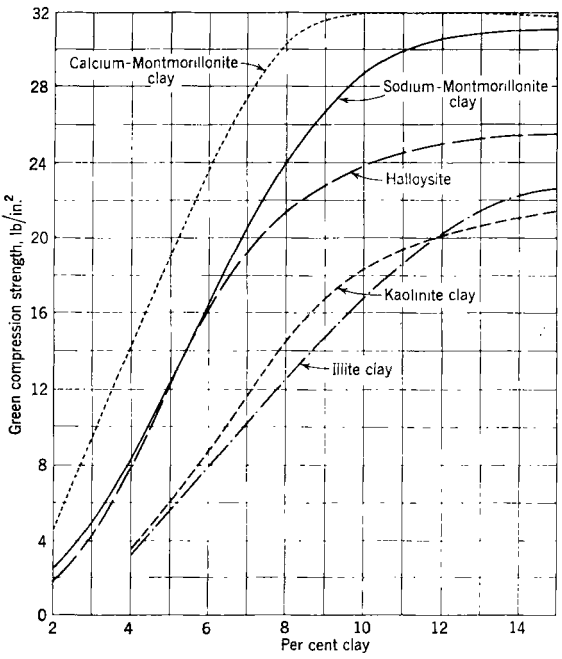

Fig. 5.4. Curves showing the maximum green compression strength developed by each type of clay in relation to the amount of clay in the sand—clay mixture.

Dry compression strength

Dry compression strength is the compressive force necessary to cause failure in a rammed specimen that has been dried in an oven to remove all tempering water and then allowed to cool in a dessicator. Again, the results vary with the amount of tempering water. Maximum dry strength is attained at a higher moisture content than maximum green strength — frequently at the point of minimum bulk density and at about the Temper Point.

The relation between dry compression strength and amount of tempering water for various quantities of a sodium bentonite and a calcium bentonite in a sand—clay mixture is shown in Figs. 5.5 and 5.6, respectively. The curves show the extremely high dry strength developed in the sand bonded with the sodium bentonite even with small (4%) amounts of clay. The curves also show the very great variation in dry strength with extremely small amounts of tempering water. A comparison of Figs. 5.5 and 5.6 shows that the calcium bentonite tends to develop much lower dry strength than the sodium bentonite. Further, the dry strength of the calcium bentonite bonded sand increases with the amount of tempering water up to a maximum value which is reached abruptly. The maximum value is about the same

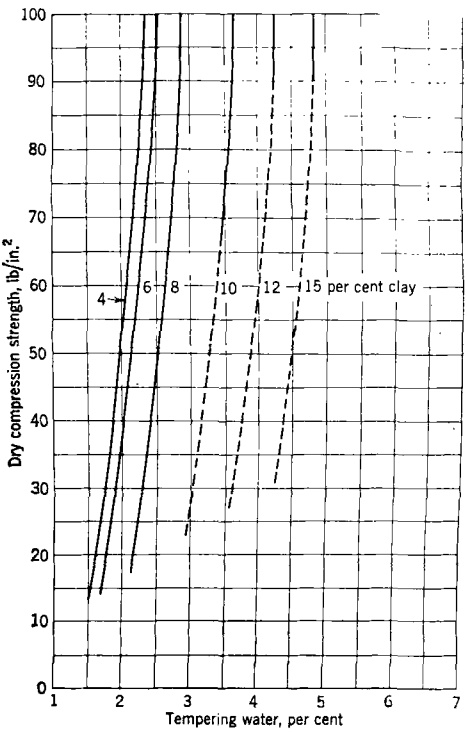

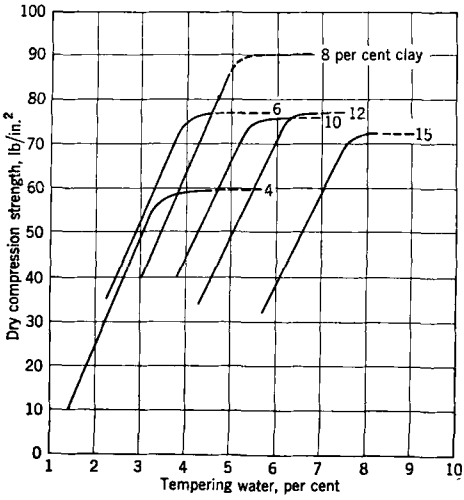

Fig. 5.5. Dry compression strength versus amount of tempering water in sands bonded with varying amounts of a sodium bentonite.

Fig. 5.6. Dry compression strength versus amount of tempering water in sands bonded with varying amounts of a calcium bentonite.

for mixtures containing about 6 or a higher percentage of clay. Hofmann (1956) has shown that treating some calcium smectite clays with sodium salts tends to increase dry strength. This author (Hofmann, 1970) also has indicated that bentonites with relatively high contents of magnesium and iron are likely to have superior bonding properties.

Hot strength

Hot strength is the compressive force necessary to cause failure of a rammed test specimen at an elevated temperature. Although test data are scant, it appears that hot strength also varies with the amount of tempering water. The practical value of hot strength data have been questioned, because the test procedures may not be closely related to the actual use of molding sands in practice.

Fig. 5.7 shows that the compression strength of a sodium bentonite bonded sand increases slowly (up to about 1000°F), then rapidly increases (to 1800°F), after which it declines abruptly. A calcium bentonite bonded sand developed much less hot strength than the sand bonded with the sodium bentonite. The strength of specimens allowed to cool after heating generally is much less than its hot strength.

Flowability

Dunbeck (1942) has listed flowability in relation to clay mineral composition as follows in decreasing order: calcium smectite, illite, kaolinite, and sodium smectite. Grim and Johns (1957) have shown that for smectite bonded sands, good flowability may require tempering water considerably in excess of that required for maximum green strength.

Permeability

Permeability may be determined on the green or dried test specimens. The particle-size distribution of the sand grains rather than the clay is the major factor influencing permeability. However, because relatively small amounts of smectite clays are required in molding sands, the permeability of such sands is relatively high as compared to sands bonded with other clay minerals.

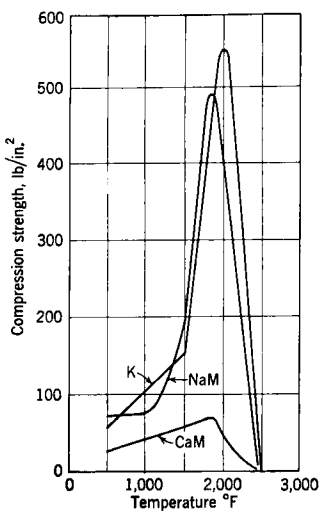

Fig. 5.7. Hot compression strength of sand bonded with sodium bentonite (NaM), calcium bentonite (CaM) and kaolin (K), with 5% NaM, 4% CaM, and 12% K at about temper point (modified after Dunbeck, 1942).

General comments

Although the potential value of a clay for use in molding sands can be evaluated by the determination of green strength, dry strength, etc., a final evaluation can only be made after the clay is actually used in foundry practice. The reason is that flowability, durability, ease of shake out of the casting from the mold, cleanness of the surface of the cast metal, etc., cannot be determined except by preparing molds using the clay and casting hot metal into it.

Recently, foundry sand mixtures have come into use which are bonded with a clay so prepared that it is wettable in oil, and oil instead of tempering water is used. It is claimed that such sands are advantageous for small castings which are required to have an especially clean surface. Smectite-clays that have been reacted with organic molecules to coat the surfaces of the particles and thereby to render the surface oleophyllic have been used in such foundry sand mixtures.

Sakawa et al. (1969) have reported that irradiation of bentonite with gamma or X-rays alters their bonding properties.

5.4. PROPERTIES RELATED TO USES IN THE PETROLEUM INDUSTRY

The unique properties of bentonites cause them to have several uses in the petroleum industry — as components of drilling fluids in the recovery of petroleum, and as source materials for catalysts, decolorizing agents, etc., in the refining of petroleum. The clay mineral component of bentonites, i.e smectites, when present in reservoir rocks is important in secondary recovery operations, because of its influence on permeability (Grim, 1962). Further, it has been suggested (Grim, 1947; Johns and Shimoyama, 1972) that the clay minerals acted as catalysts in the transformation of buried organic material to petroleum.

Drilling fluids

In drilling operations by the rotary method, a fluid is maintained in the hole at all times. The fluid is pumped down through the hollow drill stem emerging at the bottom through "eyes" in the bit. It rises to the surface in the annular space between the drill stem and the walls of the hole and flows into a pit for the removal of cuttings and entrained gas. From the pit it is recirculated down the hole. The function of the drilling fluid is to remove cuttings, to keep formations fluids confined to their formations, to lubricate the bit, and to build an impervious coating on the wall of the hole in order to impede the penetration of water from the drilling fluid into the formation. The impervious character must be developed in a very thin coating that has a certain strength and toughness making it resistant to erosion by abra-

sion of the drill stem in the drilling operation.

Viscosities greater than that of water are required to facilitate the removal of cuttings. Viscosities of about 15 centipoises are common. Further, the drilling fluid should be markedly thixotropic so that cuttings do not settle to the bottom of the hole and "freeze" the drill stem when pumping or agitation of the drilling fluid ceases temporarily. It is desirable that the viscosity and thixotropy of the drilling fluid be altered relatively little by large variations in concentrations of electrolytes as may be encountered in the drilling operation. Further, the fluid should be little influenced by elevated temperatures which may be encountered in deep drilling operations.

It is obvious from the foregoing statements that water alone is not a satisfactory drilling fluid. Bentonites as ingredients in drilling fluids have been found to yield the desired properties, and thus are widely used for this purpose. Various organic and inorganic chemicals and weighting materials, such as barites, to increase the specific gravity of the fluid, may also be components of the drilling fluid to attain the desired properties and to maintain them in the drilling operations. Indeed, an elaborate and important drilling mud technology to develop and maintain desired properties has developed in recent years which is beyond the scope of this volume.

The qualification of clays for use in drilling fluids is measured primarily by the number of barrels of mud of a given viscosity (usually 15 centipoises) obtained from a ton of clay in fresh water and salt water; by the gel strength, which is the difference in yield value immediately after agitation and after standing 10 minutes; and by the wall building properties as measured by the water loss through a filter paper when a 15-centipoises clay is subjected to a pressure of 100 psi and as determined by the thickness and character of the filter cake produced in the standard American Petroleum Institute water loss test. The data in Figs. 5.8 and 5.9 and Table 5.5 after Larsen (1955), giving the characteristics of a sodium bentonite and a calcium bentonite as well as similar data for other clays show the suitability of bentonites for use in drilling fluids. It is generally known that weathering of bentonites tends to enhance their drilling mud properties.

Some of the bentonites from the Wyoming area are extensively and widely used all over the world as ingredients in drilling fluids. The particular valuable property of this bentonite carrying sodium as the major exchangeable cation is that the smectite component is made up of relatively large flakes which disperse readily in water into very thin units (see p. 20). Because of these characteristics of the smectite, the bentonite gives yields commonly in excess of 100 barrels/ton. Only 5% of the bentonite is necessary to produce the desired viscosity. This clay also has very high gel strength, but is particularly outstanding for its low filter cake permeability. Commonly the yield of bentonites can be improved by treatment with a sodium salt, usually soda ash, but in general such treatment does not improve substantially the water loss property.

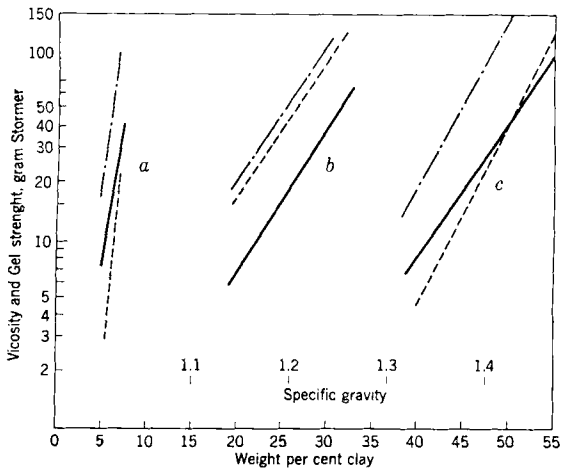

Fig. 5.8. Viscosity and gel strength of sodium bentonite (*a*), calcium bentonite (*b*), and an illite clay (*c*) (after Larsen, 1955). — · — · = shear strength after 10 min; · · · · = shear strength immediately after agitation; ——— = so-called stormer viscosity at 600 rpm.

Clays composed of the hectorite member of the smectite group as indicated in Table 5.5 give very high yields. Recently clays from the Amargosa Valley in Nevada which are composed of sepiolite and the saponite member of the smectite group are reported to yield very satisfactory drilling fluids. Drilling fluids prepared with the sepiolite have proven to be especially resistant to high pH environments and elevated temperatures.

Catalysts

In the cracking process of petroleum refining, heavy oil in the vapor state is contacted with a catalyst at 425 to 500°C under atmospheric pressure and for contact times of 6—20 sec. Under the influence of the catalyst, a series of complicated reactions take place leading to the formation of about 5% methane and propane, 10% butane, 45% gasoline, and 40% unchanged feed stock. In addition, 1 to about 3% of the charged stock is reduced to carbon which is deposited on the catalyst.

Two types of catalysts, both essentially composed of aluminum and silicon are used. One type is synthesized from silicon and aluminum compounds, and the other type is produced from clays of certain types. The catalyst must give the desired level of conversion and a satisfactory product distribution. In addition, the catalyst must be very hard to resist abrasion in the operation of the cracking unit, must have long life, and must be resistant to poisoning by such elements as sulfur in the feed stock.

Clay catalysts are produced from bentonites and from halloysite and kaolinite clays. The specifications required of bentonites for catalyst

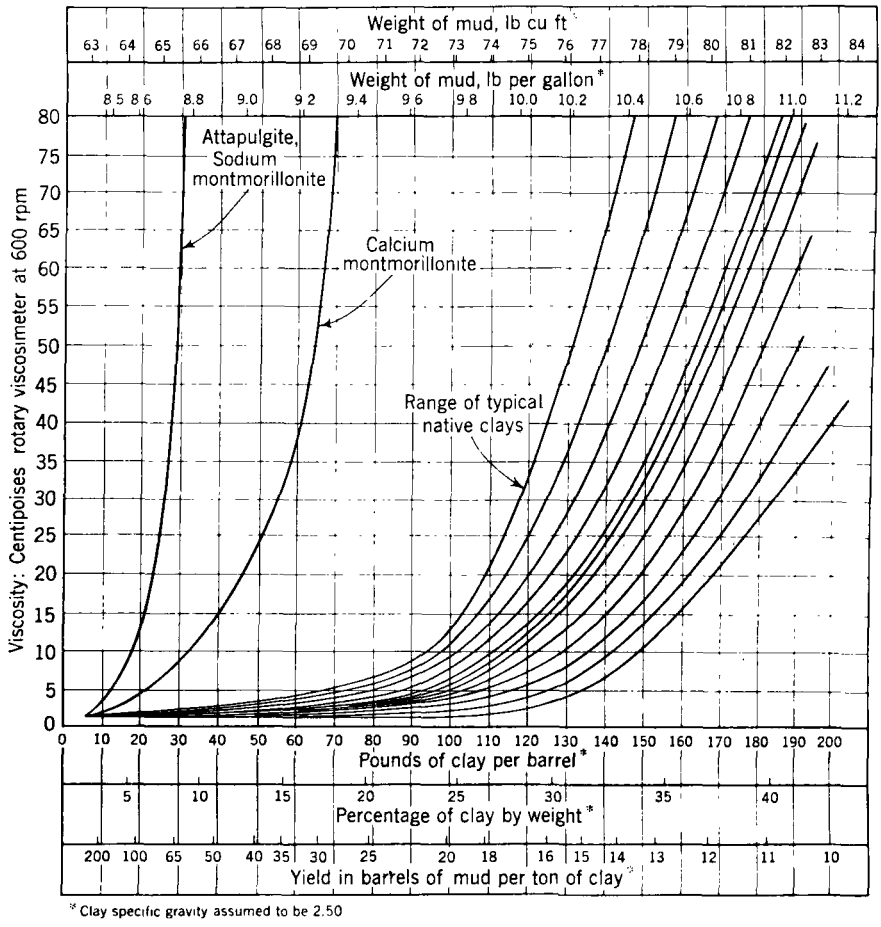

Fig. 5.9. Viscosity and weight of mud in relation to percentage of bentonites and native clays in fresh water (after "Drilling Mud" — Anon. Baroid Division National Lead Co., 1953).

manufacture are not well known, except that they must be substantially pure smectite, and the smectite must have an extremely low iron content.

Details of the procedures for the production of catalysts from bentonite have not been revealed in detail by the manufacturers, but in general the process involves treatment of the crude clay with sulfuric or hydrochloric acid at moderately elevated temperatures followed by washing, drying, and preparation into the desired particle-size distribution, and calcining at about 500—600°C. The process involves the removal of adsorbed alkalies and alkaline earths, and a fairly complete removal of iron and partial removal of magnesium and aluminum from the smectite lattice. Acid treatment

TABLE 5.5

Yield and water loss data for various types of clay minerals (after Larsen, 1955)

Clay mineral	Yield bbl. 15 cp mud/ton in fresh water	Solids in filter cake (wt. %)	A.P.I. water loss at 15 cp	Filter cake permeability (microdarcys)	pH
Hectorite, Calif.	160	6.5	7	0.85	8.6
Na-bentonite, Wyom.	125	10	11	1.8	8.2
Ca-bentonite, Calif.	71	16	15	2.1	8.7
Ca-bentonite, Texas	18	50	11	1.5	7.5
Attapulgite, Georgia	105	23	105	68	7.1
Illite, Illinois	13	67	57	38	7.4

increases the surface area and alters the pore-size distribution of the material. X-ray diffraction patterns of the catalyst preparations show that some smectite crystallization is retained, but the patterns are more diffuse than those of the untreated clay indicating that the smectite has less order, is of smaller particle size, and/or contains some material with very little order.

For kaolinite or halloysite clays the process may be different involving reaction with sodium compounds and the development of a zeolitic structure.

For references to theories explaining the catalytic activity, and to the catalytic activity of clays for other material than petroleum, the volume by Grim (1962) should be consulted.

Decolorization

Clay materials are widely used to decolorize various mineral, vegetable, and animal oils, such as hydrocarbons, cottonseed, soy, palm, and lard. The earths may serve to deodorize, dehydrate, and neutralize as well as decolorize the oils. The clay or earth must cause a large amount of color reduction, must have low oil retention, must have good filtration characteristics, must not alter detrimentally the character of the oil, and must not impart objectionable color or taste to the oil.

Some clay materials and silts with no more processing than drying and pulverizing possess adequate decolorizing ability for commercial use. Such materials are so-called *fuller's earths.* Some bentonites as well as clays composed of attapulgite can be classed as fuller's earths. The reason why some bentonites and not others are satisfactory as fuller's earths is not known.

Acid activation frequently enhances the decolorizing property of bentonites several fold. The activation process is in general terms similar to that used in the manufacture of catalysts from bentonites. Some bentonites are

more susceptible to acid activation than others and the optimum treatment process, i.e. acid concentration, temperature, reaction time, etc., varies from one bentonite to another. Further, the optimum treating conditions are not the same for all types of oil to be decolorized. The fundamental factors of smectite structure and composition that control the susceptibility, etc., to acid activation are not well known.

There are some bentonites commonly designated as "acid clays", for example, Japanese acid earths (Yamamoto, 1940) and clays from the Pembina area in Manitoba, Canada, which apparently have been subjected to natural leaching with low-Ph water so that they have been changed naturally in the direction of acid activation.

Other uses

Bentonites are used in the refining of petroleum for a considerable variety of miscellaneous uses. Thus, they may be used to remove sulfur and other deleterious elements that would tend to poison catalysts, to remove undesirable asphaltic and resinous material from petroleum products, to neutralize residual acid in acid treated oil stocks, and as dehydrating agents in refining operations.

5.5. MISCELLANEOUS USES OF BENTONITES

Adhesives

The high dispersion and suspension characteristics of bentonites make them useful in some adhesives such as those made with latex and asphaltic material. A considerable number of United States Patents disclose starch, casein and sodium silicate adhesives containing bentonite as well as those compounded with latex and asphalt. Organic-clad smectites are said to be used in some types of adhesives because of their gelling properties in certain organic liquids.

Animal bedding

Granular grades of clay about 10—30 mesh are used for animal bedding, particularly for household pets. The clay serves as an absorbent and deodorizing agent and must have fairly high absorbent capacity. The clays are heated above 400°C and below 1000°C to develop absorbent capacity, and to provide a material which will not break down to fine particles on use either when wet or dry. It must not form a sticky or plastic mass nor must it become dusty. Some bentonites have been found satisfactory for this use. Various chemicals may be added to the dried granular clay to further control odor, and to provide disinfectant and pesticide properties.

Atomic (radioactive) waste disposal

The disposal of waste waters and solutions carrying radioactive materials of high biological toxicity is a vital factor in the development of atomic energy. Isotopes of strontium and cesium are particularly important because of their long half life. The use of clay has been suggested as a means of absorbing the isotopes and then fixing them against leaching by calcining to temperatures adequate to vitrify the clay and thereby to tie up the radioactive material in insoluble compounds. Early work suggested that clays, such as bentonites, with high cation exchange capacity were required. More recently it has appeared that some illites, particularly degraded varieties, might be very suitable because of their specific fixation qualities, even though their cation exchange capacity is relatively low (Kerr, 1954).

Cement, mortar, and aggregates

The addition of small amounts of bentonite (1—2%) to Portland cement in concrete and cement slurries is reported to improve workability, lessen aggregate segregation, and enhance impermeability.

Pozzolanas are siliceous or siliceous—aluminous materials, natural or artificial, processed or unprocessed, which, though not cementitious in themselves, contain constituents that will combine with lime in the presence of water at ordinary temperatures to form compounds which have low solubility and possess cementing properties (Lea, 1938). After calcination in the range of 1200—1800°F, the clay minerals undergo dehydration and structural changes and as a consequence some of them develop pozzolanic properties. In general, kaolinitic clays become more pozzolanic than bentonites (Mielenz et al., 1951). According to Mielenz and King (1955), bentonitic shales have been used in the preparation of pozzolanas.

Clarification of wines, cider, beer, etc.

According to Saywell (1935), some bentonites are effective agents in clarifying wine and reducing its iron content. This author states that such clay can be used also to clarify cider and vinegar. According to Silva (1948), bentonite when used in conjunction with lime is superior to lime alone for the clarification, purification, and decolorization of sugar cane juice. Déribéré and Esme (1951) have summarized the considerable literature on the use of bentonites for the clarification of wines, liquors, cider, beer, vinegar, etc.

Emulsifying, suspending, and stabilizing agents

Bentonites, particularly the highly colloidal sodium variety, are widely used as emulsifying and stabilizing agents in many oil and/or water systems,

and as suspending agents for solid particles in many liquid vehicles. For example, bentonites are used as suspending agents in liquid fertilizers. Organic-clad smectites are used for the same purpose in many organic liquid systems.

Fabrics

There are many reports, particularly in the patent literature, of the possible use of bentonites in fabrics for dressing and finishing, in yarns to reduce shrinkage, undue filament adherence, etc. (Grim, 1962). There is, however, little specific information on the actual use of bentonites for this purpose.

Floor absorbents

Granular bentonites of 10—60 mesh calcined to 400—1000°F to develop absorbent qualities and destroy dispersion properties are used as absorbents for floor cleaning. The major function is to absorb oily substances which would cause slipperiness.

Food

Bentonites are reportedly used in small amounts (1—5%) as bonding agents in pelletizing animal feed, and as suspending agents in wet-mash type feeds. Holden (1948) claims that the addition of 0.25—1.25% by weight of the total cereal content of flour reduces staling in bread and other baked products.

Greases

Organic-clad smectites prepared from bentonites have come to be widely used for stabilizing the gel properties of lubricating greases in place of various soaps. Hauser (1950) and Jordan (1950) have emphasized the superior properties of the greases prepared with organic-clad smectites. Various types of organic molecules are used to coat the particles — the type depending on the composition of the grease to be stabilized.

Ink

Organic-clad smectites are reportedly used (Curado and Praeg, 1956; Voet and Yelmgren, 1956) in some inks to control consistency, penetration, and misting during the printing operation.

Medicines, pharmaceuticals, and cosmetics

The literature, particularly the patent literature, contains many suggested formulations which contain bentonite, but how widely bentonite is actually

used in such preparations is not generally known. Cuciureanu et al. (1972) report that the stability of some antibiotics is increased when they are incorporated in bentonite pastes. Novelli (1972) has recently pointed out that the medicinal use of bentonite includes its antidotal effect in morphine, cocaine, nicotine, and strychnine toxicities; improvement of barium sulphate suspensions for radiological examinations; and its use in the purification and concentration of vitamin preparations.

Paint

The vehicle in paint may be oil, latex, water, or any one of a large number of organic chemicals. The various types of clay used in paint are not necessarily only inert fillers but may add valuable properties to the paint, and indeed they are essential components of some types of paint.

Bentonites are used in both oil and water-based paints. In water-based paints, the bentonite acts as a suspending and thickening agent. It is also used as an emulsifying agent in water and oil-based paints.

Organic-clad smectites, tailor-made with a variety of organic compounds to meet the requirements of different vehicles, such as lacquers, epoxy resins and vinyl resins, are widely used in paint formulations. These clays are said to improve pigment suspensions, viscosity, and thixotropy control. They also improve brushability and spraying characteristics, and permit some control of the penetration of the vehicle into porous surfaces.

Paper

Clays composed of kaolinite rather than bentonite are used extensively in filling and coating paper. The thixotropic and viscosity characteristics of bentonites are in general not desirable attributes in paper manufacture. However, there are reported special uses of bentonite in the paper industry (Grim, 1962). Thus, it is claimed that the addition of about 1% of bentonite to the pulp slurry tends to prevent the agglomeration of fine particles of pitch, tar, waxes, and resinous material which cause defects in the paper sheet. It is also claimed that this amount of bentonite in the pulp will increase the retention of pigments in the paper stock and enhance the uniformity of the distribution of pigment throughout the paper.

Bentonite is said to be used in de-inking old newsprint paper. Following chemical treatment to free the ink pigment, bentonite is used to disperse the pigment particles and to adsorb them.

Pelletizing ores, fluxes, fuels, etc.

Bentonites are widely used in pelletizing iron ores (De Vaney, 1956). Finely ground ore concentrate must be pelletized into units of the order of one inch or more in diameter before it can be used as blast furnace feed. In recent years this has become an extremely large and important use of bentonites. It has been found that pelletized ore, perhaps because of its uniform-

ity in composition and particle size, is a superior blast furnace feed. Bentonite with high dry strength in amounts of about 0.5% of the weight of the ore is commonly used. According to Abbot and Anderson (1940), Rick and Loetel (1940), and Klinefelter (1946), bentonite may be used for pelletizing other ores as well as fuels and fluxes.

Pesticides

Various types of clay are used as carriers and diluents in pesticide preparation. The clay is important in attaining uniform dispersions of the toxicant, in the retention of the pesticide by the plants, and in the preservation of the toxicity of the pesticide. The latter point has not always been realized, and only in recent years has much attention been given to the way in which clay additives may influence the toxicity of the pesticides. In this instance, the catalytic property of the clay mineral may be undesirable. Judging by the patent literature, bentonites are components of many pesticide formulations.

Rubber

Bentonite clays are used as additives to latex for the purpose of thickening and stabilizing. They are also used as emulsion stabilizers, for example, in rubber-based paints, and in rubber adhesives (Hauser, 1955).

Smectite-organic complexes

It has been known for a long time that smectite-organic complexes can be formed by ion-exchange reactions. Depending on the size and nature of the organic cation, the smectite particles of bentonite may be completely clad with organic molecules one or more molecular layers in thickness. Such organic-clad particles are hydrophobic and oleophylic. They may be polymerized with a variety of organic compounds.

It has been known for a long time that smectite-organic complexes can be formed by the reaction of smectites with polar organic molecules. The acidity of the reaction increases with the polarity of the organic molecule and may be sufficient to replace adsorbed water. The polar molecules are thought to be held through hydrogen bonds. In the case of highly polar molecules, layers several molecules thick can be adsorbed on the basal surfaces of smectites.

In recent years a vast amount of research has been done on the types of organics which will react with the clay minerals, the orientation of the organic molecules on the clay mineral surfaces, the properties of the resulting complex, etc. For an introduction to this subject, see Grim (1968).

Organic-clad bentonites are produced commercially and sold under the trade names BENTONE, ASTROTONE, etc. Some of the commercial uses of such products are indicated elsewhere in this chapter.

Soaps, cleaning, and polishing compounds

According to Déribéré and Esme (1951), bentonites are used in soaps as a partial replacement for the fatty-acid component because of their emulsifying action, their affinity for carbon particles, and their detergent effect. According to Fleury-Larsonneau and André (1942), acid treatment of the bentonite improves the detergent action. Hirschmann and Bechtner (1938) claim that bentonite in addition to its detergent action, acts as a dispersing agent to improve the efficiency of soaps. Further, the sodium bentonites have a beneficial water softening action.

The literature, particularly the patent literature (see Grim, 1962), mentions many cleaning and polishing formulations containing bentonite.

Water clarification

Bentonites, because of their dispersion and absorbing properties, have been used in water clarification. Frequently the bentonite is added to the water followed by the addition of alum. The alum flocculates the clay which serves to gather up and collect the colloidal material which would otherwise not settle. According to Olin et al. (1942), similar treatment of paper mill wastes, sewage, and industrial wastes by bentonite is satisfactory for their clarification.

Water impedance

Bentonite, particularly the sodium variety from Wyoming, is used extensively to impede the movement of water through earthen structures and to retard or stop similar movement through cracks and fissures in rock and concrete structures. It is used to stop the seepage of water from ponds and irrigation ditches, and to waterproof the outsides of basement walls of homes.

The bentonite may be used as a grout in which a bentonite suspension is injected under pressure into a porous strata, fissure, or crack. The bentonite may be placed as a blanket between the earth and the water, or mixed with the surface soil of the structure to render the soil impervious. Frequently one part of bentonite to five parts of soil is adequate to develop the imperviousness desired.

5.6. PROPERTIES RELATED TO ENGINEERING APPLICATIONS

It is necessary frequently to build structures on, through, or with clay materials. The properties of such clay materials is obviously important to the engineer in the design and building of such structures. The clay mineral

characteristics of such materials are therefore important as they exert a major influence on the various properties that are important to the engineer. At places bentonites or clays with significant contents of smectites are the clay materials involved in construction. It is the object of the following statements to summarize the available data on the influence of such clay materials on the various physical properties of interest and importance to the construction engineer.

Plasticity

Engineers have found it convenient to express the plastic properties of clay materials in terms of the Atterberg Limits (see discussion of Ceramic Properties, p. 218). They have found limit values to be very useful as index properties which may be correlated with other properties such as shear strength and compressibility.

Atterberg Limit values for bentonites, as shown in Table 5.6, are significantly higher than those for illite clays and kaolins which are in the range of common nonbentonic clay materials. The data also show that the limit values for bentonites may vary substantially depending on the nature of the exchangeable cation whereas for the illite clays and kaolin the variations are very small.

The presence of sodium and lithium as exchangeable cations in smectite clays leads to high plastic limits and extremely high liquid limits — in fact the liquid limit is so high, and because of the thixotropic character of such material, it is difficult to determine.

Natural bentonites commonly carry sodium or calcium as the dominant exchangeable cation. The data in Table 5.6 show, therefore, that the limit values for natural bentonites can vary widely. The very high limit values for the sodium variety of bentonites would make such material extremely difficult for the engineer because of its other properties, such as shear strength, compaction, etc. Since the limit values for bentonites vary substantially with the nature of the adsorbed cation, any change in the environment in which such clays existed during or after construction could lead to a significant change in properties. In other words, the later properties might be significantly different from those determined on the original undisturbed clay.

Activity

Activity (Skempton, 1953) is the ratio of the Atterberg Plastic Index to the abundance of the clay fraction of a material, defined as the percent dry weight of the minus 2 μm fraction of the sample. Activity, therefore, indicates the plastic index of the clay-size fraction of the material which is generally the clay mineral component. Activity for three bentonites and for

TABLE 5.6

Atterberg Limit values and activities (after White, 1955)

	Ca			Mg			K			NH_4			Na			Li		
	Pw	Lw	Ac	Pw	Lw	Ac	Pw	Lw	Ac	Pw	Lw	Ac	Pw	Lw	Ac	Pw	Lw	Ac
Bentonite A	65	166	1.26	59	158	1.24	57	161	1.30	75	214	1.74	93	344	3.14	80	638	6.98
Bentonite B	65	155	1.20	51	199	1.97	57	125	0.91	75	114	0.52	89	443	4.72	59	565	6.75
Bentonite C	63	177	1.34	53	162	1.24	60	297	2.79	60	323	3.09	97	700	7.09	60	600	6.35
Illite clay A	40	90	0.53	39	83	0.44	43	81	0.38	42	82	0.40	34	61	0.27	41	68	0.27
Illite clay B	36	69	0.33	35	71	0.36	40	72	0.32	37	60	0.23	34	59	0.25	38	63	0.25
Kaolin A	36	73	0.37	30	60	0.30	38	69	0.31	34	75	0.41	26	52	0.26	33	67	0.34
Kaolin B	26	34	0.08	28	39	0.11	28	35	0.07	28	35	0.07	28	29	0.01	28	37	0.09

Pw = plastic limit; Lw = liquid limit; Ac = activity.
Bentonite A, Pontotoc, Mississippi; B, Cheto, Arizona; C, Belle Fourche, Wyoming.
Illite A, Fithian, Illinois; B, Jackson County, Ohio.
Kaolin A, Anna, Illinois; B, Dry Branch, Georgia.

illite clays and kaolin are given in Table 5.6. Activity values (Ac) for the bentonites range from about 0.5 to 7 with the values for sodium bentonites several times greater than the values for the calcium bentonites. Clays with high activity values have relatively high water holding capacity, high compaction under load, low permeability, and low resistance to shear. Because of the high cation-exchange capacity of bentonites, their activity values vary greatly with the nature of the exchangeable cation as shown in Table 5.6.

For a discussion of the theory of plasticity in clay materials, the work of Grim (1962) should be consulted.

Water sorption

The rate of water sorption for a calcium bentonite, a sodium bentonite, two illite clays, and two kaolins is shown in Fig. 5.10 (after White and Pichler, 1959). These data show the very great water sorption for sodium bentonite continuing without a break, whereas the water sorption for the calcium bentonite is rapid initially and then sharply reduced. The break in the curve is at about the liquid limit for the calcium bentonite. The illite clays and the kaolins show much smaller sorption values than either of the bentonites — again there is a break in the curves at about the liquid limit.

Unconfined compression strength

Unconfined compression strength of a clay is the compressive force required to cause failure of an undisturbed sample tested under unconfined conditions. Mielenz and King (1955) give values of 55.5 psi for a sodium bentonite and 100.3 psi for a kaolin for their compressive strengths. These values are only significant in indicating the lower value for the bentonite as compared to clays composed of other minerals than smectites. These authors have also shown that, particularly for clays composed of smectites, the compressive strength of a material composed of a mixture of nonclay minerals and clay minerals may be greater than the strength of the pure clay minerals. This conclusion is shown also by the data presented for bonding clays (pp. 222—225) illustrating the substantial variation of the compressive strength of sand—clay mixtures with varying amounts of various clay minerals. In general, in mixtures of clay minerals and nonclay minerals, smectites tend to produce the highest compressive strength.

Shear strength

Shear strength is measured by the shearing stress at maximum displacement before failure. It is usually determined under conditions of increasing load pressure. Samuels (1950) has shown (Fig. 5.11) the lower shear resistance of sodium bentonite as compared to calcium bentonite, and that the

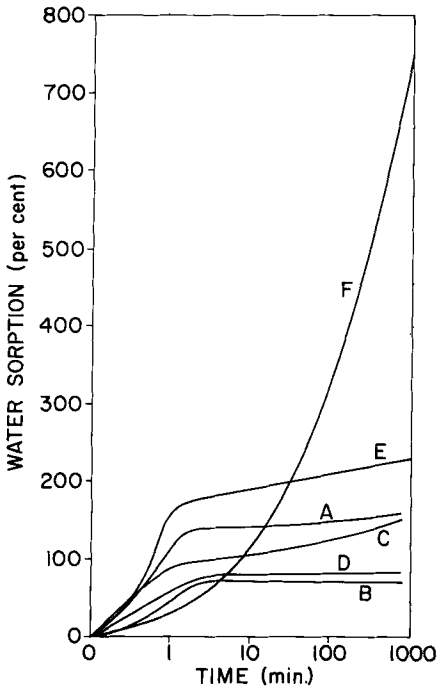

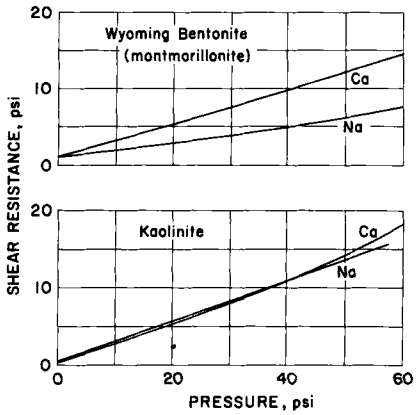

Fig. 5.10. Water-sorption curves. *A* = Illite, Grundy County, Illinois; *B* = Illite, Vermillion County, Illinois; *C* = Kaolin, Union County, Illinois; *D* = Kaolin, Dry Branch, Georgia; *E* = Ca-bentonite, Cheto, Arizona; *F* = Na-bentonite, Belle Fourche, South Dakota.

Fig. 5.11. Shear resistance (after Samuels, 1950).

values for calcium bentonite are only slightly lower than those for a kaolin (and probably also for illite clays). This conclusion must be considered only to have general value as the shear strength of a clay varies with the amount of nonclay components, the moisture content, the load placed on the material, and probably also on its geologic history.

The shear strength of a clay is made up of two parts, namely cohesion and internal friction. Gibson (1953) has shown (Fig. 5.12) that the true angle of internal friction is much smaller for bentonites than for illite clays or kaolins. This means that in bentonites, cohesion contributes a relatively high percentage of the shear strength. According to this same author, in a sodium bentonite sample from Wyoming, cohesion contributed about 80% of the shear strength; in illite clay samples from 40 to 60% of the shear strength; and in a kaolin sample less than 20% of the shear strength. For a calcium bentonite, the contribution of cohesion would be expected to be in the range of the higher illite clay values.

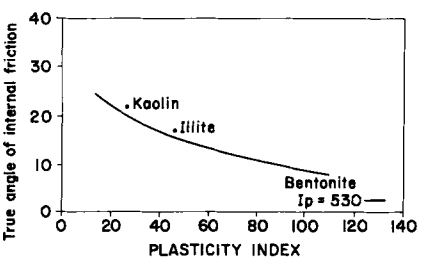

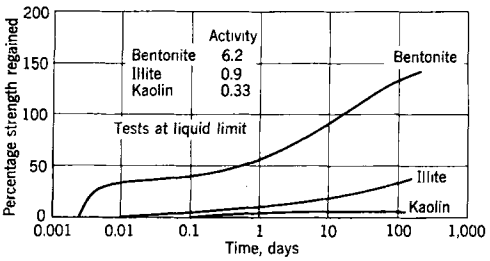

Fig. 5.12. Relation between plasticity index and true angle of internal friction (after Gibson, 1953).

Fig. 5.13. Regain of strength versus time (after Skempton and Northey, 1952).

Sensitivity

Sensitivity is defined by Terzaghi (1944) as the ratio of the strength of a clay material in an undisturbed state to the strength of the remolded material at the same moisture content. Clay materials with high sensitivity values are obviously ones with little or no strength after being disturbed.

Skempton and Northey (1952) show that the sensitivity values for clay materials range from less than one to more than 16. Bentonites fall in the range from 4 to about 8 which are considered reasonably high values. The so-called "Quick Clays" with the highest sensitivity are not bentonites, but generally silty materials with a distinct texture, high liquidity, and a unique geologic history.

Bentonites tend to show a regain in strength when the remolded sample is allowed to stand without the loss of moisture. This characteristic is shown in Fig. 5.13 which also shows that illite clays and kaolins show very slight if any regain in strength. The regain in strength of bentonites is a consequence of the thixotropic property of clays composed of smectite clay minerals.

Permeability

Values for permeability of mica, kaolin, a calcium bentonite, and a sodium bentonite are given in Table 5.7 (after Endell et al., 1938). The values show the relative impermeability of sodium bentonite and the great reduction in permeability of sands with the addition of only very small amounts of sodium bentonite. The calcium bentonite has much less influence on permeability than the sodium bentonite.

Frost heaving

Frost heaving is raising the ground surface by the development of bodies of ice within the clay material. It has been well demonstrated that frost

TABLE 5.7

Permeability of clays and sand—clay mixtures (after Endell et al., 1938)

		Permeability in k (cm/min at 65 kg/cm^2)
Quartz sand		$1 \cdot 10^{-3}$
Quartz sand : mica	9 : 1	$4.6 \cdot 10^{-4}$
	7 : 3	$4.2 \cdot 10^{-4}$
	1 : 1	$5.8 \cdot 10^{-4}$
	0 : 1	$4.9 \cdot 10^{-4}$
Quartz sand : kaolin	9 : 1	$9.5 \cdot 10^{-5}$
	7 : 3	$8.9 \cdot 10^{-6}$
	1 : 1	$2.5 \cdot 10^{-6}$
	0 : 1	$3.0 \cdot 10^{-6}$
Quartz sand : calcium bentonite	9 : 1	$4.3 \cdot 10^{-5}$
	7 : 3	$2.1 \cdot 10^{-6}$
	1 : 1	$5.5 \cdot 10^{-7}$
	0 : 1	$2.0 \cdot 10^{-7}$
Quartz sand : sodium bentonite	9 : 1	$1.6 \cdot 10^{-7}$
	7 : 3	$3.0 \cdot 10^{-8}$
	1 : 1	impermeable
	0 : 1	impermeable

heaving is caused by the movement of water into the freezing zone. Lambe (1953) has shown that bentonites are relatively less prone to frost heaving than materials composed of other clay minerals. The very low permeability of bentonites provides an explanation for this characteristic.

Compressibility and consolidation

Compression refers to the relationship between the increase of unit load on a laterally confined specimen and the corresponding decrease of its void ratio. Void ratio is defined as the ratio of the total volume of voids to the volume of solid constituents of the material.

Samuels (1950) working with samples prepared with initial moisture contents equal to their liquid limit has shown (Fig. 5.14) that for sodium bentonite there is a very large reduction in volume with the application of small pressure, and that further increases in pressure cause only relatively slight reductions in volume. For calcium bentonites the amount of compression is reduced, but there is also a relatively large reduction in volume at low applied pressures. The compressibility of kaolin is considerably less than that of the bentonites with a relatively small initial reduction in volume at small loads. Illite clays would be expected to be generally similar to the kaolins.

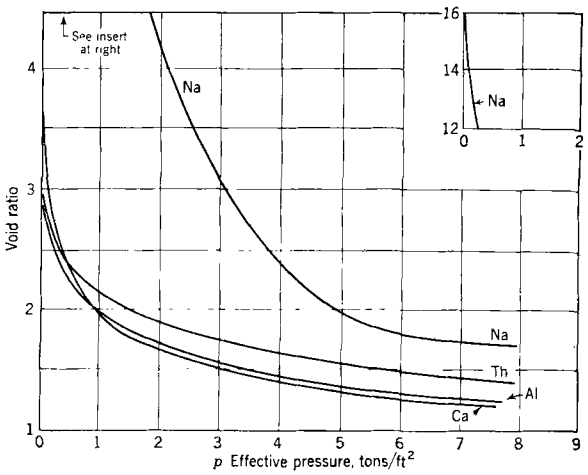

Fig. 5.14. Pressure—void-ratio curves for bentonites (after Samuels, 1950).

The data in Fig. 5.15, also after Samuels (1950), show that the bentonites exhibit a slow initial rate of consolidation with the rate increasing with increasing time. The slow initial rate is particularly slow for the sodium bentonite. In the case of kaolin, there is an initial large reduction in volume at small loads and small rather uniform decreases in volume with increasing loads.

Samuels (1950) has also shown that for bentonites with increasing loads, the rate of consolidation decreases somewhat initially, but after short periods of time an increase in pressure has little effect on the rate. On the other hand for kaolins, increasing pressure increases the rate of consolidation throughout the time of its application. Grim (1962) has offered an explanation for this varying characteristic of bentonites versus kaolin based on the character of the adsorbed water held by smectites versus kaolinites.

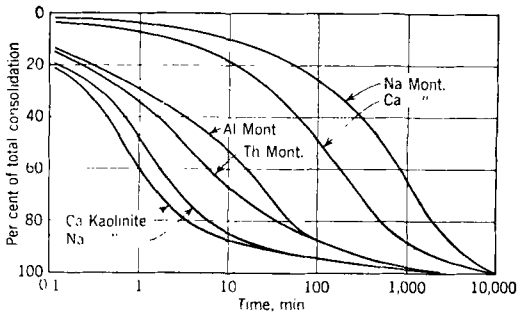

Fig. 5.15. Rate of consolidation of bentonites and kaolin at 4—8 tons/ft.^{2}, after Samuels (1950).

Soil stabilization

The object of soil stabilization is to bind the soil particles together so that a rigid nondispersable mass is quickly obtained with high load-bearing strength and resistance to the effects of weathering. The addition of lime to expansive clays (e.g. bentonites) reduces the plasticity index, and increases the load-bearing values. Eades and Grim (1960) have shown that there is an actual chemical reaction between the lime and kaolinite, illite and smectite accompanying the increases in bearing power. The reaction products appeared to be calcium silicate hydrates and calcium aluminum hydrates. In the case of bentonites an appreciable amount of lime is required to satisfy the exchange capacity so that the initial increments of lime cause little or no increase in strength. Sodium bentonites require more lime to become wholely saturated than the calcium variety, and thus there is a larger lag in the development of strength with lime additions for sodium than for calcium bentonites. Bentonites required 8% or more lime as the optimum amount for stabilization whereas for kaolins the optimum amount was of the order of 4%.

Organic compounds, such as petroleum fractions and bitumin, have been widely used for a long time to stabilize earthen roads. There is very little specific information available on the relative effect of various types of organic compounds on specific clay minerals or on types of soil. One would expect that the ability of bentonites to react with and fix certain organic compounds (see pp. 236—237) would be a significant factor in the relative stabilization properties of such compounds. One would suspect also that for the same reason, the stabilization effect would be different for bentonites than for other clay materials. One would also expect that it would be difficult to adequately mix organic compounds with bentonites. The high water-holding capacity of bentonites would make the addition of organic compounds extremely difficult, and retard their reaction. Kaolinite and illite clays would appear to be much more susceptible to such stabilization than bentonites.

5.7. PROPERTIES RELATED TO AGRICULTURAL USE

From an agricultural standpoint there are certain attributes that a soil requires in order to make it desirable for the growth of vegetation. These may be listed as follows — not necessarily in their order of importance.

There is an optimum water retention capacity so that the soil will not dry out too quickly or remain wet too long after a rain.

On drying the soil must not become so hard that the penetration of plant roots is difficult.

The soil must have a certain tilth, i.e. it must be amenable to easy plowing and working.

The soil must have substantial retention capacity for fertilizers. The soil must retain added ingredients so that they are not leached out following the first rain after fertilizing.

Although the soil must retain added ingredients, they must not be fixed so that they are unavailable to the plants.

There should be the capacity to retain organic material so that its elimination by decay and oxidation is retarded.

It is desirable that the soil contain chemical components, e.g. potassium and calcium, that plant growth requires.

It is important that the soil does not contain chemical elements, e.g. sodium, in such abundance that plant growth is retarded or prevented.

Bentonites can be evaluated from an agricultural standpoint by considering the possible correlation of their properties with the attributes noted above. Bentonites have the property of absorbing and holding large amounts of water. The sodium variety tends to absorb such extremely large amounts of water that it could become excessively wet and plastic. The water absorption capacity of calcium bentonites is more moderate and this characteristic should not be detrimental for them.

On drying bentonites shrink and tend to become hard. This is particularly true for the sodium variety, and it especially should not be valuable from an agricultural standpoint.

The tilth of bentonites is likely to be marginal for the calcium variety and unsatisfactory for the sodium variety. For plowing, they would be very soft and plastic when wet and very hard after drying.

Their high cation exchange capacity would give bentonites excellent capacity to hold plant nutrients. Further, such added ingredients would probably not be fixed so that they would be unavailable for plant growth.

Bentonites should also be satisfactory from the point of view of the need to hold organic material. However, there may be some question about this conclusion because of the catalytic property of the smectite clay minerals, and their ability to adsorb various organic molecules and thereby become oleophylic.

The calcium bentonites would provide a source of calcium as may be needed for plant growth. It is now well known that traces of certain elements may be extremely favorable or detrimental for the growth of certain plants (e.g. copper favorable for tomatoes, and manganese for certain berries). By their very nature and mode of origin some bentonites may naturally contain such elements. Because of their sorption properties, it should be relatively easy to provide such elements to bentonitic soils.

REFERENCES

Abbot, F.C. and Anderson, C.O., 1940. Metalurgical Flux and Method of Producing It. U.S. Patent, 2,220,385.

Anonymous, 1959. Drilling Mud. Baroid Division, National Lead Company.
Atterberg, A., 1911. Die Plastizität der Tone. Int. Mitt. Bodenk., I: 4—37.
Atterberg, A., 1912. Die Konsistenz und Bindigkeit der Boden. Int. Mitt. Bodenk., II.
Cuciureanu, G., Verbuta, A., Oita, N. and Craita, V., 1972. Delivery and stability of some antibiotics in bentonite. Farmacia (Bucharest), 20: 119—127.
Curado, J.G. and Praeg, D.H., 1956. Printing Ink. U.S. Patent, 2,750,296.
De Vaney, F.D., 1956. Process of Preparing Indurated Pellets of Iron Ore Fines. U.S. Patent, 2,743,172.
Déribéré, M. and Esme, S., 1951. La Bentonite. Dunod, 3rd Ed., Paris.
Dunbeck, N.J., 1942. American synthetic sand practice. Trans. Am. Foundrymen's Soc. 50: 141—164.
Eades, J.L. and Grim, R.E., 1960. The reaction of hydrated lime and pure clay minerals in soil stabilization. U.S. Highway Res. Board Meet., January, 1960.
Endell, K., Loos, W., Meischeider, H. and Berg, V., 1938. Über Zusammenhänge zwischen Wasserhaushalt der Tonminerale und Bodenphysikalischen Eigenschaften Bindiger Böden. Veröff. Dtsch. Forsch. Bodenmech. 5.
Fendius, H. and Endell, K., 1935. Über die Bestimmung der Verformbarkeit und Plastizität verschiedener Tone und Massen. Sprechsaal, 14.
Fleury-Larsonneau, A. and André, M., 1942. Étude du pouvoir de saven charges. Chim. Ind. (Paris), 47: 333—350.
Gibson, R.E., 1953. Experimental determination of the true cohesion and true angle of internal friction in clays. Proc. Int. Congr. Soil Mech., 3rd., I: 126—130.
Graham, R.P. and Sullivan, J.D., 1939. Workability of clays. J. Am. Ceram. Soc., 22: 152—157.
Grim, R.E., 1947. Relation of clay mineralogy to the origin and recovery of petroleum. Bull. Am. Assoc. Pet. Geol., 31: 1491—1499.
Grim, R.E., 1962. Applied Clay Mineralogy. McGraw-Hill, New York, N.Y., 422 pp.
Grim, R.E., 1968. Clay Mineralogy. McGraw-Hill, New York, N.Y., 2nd Ed., 596 pp.
Grim, R.E. and Cuthbert, F.L., 1945. The bonding action of clays. Part I. Clays in green molding sands. Ill. State Geol. Surv., Rep. Inv., 102. Part II. Clays in dry molding sands. Ill. State Geol. Surv., Rep. Invest., 110.
Grim, R.E. and Johns, W.D., 1957. Compaction studies of molding sands. Trans. Am. Foundrymen's Soc., 59: 90—95.
Grimshaw, R.W., 1971. The Chemistry and Properties of Clays. Interscience, New York, N.Y., 4th Ed.
Hauser, E.A., 1950. Modified Gel-forming Clay and Process of Producing Same. U.S. Patent, 2,251,427.
Hauser, E.A., 1955. Silicic Science. Van Nostrand, Princeton, N.J.
Hirshmann, W.R. and Bechtner, P., 1938. Bentonite. Soap Sanit. Chem., 14: 24—26.
Hofmann, F., 1956. Beitrag zur Kenntnis und zur Untersuchung der Eigenschaften von Bentoniten. Giesserei, 16: 857—864.
Hofmann, F., 1970. Relation between origin and technical properties of various bentonites. Rep. Int. Comm. Study Clays, Int. Geol. Congr., Copenhagen, 5.
Hofmann, U., 1954. Füllstoffe und Keramische Rohmaterialien. Rapp. Europees Congr. Electronenmikroskopie, pp. 161—172,
Holden, E.G., 1948. Preservation of Baked Cereal Food. U.S. Patent, 2,443,138.
Johns, W.D. and Shimoyama, A., 1972. Clay minerals and petroleum refining reactions during burial and diagenesis. Bull. Am. Assoc. Pet. Geol., 56: 2160—2167.
Jordan, J.W., 1950. Lubricants. U.S. Patent, 2,531,440.
Kerr, J.M., 1954. Preliminary tests on clay sinters to retain reactor wastes. Bull. Am. Ceram. Soc., 38: 374—376.
Klinefelter, T.A., 1946. Evaluation of some binders for use in pelletizing slimes. U.S. Bur. Mines, Rep. Invest., 3846.

Lambe, T.W., 1953. Cold room studies. Appendix D., Minerals and chemical studies. In: Frost Investigation. U.S. Army Corp. Eng.
Larsen, D.H., 1955. Use of clays in drilling fluids. Calif., Div. Mines Geol. Bull., 169: 269—281.
Lea, F.M., 1938. The chemistry of Pozzolannas. Proc. Symp. Cement Chem., 460—490.
Mielenz, R.C. and King, M.E., 1955. Physical chemical properties and engineering performance of clays. Calif., Div. Mines Geol. Bull., 169: 196—254.
Mielenz, R.C., Greene, K.T. and Schieltz, N.C., 1951. Natural Pozzolannas for Concrete. Econ. Geol., 46: 311—328.
Novelli, G., 1972. Properties and possible use of montmorillonite in pharmaceutical and cosmetic preparations. Riv. Ital. Essenze, Profumi, Piante Off., Olii Veget., Saponi, 54: 267—270.
Olin, H.L., Box, P.J. and Whitson, R.E., 1942. Bentonite as a coagulant for sewages and industrial wastes. Water Sewage Works, December.
Rick, G.G. and Loetel, C.E., 1940. Fuel Briquettes and method of making same. U.S. Patent, 2,217,994.
Sakawa, W., Szymanski, J., Jura, S. and Gawarecki, S., 1969. Improvement of montmorillonite clays for foundry practice. Politech. Gliwice, Pol., 58, 190, (cl. B 03b).
Samuels, S.G., 1950. The effect of base exchange on the engineering properties of soils. Build. Res. Stn. G.B., Note, C176.
Saywell, L.G., 1935. The bentonite process of clarifying wine. Calif. Wine Rev., January.
Silva, F.J., 1948. Colloidal bentonite as a clarifying agent. Sugar J., October.
Skempton, A., 1953. The colloidal activity of clays. Proc. Int. Conf. Soil Mech., 3rd, I: 57—61.
Skempton, A. and Northey, R.D., 1952. The sensitivity of clays. Geotechnique, 3: 30—53.
Terzaghi, K., 1944. Ends and means of soil mechanics. Harvard Univ., Grad. Sch. Eng., Publ., 402.
Voet, A. and Yelmgren, A.E., 1952. Anti-misting Printing Ink. U.S. Patent, 2,754,219.
White, W.A., 1947. The Properties of Clays. M.S. Thesis, Univ. of Illinois.
White, W.A., 1955. Water Sorption Properties of Homoionic Clay Minerals. Ph.D. Thesis, Univ. of Illinois.
White, W.A. and Pichler, E., 1959. Water sorption characteristics of clay minerals. Ill. State Geol. Surv., Circ., 266.
Whittemore, J.W., 1935. Mechanical methods for measurement of plasticity of clay. J. Am. Ceram. Soc., 18: 352—360.
Yamamoto, K., 1940. Acid clay and activated clay in Japan. J. Soc. Chem. Ind., Japan, 43: 303—304B.

INDEX